GEL LAYER FORMATION ON MEMBRANES IN MEMBRANE BIOREACTORS

Paula van den Brink

van den Brink, P.F.H., 2014
Gel layer formation on membranes in Membrane Bioreactors

Cover picture: Cross section of a gel layer fouled membrane. The scanning electron microscopy image was prepared by dr. Arie Zwijnenburg.
Cover design by: Silvia Ardesch
Lay-out by: Ridderprint BV, Ridderkerk, the Netherlands
Printed by: Ridderprint BV, Ridderkerk, the Netherlands

GEL LAYER FORMATION ON MEMBRANES IN MEMBRANE BIOREACTORS

PROEFSCHRIFT

ter verkrijging van de graad van doctor
aan de Technische Universiteit Delft,
op gezag van de Rector Magnificus prof.ir. K.C.A.M. Luyben,
voorzitter van het College voor Promoties,
in het openbaar te verdedigen

op dinsdag 16 september 2014 om 15.00 uur

door
Paula Frederica Henrica VAN DEN BRINK

Ingenieur Bioprocestechnologie
geboren te Nijmegen

Dit proefschrift is goedgekeurd door de promotor:
Prof.dr.ir. M.C.M. van Loosdrecht

Copromotor: Dr.ir. H. Temmink

Samenstelling promotiecommissie:

Rector Magnificus	Technische Universiteit Delft, *voorzitter*
Prof. M.C.M. van Loosdrecht	Technische Universiteit Delft, *promotor*
Dr.ir. H. Temmink	Wageningen Universiteit, *copromotor*
Prof.dr.ir. D.C. Nijmeijer	Universiteit Twente
Prof.dr.ir. H.D.W. Roesink	Universiteit Twente
Prof.dr. M.D. Kennedy	Technische Universiteit Delft/UNESCO-IHE
Prof.dr.ir. J.B. van Lier	Technische Universiteit Delft
Dr. C.M. Plugge	Wageningen Universiteit

Dr. A. Zwijnenburg (Wetsus) heeft als begeleider in belangrijke mate aan de totstandkoming van dit proefschrift bijgedragen

This work was performed in the cooperation framework of Wetsus, centre of excellence for sustainable water technology (www.wetsus.nl)

© 2014 by P.F.H. van den Brink

ISBN: 978-90-5335-895-5

TABLE OF CONTENTS

Summary		**7**
Samenvatting		**11**
Chapter 1	Introduction	**15**
Chapter 2	Effect of free calcium concentration and ionic strength on alginate fouling in cross-flow membrane filtration	**39**
Chapter 3	Gel layer formation on membranes increases particle retention and fouling	**65**
Chapter 4	Potential of mechanical cleaning of membranes from a membrane bioreactor	**91**
Chapter 5	Bacterial communities in sludge fractions and membrane biofilms in a membrane bioreactor	**117**
Chapter 6	Effect of temperature shocks on membrane fouling in membrane bioreactors	**145**
Chapter 7	Concluding remarks	**169**
Curriculum Vitae		**181**
List of Publications		**185**
Dankwoord		**189**

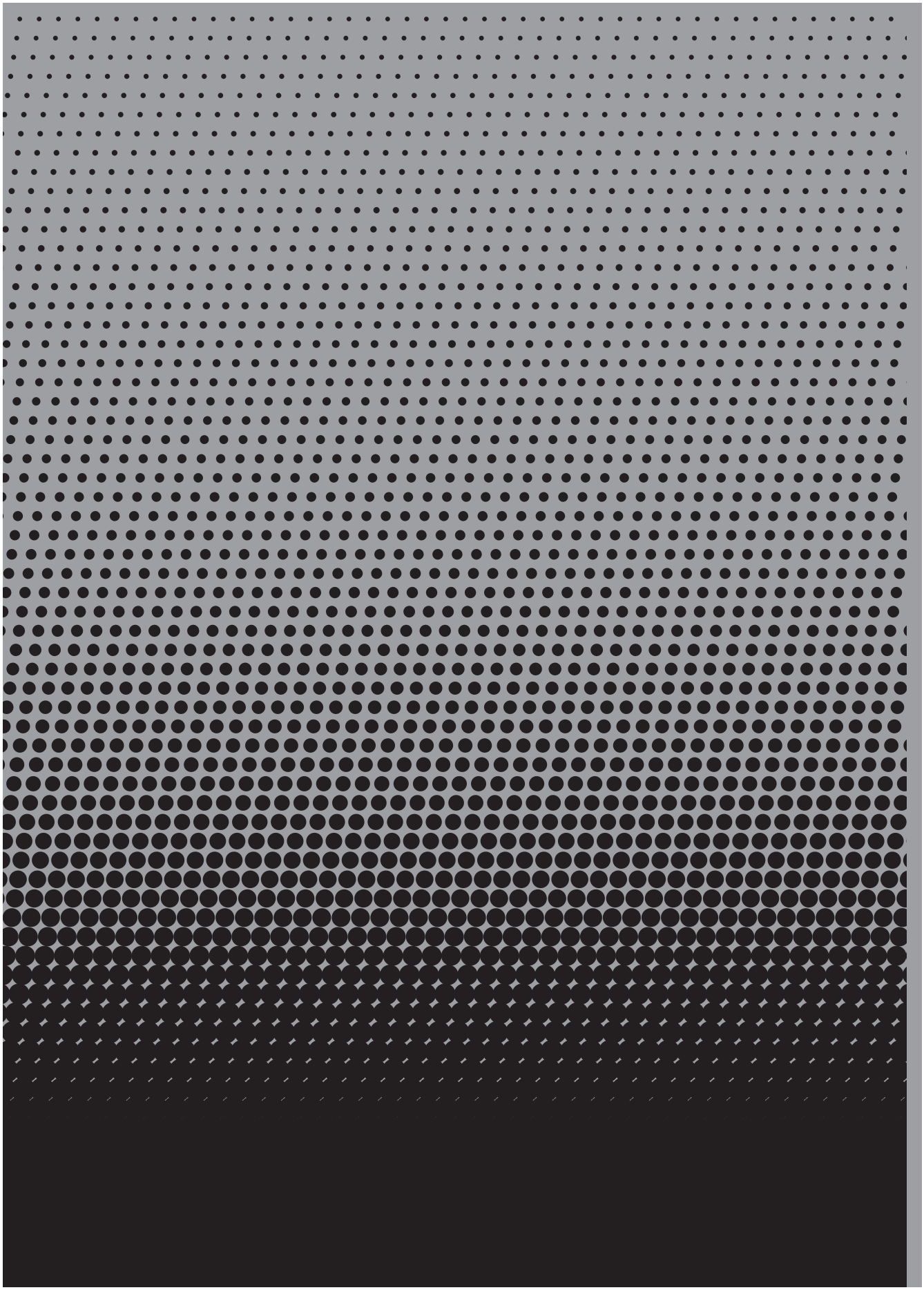

SUMMARY

The widespread application of membrane bioreactors (MBRs) for municipal wastewater treatment is hampered by membrane fouling. Fouling increases energy demand, reduces process performance and creates the need for more frequent (chemical) membrane cleaning or replacement. Membrane fouling in MBRs is known to be caused by several membrane fouling mechanisms. Extracellular polymeric substances (EPS) play a major role during fouling development. However, EPS concentration in the bulk solution can not be generally used as an indicator for fouling propensity. The term "EPS" comprises several types of compounds, originating from the biomass: proteins, polysaccharides, nucleic acids, lipids and other polymeric substances. In this thesis, several findings are described concerning the role and behaviour of EPS during membrane fouling in MBRs.

Chapter 1 gives an introduction to membrane filtration and more particularly to membrane bioreactors and membrane fouling. Fouling mechanisms are extensively described, as well as methods to prevent and control fouling. This chapter also contains the objective of this thesis and an introduction to its contents.

In **chapter 2**, alginate is used as a model compound to simulate fouling by polysaccharides, which are the main constituents of EPS. Polysaccharides are known to play an important role in membrane fouling. The effect of water chemistry of alginate feed solution (calcium concentration, foulant concentration and ionic strength) on fouling rate and reversibility was studied in flux step experiments. There was a strong relation between calcium concentration and fouling rate. An increased ionic strength had no impact on fouling rate in low fouling experiments, but decreased fouling with 66–72% at high fouling conditions. Reversibility of the fouling decreased with increasing calcium concentrations to values as low as 3%.

The interaction between fouling by particles and gel formation was studied in **chapter 3**. Membranes fouled by alginate gels or by gels formed in an MBR treating municipal wastewater show increased retention for particles. Increased retention for particles was also observed when particles and alginate were filtered simultaneously. Comparing filtration times and plateau values for alginate with and without particles, alginate plus particles fouls more than the sole alginate solution.

In **chapter 4**, harsh mechanical cleaning was applied on membranes operated at different relatively low fluxes to evaluate how much fouling could be maximally removed and distribution of remaining fouling was investigated. Even after harsh mechanical cleaning, membrane samples showed considerable oxygen consumption. No fouling was observed inside the membrane. Of several membranes operated for at least 1 year, the permeate side was covered with bacteria and extracellular polymeric substances (EPS).

This fouling on the permeate side should not be neglected when designing membrane cleaning.

In **chapter 5**, the community structure and dynamics of sludge fractions in an MBR treating municipal wastewater were compared with those of the wastewater and membrane biofilms using cultivation independent molecular techniques. Constant flux filtrations were performed and samples were taken at three different dates. Denaturating gradient gel electrophoreses (DGGE) and sequence analysis revealed a high bacterial diversity in the wastewater, sludge fractions and membrane biofilms. An increase in diversity was shown in the following order: wastewater < mixed liquor supernatant < mixed liquor < membrane biofilm. No higher similarity of biofilm communities with one specific other MBR fraction was observed. The bacterial communities in the wastewater, sludge fractions and membrane biofilms were time variable. Only at higher biofilms ages, a clear effect of biofilm age on biofilm communities was observed: communities, distinct from those in wastewater and sludge fractions, developed at higher biofilm ages. This indicates occurrence of active bacterial growth on the membrane. No effect of flux on bacterial diversity of the biofilms could be observed and few bacterial genera could be removed by harsh mechanical cleaning.

Chapter 6 describes the effect of temperature shocks on membrane fouling in membrane bioreactors. Flux step experiments were performed in an experimental system at 7, 15, and 25° C with sludge that was continuously recirculated from a pilot-scale MBR. Higher membrane fouling rates were obtained for the lower temperature in combination with low fouling reversibility. At low temperature, a high polysaccharide concentration was found in the mixed liquor supernatant of the experimental system as compared to the MBR pilot. Upon decreasing the temperature of the mixed liquor, a shift was found in particle size in the mixed liquor supernatant towards smaller particles. These results show that the release of polysaccharides and/or submicron particles from sludge flocs could explain the increased membrane fouling at low temperatures.

The main results and conclusions presented in this thesis are summarized in **chapter 7.** The origin of EPS in MBRs is discussed and an overview is given of EPS measuring methods and their restrictions. In this chapter also practical implications of EPS fouling in MBRs are mentioned and suggestions for further research are provided.

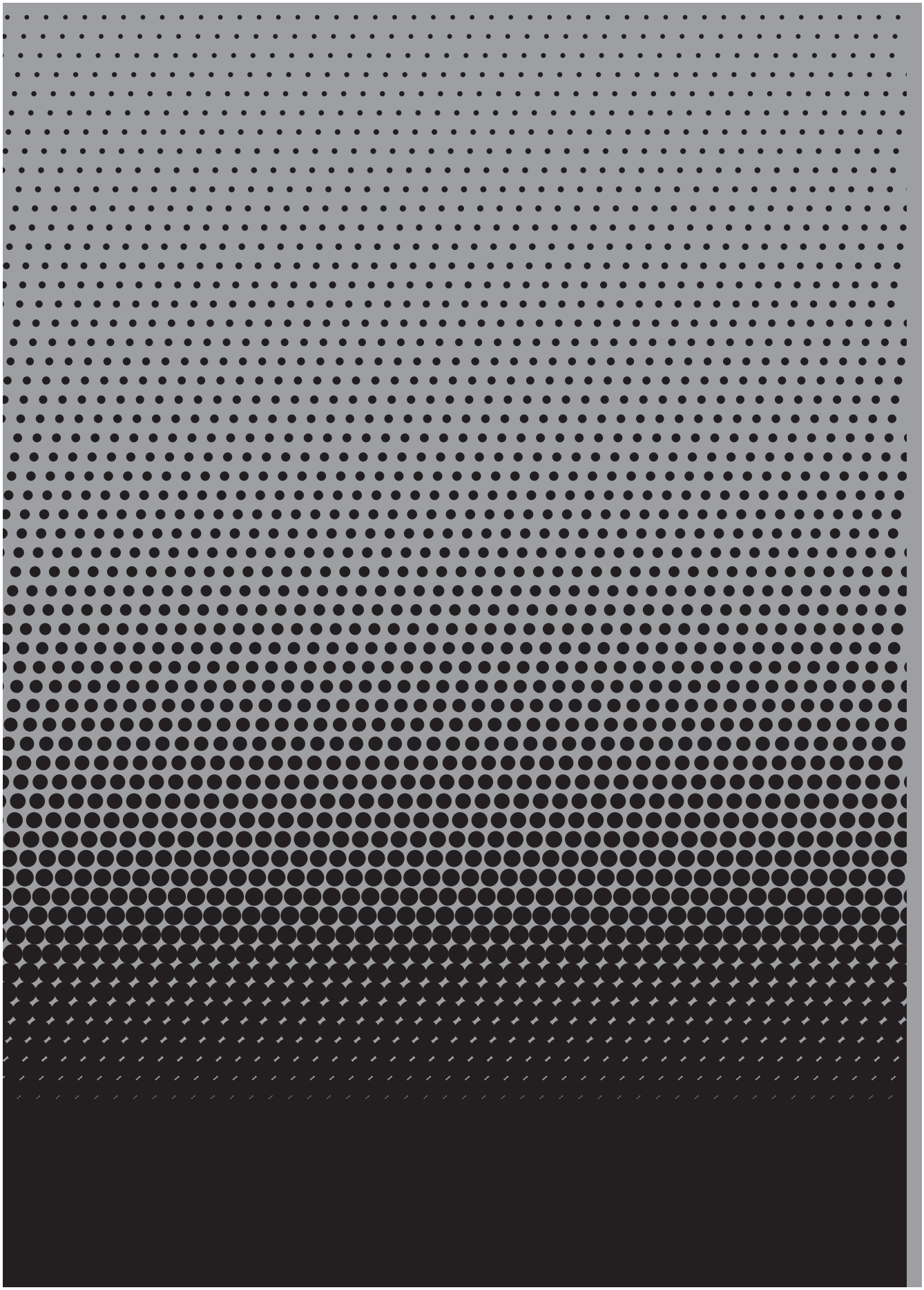

SAMENVATTING

De grootschalige toepassing van membraan bioreactoren (MBR) voor behandeling van huishoudelijk afvalwater wordt verhinderd door membraanvervuiling. Vervuiling van membranen zorgt voor een verhoogd energieverbruik, verminderde prestaties van het proces en zorgt ervoor dat de membranen vaker (met chemische middelen) schoongemaakt of vervangen moeten worden. Membraanvervuiling in membraan bioreactoren wordt veroorzaakt door verscheidene membraanvervuilingsmechanismen. Extracellulaire polymere substanties (EPS) spelen een belangrijke rol tijdens de ontwikkeling van vervuiling. Desondanks kan de concentratie van EPS in de oplossing niet algemeen gebruikt worden als een indicator voor neiging tot vervuiling. De term "EPS" omvat verscheidene typen stoffen die voortkomen uit de biomassa: eiwitten, polysacchariden, nucleïnezuren, lipiden en andere polymere stoffen. In dit proefschrift worden diverse bevindingen beschreven betreffende de rol en het gedrag van EPS tijdens membraanvervuiling in MBRs.

Hoofdstuk 1 geeft een inleiding op membraanfiltratie en meer specifiek op membraan bioreactoren en membraanvervuiling. Membraanvervuilingsmechanismen worden uitgebreid beschreven, en daarnaast ook methoden om vervuiling te voorkomen en onder controle te houden. Dit hoofdstuk bevat ook het doel van dit proefschrift.

In **hoofdstuk 2** wordt alginaat gebruikt als een modelstof om vervuiling door polysacchariden, welke de belangrijkste bestanddelen van EPS zijn, na te bootsen. Van polysacchariden is bekend dat zij een belangrijke rol spelen bij membraanvervuiling. Het effect van de waterchemie van de alginaat voedingsoplossing (calcium concentratie, concentratie alginaat en ionsterkte) op vervuilingssnelheid en reversibiliteit werd bestudeerd in "flux stap" experimenten. Er is een sterke relatie tussen calcium concentratie en vervuilingssnelheid gevonden. Een verhoogde ionsterkte had geen effect op de vervuilingssnelheid in experimenten met weinig vervuiling, maar verminderde deze met 66–72% in experimenten met veel vervuiling. Reversibiliteit van de vervuiling verminderde bij verhoogde calcium concentraties tot waarden van 3%.

De interactie tussen deeltjesvervuiling en gelvorming is bestudeerd in **hoofdstuk 3**. Membranen vervuild met alginaat gels of met gels gevormd in een MBR die huishoudelijk afvalwater behandelde lieten verhoogde retentie voor deeltjes zien. Verhoogde retentie voor deeltjes is ook waargenomen wanneer deeltjes en alginaat tegelijkertijd werden gefiltreerd. Wanneer filtratietijden en plateauwaarden vergeleken werden voor alginaat met en zonder deeltjes, vervuilde alginaat met deeltjes meer dan de alginaatoplossing alleen.

In **hoofdstuk 4** is ruwe mechanische reiniging toegepast op membranen die bedreven zijn bij verschillende relatieve lage fluxen om te zien hoeveel vervuiling maximaal verwijderd kon worden. Daarnaast is de verdeling van de overgebleven vervuiling over het membraan bestudeerd. Zelfs na ruwe mechanische reiniging lieten de membraanmonsters behoorlijke

zuurstofconsumptie zien. Geen vervuiling is waargenomen binnen in het membraan. Van diverse membranen die bedreven zijn voor minstens één jaar, was de permeaatzijde bedekt met bacteriën en extracellulaire polymere substanties (EPS). Deze vervuiling aan de permeaatzijde moet niet worden verwaarloosd bij de membraanreiniging.

In **hoofdstuk 5**, werden de structuur en dynamiek van de bacteriële populaties in de slibfracties in een MBR, die huishoudelijk afvalwater behandelde, vergeleken met de populaties in het afvalwater en de biofilms op de membranen. Hierbij is gebruik gemaakt van kweek onafhankelijke moleculaire technieken. Constante flux filtraties werden uitgevoerd en monsters werden genomen op drie verschillende data. Denaturating gradient gel electrophoresis (DGGE) en sequentie analyse lieten een hoge bacteriële diversiteit zien in het afvalwater, de slibfracties en de biofilms op de membranen. De diversiteit van de verschillende monsters liep als volgt op: afvalwater < supernatant van het actief slib < actief slib mengsel < membraan biofilm. Geen hogere gelijkenis van de biofilm populaties is waargenomen met één specifieke andere MBR fractie. De bacteriële populaties in het afvalwater, slibfracties en de biofilms op de membranen varieerden in de tijd. Alleen bij hogere biofilm leeftijden werd een duidelijk effect van biofilm leeftijd op populaties in de biofilm opgemerkt: populaties, verschillend van die in afvalwater en slibfracties, ontwikkelden zich bij hogere biofilm leeftijden. Dit geeft aan dat actieve bacteriële groei plaatsvindt op het membraan. Geen effect van flux op diversiteit in de bacteriële populaties kon opgemerkt worden en enkele bacteriële genera konden verwijderd worden door ruwe mechanische reiniging.

Hoofdstuk 6 beschrijft het effect van temperatuurschokken op membraanvervuiling in membraan bioreactoren. “Flux stap” experimenten werden uitgevoerd in een experimenteel system bij 7, 15, en 25°C met actief slib dat continu werd gerecirculeerd vanuit een pilot-scale MBR. Hogere membraanvervuilingssnelheden in combinatie met lage reversibiliteit van de vervuiling werden verkregen voor de lagere temperatuur. Bij lage temperatuur werd een hoge polysaccharide concentratie gevonden in het supernatant van het actief slib van het experimentele systeem vergeleken met de MBR pilot. Nadat de temperatuur van het actief slib werd verlaagd, werd een verschuiving gezien in de deeltjesgrootte in het supernatant van het actief slib naar kleinere deeltjes. Deze resultaten laten zien dat het vrijkomen van polysacchariden en/of submicron deeltjes vanuit de slibvlokken de verhoogde membraanvervuiling bij lage temperaturen kan verklaren.

De belangrijkste resultaten en conclusies gepresenteerd in dit proefschrift worden samengevat in **hoofdstuk 7**. De oorsprong van EPS in MBRs wordt besproken en er wordt een overzicht gegeven van meetmethoden voor EPS en hun beperkingen. In dit hoofdstuk worden ook praktische consequenties van EPS vervuiling in MBRs genoemd en suggesties voor verder onderzoek gedaan.

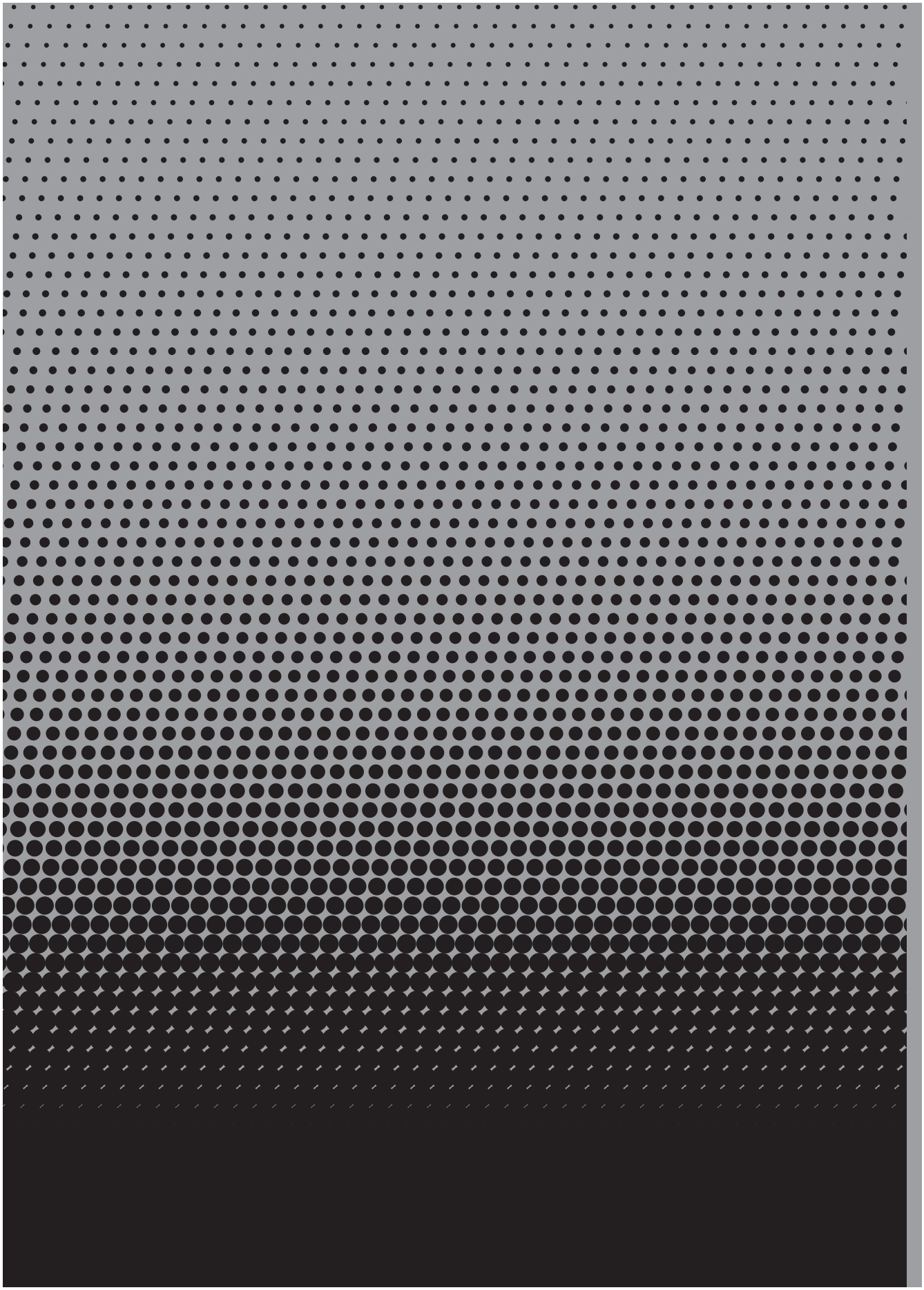

Chapter 1

INTRODUCTION

MEMBRANE FILTRATION

In membrane processes, the feed stream is divided into two streams, i.e. the retentate or concentrate stream and the permeate stream (Figure 1.1). Either the concentrate or permeate stream is the product. The two streams are separated by the membrane, which is defined by Mulder as "a selective barrier between two phases, the term 'selective' being inherent to a membrane or a membrane process" (Mulder, 1996).

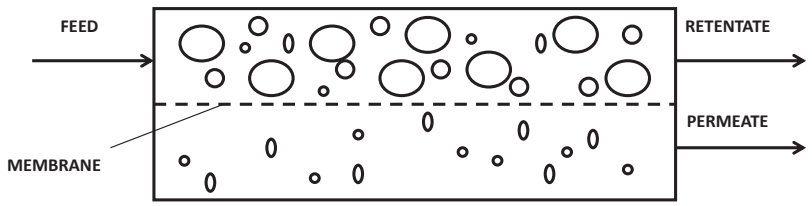

Figure 1.1 Schematic representation of a membrane process.

Different driving forces play a role in membrane separations: fluid pressure (e.g. microfiltration, reverse osmosis), vapor pressure (e.g. gas separation), osmotic pressure (e.g. dialysis, forward osmosis), temperature difference triggering a vapor pressure difference (e.g. membrane distillation) and electric potential difference (e.g. electrodialysis, electrophoresis) (Mulder, 1996). Two characteristics of a membrane that are mainly used to describe its performance are selectivity and flow through the membrane. For dilute aqueous solutions, as is the case for membrane bioreactors (MBRs) that are studied in this thesis, the term "retention" is used instead of "selectivity". In MBRs, the fluid pressure is used to perform the separation, and this type of membrane process will therefore be explained in more detail below.

In micro- and ultrafiltration of aqueous solutions, separation is based on differences in particle size, i.e. particles larger than the membrane's pore size are retained by the membrane. These filtration processes can be categorized according to the membrane's pore size, and consequently to the particle size that can be retained by membrane. When the pore size decreases, the required transmembrane pressure (TMP) increases. Table 1.1 shows several membrane processes for aqueous solutions, including the corresponding pore sizes, porosities and applied TMPs. Different ranges of pore sizes and TMPs are reported, which means that the distinction between membrane filtration types is not very strict. Membrane processes for aqueous solutions are applied in the fields of food and dairy production, pharmaceuticals, wastewater treatment and drinking water production. A few applications are also included in the Table.

Table 1.1 Different membrane processes for aqueous solutions and their characteristics (based on Mulder, 1996).

Membrane filtration type	Separation mechanism	Pore size	Porosity	Applied TMP (bar)	Example of applications
Microfiltration	Size exclusion	0,1-10 µm	High	0.1-2	- clarification fermentation broths - water treatment
Ultrafiltration	Size exclusion	5-100 nm	High	0.5-10	- dairy & food - pharmaceutical - water treatment
Nanofiltration	Solution/diffusion	<2 nm	Small	5-20	- water softening - removal of micropollutants
Reverse Osmosis	Solution/diffusion	<2 nm	Small (dense)	10-80	- desalination - concentration juices/milk

In the field of wastewater treatment, micro- or ultrafiltration membranes are often used in MBRs, which combine biological treatment with a physical separation step.

MEMBRANE BIOREACTORS

The membrane in the MBR is an alternative to the settling tank in the conventional activated sludge process. It combines the activated sludge process with membrane filtration for biomass retention, thereby making a separate settling step redundant.

The main advantages of MBRs over conventional activated sludge (CAS) processes are (Chang et al., 2002; Kim and Jang, 2006; Wintgens et al., 2003; Le-Clech, 2010):

1. Higher effluent quality

MBRs show a complete removal of solids resulting in a high and consistent effluent quality, which can be upgraded to process water by application of nanofiltration or reverse osmosis (RO). MBR-RO permeate quality concerning TOC, NH_4 and NO_3^- was shown to be the same or better than that of a CAS-MF-RO process treating domestic sewage, while the RO could be operated at a 30% higher flux in the MBR-RO process (Qin et al., 2006). Because of the high retention of bacterial and viral indicators by the membrane (Marti et al., 2011; Francy et al., 2012; de Luca et al., 2013), MBR effluent can be discharged in water bodies where recreational activities take place (van Nieuwenhuijzen et al., 2008) and reused for example as irrigation water or, after additional treatment, as drinking water.

2. Smaller plant footprint

By replacing the secondary settler with a membrane process, a smaller footprint is required for the plant because less space is needed for the membranes than for the settler (Defrance et al., 2000; Visvanathan et al., 2000). Also, higher mixed liquor suspended solids (MLSS)

concentrations in the MBR allow for smaller biological reactor volumes (Melin et al., 2006). Approximately 50% can be saved on space requirements, depending on the applied MLSS concentrations and the need for tertiary treatment (Hai and Yamamoto, 2011). In the case of retrofitting of Brescia wastewater treatment plant (WWTP), space savings can be easily quantified as both CAS and MBR are installed treating the same wastewater (Judd and Judd, 2010). In highly populated or coastal areas, in some cases of retrofitting or upgrading existing WWTPs, or in industrial wastewater treatment, the space savings can be decisive to apply a MBR instead of a conventional activated sludge system.

3. Robustness

The MBR is able to handle wide fluctuations in influent quality (Chang et al., 2002) and has a lower sensitivity to contaminant peaks (Melin et al., 2006). In a CAS system, shock loads or high salt concentrations can be a problem when the settleability of the sludge is affected. In this case, which is of most importance for industrial wastewaters, the MBR is more robust because the sludge is retained by the membrane.

Reduced excess sludge production is often mentioned as another advantage of MBRs, resulting from low sludge loading rates and high SRTs (Drews, 2010). In practice, high SRTs and high MLSS concentrations are not feasible because high MLSS concentrations have a negative effect on the α-factor (which is the ratio of the volumetric mass transfer coefficient K_La in the mixed liquor to the K_La in clean water (Stenstrom, 2007) and thus on energy input (Henze, 2008). Therefore, sludge loading rates applied for full scale CAS and MBR systems are similar and this results in similar excess sludge production (Hai and Yamamoto, 2011).

MBRs also have disadvantages when comparing them to CAS systems, of which the main are mentioned below.

1. High capital and operating costs

Although membranes show a decreasing price development since the early 1990s (Hai and Yamamoto, 2011), MBRs are still relatively expensive to install and operate (Le-Clech, 2010). When comparing MBR and CAS systems, the reference system should be a CAS system that produces the same effluent quality. Several other assumptions (e.g. plant capacity, membrane lifetime) greatly influence the outcome of this cost comparison.

2. High energy consumption

In the MBR, aeration is used for both the biological process and membrane cleaning, and different bubble sizes are needed for each process. Therefore, more air and, hence, also more energy is used in the MBR process as compared to the CAS process (Hai and Yamamoto,

2011). A total energy consumption for CAS-UF/MF of 0.35-0.5 kWh m^{-3} was estimated for a new facility (Lesjean et al., 2004), while values for MBRs range from 0.64 (for large scale commercial MBRs such as MBR Schilde) to 1.2-1.5 kWh m^{-3} or higher (for smaller-scale facilities) (Judd, 2006; van Bentem et al., 2007; Fenu et al., 2010).

3. Frequent membrane monitoring and cleaning

Due to membrane fouling, cleaning of the membranes is frequently needed to restore their performance. The use of chemicals for membrane cleaning has a negative impact on the environment (Drews, 2010).

4. Complexity of the process

The membrane separation adds complexity to the wastewater treatment process, which entails the need for highly skilled operators.

A schematic representation of a MBR system in its two possible configurations is shown in Figure 1.2. The submerged configuration is most often applied for large scale low strength applications because of reduced fouling and lower energy consumption of 0.64-1.5 kWh m^{-3} as compared to up to 4 kWh m^{-3} for the side-stream configuration (Gander et al., 2000; Huang et al., 2001; Judd, 2006; Fenu et al., 2010). Recent developments concerning lowering energy consumption are, for example, intermittent aeration for submerged systems and the airlift concept of Pentair.

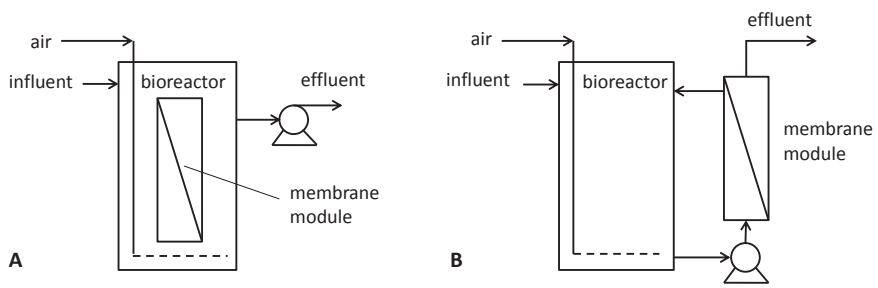

Figure 1.2 MBR configurations (**A**) Submerged (**B**) Side-stream (after Metcalf & Eddy, 2003).

There are two main types of configuration of the membrane, called the tubular membrane system and the flat sheet membrane system (Mulder, 1996). In the first category, the following types can be distinguished, based on dimensions: hollow fiber membranes (diameter <0.5 mm, inside-out and outside-in), capillary (diameter 0.5-5 mm) and tubular membranes (diameter >5 mm). Flat sheet membranes are divided up in spiral-wound membranes that are mainly used in nanofiltration (NF) and reverse osmosis (RO), and plate and frame membranes. Due to potential clogging of the module, not all membrane types

can be applied in each configuration. In the submerged MBR, outside-in hollow fibres and capillaries, and plate and frame membranes are used. For side-stream MBRs, inside-out tubular membranes are mostly applied. The different membrane configurations used in MBRs are shown in Figure 1.3.

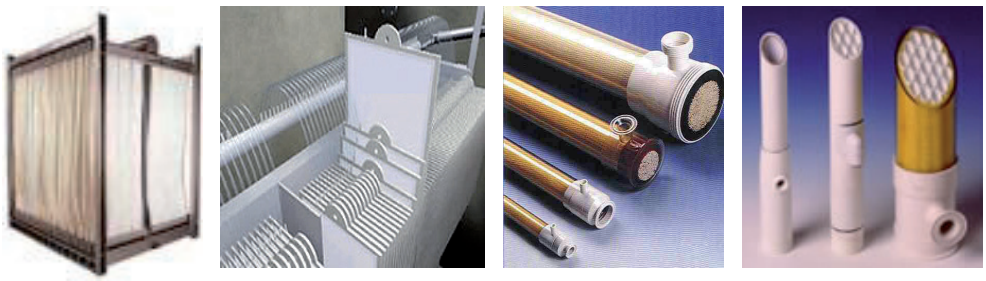

Figure 1.3 Different membrane configurations, from left to right: hollow fiber, plate and frame (both submerged), capillary, tubular (both side-stream).

The two main suppliers of membranes for MBR systems are GE-Zenon (using capillaries of 1.9 mm in diameter), building some of the largest MBRs, and Kubota (using flat sheet membranes), having a very large number of small-scale systems (Judd and Judd, 2010). When the capacities of MBR systems treating municipal and industrial wastewater in Europe are compared, GE-Zenon and Kubota are the main suppliers, treating 63 % and 30 % of the wastewater, respectively. Almost all installed membrane surface (99 %) for MBR applications are used for submerged systems (Lesjean and Huisjes, 2008). Also many MBR plants are located in Japan (mostly small scale systems for wastewater reuse in large buildings and industrial MBRs), other Asian countries, North America, Middle East and Australia. Areas with high water stress show highest growth rates of MBR technology. The most common capacity range for MBRs currently installed worldwide is 200-2000 m^3 d^{-1} (Hai and Yamamoto, 2011).

Many different materials can be used for the production of membranes, like ceramics and polymers (Baker, 2000). Although ceramic membranes are highly resistant against high temperatures and acid/base cleaning (Chang et al., 2002), most of the membranes used in MBRs are polymeric (polyvinylidene fluoride (GE-Zenon, Pentair, Mitsubishi, Toray), polyether sulfon (Pentair) and chlorinated polyolefin (Kubota)) because of their resistance against the commonly used cleaning agent NaOCl (Hai and Yamamoto, 2011). Another important feature of a membrane is whether it is susceptible to membrane fouling, although membrane material is only one of the factors influencing membrane fouling.

MEMBRANE FOULING

Membrane fouling, which can be referred to as "process resulting in (partial) loss of performance of a membrane due to the deposition of suspended or dissolved substances on its external surfaces, at its pore openings, or within its pores" (Koros et al., 1996), is still a major drawback of membrane bioreactors. Fouling leads to an increase in hydraulic resistance and, consequently, permeate flux decline (Le-Clech et al., 2003). In case a constant permeate flux is chosen, increasing TMPs need to be applied. When the TMP is fixed, the flux decreases. In both cases, operating costs will increase because of higher energy costs and the need to clean the membranes. Furthermore, membrane fouling increases the frequency with which membranes should be replaced. Finally, effluent quality can be either positively (by formation of a dynamic membrane (Fan and Huang, 2002)) or negatively influenced (in case of internal or permeate side fouling (van den Brink et al., 2013)) by membrane fouling. Membrane fouling mechanisms and methods to prevent and control fouling to a certain extent will be discussed in this paragraph.

Fouling mechanisms in membrane bioreactors

Mechanisms that may influence membrane fouling in MBRs are cake and/or gel layer formation, precipitation, adsorption/adhesion, pore narrowing, pore blocking and biofilm growth. Figure 1.4 shows a schematic representation of these fouling mechanisms.

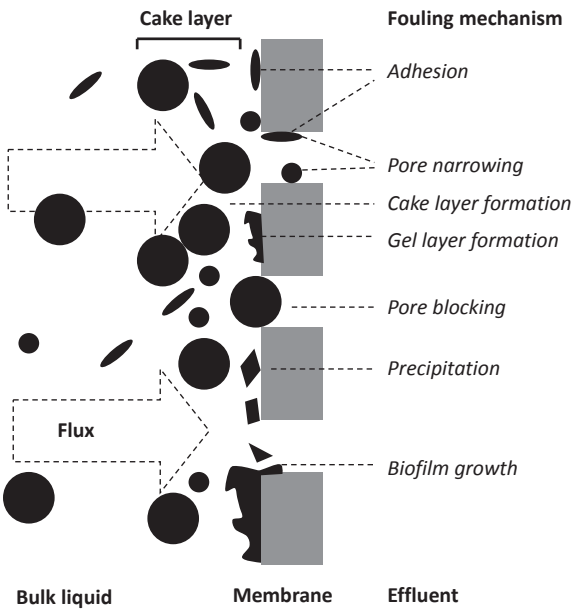

Figure 1.4 Membrane fouling mechanisms.

Before focusing on membrane fouling mechanisms, it is important that they are clearly defined. As much as possible, the terminology proposed by the International Union of Pure and Applied Chemistry in their recommendations of 1996 is used (Koros et al., 1996).

Adhesion: the physical attraction of particles to a solid surface, resulting in relatively high concentration of the molecules at the place of contact. In case of membrane fouling, the solid surface is the membrane. Adhesion is a reversible process.

Adsorption: the tendency for one component of a system to have a higher (or lower) concentration at the interface than it has in the adjacent bulk phase (Barnes and Gentle, 2005).

In the strict sense of these definitions, adsorption applies to dissolved substances and adhesion to particles. However, a third group of compounds, colloidal matters also is important in MBR systems. Because it is difficult to distinguish colloids from particles, and because both adsorption and adhesion result in a higher concentration of compounds at the membrane surface, only one term will be used for both mechanisms: adhesion.

The kinetics of adhesion can be crucial as conformational changes of the adhered layer changes the properties of the membrane surface with time (Le-Clech et al., 2006). This most likely only is important during the first stages of the filtration process, but is relevant for interpretation of lab study results. Pore narrowing is most often associated with adhesion (Bhattacharjee and Hong, 2005) and this decreases the effective pore diameter, which was shown to result in flux decline and higher solute rejection (Clark et al., 1991). Also, when adhesion continues, smaller pores may be blocked, causing redistribution of the flow throughout the membrane structure (Le-Clech et al., 2006). This redistribution of flow is the basis of the local critical flux concept (Ognier et al., 2004).

The idea of a critical flux was first suggested in 1995 by Field and coworkers (Field et al., 2005). It is defined by the flux value below which a decline of flux with time does not occur. Above the critical flux, fouling is observed. Many methods have been developed to quantify the critical flux, for example relating deposition of particles to hydrodynamic conditions (Kwon and Vigneswaran, 1998) or observing deposition directly through the microscope (DOTM) (Kwon et al., 2000).
A method that was further refined by Le-Clech involves the step-wise increase of the flux while measuring the TMP (2003). In a strict sense, the critical flux is the flux below which the TMP stays constant in time. Although critical flux measurements do not give any insight into the membrane fouling mechanisms, it provides a tool in practical applications, for example

to select the proper membrane material (van der Marel et al., 2010). The local critical flux concept shows that, even when a constant flux below the critical flux is applied, the critical flux can be reached at a local scale. This results in the formation of deposits which induce an abrupt increase of the TMP.

Precipitation: the formation of a solid in a solution when the ion product (reflecting the concentrations of the ions) is above the solubility product.

The ion product can be influenced by chemical or biological conversions or physical processes (e.g. stripping of CO_2 from a solution). Precipitation may occur on the membrane surface or even inside the membrane due to high local concentrations, or precipitates can form from solution and then be transported to the membrane. In both situations, the membrane may get fouled by pore blocking or narrowing, or by cake layer formation. The membrane fouling effect of precipitation is often referred to as "scaling". Although both organic (e.g. proteins) and inorganic compounds may precipitate, the term is mostly used for inorganic substances. Scaling often occurs in RO sytems. Antiscalants are dosed to the feed solution to increase the threshold for scaling and allow a higher water recovery by inhibiting the ordering stage and/or growth stage during crystallization (Antony et al., 2011).

Concerning membrane bioreactors, precipitation that causes membrane fouling is often found in anaerobic systems. The compound that causes severe membrane fouling in anaerobic MBRs is struvite $(NH_4)MgPO_4 \cdot (6H_2O)$ (Choo and Lee, 1996; Kang et al., 2002). Also, deposition of calcium carbonate crystals was suggested to cause membrane fouling in a denitrifying MBR, which was operated at pH values between 8 and 9 (Ognier et al., 2002).
Although precipitation causes membrane fouling in aerobic MBR systems as well, it has not been described in literature extensively. Cicek et al. reported deterioration of ceramic aerobic MBR performance by crystals upon application of shock loads of phosphate (1999). In another study, wastewater treated anaerobically was sent to aerobic submerged and side-stream MBRs. The submerged MBR showed significant $CaCO_3$ scaling upon spiking with $CaCl_2$. The $CaCO_3$ precipitation was induced by a rise in pH (to approx. 8.2-8.5) upon stripping of CO_2 from the liquid phase by aeration (You et al., 2006).

Pore narrowing: partly obstruction of the pore by particles which are considerably smaller than the pore size.

Pore narrowing is important in the presence of particles in the mixed feed with a particle diameter smaller than pore size. Pore narrowing is most often associated with adhesion (Bhattacharjee and Hong, 2005), but may also be caused by other mechanisms like

precipitation on the pore walls. Pore narrowing decreases the effective pore diameter, which was shown to result in a flux decline and higher solute rejection (Clark et al., 1991). Because pore narrowing, in modeling work often referred to as “pore constriction”, is one of the mechanisms in the classical filtration models, it has been modeled extensively. It can be of importance in MBRs due to the wide particle size distribution in the bioreactor mixed liquor (van den Brink et al., 2011), and especially at the start-up period when the membrane is still clean.

Pore blocking: obstruction of the pore by particles in the range of the pore size

Pore blocking is important for particles with a diameter in the same range as the pore size. In most membrane filtrations, the particles to be retained by the membrane are larger than the pore size. Because of the broad pore size distribution of commercially available membranes (Bowen et al., 1997) in combination with the large particle size distribution in MBR mixed liquor (van den Brink et al., 2011), a certain fraction of the particles in the MBR mixed liquor can enter the pores.
Pore blocking is an important process during the initial start-up of a membrane filtration (Bhattacharjee and Hong, 2005). Once a pore is blocked, this results in a reduction of the overall flux of the membrane or (depending on the operation mode) an increase in TMP. Because the flow through a pore is proportional to the 4nd power of the pore radius according to the Hagen-Poiseuille equation (assuming cylindrical pores capillaries perpendicular to the face of the membrane), large pores have the biggest share of the permeate flux (Bhattacharjee and Hong, 2005). In case such large pores are blocked, the resistance increases very fast causing a TMP jump during fixed flux operation. Pore blocking may be preceded by precipitation or pore narrowing. Pore blocking is one of the fouling mechanisms that is most often taken into account in modeling.

Cake layer formation: deposition of particles on the membrane surface

Cake layer formation is a reversible process (Lindau et al., 1995; Maartens et al., 1998), unless coagulation or aggregation of the particles with the existing fouling occurs (Le-Clech et al., 2006). The cake layer can be removed by several methods, which will be further discussed in the paragraph on fouling control.

Generally, cake layer formation is considered the most dominant mechanism in long term membrane fouling (Belfort et al., 1994; Song, 1998). If the diameter of a particle in the bulk solution is larger than the pore size, it is retained by the membrane and deposits on the membrane surface, thereby forming a cake layer (Bhattacharjee and Hong, 2005). The cake

layer adds an increasing resistance to the flow and causes a decline in permeate flux. In dead-end filtration, with the fluid flow perpendicular to the membrane surface, the cake grows until the filtration is stopped (Belfort et al., 1994). In cross-flow filtration the tangential fluid flow limits cake layer growth (Schmitz et al., 1992), allowing for operation at higher fluxes.

The propensity of a particle to deposit on the membrane as a stationary cake layer can be predicted by adding up all individual force components acting on the particle (Fu and Dempsey, 1998). These force components can be grouped in hydrodynamic interactions resulting from the relative motion of the solvent with respect to the colloidal particle and various thermodynamic forces including interparticle and membrane-particle interactions (Bhattacharjee and Hong, 2005). The hydrodynamic forces influencing cake layer formation are:

1. Permeation drag (normal to membrane surface)
2. Gravitational (for particles with diameter > 10 µm)
3. Brownian (diffusion from cake to bulk solution)
4. Inertial lift (between particles and flow boundary)

The magnitudes of the first four forces as a function of the particle size are shown in Figure 1.5. Interparticle interactions are independent of the particles size and mentioned as “colloidal forces” in the same graph. Gravity and inertial and lift forces are negligible for colloidal particles. Inertial lift forces become more important for larger particles and when operating at high cross flow velocities (Altmann and Ripperger, 1997). The forces shown in this Figure are calculated for a flow velocity in the pore of $2*10^{-5}$ m s^{-1}, which corresponds to a flux of 21.60 L m^{-2} h^{-1} assuming a membrane porosity of 30%. The intersection of the curves for Brownian forces and permeation drag defines the particle size above which particles will deposit. In Figure 1.5, the intersection gives a critical particle size of 100-200 nm, which is in the range of the pore size of microfiltration/ultrafiltration membranes (Table 1.1). At higher fluxes, the permeation drag increases, causing this intersection to shift to the left and smaller particles to deposit.

An interesting phenomenon is the formation of a secondary or dynamic membrane layer, which results in an increased rejection compared to the original cut-off of the membrane (Choi et al., 2006), and increased reversibility of the fouling layer (Wu et al., 2008a). Dynamic membranes can be categorized in two groups: precoated and self-forming (Meng et al., 2009). Many efforts were undertaken to induce the formation of a dynamic membrane by for example using kaolinite suspensions (Li et al., 2006), starting up at a high flux (60 L m^{-2} h^{-1}) for 1-2 min, followed by a lower flux (Wu et al., 2008a) and by applying a 100 µm mesh instead of a microfiltration membrane (Fan and Huang, 2002). These first studies each

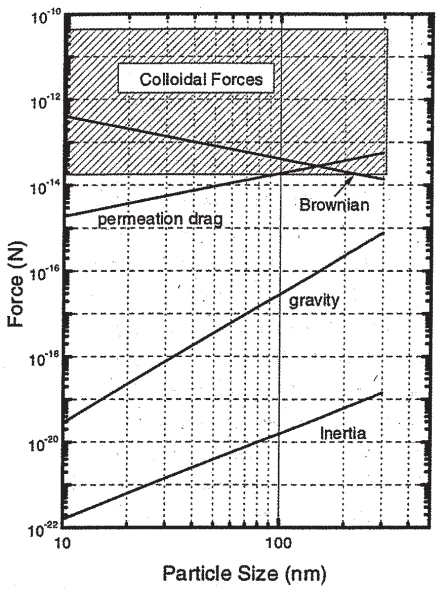

Figure 1.5 Magnitudes of physico-chemical forces acting on a colloidal particle during membrane filtration as function of its particle size (Bhattacharjee and Hong, 2005).

show different promising results, such as increased rejection, permeability or reversibility of the fouling layer. Increased retention could help to improve effluent quality. Because also contradictory results have been reported (Metzger et al., 2007; Wu et al., 2008b), more research should be performed to properly estimate the potential of this fouling control strategy. The review by Meng et al. gives a more extensive overview of the work done in this field (2009).

Biofilm formation: the formation of a complex aggregation of microorganisms marked by the excretion of a protective and adhesive matrix.

Although in some systems the biofilm is formed on purpose (e.g. trickling filters and rotating biological contactors), often biofilm formation has a negative effect on process performance (Characklis et al., 1982). A few examples of systems that suffer from biofilm formation are heat exchangers, cooling towers, drinking water distribution systems, and ion exchange and membrane processes (Characklis et al., 1982). Most literature on biofilms in relation with membrane filtration processes is on reverse osmosis membranes. In case biofilm formation creates an operational problem, in the sense that a higher pressure drop is needed to produce the same permeate flux, it is called “biofouling”. Biofouling is referred to as the unwanted deposition and growth of biofilms (Flemming, 2002).
Recently, biofilm formation, and associated EPS production, has gained attention as an

important fouling mechanism in membrane bioreactors as well (Ng et al., 2006; Zhang et al., 2006; Miura et al., 2007; Huang et al., 2008). Because characteristic times of biofilm formation are reported to be as long as weeks or months, depending on the conditions in the membrane process (Al-Ahmad et al., 2000), biofilm growth might be responsible for long-term membrane fouling effects. One important factor that influences biofilm formation is the availability of (easily) biodegradable compounds at the membrane surface in case the membrane is placed in an ideally mixed bioreactor. There is also sufficient oxygen present for microbial growth as aeration is used for both the biological process and membrane cleaning. Another important factor is the hydrodynamics of the system. Shear stress was shown to increase biofilm density (Characklis et al., 1982), and the hydrodynamics are one of the key factors that determine the structure in which a biofilm develops (van Loosdrecht et al., 1997; Ohl et al., 2004; Vrouwenvelder et al., 2010). Other factors that influence biofilm formation are temperature, pH, roughness of the membrane, presence of particulates (that may be entrapped) and the effectivity of biofouling control measures (Cloete et al., 1992). Several studies were performed to identify the microbial communities on membranes and to study colonization of the membranes by bacteria in MBRs (Chen et al., 2004; Jin et al., 2006; Jinhua et al., 2006; Ng et al., 2006; Zhang et al., 2006; Miura et al., 2007; Huang et al., 2008; Lee et al., 2009). Microbial communities in the biofilm were found to be different from those in the activated sludge. Some phylogenetic groups of bacteria may play a key role in early biofilm development.

Gel layer formation: formation of a highly swollen fouling layer comprising a three-dimensional network structure residing at the surface of a membrane.

The attention for gel layer formation as fouling mechanism is a rather recent development and therefore the amount of research papers on this topic is limited. Gel layers are formed at sub-critical fluxes (fluxes that stay constant in time) and are different from cake layers (Wang et al., 2008; van der Marel et al., 2010). Cake layers are removable by for example (chemically enhanced) backwashing, while gel layers can only be removed by thorough off-line cleaning of the membranes (Le-Clech et al., 2006; Wang et al., 2008; van der Marel et al., 2010). The composition of this gel layer still is largely unknown (Wang et al., 2008). Gel layers may be formed by solidification from the solution when the critical gel concentration is reached (Wijmans et al., 1984), by transport from the bulk solution, or by production by bacteria in the biofilm (Chang and Lee, 1998; Skillman et al., 1999; Sutherland, 2001). In the last case, the gel layer formation is a part of biofilm growth.

Membrane fouling in MBR systems is often ascribed to one or more of the before-mentioned mechanisms. However, no studies have been done for MBRs in which experimental

membrane fouling is compared with the theory describing the fouling mechanisms. The complex nature of the mixed liquid in the MBR makes this a very difficult task, with many different types of compounds that may influence each other's fouling behavior, resulting in unexpected and rapid changes in fouling (Le-Clech et al., 2006), and also have different interactions with the membrane surface. Studying membrane fouling mechanisms in detail with model compounds can help to better understand the overall fouling process.

Fouling control

Membrane fouling is a complex phenomenon in which many parameters are involved. It is therefore important to understand the fouling mechanisms when developing fouling control strategies. Because membrane fouling increases with flux, the operating flux should be below the critical flux (Field et al., 1995). However, because some fouling mechanisms (e.g. adhesion) are flux-independent, fouling occurs already at sub-critical conditions. Fouling control strategies can be categorized in two main groups: fouling removal and fouling limitation. Because controlling of membrane fouling is necessary for the widespread application of membrane bioreactor and membrane filtration in general, many research projects have been devoted to investigation, modeling and control of membrane fouling processes (Chang et al., 2002). A short overview of the main fouling control strategies is provided below.

Fouling removal

Usually several of the cleaning methods are used in combination:

Intermittent permeation (also called: membrane relaxation) was shown to be an effective technique for fouling control (Howell et al., 2004). During membrane relaxation, deposited particles can be removed by the crossflow. Application of intermittent permeations can significantly improve productivity (Yamamoto et al., 1989), and is a rather established operation mode by now.

Permeate backwashing and chemical cleaning are other commonly used techniques to minimize fouling of membranes (Judd, 2005). Backwashing can be performed with permeate (Bouhabila et al., 2001), possibly containing chemicals (chemically enhanced backwash, CEB) (Le-Clech et al., 2006) and with air (Visvanathan et al., 1997). Chemical cleaning is often a combination of maintenance cleaning at a regular basis (e.g. weekly) and intensive or recovery cleaning once or twice a year (Le-Clech et al., 2006). These techniques result in lower net filtration efficiency and damage the membrane (Wintgens et al., 2003; Le-Clech et al., 2006).

Fouling limitation

Three strategies methods to limit fouling are (1) optimization of operating conditions, (2) membrane surface modification and, (3) biomass pre-treatment. The most important studies are discussed below:

Optimization of operating conditions

In aerobic MBRs, aeration is used for both the biological process and to induce flow circulation and shear stress on the membrane surface. Different bubble sizes are needed for each process: fine bubbles for providing oxygen to the activated sludge and coarse bubbles for fouling limitation. Coarse bubbles have a scouring effect on the membrane surface which limits the buildup of a cake layer (Cicek, 2003; Judd, 2005). The air bubbles create shear stress on the membrane surface, thereby promoting back transport of particles (Liu et al., 2000). This results in an increase of the critical flux.

Membrane surface modification

Membrane surface modification could be another way to control membrane fouling. Several membrane properties are known to influence fouling during the start-up of MBRs: roughness, hydrophobicity, surface charge, pore structure and pore size (Chang et al., 2002). Pore sizes used in MBRs range from 0.04 to 5 µm, although pore sizes larger than 1 µm are exceptions (Stephenson et al., 2000). Because the interactions between solutes, microbial cells and the membrane material are hydrophobic, hydrophobic membranes are expected to show worse filtration behaviour than hydrophilic membranes (Madaeni et al., 1999; Yu et al., 2005). Improved filtration performances concerning remaining flux after fouling and recovery after cleaning were found in a submerged MBR for acrylic acid-grafted membranes and for non-polymeric NH_3 and CO_2 plasma treated membranes. The surface-grafted membranes showed better filtration performances than the plasma-treated membranes (Yu et al., 2008).

However, the effect of hydrophobicity of the membrane is most likely only playing a role during the first stages of filtration. Thereafter, a fouling layer has formed on the membrane which is covering the membrane surface properties and governing the interactions with the bulk liquid (Le-Clech et al., 2006). Roughness was also suggested to affect membrane fouling, with ultrafiltration membranes with a higher roughness (produced by UV irradiation) showing a higher fouling tendency (Pieracci et al., 1999).

Biomass pre-treatment

Rather recently, some new strategies came up, such as addition of powdered activated carbon (PAC) to strengthen the sludge flocs (Remy et al., 2009), coagulants or flocculants such as alum (Holbrook et al., 2004) or ferric chloride and zeolite (Lee et al., 2001), or flux

enhancers such as starch and the cationic polymers MPE50 and KD 452 (Iversen et al., 2009). Generally, flux enhancement has been found in short term experiments, while the positive effect of PAC on filterability was found in a pilot plant treating municipal wastewater for several months. This beneficial effect of PAC addition was explained by improved strength of the sludge floc (Remy et al., 2010), but other effects could play a role as well, such as creating a more open cake layer or adsorption of foulants. For all additives, the environmental impact of these compounds, their effect on the biomass and their costs should be considered and balanced against their positive effect of permeability increase.

Table 1.2 summarizes the discussed membrane fouling mechanisms based on their fouling rate, time constants and associated fouling control technique. The time constants can be very different for the same mechanisms. This is partly due to their dependency on the properties of the feed stream (type of particle(s), particle concentration), the operating conditions such as the shear and imposed flux, on membrane properties and on module configuration and plant design. Moreover, the definition of the characteristic time is rather arbitrary. For example, Song reports characteristic times for pore blocking and cake formation at 99% blocking and 99% flux reduction, respectively (1998), while Duclos-Orsello et al. apply flux reduction values of 37% (pore blockage), 25% (pore constriction) and resistance ratio of cake layer to membrane of 0.73 (2006).

Table 1.2 Comparison membrane fouling mechanisms.

Mechanism	Fouling rate (mbar min^{-1})	Time constant	Fouling control technique	Reference
Adhesion	n/a	minutes/hours	Surface modification	Sweity, 2011
Precipitation	0.06-0.5	days/weeks	Aeration, chemical cleaning	You, 2006
Biofilm formation	0.01-0.1	weeks/months	Chemical cleaning	Al-Ahmad, 2000
Cake layer formation	n/a	5.94-9.46 min*	Backwashing, relaxation, aeration	Duclos-Orsello, 2006
Gel layer formation	1-10	hours/days	Chemical cleaning	van der Marel, 2010

* Values for 1 g L^{-1} BSA microfiltration (9.46) and 0.00025% polysterene microspheres (5.94).

In general, all fouling control techniques presented above contribute to minimizing fouling development to some extent. All of them involve cost increases, because of more frequent membrane replacement (chemical/physical cleaning), decreasing capacity leading to requirement of higher installed membrane areas (backflushing, intermittent permeation, operation below critical flux), higher energy (increasing aeration), operating costs (use of additives), or membrane investment costs (surface modification). To come to a better prediction of membrane fouling and to identify possible solutions, it is necessary to identify which fouling mechanisms are playing a dominant role in MBRs.
In addition, the location of fouling needs to be known on the micro-level (outside of the

membrane, inside the pores, permeate side) as this defines which prevention or control method could be suitable. Development of (in situ) measurement techniques and/or micro scale modeling can support this search.

OBJECTIVE AND OUTLINE OF THE THESIS

The objective of this thesis is to get more insight in the membrane fouling mechanisms that are of importance in membrane bioreactors. Extracellular polymeric substances (EPS) play a major role during fouling development. Specific attention is paid to gel layer and biofilm formation in relation to the bioreactor mixed liquor composition and the possibility to remove gel layers by harsh mechanical cleaning. The microbial composition of the fouling layers as well as the effect of temperature on gel layer formation is investigated. Combined cake and gel layer formation is also subject of study.

In **chapter 2**, alginate is used as a model compound to simulate fouling by polysaccharides, which are the main constituents of EPS. Polysaccharides are known to play an important role in membrane fouling. The effect of water chemistry of alginate feed solution (calcium concentration, foulant concentration and ionic strength) on fouling rate and reversibility was studied in flux step experiments. There was a strong relation between calcium concentration and fouling rate. An increased ionic strength had no impact on fouling rate in low fouling experiments, but decreased fouling with 66–72% at high fouling conditions. Reversibility of the fouling decreased with increasing calcium concentrations to values as low as 3%.

The interaction between fouling by particles and gel formation was studied in **chapter 3**. Membranes fouled by alginate gels or by gels formed in an MBR treating municipal wastewater show increased retention for particles. Increased retention for particles was also observed when particles and alginate were filtered simultaneously. Comparing filtration times and plateau values for alginate with and without particles, alginate plus particles fouls more than the sole alginate solution.

In **chapter 4**, harsh mechanical cleaning was applied on membranes operated at different relatively low fluxes to evaluate how much fouling could be maximally removed and distribution of remaining fouling was investigated. Even after harsh mechanical cleaning, membrane samples showed considerable oxygen consumption. No fouling was observed inside the membrane. Of several membranes operated for at least 1 year, the permeate side was covered with bacteria and extracellular polymeric substances (EPS). This fouling on the permeate side should not be neglected when designing membrane cleaning.

In **Chapter 5**, the community structure and dynamics of sludge fractions in an MBR treating municipal wastewater were compared with those of the wastewater and membrane biofilms using cultivation independent molecular techniques. Constant flux filtrations were performed and samples were taken at three different dates. Denaturating gradient gel electrophoreses (DGGE) and sequence analysis revealed a high bacterial diversity in the wastewater, sludge fractions and membrane biofilms. An increase in diversity was shown in the following order: wastewater < mixed liquor supernatant < mixed liquor < membrane biofilm. No higher similarity of biofilm communities with one specific other MBR fraction was observed. The bacterial communities in the wastewater, sludge fractions and membrane biofilms were time variable. Only at higher biofilms ages, a clear effect of biofilm age on biofilm communities was observed: communities, distinct from those in wastewater and sludge fractions, developed at higher biofilm ages. This indicates occurrence of active bacterial growth on the membrane. No effect of flux on bacterial diversity of the biofilms could be observed and few bacterial genera could be removed by harsh mechanical cleaning.

Chapter 6 describes the effect of temperature shocks on membrane fouling in membrane bioreactors. Flux step experiments were performed in an experimental system at 7, 15, and 25°C with sludge that was continuously recirculated from a pilot-scale MBR. Higher membrane fouling rates were obtained for the lower temperature in combination with low fouling reversibility. At low temperature, a high polysaccharide concentration was found in the mixed liquor supernatant of the experimental system as compared to the MBR pilot. Upon decreasing the temperature of the mixed liquor, a shift was found in particle size in the mixed liquor supernatant towards smaller particles. These results show that the release of polysaccharides and/or submicron particles from sludge flocs could explain the increased membrane fouling at low temperatures.

The main results and conclusions presented in this thesis are summarized in **chapter 7**. The origin of EPS in MBRs is discussed and an overview is given of EPS measuring methods and their restrictions. In this chapter also practical implications of EPS fouling in MBRs are mentioned and suggestions for further research are provided.

REFERENCES

Al-Ahmad M, Abdul Aleem FA, Mutiri A, Ubaisy A (2000) Biofouling in RO membrane systems. Part 1: Fundamentals and control *Desalination* **132** (1-3), 173-179

Altmann J, Ripperger S, (1997) Particle deposition and layer formation at the crossflow microfiltration *J. Membrane Sci.* **124** (1), 119 -128

Antony A, Low JH, Gray S, Childress AE, Le-Clech P, Leslie, G (2011) Scale formation and control in high pressure membrane water treatment systems: A review *J. Membrane Sci.* **383** (1-2), 1-16

Baker RW (2000) Membrane technology and applications McGraw-Hill, New York, USA

Barnes GT, Gentle IR (2005) Interfacial science - an introduction Oxford University Press, New York, USA

Belfort G, Davis RH, Zydney AL (1994) The behavior of suspensions and macromolecular solutions in crossflow microfiltration *J. Membrane Sci.* **96** (1-2), 1-58

Bhattacharjee S, Hong S (2005) Fundamentals of particle fouling in membrane processes *Korean Membrane J.* **7** (1), 1-18

Bouhabila EH, Ben Aim R, Buisson H (2001) Fouling characterization in membrane bioreactors *Sep. Purif. Technol.* **22-23**, 123-132

Bowen WR, Hilal N, Lovitt RW, Sharif AO, Williams PM (1997) Atomic force microscope studies of membranes: Force measurement and imaging in electrolyte solutions *J. Membrane Sci.* **126** (1), 77-89

Characklis WG, Trulear MG, Bryers JD, Zelver N (1982) Dynamics of biofilm processes: methods *Water Res.* **16** (7), 1207 -1216

Chang IS, Lee CH (1998) Membrane filtration characteristics in membrane coupled activated sludge system—the effect of physiological states of activated sludge on membrane fouling *Desalination* **120** (3), 221–233

Chang IS, Le-Clech P, Jefferson B, Judd SJ (2002) Membrane fouling in membrane bioreactors for wastewater treatment *J. Environ. Eng.* **128** (11), 1018-1029

Chen CL, Liu WT, Chong ML, Wong MT, Ong SL, Seah H, Ng WJ (2004) Community structure of microbial biofilms associated with membrane-based water purification processes as revealed using a polyphasic approach *Appl. Microbiol. Biotechnol.* **63** (4), 466-473

Choi H, Zhang K, Dionysiou DD, Oerther DB, Sorial GA (2006) Effect of activated sludge properties and membrane operation conditions on fouling characteristics in membrane bioreactors *Chemosphere* **63** (10), 1699-1708

Choo KH, Lee CH (1996) Membrane fouling mechanisms in the membrane-coupled anaerobic bioreactor *Water Res.* **30** (8), 1771-1780

Cicek N (2003) A review of membrane bioreactors and their potential application in the treatment of agricultural wastewater *Can. Biosystems Eng.* **45**, 6.37-6.49

Cicek N, Dionysiou D, Suidan MT, Ginestet P, Audic JM (1999) Performance deterioration and structural changes of a ceramic membrane bioreactor due to inorganic abrasion. *J. Membrane Sci.* **163** (1), 19-28

Clark WM, Bansal A, Sontakke M, Ma YH (1991) Protein adsorption and fouling in ceramic ultrafiltration membranes *J. Membrane Sci.* **55** (1-2), 21-38

Cloete TE, Brozel VS, Holy AV (1992) Practical aspects of biofouling control in industrial water systems *Int. Biodeter. Biodegr.* **29** (3-4), 299-341

Defrance L, Jaffrin MY, Gupta B, Paullier P, Geaugey V (2000) Contribution of various constituents of activated sludge to membrane bioreactor fouling *Bioresource Technol.* **73** (2), 105-122

De Luca G, Sacchetti R, Leoni E, Zanetti F (2012) Removal of indicator bacteriophages from municipal wastewater by a full-scale membrane bioreactor and a conventional activated sludge process: Implications to water reuse *Bioresource Technol.* **129**, 526-531

Drews A (2010) Membrane fouling in membrane bioreactors - Characterisation, contradictions, cause and cures *J. Membrane Sci.* **363** (1-2), 1-28

Duclos-Orsello C, Li W, Ho CC (2006) A three mechanism model to describe fouling of microfiltration membranes *J. Membrane Sci.* **280** (1-2), 856-866

Fan B, Huang X (2002) Characteristics of a self-forming dynamic membrane coupled with a bioreactor for municipal wastewater treatment *Environ. Sci. Technol.* **36** (23), 4245-4251

Fenu A, Roels J, Wambecq T, De Gussem K, Thoeye C, De Gueldre G, Van De Steene B (2010) Energy audit of a full scale MBR system *Desalination* **262** (1-3) 121–128

Field RW, Wu D, Howell JA, Gupta BB (1995) Critical flux concept for microfiltration fouling *J. Membrane Sci.* **100** (3), 259-272

Flemming HC (2002) Biofouling in water systems - Cases, causes and countermeasures *Appl. Microbiol. Biotechnol.* **59** (6), 629-640

Francy DS, Stelzer EA, Bushon RN, Brady AM, Williston AG, Riddell KR, Borchardt MA, Spencer SK, Gellner TM (2012) Comparative effectiveness of membrane bioreactor, conventional secondary treatment, and chlorine and UV disinfection to remove microorganisms from municipal wastewater *Water Res.* **46** (13), 4164–4178

Fu LF, Dempsey BA (1998) Modelling the effect of particle size and charge on the structure of the filter cake in ultrafiltration *J. Membrane Sci.* **149** (2) 221-240

Gander MA, Jefferson B, Judd SJ (2000) Aerobic MBRs for domestic wastewater treatment: a review with cost considerations *Sep. Purif. Technol.* **18** (2), 119–130

Hai FI, Yamamoto K (2001) Membrane Biological Reactors. In P. Wilderer (Eds.), Treatise on Water Science (pp. 571-613), Elsevier, UK.

Henze M, van Loosdrecht MCM, Ekama GA, Brdjanovic D (2008) Biological Wastewater Treatment: Principles, Modeling, and Design, IWA Publishing, London, UK.

Holbrook RD, Higgins MJ, Murthy SN, Fonseca AD, Fleischer EJ, Daigger GT, Grizzard TJ, Love NG, Novak JT (2004) Effect of alum addition on the performance of submerged membranes for wastewater treatment *Water Environ. Res*. **76** (7), 2699-2702

Howell JA, Chua HC, Arnot TC (2004) In situ manipulation of critical flux in a submerged membrane bioreactor using variable aeration rates, and effects of membrane history *J. Membrane Sci.* **242** (1-2), 13–19

Huang X, Gui P, Qian Y (2001) Effect of sludge retention time on microbial behaviour in a submerged membrane bioreactor *Process Biochem.* **36** (10), 1001-1006

Huang LN, de Wever H, Diels L (2008) Diverse and distinct bacterial communities induced biofilm fouling in membrane bioreactors operated under different conditions *Environ. Sci. Technol.* **42** (22), 8360–8366

Iversen V, Koseoglu H, Yigit NO, Drews A, Kitis M, Lesjean B, Kraume M (2009) Impacts of membrane flux enhancers on activated sludge respiration and nutrient removal in MBRs *Water Res.* **43** (3), 822-830

Jin YL, Lee WN, Lee CH, Chang IS, Huang X, Swaminathan T (2006) Effect of DO concentration on biofilm structure and membrane filterability in submerged membrane bioreactor *Water Res.* **40** (15), 2829-2836

Jinhua P, Fukushi K, Yamamoto K (2006 Bacterial community structure on membrane surface and characteristics of strains isolated from membrane surface in submerged membrane bioreactor *Separ. Sci. Technol.* **41** (7), 1527-1549

Judd SJ (2005) Fouling control in submerged membrane bioreactors *Water Sci. Technol.* **51** (6-7), 27-34

Judd SJ (2006) The MBR Book: Principles & Applications of MBRs in Water & Wastewater Treatment, Elsevier, Oxford, UK

Judd SJ, Judd C (2010) The MBR Book (2nd ed.): Principles and applications of membrane bioreactors in water and wastewater treatment, Elsevier, Oxford, UK

Kang IJ, Yoon SH, Lee CH (2002) Comparison of the filtration characteristics of organic and inorganic membranes in a membrane-coupled anaerobic bioreactor *Water Res.* **36** (7), 1803-1813

Kim IS, Jang N (2006) The effect of calcium on the membrane biofouling in the membrane bioreactor (MBR) *Water Res.* **40** (14), 2756-2764

Koros WJ, Ma YH, Shimizu T (1996) Terminology for membranes and membrane processes. IUPAC recommendations *J. Membrane Sci.* **120** (2), 149-159

Kwon DY, Vigneswaran S (1998) Influence of particle size and surface charge on critical flux of crossflow microfiltration *Water Sci. Technol.* **38** (4-5), 481-488

Kwon DY, Vigneswaran S, Fane AG, Ben Aim R (2000) Experimental determination of critical flux in cross-flow microfiltration *Sep. Purif. Technol.* **19** (3), 169-181

Le-Clech P, Jefferson B, Chang IS, Judd SJ (2003) Critical flux determination by the flux-step method in a submerged membrane bioreactor *J. Membrane Sci.* **227** (1-2), 81-93

Le-Clech P, Chen V, Fane AG (2006) Fouling in membrane bioreactors used in wastewater treatment – A review *J. Membrane Sci.* **284** (1-2), 17-53

Le-Clech P (2010) Membrane bioreactors and their uses in wastewater treatments *Appl. Microbiol. Biotechnol.* **88** (6), 1253-1260

Lee WN, Cheong WS, Yeon KM, Hwang BK, Lee CH (2009) Correlation between local TMP distribution and bio-cake porosity on the membrane in a submerged MBR *J. Membrane Sci.* **332** (1-2), 50-55

Lee JC, Kim JS, Kang IJ, Cho MH, Park PK, Lee CH (2001) Potential and limitations of alum or zeolite addition to improve the performance of a submerged membrane bioreactor *Water Sci. Technol.* **43** (11), 59-66

Le Gouellec YA, Elimelech M (2002) Calcium sulfate (gypsum) scaling in nanofiltration of agricultural drainage water *J. Membrane Sci.* **205** (1-2), 279–291

Lesjean B, Huisjes EH (2008) Survey of the European MBR market, trends and perspectives *Desalination* **231** (1-3), 71-81

Lesjean B, Rosenberger S, Schrotter JC, Recherche A (2004) Membrane-aided biological wastewater treatment – an overview of applied systems *Membrane Technol.* **2004** (8), 5-10

Li F, Chen J, Deng C (2006) The kinetics of crossflow dynamic membrane bioreactor *Water SA* **32** (2), 199-204

Lindau J, Jönsson AS, Wimmerstedt R (1995) The influence of a low-molecular hydrophobic solute on the flux of polysulfone ultrafiltration membranes with different cutoff *J. Membrane Sci.* **106** (1-2), 9-16

Liu R, Huang X, Wang C, Chen L, Qian Y (2000) Study on hydraulic characteristics in a submerged membrane bioreactor process *Process Biochem.* **36** (3), 249-254

Maartens A, Swart P, Jacobs EP (1998) Humic membrane foulants in natural brown water – characterization and removal *Desalination* **115** (3), 215-227

Madaeni SS, Fane AG, Wiley D (1999) Factors influencing critical flux in membrane filtration of activated sludge *J. Chem. Technol. Biot.* **74** (6), 539-543

Marti E, Monclús H, Jofre J, Rodriguez-Roda I, Comas J, Balcázar JL (2011) Removal of microbial indicators from municipal wastewater by a membrane bioreactor (MBR) *Bioresource Technol.* **102** (8), 5004-5009

Melin T, Jefferson B, Bixio D, Thoeye C, de Wilde W, de Koning J, van der Graaf J, Wintgens T (2006) Membrane bioreactor technology for wastewater treatment and reuse *Desalination* **187** (1-3), 271-282

Meng F, Chae SR, Drews A, Kraume M, Shin HS, Yang F (2009) Recent advances in membrane bioreactors (MBRs): Membrane fouling and membrane material *Water Res.* **43** (6), 1489-1512

Metcalf and Eddy, Inc. (2003) Wastewater Engineering, Treatment and Reuse, 4th Int. Ed., McGraw Hill Education, New York, USA

Metzger U, Le-Clech P, Stuetz RM, Frimmel FH, Chen V (2007) Characterisation of polymeric fouling in membrane bioreactors and the effect of different filtration modes *J. Membrane Sci.* **301** (1-2), 180-189

Miura Y, Watanabe Y, Okabe S (2007) Membrane biofouling in pilot-scale membrane bioreactors (MBRs) treating municipal wastewater: impact of biofilm formation *Environ. Sci. Technol.* **41** (2), 632-638

Mulder M (1996) Basic principles of membrane technology. Kluwer Academic Publishers, Dordrecht, the Netherlands

Ng HY, Tan TW, Ong SL (2006) Membrane fouling of submerged membrane bioreactors: impact of mean cell residence time and the contributing factors *Environ. Sci. Technol.* **40** (8), 2706-2713

Ognier S, Wisniewski C, Grasmick A (2002) Characterisation and modelling of fouling in membrane bioreactors *Desalination* **146** (1-3), 141-14.

Ognier S, Wisniewski C, Grasmick A (2004) Membrane bioreactor fouling in sub-critical filtration conditions: a local critical flux concept *J. Membrane Sci.* **229** (1-2), 171-177

Ohl AL, Horn H, Hempel DC (2004) Behaviour of biofilm systems under varying hydrodynamic conditions *Water Sci. Tech.* **49** (11-12), 345-351

Ohlinger KN, Young TM, Schroeder ED (1998) Predicting struvite formation in digestion *Water Res.* **32** (12), 3607-3614

Pieracci J, Crivello JV, Belfort G (1999) Photochemical modification of 10 kDa polyethersulfone ultrafiltration membranes for reduction of biofouling *J. Membrane Sci.* **156** (2), 223-240

Qin JJ, Kekre KA, Tao G, Oo MH, Wai MN, Lee TC, Viswanath B, Seah H (2006) New option of MBR-RO process for production or NEWater from domestic sewage *J. Membrane Sci.* **272** (1-2), 70-77

Remy M, Potier V, Temmink H, Rulkens W (2010) Why low powdered activated carbon addition reduces membrane fouling in MBRs *Water Res.* **44** (3), 861-867

Remy M (2012) Low concentration of powdered activated carbon decreases fouling in membrane bioreactors. PhD thesis, Wageningen University, the Netherlands

Remy M, van der Marel P, Zwijnenburg A, Rulkens W, Temmink H (2009 Low dose powdered activated carbon addition at high sludge retention times to reduce fouling in membrane bioreactors *Water Res.* **43** (2), 345-350

Schmitz P, Houi D, Wandelt B (1992) Hydrodynamic aspects of cross-flow microfiltration – Analysis of particle deposition at the membrane surface *J. Membrane Sci.* **71** (1-2), 29-40

Schrader GA (2006) Direct nanofiltration of wastewater treatment plant effluent. PhD Thesis, University of Twente, Enschede, the Netherlands

Skillman L, Sutherland IW, Jonse MV (1999) The role of exopolysaccharides in dual species biofilm development *J. Appl. Microbiol*. **85** (28), 13S-18S

Song L (1998) Flux decline in crossflow microfiltration and ultrafiltration: mechanisms and modeling of membrane fouling *J. Membrane Sci.* **139** (2), 183-200

Stenstrom MK (2007) Measurement of oxygen transfer in clean water. American Society of Civil Engineers, Reston, USA

Stephenson T, Brindle K, Judd S, Jefferson B (2000) Membrane bioreactors for wastewater treatment. IWA Publishing, London, UK

Stocks-Fischer S, Galinat JK, Bang SS (1999) Microbiological precipitation of CaCO3 *Soil Biol. Biochem.* **31** (11), 1563-1571

Sutherland IW (2001) Exopolysaccharides in biofilms, flocs and related structures *Water Sci. Technol.* **43** (6), 77–86

Sweity A, Ying W, Belfer S, Oron G, Herzberg M (2011) pH effects on the adherence and fouling propensity of extracellular polymeric substances in a membrane bioreactor *J. Membrane Sci.* **378** (1-2), 186-193

van Bentem AGN, Petri CP, Schyns PFT (2007) Membrane bioreactors: Operation and results of a MBR wastewater treatment plant - STOWA Report, IWA publishing, ISBN: 1843391732

van den Brink P, Satpradit OA, van Bentem A, Zwijnenburg A, Temmink H, van Loosdrecht MCM (2011) Effect of temperature shocks on membrane fouling in membrane bioreactors *Water Res.* **45** (15), 4491-4500

van den Brink P, Vergeldt F, van As H, Zwijnenburg A, Temmink H, van Loosdrecht MCM (2013) Potential of mechanical cleaning of membranes from a membrane bioreactor *J. Membrane Sci.* **429**, 259-267

van der Marel P, Zwijnenburg A, Kemperman A, Wessling M, Temmink H, van der Meer W (2010) Influence of membrane properties on fouling in submerged membrane bioreactors *J. Membrane Sci.* **348** (1-2), 66-74

van Loosdrecht MCM, Picioreanu C, Heijnen JJ (1997) A more unifying hypothesis for biofilm structures *FEMS Microbiol. Ecol.* **24** (2), 181-183

van Nieuwenhuijzen AF, Evenblij H, Uijterlinde CA, Schulting FL (2008) Review on the state of science on membrane bioreactors for municipal wastewater treatment *Water Sci. Technol.* **57** (7), 979-986

Visvanathan C, Ben Aim R, Parameshwaran K (2000) Membrane separation bioreactors for wastewater treatment *Crit. Rev. Env. Sci. Tec*. **30** (1), 1-48

Visvanathan C, Byung-Soo Y, Muttamara S, Maythanukhraw R (1997) Application of air backflushing technique in membrane bioreactor *Water Sci. Technol.* **36** (12), 259-266

Vrouwenvelder JS, Buiter J, Riviere M, van der Meer WGJ, van Loosdrecht MCM, Kruithof JC (2010) Impact of flow regime on pressure drop increase and biomass accumulation and morphology in membrane systems *Water Res.* **44** (3), 689-702

Wang Z, Wu Z, Yin X, Tian L (2008) Membrane fouling in a submerged membrane bioreactor (MBR) under sub-critical flux operation: membrane foulant and gel layer characterization *J. Membrane Sci.* **325** (1), 238-244

Wintgens T, Rosen J, Melin T, Brepols C, Drensla K, Engelhardt N (2003) Modelling of a membrane bioreactor system for municipal wastewater treatment *J. Membrane Sci.* **216** (1-2), 55-65

Wijmans JG, Nakao S, Smolders CA (1984) Flux limitation in ultrafiltration: Osmotic pressure model and gel layer model *J. Membrane Sci.* **20** (2), 115-124

Wu J, Le-Clech P, Stuetz RM, Fane AG, Chen V (2008a) Novel filtration mode for fouling limitation in membrane bioreactors *Water Res.* **42** (14), 3677-3684

Wu J, Le-Clech P, Stuetz RM, Fane AG, Chen V (2008b) Effects of relaxation and backwashing conditions on fouling in membrane bioreactors *J. Membrane Sci.* **324** (1-2), 26-32

Yamamoto K, Hiasa H, Talat M, Matsuo T (1989) Direct solid liquid separation using hollow fiber membranes in activated sludge aeration tank *Water Sci. Technol.* **21** (4-5), 43-54

You HS, Huang CP, Pan JR, Chang SC (2006) Behavior of membrane scaling during crossflow filtration in the anaerobic MBR system *Separ. Sci. Technol.* **41** (7), 1265-1278.

Yu HY, Hu MX, Xu ZK, Wang JL, Wang SY (2005) Surface modification of polypropylene microporous membranes to improve their antifouling property in MBR: NH3 plasma treatment *Sep. Purif. Technol.* **45** (1), 8-15

Yu HY, Liu LQ, Tang ZQ, Yan MG, Gu JS, Wei XW (2008) Mitigated membrane fouling in an SMBR by surface modification *J. Membrane Sci.* **310** (1-2), 409-417

Zhang K, Choi H, Dionysiou DD, Sorial GA, Oerther DB (2006) Identifying pioneer bacterial species responsible for biofouling membrane bioreactors *Environ. Microbiol.* **8** (3), 433-440

Chapter 2

EFFECT OF FREE CALCIUM CONCENTRATION AND IONIC STRENGTH ON ALGINATE FOULING IN CROSS-FLOW MEMBRANE FILTRATION

This chapter has been published as:

van den Brink P, Zwijnenburg A, Smith G, Temmink H, van Loosdrecht MCM (2009) Effect of free calcium concentration and ionic strength on alginate fouling in cross-flow membrane filtration *J. Membrane Sci.* **345** (1-2), 207-216

ABSTRACT

Extracellular polymeric substances (EPS) are generally negatively charged polymers. Membrane fouling in membrane bioreactors (MBRs) by EPS is therefore influenced by the water chemistry of the mixed liquor (calcium concentration, foulant concentration and ionic strength). We used alginate as a model compound to study this fouling in detail. Flux-step experiments were performed with a flat sheet test cell, varying the free calcium concentration, total ionic strength and alginate concentration. There was a strong relation between calcium concentration and fouling rate. An increased ionic strength had no impact on fouling rate in low fouling experiments, but decreased fouling with 66 % to 72 % at high fouling conditions. Reversibility of the fouling decreased with increasing calcium concentrations to values as low as 3 %. Several fouling mechanisms were identified and the reducing effect of increased ionic strength on alginate fouling was explained by competition for carboxyl groups on the alginate polymer. Further research will focus on the interaction of polysaccharides with other compounds typically present in the MBR supernatant (e.g. proteins, humic acids and sludge particles) and a more detailed analysis of the fouling layer.

Key words: EPS fouling, cross-flow filtration, alginate, membrane bioreactor, water chemistry.

INTRODUCTION

Extracellular polymeric substances (EPS) have often been reported to be major foulants in membrane bioreactors (MBRs) (Chang et al., 2002; Shannon et al., 2008). The term "EPS" comprises several types of compounds, originating from the biomass: proteins, polysaccharides, nucleic acids, lipids and other polymeric substances (Bura et al., 1998; Flemming et al., 2001). Several fouling mechanisms were identified as important for fouling by EPS, such as adsorption and gel or cake layer formation (Ye et al., 2005b). Biofilm formation could also be of influence (Le-Clech et al., 2006; Yun et al., 2006; Miura et al., 2007), as bacteria actively excrete EPS. Recently, more attention was paid to gel layers, which are formed at sub-critical fluxes and are different from cake layers (Wang et al., 2008). Cake layers are removable by backwashing, while gel layers can only be removed by thorough off-line cleaning of the membranes. The composition of this gel layer is however still largely unknown (Wang et al., 2008). Because of their unknown composition and large effect on sub-critical fouling, it was decided to study gel layer formation with a model compound.

A model compound for polysaccharides was used because polysaccharides are reported to play a significant role in membrane fouling due to their wide molecular weight distributions as compared to proteins and being the main constituents of EPS (Ye et al., 2005b; Chu et al., 2004; Zhang et al., 2006). Moreover, a linear relation between the concentration of polysaccharides in the activated sludge supernatant (paper filtered mixed liquor) of a submerged membrane bioreactor and fouling rate was found in two pilot systems that were monitored for a period of 1 year (Rosenberger et al., 2005). Sodium alginate is the most commonly used model compound for polysaccharides, because it is an important microbial polysaccharide and it has been extensively studied (Mayer et al., 1999; Katsoufidou et al., 2007; Davis et al., 2008). Studies with sodium alginate were performed in dead-end (Katsoufidou et al., 2007; van de Ven et al., 2007) as well as in cross-flow filtration (Ye et al., 2005b).

In earlier experiments with alginate fouling performed in cross-flow filtration using micro- or ultrafiltration membranes, the water chemistry was not taken into account (Ye et al., 2005b; Nataraj et al., 2008). For many years, multivalent cations such as calcium and, to a lower extent, magnesium are known to act as "bridging agents" with alginate, forming highly compacted gels (Haug, 1961). A decade later, this complexation between polysaccharides and divalent cations was explained by the so-called "egg-box" model (Grant et al., 1973). Ca^{2+} ions may affect membrane fouling in MBRs in several ways, because these cations are involved in several processes taking place in the bioreactor: bioflocculation of the sludge according to the divalent cation bridging theory or the double layer or DLVO theory (Sobeck

and Higgins, 2002), formation of polysaccharide gels as described above, and inorganic fouling (Arabi and Nakhla, 2008). Although low SRT sludges were shown to contain lower metal concentrations (including calcium) than high SRT sludges, more metals were deposited when filtering the low SRT sludges (Al-Halbouni et al., 2008). Because these different processes are interrelated, it is difficult to study them individually in an MBR system. By isolating polysaccharide gel formation, the influence of Ca^{2+} on this process and membrane fouling can be tested. Wastewater may contain considerable amounts of free calcium as tap water can contain up to 2,5 mM, dependent on its source. Free calcium concentrations of 0,625 -1 mM were measured in the waste activated sludges of 6 different wastewater treatment plants treating domestic wastewater (Park et al., 2006) and other researchers reported typical calcium concentrations of 0.5-3 mM for municipal wastewaters (Arabi and Nakhla, 2008).

Although the effect is less pronounced than for free calcium ions that can act as bridging compounds, the total ionic strength of the solution was shown to promote alginate gel formation by compaction of the electric double layers on the membrane and the alginate molecule, which resulted in a lower electrostatic repulsion and a denser fouling layer with a higher absolute resistance according to the DLVO theory (van de Ven et al., 2007). More severe fouling was observed as well upon increasing the ionic strength with NaCl when studying alginate fouling on RO membranes (Lee and Elimelech, 2006).
In the experiments presented here, information was obtained on alginate gel layer formation by studying the rate of fouling build-up, fouling reversibility and retention. This was achieved with an improved flux step method, which was developed to test fouling reversibility and fouling rate (van der Marel et al., 2009). The main objectives of this study were to determine the influence of

1. free calcium concentration
2. ionic strength
3. membrane flux

on alginate fouling behaviour (fouling rates, reversibility) in a cross flow membrane filtration test cell. A cross flow test cell was chosen to be able to work at well defined operating conditions. Because no aeration was applied, the hydrodynamics were determined by the cross flow velocity. The results are discussed to get a better understanding of gel layer formation in MBRs, and to develop membrane fouling control strategies.

MATERIALS AND METHODS

Materials

Commercially available low viscosity sodium alginate with a molecular weight distribution between 80 and 120 kDa (Sigma) extracted from brown algae was used in all experiments. Thirty litres of feed solution were prepared by dissolving the required amount of sodium alginate, typically 10 ppm, in demineralised water while continuously stirring. The ionic strength was adjusted by adding KCl (Boom, the Netherlands). $CaCl_2 \cdot 2H_2O$ (Boom, the Netherlands) was added to set the calcium concentration. In one experiment ("No I"), no KCl was added and the total ionic strength was determined by the addition of $CaCl_2 \cdot 2H_2O$. Although pH was not adjusted, it remained approximately 7.4 in all experiments. The applied concentrations of free calcium and total ionic strength in the experiments agreed with alginate fouling experiments previously performed in dead-end mode by others (Katsoufidou et al., 2007; van de Ven et al., 2007). 10 ppm of alginate is a representative amount when compared to concentrations of polysaccharides found in the activated sludge liquid phase of three MBR pilot plants fed with municipal wastewater (Rosenberger et al., 2005; Evenblij et al., 2004)

Polycarbonate membranes (GE Osmonics, US) with an absolute pore size of 0.1 µm and nominal thickness of 6 µm were used in all experiments, because the authors wanted to focus on the effect of water chemistry on alginate fouling, and wished to exclude membrane-related factors like pore size distribution and interconnectivity between pores. The membrane was used in combination with polyester non-woven FO2416 as product spacer (Freudenberg, Germany). A new membrane was used for each experiment.

Filtration set-up

The experiments were performed in a typical cross-flow filtration test cell with an 800 µm high, 4 cm wide and 20 cm long flow channel (Vrouwenvelder et al., 2006). Feed solutions were stored in a 50 liter reservoir which was continuously stirred to prevent aggregate formation. Feed solution was transported to the test cell using a positive displacement pump (Hydra Cell, Wanner Engineering, US) and permeate was extracted with a peristaltic pump (Masterflex, Cole-Parmer, US). The concentrate was recirculated to the feed reservoir. A floating disk rotameter (Kobold, Germany) was used to monitor the concentrate flow rate. Temperature of the feed stream was continuously measured with a temperature probe (Pt 100, Kobold, Germany). Absolute pressure sensors (Endress+Hauser, Germany) measured the pressures at the feed and permeate side of the membrane and a differential pressure transducer (Endress+Hauser, Germany) was installed to measure the pressure drop over the feed channel of the test cell. The signals from the sensors (apart from the mass flow controllers) were logged by an Ecograph T datalogger from Endress+Hauser, Germany. The

transmembrane pressure (TMP) was calculated from the pressure data as follows:

$$TMP = (P_{feed} - (0.5\Delta P)) - P_{perm} \quad (1)$$

where P_{feed} is the absolute pressure of the feed stream (Pa), ΔP is the pressure drop over the feed channel (Pa) and P_{perm} is the absolute pressure of the permeate stream (Pa). The total resistance was calculated from the TMP, membrane flux and feed solution viscosity, according to the following expression:

$$R_t = TMP/(\eta J) \quad (2)$$

where R_t is total resistance (m^{-1}), η the feed solution viscosity (Pa s) and J the membrane flux ($m^3\ m^{-2}\ s^{-1}$) . A temperature correction was performed on the feed solution viscosity, according to the following relation (Roorda et al., 2001)

$$\mu = 0.497(T+42.5)^{-1.5} \quad (3)$$

with temperature T in degrees Celsius.

Experimental procedure

The filtrations were performed according to the flux-step method as described by van der Marel et al. (2009). The procedure was slightly adjusted: the relaxation step was done at a membrane flux of 15 L m^{-2} h^{-1} and 6 membrane flux values were tested: 30, 35, 40, 45, 50, and 55 L m^{-2} h^{-1}. The duration of the relaxation step was 15 minutes and the other steps each took 45 minutes. Before starting the experiment, a clean water filtration was performed for 20 minutes. The cross-flow velocity in all experiments was 0.26 m s^{-1}, as this is a representative mixed liquor cross-flow velocity for submerged systems (Bérubé and Lei, 2006; Kang et al., 2008). A typical example of the resistance data in a flux-step experiment is shown in Figure 2.1.

Total fouling rates were calculated from the slope of the resistance in time (R(t)) after 30 minutes of filtration. This time point was chosen arbitrarily. The initial stage of the filtration curve, just after the relaxation step, can not be used for fouling rate calculation. During the short time after the relaxation period, which lasts only for 1-2 minutes as can be seen in Figures 2.1 and 2.2 (1 data point per minute), the pump needs to switch from a low flow in the relaxation step to a higher flow in the flux step. It takes some time before the higher flow is actually given by the pump, and therefore this part of the curve is not representative for the actual flux step. Reversibility by relaxation for 15 minutes at a membrane flux of 15

L m^{-2} h^{-1} was expressed as a percentage of the total resistance increase for one membrane flux step:

$$\% \text{ Reversibility} = (R_{high\ n} - R_{low\ n})/(R_{high\ n} - R_{low\ n-1})*100 \quad (4)$$

$R_{high\ n}$ represents the resistance at the end of one filtration step, $R_{low\ n}$ represents the average resistance at the corresponding relaxation step and $R_{low\ n-1}$ represents the average resistance at the previous relaxation step.

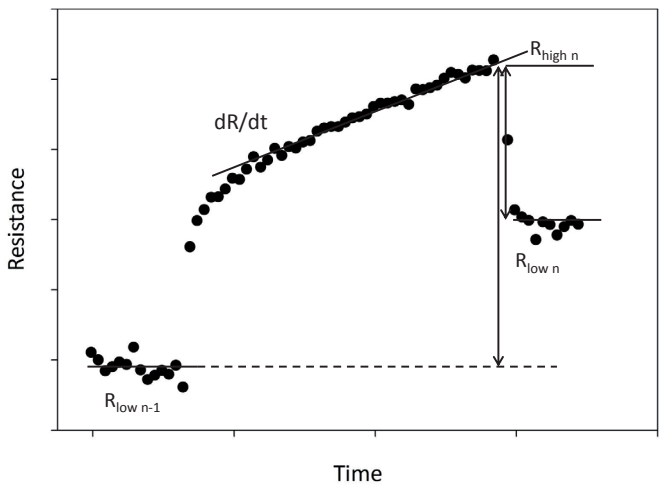

Figure 2.1 Calculation of fouling rate (dR/dt) at t=30 min and reversibility (eq. 4) from filtration data.

To assess the rejection of alginate by the membrane, samples of the permeate were taken at every membrane flux and relaxation step, and analysed for total organic carbon (TOC) concentrations with a Shimadzu analyzer (TOC-V_{CPH}, Shimadzu, Japan). In addition, the TOC concentration of the feed alginate solution was measured. No release of TOC from the membrane material was detected (data not shown), and therefore all TOC can be considered to originate from the feed solution.

Experiments

Applied concentrations of alginate, free calcium and total ionic strengths for the different experiments can be found in Table 2.1.

Table 2.1 Concentrations applied in the different filtration experiments.*

Name	Concentration alginate (ppm)	Concentration free Ca^{2+} (mM)	Total ionic strength (I) (mM)
Base case (n=4)	10	1	10
High Ca^{2+} (n=4)	10	2	10
High I	10	1	20
High Ca^{2+} + I	10	2	20
High alginate	20	1	10
High alginate + Ca^{2+}	20	2	10
High all	20	2	20
No Ca^{2+}	10	0	10
No I	10	1	3
No alginate	0	1	10

* n=1 unless stated otherwise.

RESULTS

Base case

The resistance development in the improved flux-step method for the base case (Exp.1) is shown in Figure 2.2. The first phase in the graph shows the resistance during clean water filtration (phase I), which was performed to measure the membrane resistance. Subsequently, the system was switched from clean water to alginate solution and the first relaxation step was performed (phase II). The 6 filtration steps of 45 minutes can be clearly identified (phase III). The relaxation step (phase IV), is visible from the lower resistance values.

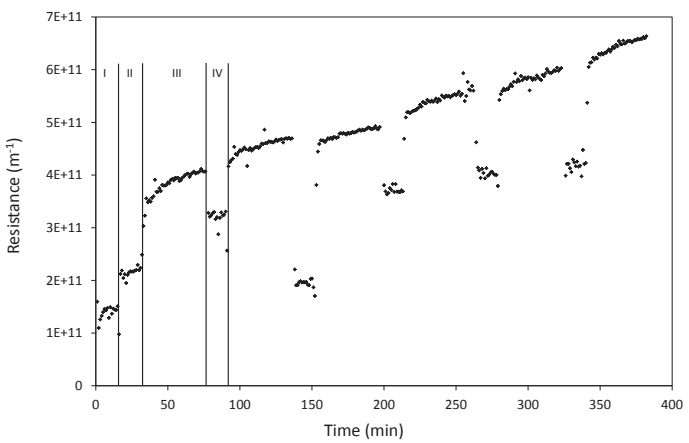

Figure 2.2 Resistance in time for the base case experiment (1 mM Ca2+, total ionic strength 10 mM, alginate 10 ppm).

Fouling rates at different membrane fluxes for the base case (10 ppm alginate, 1 mM free Ca^{2+} and 10 mM total ionic strength) the largest fouling rate at 30 L m^{-2} h^{-1} (Figure 2.3). Reversibility of fouling increased with the applied membrane flux from a low value (41-53%) at the lower membrane fluxes (30-40 L m^{-2} h^{-1}) to 87% reversibility at a membrane flux 50 L m^{-2} h^{-1} (Figure 2.3).

The increase in reversibility in the course of the experiment and the high fouling rate at the first flux step can be explained by a "loading effect": in the first flux steps, the clean membrane surface was exposed to the alginate, resulting in an interaction between the membrane surface and the alginate and creating a strong fouling layer. In later flux steps in time, i.e. the ones at higher membrane fluxes, the alginate could not interact with the membrane anymore as it was already covered by the fouling layer. Even though relaxation is not the most effective cleaning method, the fouling that was formed during the higher flux steps could, for a large part, be removed by this relaxation step. This shows that the alginate that is transported to the membrane during the filtration steps in solution or as aggregate was not very adhesive to the existing fouling layer. The two-phase process can be clearly identified in Figure 2.3: until membrane flux 40 L m^{-2} h^{-1}, an alginate gel layer was formed at high but decreasing fouling rates and low reversibilities and at higher membrane fluxes this gel layer became more stable with high reversibilities.

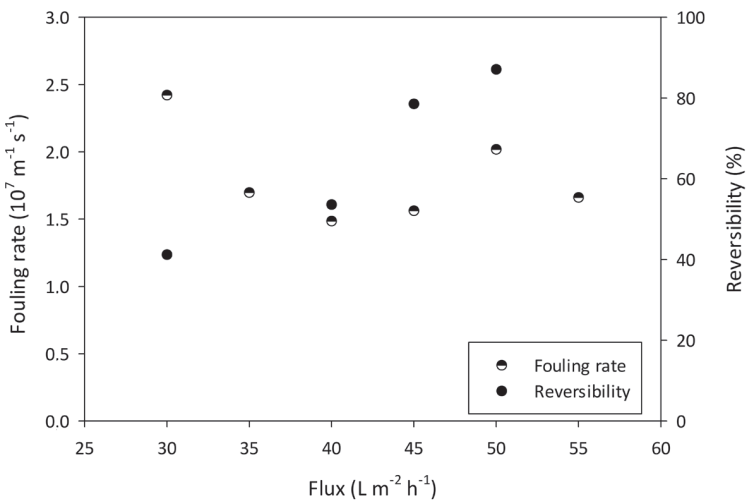

Figure 2.3 Total fouling rates and reversibility values at different membrane fluxes for the base case (1 mM Ca^{2+}, total ionic strength 10 mM, alginate 10 ppm). Note: the y-axis in this Figure has a smaller scale as compared to Figures 2.4 and 2.5.

Fouling behaviour at a certain step may have been influenced by the fouling that was not removed during the relaxation step. This would mean the effect of the membrane flux is masked by the fouling already present on the membrane. To test whether this is an issue that needs to be considered, an experiment was performed in which six flux steps where done at 30 L m^{-2} h^{-1} and fouling rates and reversibilities were compared with a flux step experiment filtering the same solution at membrane fluxes of 30 to 55 L m^{-2} h^{-1} as described above.

Figure 2.4 shows that the fouling rates for the equal flux step experiment varying around an average of 5.2 x 10^7 m^{-1} s^{-1}, whereas in the increasing flux step experiment the fouling rates were increasing linearly with the membrane flux. This shows the direct effect of the membrane flux on fouling rate and also proves that the fouling history (i.e. fouling built up in previous flux steps) is not overshadowing the effect of the membrane flux on fouling behaviour. Consequently, although fouling history can play a role in the presented flux step experiments, the effects of membrane flux can still be identified and this justifies the use of the flux step method.

The first flux step gave a relatively low reversibility. This was previously described as the "loading effect". Reversibilities were decreasing in time in the experiment with increasing flux steps, while they were higher and increasing for the equal flux experiment. The fifth and sixth flux steps show clear differences in reversibilities between the two experiments, indicating that the membrane flux indeed had an effect on fouling behaviour.

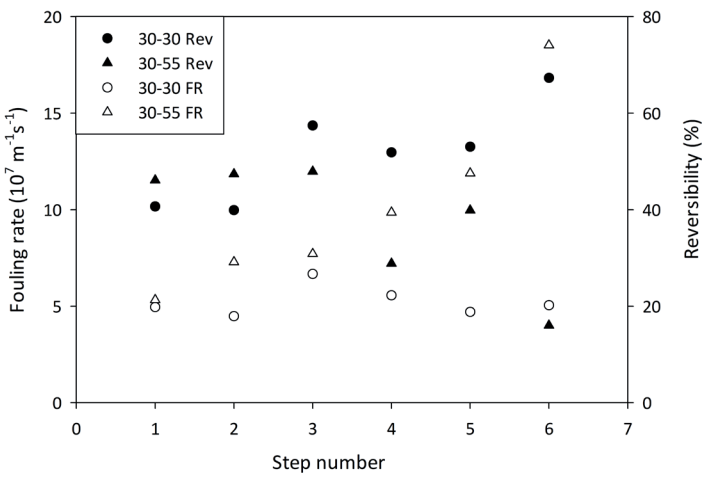

Figure 2.4 Comparison between equal flux steps (30-30) and increasing flux steps (30-55): total fouling rates (FR) and reversibility values (Rev),(2 mM Ca^{2+}, total ionic strength 10 mM, alginate 10 ppm).

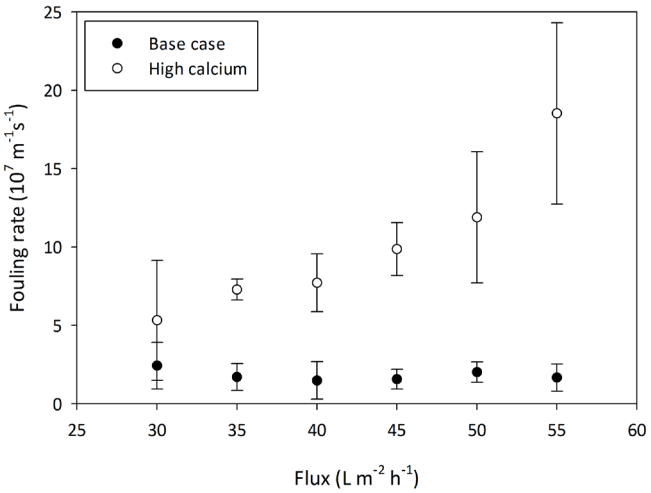

Figure 2.5 Total fouling rates at different membrane fluxes for the base case (1 mM Ca^{2+}, total ionic strength 10 mM, alginate 10 ppm) and for a high calcium concentration (2 mM Ca^{2+}), including error bars (n=4).

To test the reproducibility of the flux step experiments, two experiments have been performed in quadruple: the base case experiment and the experiment with a high calcium concentration (Figure 2.5). Although there is variation between the quadruplicates, there is no overlap between the two experiments. Therefore, the differences in fouling rate can be assigned to the composition of the alginate solution and the reproducibility of the experiments was regarded as sufficient. This was also found for the reversibility values of the experiments presented in Figure 2.5 (data not shown).

Membrane flux

In most experiments, fouling rates stayed constant at increasing fluxes. For the high fouling rates however, an increase in fouling rate was found with increasing membrane flux (Figure 2.6). For the experiment with a high calcium concentration, the fouling rate was exponential with the membrane flux (Figure 2.4 and Figure 2.6). Moreover, reversibility increased from 40 % for the first flux step to 67% for the last flux step in the experiment with equal flux steps, showing the difference in fouling between the first and the later flux steps (Figure 2.4).

The high membrane fluxes in the experiment with high alginate and calcium concentrations do not show the before mentioned relation of fouling rate with membrane flux (Figure 2.6). This may have been caused by the high TMP (>300 mbar) at these flux steps: a lower effective membrane flux was reached than was set because the pump could not manage to give the set flow at this TMP.

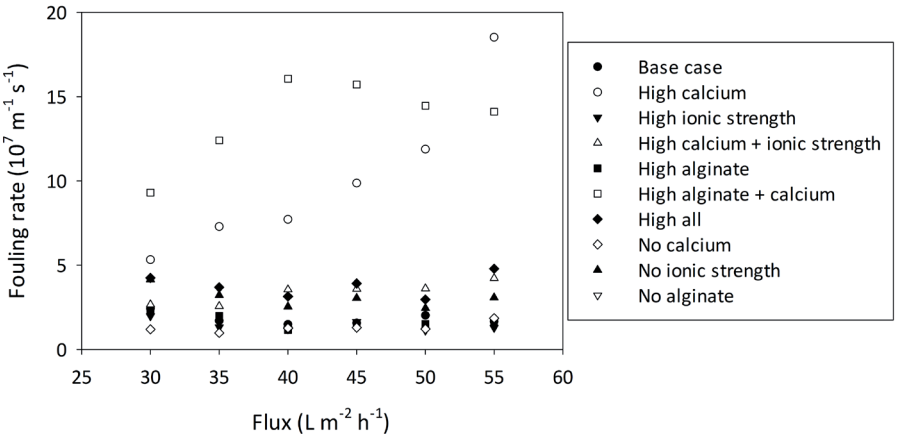

Figure 2.6 Total fouling rates at different membrane fluxes. Applied concentrations are for the base case: 1 mM Ca^{2+}, total ionic strength 10 mM, alginate 10 ppm and the elevated levels are 2 mM Ca^{2+}, total ionic strength 20 mM, alginate 20 ppm (see also Table 2.1).

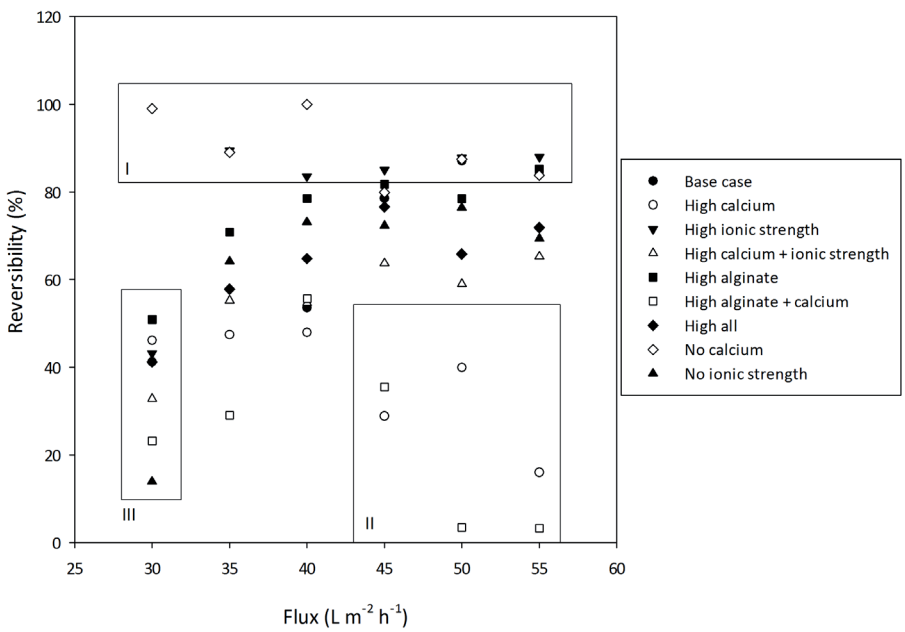

Figure 2.7 Fouling reversibility (%) at different membrane fluxes. Applied concentrations are for the base case: 1 mM Ca^{2+}, total ionic strength 10 mM, alginate 10 ppm and the elevated levels are 2 mM Ca^{2+}, total ionic strength 20 mM, alginate 20 ppm(see also Table 2.1). The experiments highlighted in box I, II and III are explained extensively in the text.

At high fouling conditions (i.e. high calcium and high alginate + high calcium), reversibility decreased when membrane flux increased (Figure 2.7II). This trend was not seen in the other experiments, in which reversibility increased about 10% from the second to the sixth flux step. The only exception here was the lowest flux step of 30 L m^{-2} h^{-1} which gave a much smaller reversibility value (14-50%) compared to the other flux steps, in which the reversibility was mostly above 50% (Figure 2.7III).
As mentioned before, fouling rate and fouling reversibility are inversely related; high fouling rates give low reversibilities. This effect is most clearly observed at the higher flux steps.

Calcium to alginate ratio

A strong increase in fouling rate (factor 6-11 compared to base case) was observed in case the calcium to alginate ratio was increased compared to the base case, and an even stronger effect when the total alginate and calcium concentrations were both high (Figure 2.6). The same trend was seen when evaluating the end resistances of the last flux steps (Figure 2.8). By doubling the alginate concentration and keeping the calcium concentration constant compared to the base case, total fouling rates and end resistances were similar to those of the base case (Figures 2.6, 2.8). This shows that not just the absolute calcium and alginate concentrations determine the fouling behaviour of alginate solution, but it is important to also consider the ratio of the two compounds. In case alginate was absent, low fouling rates were observed (Figure 2.6). This fouling can be explained by the presence of impurities in the filtered solution, which could not be avoided.
Without calcium, the alginate fouling was reversible with values above 80%, and independent of the alginate concentration (Figure 2.7I). The experiments in which a high fouling rate was observed (high calcium to alginate ratio and high calcium and alginate concentrations) showed a lower reversibility, especially at the higher membrane fluxes (Figure 2.7II). For these two experiments the highest reversibility was found around 35-40 L m^{-2} h^{-1}. Concerning the first flux step, lower reversibilities were found for the high calcium solutions (Figure 2.7III), indicating stronger interaction of the alginate with the clean membrane or increased pore blocking by alginate aggregates.

Ionic strength

When the total ionic strength of the solution was doubled compared to the base case, the average total fouling rate was similar to the base case (Figure 2.8). In case both ionic strength and free calcium concentration were increased, the average fouling rate was 66% lower compared to just an elevated free calcium concentration (Figure 2.8). A decrease in average fouling rate was also observed when the ionic strength was increased in the experiment with high alginate and calcium concentration. In this case, the average fouling rate decreased with 72%. Without adjusting the ionic strength with KCl (only $CaCl_2 \cdot 2H_2O$

is added), the average fouling rate was in the same range as in the experiments with high ionic strength and calcium concentration and for the "all high" experiment (Figure 2.8). From the above mentioned observations it can be concluded that increasing the ionic strength decreases the fouling rate of alginate solutions, but only if the calcium concentration is high as well.

Concerning reversibility, increasing the ionic strength gave a positive effect (Figure 2.8). Reversibility at high ionic strengths was found to be rather constant, on average 80%, at different membrane fluxes. When the free calcium concentration was increased as well, the average reversibility dropped to 55% (Figure 2.8). Without adjusting the ionic strength, the average reversibility was with 62% in between the above mentioned experiments.

Combining the results for the fouling rates and the reversibility data, increasing the ionic strength has a positive effect on decreasing alginate fouling, both concerning fouling rate and reversibility. However, this positive effect only takes place when the calcium concentration is high, i.e. at high fouling conditions.

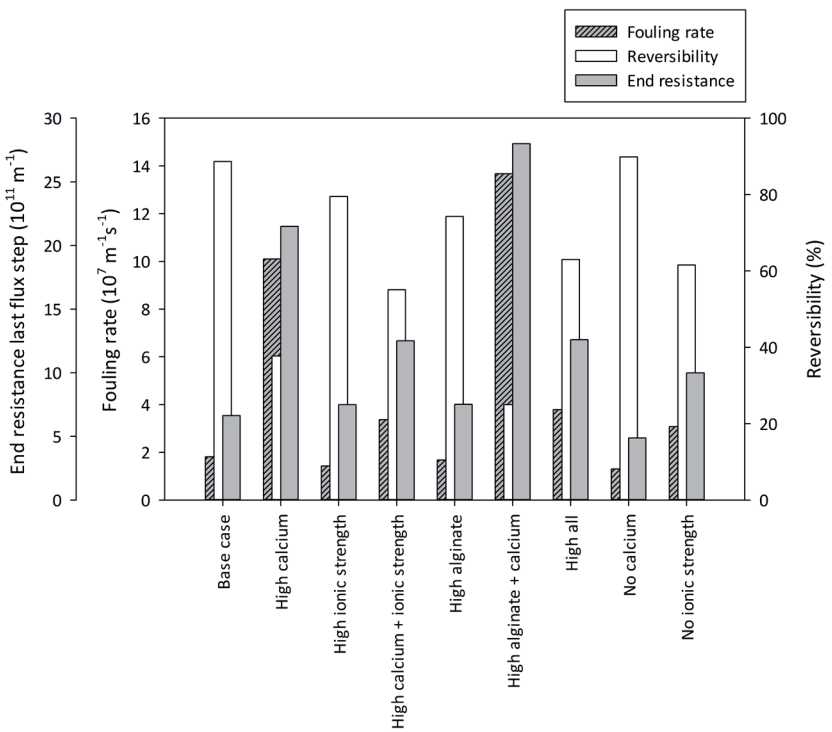

Figure 2.8 Average fouling rates and reversibilities for all experiments, and resistance at the end of the last flux step.

Retention

Alginate retention in each experiment was constant over the flux steps, except for the first flux step of 15 L m^{-2} h^{-1}, which showed lower retention values. Average retention values for each experiment are shown in Table 2.2. In case no calcium was added, retention varied widely from -65% (due to dissolution of the fouling layer) to 66%.

Table 2.2 Retention for the different experiments. No measurements are available for the experiment with high ionic strength.

Name	Average retention (%)	Lowest retention (%)	Highest retention (%)
Base case	71	40	82
High Ca^{2+}	77	63	86
High I	n/a	n/a	n/a
High Ca^{2+} + I	74	40	94
High alginate	81	58	93
High alginate + Ca^{2+}	76	57	87
High all	86	76	94
No Ca^{2+}	13	-65	66
No I	66	33	90

DISCUSSION

Fouling mechanisms

A strong fouling effect of high calcium to alginate ratios and high absolute calcium and alginate concentrations was observed. These observations can be explained by different fouling mechanisms, which act at different positions of the membrane (Table 2.3):

1. Adsorption

At the beginning of a filtration run, alginate chains adsorb to the membrane surface. In our experiments, adsorption took place during the first relaxation step and during flux step 1 (30 L m^{-2} h^{-1}). This can be concluded when comparing the reversibility values for the different flux steps (Figure 2.7III). A low reversibility upon relaxation or application of high cross flow velocity, while the fouling layer was removable by cleaning with a strong metal chelating agent, such as EDTA, has been reported before in literature (Ang et al., 2006). Initial adsorption during sodium alginate filtration through a UF membrane was also reported by Ye et al. (2005a).

The composition of the applied alginate solution influences the adsorption of alginate chains to the membrane surface. Low reversibilities were found for the high calcium solutions (Figure 2.7III), indicating stronger interaction of the alginate with the clean membrane. Absence of calcium dramatically increased reversibility for the flux step to 99% (Figure 2.7III).

Polycarbonate membranes are negatively charged and have a rather constant ζ potential over a pH range of 4-10 at 10 mM NaCl (Bowen and Cooke, 1991). Because of its negative charge, the membrane surface may bridge with the carboxyl groups of the alginate by calcium ions. When the ionic strength of an alginate solution with a high calcium concentration is increased, reversibility increases. When the ionic strength was only determined by $CaCl_2$ (no adjustment with KCl), reversibility dropped to the lowest measured value of 14% (Figure 2.7III). This shows there is competition between calcium and potassium ions for the carboxyl groups on the alginate polymer and the negative membrane surface.

2. Aggregation

Separate alginate chains in the bulk solution form aggregates. This mechanism can play a role during the entire filtration experiment, and once aggregates are formed, they are transported to the membrane surface by convection. The cake layer that is formed is reversible, but may turn into a more irreversible gel layer at high TMPs by compression because the alginate chains are being pushed more into each others vicinity. Because this is the only reversible fouling mechanism of the proposed ones, and reversibility values were high in every experiment but the first flux step (Figure 2.7), aggregation is assumed to have happened to some extent in every experiment, While only a small effect of ionic strength on the radius of gyration was reported for single alginate molecules (Strand et al., 1982), there are indications for alginate aggregate formation, also in the absence of calcium ions. Recently, the conformation of alginate molecules was studied in ultrapure water and in a 10 mM salt solution (van de Ven et al., 2009). The slopes of the conformation plots were found to decrease with increasing molar mass, which was explained by aggregation.

Compression could explain the low reversibilities observed in the experiments with high calcium and high calcium and alginate concentrations (Figure 2.7III). Aggregation has been suggested as a cause of flux decline in ultrafiltration of sodium alginate solutions, to which calcium was added (Katsoufidou et al., 2007). Indeed, retention was similar for all experiments with calcium containing solutions. The solution without added calcium showed very low retention values, indicating that little aggregation took place.

3. Gelation

Separate alginate chains form bridges with the existing gel layer at the membrane surface. This mechanism is influenced by the membrane flux, because alginate molecules are transported to the membrane surface by the flux. In case the alginate molecules are retained by the membrane or the existing gel layer, the local concentration increases and exceeds the critical gel concentration (Wijmans et al., 1984). Because of the bridges between the alginate molecules, gelation is irreversible upon relaxation. Calcium ions play an important role during gelation, as they promote bridging between the negatively charged alginate molecules. The

average adhesion force between alginate molecules in the presence of calcium ions was shown to be twice as much as without calcium ions (Mi and Elimelech, 2008). The bridging effect of calcium is extensively described in literature (Grant et al., 1973; Draget et al., 2000) and is, as well as for aggregation, in line with the high efficiency of metal chelating agents (EDTA) and anionic surfactants (SDS) as cleaning agents for organic-fouled RO membranes (Ang et al., 2006). These compounds are hypothesized to scavenge the calcium ions from the fouling layer and thereby decrease the foulant-foulant interaction. As well as for the other fouling mechanisms, competition took place between the calcium and potassium ions in the experiments with an elevated ionic strength, leading to lower fouling rates and higher reversibilities (Figure 2.8). Because the experiments with high calcium concentration and high calcium and alginate concentrations showed low reversibilities, it can be assumed that gelation was causing a relatively large part of the total fouling (Figure 2.7).

4. Pore blocking

After the separate alginate chains have aggregated, their size can be as large as the pore size. Even though the pores in the polycarbonate membrane are straight and have a narrow pore size distribution, pore blocking can be an important fouling mechanism in the presented experiments, especially during the first flux step when the membrane is still clean. Pore blocking could also explain the low reversibilities of the first flux steps (Figure 2.7III).

The described mechanisms, their time and place of action, and the effect of the variables applied in our experiments are described in Table 2.3.

Table 2.3 Fouling mechanisms in alginate filtration.

Mechanism	Space	Reversibility	Stimulating effect of Ca	Negative effect of ionic strength	Effect flux
Adsorption	Membrane	No	Yes	Yes	No
Aggregation	Bulk	Yes, at low TMPs	Yes	Yes	No
Gelation	Membrane	No	Yes	Yes	Yes
Pore blocking	Membrane	No	No (indirect effect: aggregation)	No (indirect effect on aggregation)	Yes

Although calcium has a strong fouling effect on alginate fouling in the experiments presented here, in a membrane bioreactor calcium might reduce membrane fouling. Addition of calcium or magnesium to activated sludge resulted in increased floc strength, while sodium had the opposite effect (Sobeck and Higgings, 2002). Increasing floc strength was shown to decrease fouling (Chang et al., 1999), but it might also be that the increased Ca concentration binds free alginate like polymers to the flocs. However, high calcium concentrations were shown to cause inorganic fouling or scaling (data not shown; Arabi and Nakhla, 2008).

Competition of monovalent cations

Increasing the ionic strength decreased the fouling rate of alginate solutions, but only in case the calcium concentration was high as well (Figure 2.8). The bridging effect of divalent cations with alginate is known for a long time and can be explained by the "egg-box model" (Grant et al., 1973). This theory is specific for alginate molecules and therefore also referred to as the "alginate theory" (Sobeck and Higgings, 2002). Two other theories to explain the effect of cations on bioflocculation in general are the DLVO theory and the divalent cation bridging theory (Sobeck and Higgings, 2002). The first one states that cations decrease the double layer around particles, thereby reducing repulsive forces between particles. The divalent cation bridging theory suggests a non-specific binding of divalent cations rather than the specific interaction and gel formation between calcium and alginate.

Monovalent cations were also tested for their affinity towards alginate, with Na^+ showing a slightly enhanced binding compared to K^+ (Draget et al., 1998). Competition between mono- and divalent cations for binding sites on the alginates has been reported several times and actual ion-exchange was taking place in high ionic strength solutions (Draget et al., 1998; Martinsen et al., 1989; Neiser et al., 1999; de Kerchove and Elimelech, 2006). This competition effect was found in the alginate filtration experiments reported in this work: the fouling effect of calcium was only seen in the experiments in which the Ca^{2+}:K^+ ratio is high. When the ionic strength of the solution with a high calcium concentration (2 mM) was increased from 10 mM to 20 mM, fouling rates decreased with a factor 3-4 (Figure 2.8). This decrease is not observed when the ionic strength is increased in a low calcium solution (1 mM) (Figure 2.8). Therefore, it can be concluded that the beneficial effect of ionic strength is only valid for high fouling solutions. Only if the fouling potential of an alginate solution is high (i.e. high Ca^{2+} or high Ca^{2+} and high alginate), K^+ ions can actually compete with Ca^{2+} for the binding sites on the alginate molecule. In case fouling is low, there is less bridging by Ca^{2+} ions and therefore the competition effect of K^+ ions will be smaller.

High reversibility values were found in the filtrations of alginate solutions with high ionic strengths. The only experiment with higher reversibility is the one without calcium. These two findings match the results of de Kerchove and Elimelech, who measured intermolecular adhesion forces between alginate molecules with atomic force microscopy (2006). Lowest adhesion forces were reported in the absence of calcium and a high ionic strength combined with the presence of calcium resulted in low adhesion forces. These low adhesion forces within an alginate fouling layer increased the effectiveness of the cross flow, resulting in a higher reversibility.

Effect membrane flux

In most experiments, fouling rates stayed constant at increasing fluxes, despite increased

transport of alginate molecules towards the membrane surface (Figure 2.6). The back diffusion of alginate molecules was apparently high in these experiments. On the other hand, in the high fouling experiments, the fouling rates increased with the membrane flux (Figure 2.6). The balance between convection of alginate towards the membrane and back diffusion was different here, which can be explained by the formation of aggregates that have a lower back diffusion. Because the fouling rate of the experiment with a high calcium and high alginate concentration increased proportional to the flux, the data agree with the classical cake filtration models (Ho and Zydney, 2006). However, the rate of increase of the hydraulic resistance was more than directly proportional to the (convective) flux (Figure 2.6). Therefore, it can be assumed that more than one fouling mechanism was acting. Possible other effects that could be of importance are:

1. Compaction of the gel layer. At the higher flux steps, the transmembrane pressure was higher than at the lower flux steps. This high transmembrane pressure could cause compaction of the aggregates and the existing gel layer. This compacted layer showed a higher resistance and a lower reversibility (Figure 2.7). Higher reversible fouling at higher transmembrane pressures was observed before for whey protein solutions, leading to the conclusion that instead of the amount of proteins forming the fouling layer, rather cake compaction and cake porosity play the most significant role in membrane fouling (Mourouzidis-Mourouzis and Karabelas, 2006).
2. Increase in retention by alginate layer. This causes a larger fraction of alginate to be retained resulting in higher fouling rates and has been reported before for dead-end filtration (Wang and Waite, 2008)
3. Blockage of part of the pores, increasing the local flux (Ognier et al., 2004). This is an exponential effect.

The first flux step showed different reversibilities (Figures 2.6, 2.7). On the clean membrane, alginate molecules adsorbed and a gel layer was formed at the beginning of the experiment, resulting in high fouling rates and low reversibilities for the first flux step. Retention of alginate was low during the first flux step, because single alginate molecules could still pass the membrane. The following increase of retention showed that the alginate gel layer is able to retain single alginate molecules. Ca-alginate gels have been reported to increase the retention of colloids in dead end filtration (Wang and Waite, 2008).

Retention

Alginate retention in each experiment was constant over the flux steps, except for the first flux step of 15 L m^{-2} h^{-1}, which showed lower retention values. At the first flux step, the membrane is still clean and retention is only determined by the membrane. At later flux step, the fouling layer increases the retention.

In case no Ca^{2+} was added, retention was low with an average over the flux steps of 13 %. Even negative retention values were measured, which can be explained by breakthrough of material. Higher retention values (up to 94%) were reached in case calcium was present in the feed solution.
Different radii of gyration have been reported for the alginate molecule, ranging from 50 ± 7 nm to 137 nm (Bowen and Cooke, 1991; Wedlock et al., 1986; Windhues and Borchard, 2002). Taking into account the polydispersity of alginate (Stokke et al., 1987), these high retention values for alginate can be explained by aggregate or gel layer formation. According to the gel layer theory of Wijmans and co-workers (1984), this gel will be formed near the membrane surface because of the high concentration there.

CONCLUSIONS

Studying the effect of free calcium concentration and ionic strength on alginate fouling in cross-flow membrane filtration led to the following conclusions:

1. Raising the calcium concentration in an alginate solution results in increased alginate fouling. This strong fouling effect of free calcium ions can be explained in different ways: They promote bridging between separate alginate chains, forming a gel network at the membrane surface or aggregates in the bulk solution, or they promote bridging between the membrane and the first alginate layer. All three processes are likely to happen and are all affected by the solution chemistry, but show different reversibilities and are influenced by the flux in different ways.
   The fouling obtained at high calcium to alginate ratios is mostly irreversible upon relaxation.
2. Increasing the total ionic strength of the solution decreases the total fouling rates considerably in case of high calcium to alginate ratio solutions. This might be explained by competition between mono- and divalent cations for the binding sites on the alginate molecule, which diminishes the fouling effect of the calcium ions. Moreover, high reversibility values were found in the filtrations of alginate solutions with high ionic strengths. This can be explained by low adhesion forces within the alginate fouling layer, which increase the effectiveness of the cross flow.

The proposed mechanisms for alginate fouling would be adsorption, especially at the first flux-step (low reversibilities and low retentions were measured for this step), aggregation and gel layer formation. Further research will focus on the interaction of polysaccharides with other compounds typically present in the MBR supernatant (e.g. proteins, humic acids and sludge particles) and a more detailed analysis of the fouling layer formed with MBR sludge.

ACKNOWLEDGEMENTS

This work was performed in the TTIW-cooperation framework of Wetsus, Centre of Excellence for Sustainable Water Technology (www.wetsus.nl). Wetsus is funded by the Dutch Ministry of Economic Affairs, the European Union Regional Development Fund, the Province of Fryslân, the City of Leeuwarden and the EZ/Kompas program of the 'Samenwerkingsverband Noord-Nederland". The authors like to thank the participants of the research theme "Membrane Bioreactors" for the discussions and their financial support. The input of Perry van der Marel is gratefully acknowledged.

References

Al-Halbouni D, Traber J, Lyko S, Wintgens T, Melin T, Tacke D, Janot A, Dott W, Hollender J (2008) Correlation of EPS content in activated sludge at different sludge retention times with membrane fouling phenomena *Water Res.* **42** (6-7), 1475-1488

Ang WS, Lee S, Elimelech M (2006) Chemical and physical aspects of cleaning of organic-fouled reverse osmosis membranes, *J. Membrane Sci.* **272**, 198-210

Arabi S, Nakhla G (2008) Impact of calcium on the membrane fouling in membrane bioreactors *J. Membrane Sci.* **314** (1-2) 134-142.

Bérubé PR, Lei E (2006) The effect of hydrodynamic conditions and system configurations on the permeate flux in a submerged hollow fiber membrane system, *J. Membrane Sci.* **271** (1-2) 29-37

Bowen WR, Cooke RJ (1991) Properties of microfiltration membranes: computer automated determination of the electrokinetic properties of polycarbonate membranes, *J. Colloid Interf. Sci.* **141**, 280-287

Bura R, Cheung M, Liao B, Finlayson J, Lee BC, Droppo IG, Leppard GG, Liss SN (1998) Composition of extracellular polymeric substances in the activated sludge floc matrix *Water Sci. Technol.* **37**, 325-333

Chang IS, Le-Clech P, Jefferson B, Judd SJ (2002) Membrane fouling in membrane bioreactors for wastewater treatment *J. Environ. Eng.* **128**, 1018-1029

Chang IS, Lee CH, Ahn KH (1999) Membrane filtration characteristics in membrane-coupled activated sludge system: The effect of floc structure on membrane fouling *Separ. Sci. Technol.* **34** (9), 1743-1758

Chu HP, Li XY (2004) Membrane fouling in a membrane bioreactor (MBR): Sludge cake formation and fouling characteristics *Biotechnol. Bioeng.* **90** (3), 323-331

Davis TA, Pinheiro JP, Grasdalen H, Smidsrød O, van Leeuwen HP (2008) Stability of lead(II) complexes of alginate oligomers *Environ. Sci. Technol.* **42** (5), 1673-1679

de Kerchove AJ, Elimelech M (2006) Structural growth and viscoelastic properties of adsorbed alginate layers in monovalent and divalent salts *Macromolecules* **39**, 6558-6564

Draget KI, Smidsrød O, Skjåk-Bræk G (2000) Alginates from algae, in: A. Stenbuchel, S.K. Rhee (Eds.), Polysaccharides and Polyamides in the Food Industry. Properties, Production and Patents, Wiley – VCH, Weinheim, pp. 1-30

Draget KI, Steinsvåg K, Onsøyen E, Smidsrød O (1998) Na- and K-alginate; effect on Ca^{2+} gelation, *Carbohyd. Polym.* **35** (1-2), 1-6

Evenblij H, van der Graaf JHJM (2004) Occurrence of EPS in activated sludge from a membrane bioreactor treating municipal wastewater *Water Sci. Technol.* **50** (13), 293-300

Flemming HC, Wingender J (2001) Relevance of microbial extracellular polymeric substances (EPSs) – part I: Structural and ecological aspects *Water Sci. Technol.* **43** (6), 1-8

Grant GT, Morris ER, Rees DA, Smith PJC, Thom D (1973) Biological interactions between polysaccharides and divalent cations: The egg-box model *FEBS Lett.* **32** (1), 195-198

Haug A (1961) The affinity of some divalent metals to different types of alginates *Acta Chem. Scand.* **15**, 1794-1795

Ho CC, Zydney AL (2006) Overview of fouling phenomena and modeling approaches for membrane bioreactors *Separ. Sci. Technol.* **41** (7), 1231-1251

Kang CW, Hua J, Lou J, Liu W, Jordan E (2008) Bridging the gap between membrane bio-reactor (MBR) pilot and plant studies *J. Membrane Sci.* **325** (2), 861-871

Katsoufidou K, Yiantsios SG, Karabelas AJ (2007) Experimental study of ultrafiltration membrane fouling by sodium alginate and flux recovery by backwashing *J. Membrane Sci.* **300** (1-2), 137-146

Le-Clech P, Chen V, Fane AG (2006) Fouling in membrane bioreactors used in wastewater treatment - A review *J. Membrane Sci.* **284** (1-2), 17-53

Lee S, Elimelech M (2006) Relating organic fouling of reverse osmosis membranes to intermolecular adhesion forces *Environ. Sci. Technol.* **40** (3), 980-987

Martinsen A, Skjåk-Bræk G, Smidsrød O (1989) Alginate as immobilization material I: correlation between chemical and physical properties of alginate gel beads *Biotechnol. Bioeng.* **33** (1), 79-89

Mayer C, Moritz R, Kirschner C, Borchard W, Maibaum R, Wingender J, Flemming HC (1999) The role of intermolecular interactions: studies on model systems for bacterial biofilms *Int J. Biol. Macromol.* **26** (1) 3-16

Mi B, Elimelech M (2008) Chemical and physical aspects of organic fouling of forward osmosis membranes *J. Membrane Sci.* **320** (1-2), 292–302

Miura Y, Watanabe Y, Okabe S (2007) Membrane biofouling in pilot-scale membrane bioreactors (MBRs) treating municipal wastewater: Impact of biofilm formation *Environ. Sci. Technol.* **41**, 632-638

Mourouzidis-Mourouzis SA, Karabelas AJ (2006) Whey protein fouling of microfiltration ceramic membranes - Pressure effects *J. Membrane Sci.* **282** (1-2) 124-132

Nataraj S, Schomäcker R, Kraume M, Mishra IM, Drews A (2008) Analyses of polysaccharide fouling mechanisms during cross flow membrane filtration *J. Membrane Sci.* **308** (1-2), 152-161

Neiser S, Draget KI, Smidsrød O (1999) Interactions in bovine serum albumin-calcium alginate gel systems *Food Hydrocolloid.* **13** (6), 445-458

Ognier S, Wisniewski C, Grasmick A (2004) Membrane bioreactor fouling in sub-critical filtration conditions: a local critical flux concept *J. Membrane Sci.* **229** (1-2) 171-177

Park C, Muller CD, Abu-Orf MM, Novak JT (2006) The effect of wastewater cations on activated sludge characteristics: effects of aluminium and iron in floc *Water Environ. Res.* **78** (1), 31-40

Roorda JH, van der Graaf JHJM (2001) New parameter for monitoring fouling during ultrafiltration of WWTP effluent *Water Sci. Technol.* **43** (10), 241-248

Rosenberger S, Evenblij H, te Poele S, Wintgens T, Laabs C (2005) The importance of liquid phase analyses to understand fouling in membrane assisted activated sludge processes – six case studies of different European research groups *J. Membrane Sci.* **263** (1-2) 113-126

Shannon MA, Bohn PW, Elimelech M, Georgiades JG, Mariñas BJ, Mayes AM (2008) Science and technology for water purification in the coming decades *Nature* **452** (7185) 301-310

Sobeck DC, Higgins MJ (2002) Examination of three theories for mechanisms of cation-induced bioflocculation *Water Res.* **36** (3) 527-538

Stokke BT, Elgsaeter A, Skjåk-Bræk G, Smidsrød O (1987) The molecular size and shape of xanthan, xylinan, bronchial mucin, alginate, and amylose as revealed by electron microscopy *Carbohyd. Res.* **160**, 13-28

Strand KA, Bøe A, Dalberg PS, Sikkeland T, Smidsrød O (1982) Dynamic and static light scattering on aqueous solutions of sodium alginate *Macromolecules* **15** (2), 570-579

van der Marel P, Zwijnenburg A, Kemperman AJB, Wessling M, Temmink H, van der Meer WGJ (2009) An improved flux-step method to determine the critical flux and the critical flux for irreversibility in a membrane bioreactor *J. Membrane Sci.* **332** (1-2) 24-29

van de Ven W, Pünt I, Kemperman A, Wessling M (2009) Unraveling ultrafiltration of polysaccharides with flow field flow fractionation *J. Membrane Sci.* **338** (1-2), 67-74

van de Ven WJC, van't Sant K, Pünt IGM, Zwijnenburg A, Kemperman AJB, van der Meer WGJ, Wessling M (2007) Hollow fiber dead-end ultrafiltration: Influence of ionic environment on filtration of alginates *J. Membrane Sci.* **308** (1-2), 218-229

Vrouwenvelder JS, van Paassen JAM, Wessels LP, van Dam AF, Bakker SM (2006) The membrane fouling simulator: A practical tool for fouling prediction and control *J. Membrane Sci.* **281** (1-2), 316-324

Wang XM, Waite TD (2008) Impact of gel layer formation on colloid retention in membrane filtration processes *J. Membrane Sci.* **325** (1), 486-494

Wang Z, Wu Z, Yin X, Tian L (2008) Membrane fouling in a submerged membrane bioreactor (MBR) under sub-critical flux operation: Membrane foulant and gel layer characterization *J. Membrane Sci.* **325** (1) 238-244

Wedlock DJ, Fasihuddin BA, Phillips GO (1986) Comparison of molecular weight determination of sodium alginate by sedimentation-diffusion and light scattering *Int. J. Biol. Macromol.* **8** (1), 57-61

Wijmans JG, Nakao S, Smolders CA (1984) Flux limitation in ultrafiltration: Osmotic pressure model and gel layer model *J. Membrane Sci.* **20** (2), 115-124

Windhues T, Borchard W (2002) Temperature depending light scattering measurements of aqueous gelatin and alginate solutions and their mixtures *Eur. Polym. J.* **38** (6), 1219-1227

Ye Y, Le-Clech P, Chen V, Fane AG (2005a) Evolution of fouling during cross flow filtration of model EPS solutions *J. Membrane Sci.* **264** (1-2), 190-199

Ye Y, Le-Clech P, Chen V, Fane AG, Jefferson B (2005b) Fouling mechanisms of alginate solutions as model extracellular polymeric substances *Desalination* **175** (1), 7-20

Yun MA, Yeon KM, Park JS, Lee CH, Chun J, Lim DJ (2006) Characterization of biofilm structure and its effect on membrane permeability in MBR for dye wastewater treatment *Water Res.* **40** (1), 45-52

Zhang J, Chua HC, Zhou J, Fane AG (2006) Factors affecting the membrane performance in submerged membrane bioreactors *J. Membrane Sci.* **284** (1-2), 54-66

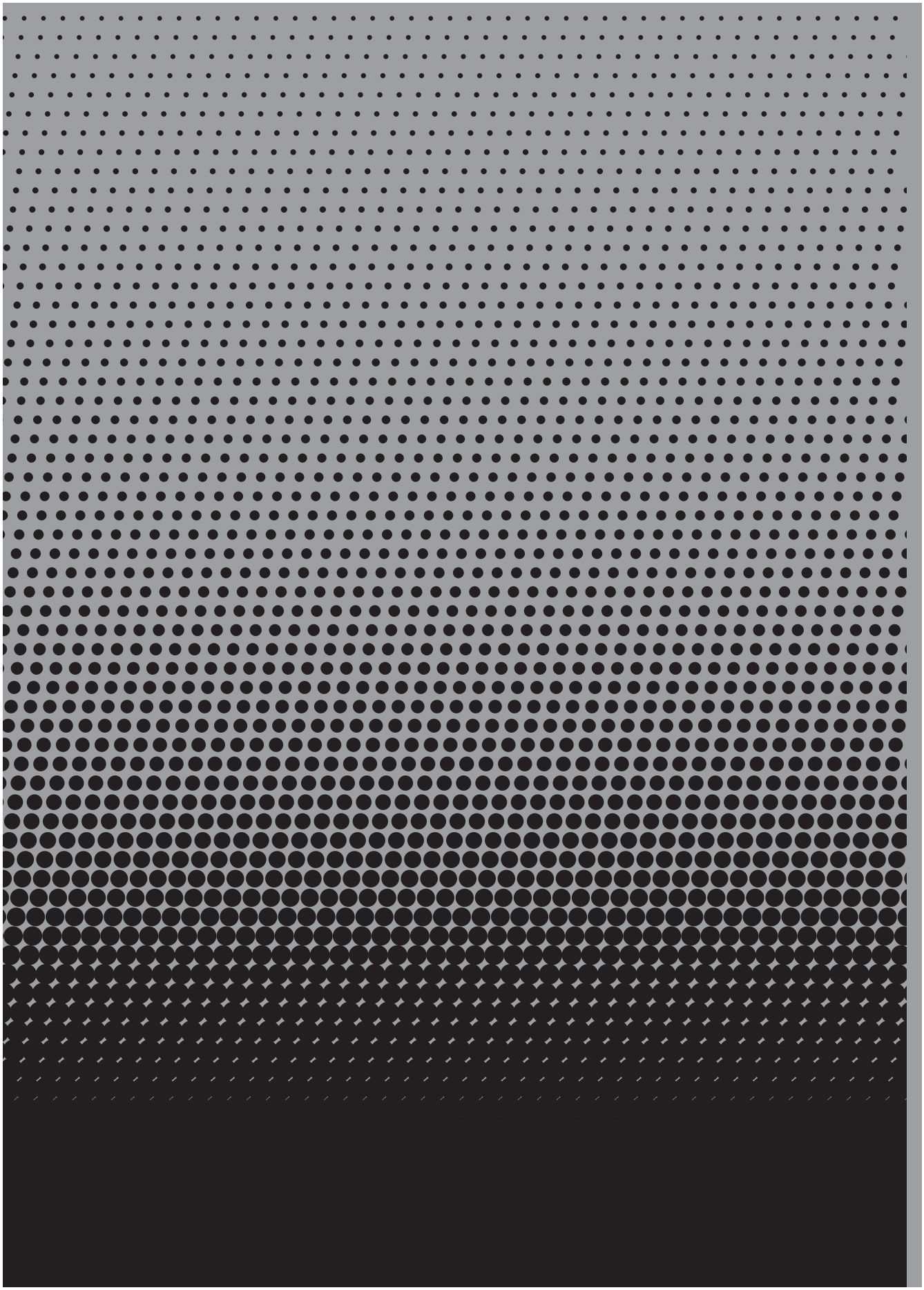

Chapter 3

GEL LAYER FORMATION ON MEMBRANES INCREASES PARTICLE RETENTION AND FOULING

ABSTRACT

Gel layer formation is an important fouling mechanism in membrane bioreactors (MBRs). Apart from fouling the membrane, gel layers might affect retention of and fouling by particles present in the MBR mixed liquor. This paper presents experiments that were performed to systematically investigate the effect of gel layer formation on retention of particles. Dead-end filtrations of particles in water and in alginate solutions were performed, as well as filtrations of particles on previously formed alginate layers and gel layers formed in a filterability set-up connected to a pilot scale MBR. Particles sizes used were smaller than or in the same range as the pores sizes of the microfiltration membranes. Particle retention and flux were monitored during the filtrations, and fouling behaviour was deducted from the flux data. Compared to filtration of particles from a water solution, increased particle retention was observed when particles were filtered from alginate solutions. Also for previously formed alginate layers and for gel layers formed in a filterability set-up connected to a pilot scale MBR extra particle retention was observed. Particle retention was not influenced by the resistance of the gel layers. Simultaneous filtration of alginate and particles showed a higher fouling rate than the solutions containing alginate or particles only. Microscopic investigation of distribution of small (diameter 0.025 µm) and big particles (diameter 0.11 µm) in both previously formed alginate layers and in gel layers formed in a filterability set-up connected to a pilot scale MBR revealed similar distribution patterns. From the alginate and gel layer cross section microscopy images, average particle layer thicknesses of 7 and 6 µm, respectively, were determined. Diameters of the applied particles are similar to those of viruses and nanoparticles. Therefore, the information obtained in this research could be useful for retention or removal of these particles in MBRs. Gel layer formation by polysaccharides present in MBR supernatant or by alginate added to the MBR mixed liquor, could be a strategy to obtain higher virus and nanoparticle retention or removal from the start of filtration.

Key words: gel layer formation, particle fouling, retention, membrane bioreactors, viruses.

INTRODUCTION

Gel layer formation is a fouling mechanism in membrane bioreactors (MBR) that is gaining increasing attention (Wang et al., 2008; van der Marel et al., 2010). Generally, gel layer formation is assumed to take place at sub-critical filtration conditions (Wang et al., 2008; Pollice et al., 2005; Wei et al., 2011). Several organic macromolecules, referred to as extracellular polymeric substances (EPS) when bound to the flocs, or as soluble microbial products (SMP) when dissolved in the supernatant, were suggested to play a major role in this process (Chang et al., 2002; Shannon et al., 2008; Drews, 2010).

Apart from fouling the membrane, gel layers might affect retention of and fouling by dissolved compounds and particles present in the MBR mixed liquor. Though the nature and size of described compounds are different, several examples of increased retention for these compounds by gel layers formed on the membrane can be found in literature. In beer filtration, a fast increase in protein retention was associated with a shift in fouling mechanism from internal fouling or pore narrowing to external gel layer formation (Blanpain-Avet et al., 1999). Increased retention of micropollutants was reported for ultrafiltration membranes fouled by natural organic matter (NOM) model compounds, and this was explained by sorption of the micropollutants onto the NOM and by the fouling layer acting as a secondary membrane (Jermann et al., 2009). Enhanced total organic carbon (TOC) rejection during filtration in a MBR treating dairy wastewater was attributed to the development of a biofouling layer (Khor et al., 2007).

Fouling layers that improve effluent quality by creating high retention compared to the original cut-off of the membrane were more and more subject of study in the past years, and were referred to as “dynamic membranes” (Fan and Huang, 2002; Choi et al., 2006; Zhang et al., 2010; Ersahin et al., 2012). A review by Meng et al. gives an extensive overview of the work done in this field (2009). Because also contradictory results were reported (Metzger et al., 2007; Wu et al., 2008a), more research should be performed to properly estimate the potential of this fouling control strategy.

Polysaccharides play a significant role in membrane fouling, being the main constituents of EPS and due to their wide molecular weight distributions as compared to proteins (Ye et al., 2005; Chu and Li, 2004; Zhang et al., 2006). Sodium alginate was used in the here presented experiments. Being an important and extensively studied microbial polysaccharide, it is the most commonly used model compound for polysaccharides (Mayer et al., 1999; Katsoufidou et al., 2007; Davis et al., 2008). Alginate fouling rates increased at higher calcium concentrations due to the bridging effect of divalent cations with alginate (van den

Brink et al., 2009), while higher ionic strengths counteract this effect to a large extent. This counteraction can be explained by competition between calcium and potassium ions for carboxyl groups on the alginate polymer (Martinsen et al., 1989; Draget et al., 1998; Neiser et al., 1999; de Kerchove and Elimelech, 2006). Not only did fouling rates increase, but also fouling reversibility decreased with increasing calcium concentrations (van den Brink et al., 2009).

While focusing mainly on the formation of alginate gels under various circumstances, research by Wang and Waite showed an increased retention of catalase by a membrane fouled with a Ca-alginate gel layer as compared to the clean membrane (2008a). Retention of bovine serum albumin (BSA) on the same gel layers was found to depend on the mass ratio of BSA to alginate. Possible explanations for the increased retention of catalase and BSA, respectively, were: (1) the apparent pore channel size was reduced by the alginate gel and caused steric hindrance, and (2) adsorption of BSA in the alginate gel layer. These experiments were performed with an alginate dispersion of 1 g L^{-1}, which is not representative for SMP (of which polysaccharides are a large fraction) concentrations in MBR supernatants (Drews, 2010). Wang and Waite used dynamic laser scattering to analyse the particle size distributions of the catalase dispersion before and after passage of the Ca-alginate layer (2008a). Although these measurements provided valuable information regarding the particles size in relation to the pore size, they were not conclusive for catalase retention as also other particles gave a signal (such as alginate aggregates). Similar to the shift in membrane fouling mechanism observed in the research on dynamic membranes and by Wang and Waite (2008a), ultrafiltration of model seawater containing alginate and humic acids showed reduced adsorption of humic acids on the membrane surface by a prefiltering action of the alginate gel layer (Resosudarmo et al., 2013).

The interactions of alginate with cations and other foulants such as humic acids, proteins and colloidal particles are well-described in literature (Wang and Waite, 2008a, Ang and Elimelech, 2007; Lee and Elimelech, 2006). As shown above, alginate fouling was also subject of several studies, because alginate is used as a model compound for SMP. Concerning alginate retention and especially its effect on retention of other compounds, only the research of Wang and Waite can be referred to (2008a). For gel layers formed in an MBR, their retention for particles is not reported in literature. The experiments presented in this paper were performed to systematically investigate the effect of gel layer formation by alginate on the retention of particles. Alginate concentrations representative for the SMP concentration in MBR supernatant were applied, as well as fluorescent particles that are easy to detect, and of which the measurement is unambiguous.

The main objectives of this study were:

1. to determine the effect of alginate gel formation on retention of particles during simultaneous filtration of alginate and particles
2. to test whether this effect on retention of particles is similar for alginate gel layers pre-formed on a clean membrane
3. to test whether gel layers formed in a lab scale membrane bioreactor have a similar effect on retention of particles
4. to find out whether combined particle fouling and gel layer formation results in faster flux decline than the separate fouling mechanisms.

MATERIALS AND METHODS

Materials

Commercially available low viscosity sodium alginate with a molecular weight distribution between 80 and 120 kDa (Sigma) extracted from brown algae was used in all experiments. Alginate solution was prepared by dissolving 50 mg of sodium alginate in 1 liter of demineralised water while continuously stirring. A CaCl2·2H2O (Boom, the Netherlands) solution was added in small steps to a final calcium concentration of 5 mM. This calcium to alginate ratio is in agreement with the ratios applied in previous studies on alginate fouling (Katsoufidou et al., 2007; van den Brink et al., 2009; van de Ven et al., 2007). The ionic strength was adjusted to 16 mM by adding KCl (Boom, the Netherlands). Home-made polyvinylidene fluoride (PVDF) membranes were casted from a PVDF/PVP/NMP solution on a polyester nonwoven support (Freudenberg FO 2406). Resulting nominal pore sizes were 0.1 µm, as determined with scanning electron microscopy (SEM, JEOL-6480LV) followed by image processing (ImageJ, NiH) and bubble point analysis (van der Marel et al., 2010). Membrane resistance of these home-made membranes was $4.3*10^{10}$ m^{-1} as reported previously (van der Marel et al., 2010). Also, commercially available PVDF membranes with a nominal pore size of 0.45 µm according to supplier's specifications (Millipore, Durapore), were used in the experiments. By performing clean water flux experiments with 0.45 µm PVDF membranes, an average membrane resistance of 0.83 $*10^{10}$ m^{-1} was determined for these membranes (Alhadidi et al., 2011). A new membrane was used for each experiment.

Experiments were carried out using commercially available suspensions (1% solids) of fluorescent polystyrene microspheres of two measured mean diameters: 0.025 µm and 0.11 µm (Thermo Scientific, USA), from this point onwards named "small" and "big" particles (SP and BP, respectively). Particle concentrations in the commercially available suspensions were $1.2*10^{15}$ and $1.4*10^{13}$ particles per ml for small (SP) and big (BP) particles, respectively.

The SP and BP had specific excitation/emission wavelengths of respectively 468/508 nm (green) and 542/612 nm (red). Particle suspensions were prepared by diluting the required volume of particle suspension in MilliQ water, 50 mg L^{-1} alginate solution, or MBR permeate.

Filtration set-up

Filtrations were performed using a dead-end filtration cell with a volume of 450 ml and an effective membrane area of 0.0040 m^2. The filtration cell was connected to pressurized air which ensured a maximum of 2 bar pressure on the membrane. Permeate production was continuously measured with a mass balance (Kern, Germany) and recorded using Labview software (National Instruments, USA).

A separate membrane filtration set-up, referred to as "filterability set-up", connected to a pilot scale MBR treating municipal wastewater, provided gel layer fouled membranes for the dead-end filtrations. The combination of the filterability set-up and the pilot MBR was described before (van den Brink et al., 2013). Total resistances of the fouled membranes just before sampling are reported in Table 3.1.

Experiments

Particle suspensions were diluted 1000 times by adding 0.4 ml of particle suspension to a total volume of 400 ml milliQ water, alginate solution, or MBR permeate and subsequently put in the test cell with a syringe (Table 3.1). This resulted in a particle concentration of 10 mg L^{-1} (number of particles per ml: $1.2*10^{12}$ for SP and $1.4*10^{10}$ for BP) and, taking into account the applied alginate concentration of 50 mg L^{-1}, a mass ratio m_{part}: $m_{alginate}$ of 0.2. For the mixture, 0.4 ml particle suspension of both particles was applied, resulting in a mass ratio m_{part}: $m_{alginate}$ of 0.4. A sample of the feed solution was taken to measure its fluorescence. The filtration was carried out at a transmembrane pressure (TMP) of 0.5 bar with either a clean or a fouled membrane. A TMP of 0.5 bar was selected for all constant pressure filtrations, because the fouled membranes required a relatively high TMP for filtration. In all filtrations the feed solution was unstirred, similar to experiments performed by Ye et al. (2005). Permeate samples were taken regularly to monitor the concentration of particles in time.

The total resistance was calculated from the TMP (Pa), membrane flux and feed solution viscosity, according to the following expression:

$$R_t = TMP/(\eta J) \quad (1)$$

where R_t is total resistance (m^{-1}), η the feed solution viscosity (Pa s) and J the membrane flux ($m^3\ m^{-2}\ s^{-1}$) .

Filtration data were plotted as total resistance versus filtrated volume (V). A typical example of this type of curve is shown in Figure 3.1. Cake filtration is assumed to be the main fouling mechanism, as occuring in colloidal fouling (Mulder, 2000). Fouling rate was obtained by determining the slope of the R vs. V curve. Because this curve is comparable with a plot of t/V as a function of V, the fouling rate obtained from this curve as shown in Figure 3.1 can be compared with the modified fouling index (MFI) (Mulder, 2000; Alhadidi et al., 2011). When fouling occurs, the curve shows a steep slope. Fouling rates for all experiments are shown in Table 3.3. Apart from the fouling rates, also total filtration times were reported in that Table.

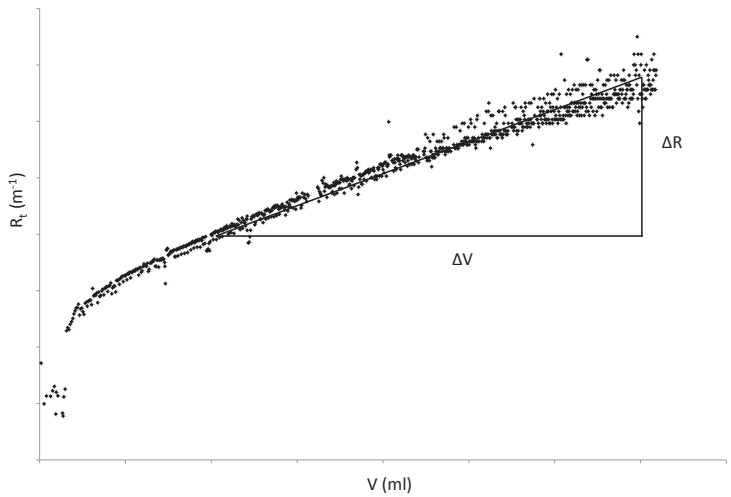

Figure 3.1 Typical curve representing increase of resistance caused by cake formation during dead-end filtration.

Apart from filtration tests with clean membranes, also fouled membranes were used for the filtrations. Alginate fouled membranes were obtained by filtering 500 ml of a 50 mg L^{-1} alginate solution in a dead-end filtration cell. The gel layer fouled membranes were taken from separate filterability set-ups, filtering sludge from a pilot scale MBR, as described above. Constant flux filtrations were performed in these filterability set-ups at fluxes between 11 and 36 L m^{-2} h^{-1}. Membrane fluxes were measured manually every day. Formation and resistance of the gel layers was estimated by on-line TMP measurements. At several points in time, membrane samples with different total resistances (reported in Tables 3.1-3.3) were taken for dead-end filtrations with particles. Membranes were sampled by cutting a circle of 0.0040 m^2 out of the membrane material. Particle filtration using the gel layer fouled membranes was performed as described above.

An overview of the different experiments is given in Table 3.1.

Table 3.1 Overview of experiments (SP = small particles, diameter 0.025 µm, BP = big particles, diameter 0.11 µm).

Name	Conc. SP (#/ml)	Conc. BP (#/ml)	Solution	Nominal membrane pore size (µm)	Total resistance before particle filtration (m^{-1})
Water – SP	$1.2*10^{12}$	-	milliQ	0.1, 0.45	n/a
Water – BP	-	$1.4*10^{10}$	milliQ	0.1, 0.45	n/a
Water – mix	$1.2*10^{12}$	$1.4*10^{10}$	milliQ	0.1, 0.45	n/a
Alginate	-	-	alginate	0.1	n/a
Alg – SP	$1.2*10^{12}$	-	alginate	0.1, 0.45	n/a
Alg – BP	-	$1.4*10^{10}$	alginate	0.1, 0.45	n/a
Alg – mix	$1.2*10^{12}$	$1.4*10^{10}$	alginate	0.1, 0.45	n/a
Alg layer – SP	$1.2*10^{12}$	-	permeate	0.1	n/a
Alg layer – mix	$1.2*10^{12}$	$1.4*10^{10}$	permeate	0.1	n/a
Gel layer – SP	$1.2*10^{12}$	-	permeate	0.1	$6.10*10^{12}$
Gel layer – SP	$1.2*10^{12}$	-	permeate	0.1	$4.55*10^{11}$
Gel layer – mix	$1.2*10^{12}$	$1.4*10^{10}$	permeate	0.1	$5.23*10^{12}$
Gel layer – mix	$1.2*10^{12}$	$1.4*10^{10}$	permeate	0.1	$1.21*10^{11}$

Analyses

Fluorescence of the samples was measured with a spectrofluorometer (Victor^3 1420, Multilabel Counter, Perkin Elmer, France). For this purpose, 1 ml sample was placed in a 24 well microtiter plate (Falcon, Becton Dickinson and Co., France) and fluorescence was measured during 1 second at the required specific excitation/emission wavelengths: 465/510 nm for small particles and 540/610 nm for big particles. Calibrations curves were constructed for particles suspended in water, permeate and alginate solution. From these calibration curves, particle concentrations could be deducted.

To assess the retention of alginate by the membrane, permeate samples were taken at the start and end of filtration, and analysed for total organic carbon (TOC) concentrations with a Shimadzu analyzer (TOC-V_{CPH}, Shimadzu, Japan).
To calculate the observed retention of the particles and alginate during filtration, the following formula was used (Mulder, 2000):

$$R = ((C_{bulk} - C_{perm})/C_{bulk})*100\% \quad (2)$$

Where R is retention (%), C_{bulk} is the concentration of particles or alginate in the bulk solution (number of particles ml^{-1} or mg l^{-1}, respectively) and C_{perm} is the concentration of particles or alginate in the permeate (number of particles ml^{-1} or mg l^{-1}, respectively).

Distribution of particles on the membrane was visualised with scanning electron microscopy (SEM) and with confocal laser scanning microscopy (CLSM). Surfaces of the fouled membranes were investigated with a JEOL-6480LV SEM (Japan). Samples were coated in a JEOL JFC-1200 fine coater with a thin (10 nm) Au (gold) layer for observation under high vacuum (HV). Au coated samples were investigated at 6 kV, working distance (WD) 10 mm and spot size (SS) 20.

A CLSM was used to visualize the fluorescent particles on the membrane in different spatial directions. A Laser Scanning Module (LSM 510) was used which was coupled to an inverse microscope (100 M BP, Zeiss, Germany). For the CLSM analysis, a gel layer was used and particles were filtered as described above. Pieces of the membrane were cut out and placed on the objective slide using a glycerol mounting solution. For imaging, a multi-track mode was used to obtain selective excitation and detection of the fluorescent particles. Images were processed using the AxioVision 3.1 software (Zeiss, Germany).

RESULTS

To investigate the effect of gel layer formation by alginate on particle retention, retention of the particles without alginate had to be studied first, as well as the retention of alginate by the membranes. For the commercially available PVDF membranes with a nominal pore size of 0.45 µm, retention values above 90% were found for 50 mg l^{-1} alginate. For the home-made PVDF with nominal pore sizes of 0.1 µm, similar or even higher retention values were expected as the pore sizes are much smaller than for the 0.45 µm membrane. High retention for alginate on membranes with pore sizes of 0.1 µm was also shown in previously reported experiments (van den Brink et al., 2009). Retention of small (diameter 0.025 µm) and big particles (diameter 0.11 µm) in water was checked for both particle sizes separately as well as for a mix of both particles. These experiments in water were followed by filtrations of a mixture of alginate and particles. Whether alginate would also influence particle retention when it had already fouled the membrane by forming a gel layer, was tested in two types of experiments: one using alginate fouled membranes, and one with gel layer fouled membranes from a filterability set-up connected to a pilot scale MBR. All retention values can be found in Table 3.2. Fluorescence of the permeate was measured at several points in time during filtration. Except for the filtration of small particles in water on a 0.1 µm membrane in which retention increased from 25 to 100% during filtration, retention stayed constant during filtration (data not shown). Apart from the retention, also the flux decline was monitored during the filtrations (Table 3.3). The distribution of particles in the alginate gel layers as well as in the gel layers formed in a filterability set-up connected to a pilot scale MBR was investigated with SEM (Figure 3.2) and CLSM (Figures 3.3 and 3.4).

Table 3.2 Retention values for all experiments (SP = small particles, diameter 0.025 µm, BP = big particles, diameter 0.11 µm). When a range is given, different retention values (constant during filtration) were found for the replicates.

Name	Total resistance before particle filtration (m^{-1})	Pore size (µm)	Number of replicates	Retention SP (%)	Retention BP (%)
Water – SP/BP	n/a	0.1	3	25 → 100*	100
	n/a	0.45	1	10	5
Water – mix	n/a	0.1	3	100	100
	n/a	0.45	1	10	10
Alg – SP/BP	n/a	0.1	3	100	100
	n/a	0.45	2	100	100
Alg – mix	n/a	0.1	3	95-100	100
	n/a	0.45	2	95-100	100
Alginate	n/a	0.45	1	90-100**	
Alg layer – SP	n/a	0.1	2	90	
Alg layer – mix	n/a	0.1	1	90	100
Gel layer – SP	$6.10*10^{12}$	0.1	1	95	
Gel layer – SP	$4.55*10^{11}$	0.1	1	90	
Gel layer – mix	$5.23*10^{12}$	0.1	1	85-90	100
Gel layer – mix	$1.21*10^{11}$	0.1	1	85-90	100

* In these experiments, retention increased during filtration from 25 % to 100 %. This increase took (on average) 5 minutes.

** Retention of alginate.

Particle retention during filtration of particles in water and in alginate solutions

Most small particles in water passed the 0.1 µm pores in the beginning of filtration (retention 25%) and showed increasing retention during filtration, despite their 4 times smaller diameter than the pore size. Due to dilution of particles in the permeate by "dead volume" water present in the membrane, support material, support plate and tubing of the filtration cell, initial retention could be overestimated. The real initial retention could then be even lower than 25%. Increasing retention during filtration could be explained by adsorption of these particles in the internal membrane surface or by aggregation of small particles in solution or at the membrane surface. Big particles in water were retained by the membrane with 0.1 µm pores already from the start of filtration. In a mixture of small and big particles in water, both particles were retained on the membrane with 0.1 µm pores from the start of filtration. No matter whether the particles are filtered separately, or in a mixture, both types of particles passed the membrane with 0.45 µm pores.

When filtered in alginate solution, small and big particles were retained by both 0.1 µm and 0.45 µm pores. This held for the mixture as well.

Particle retention by previously formed layers

Alginate layers and gel layers formed in a filterability set-up connected to a pilot scale MBR increased retention for both particles up to 90-100% as compared to filtration of these particles in water using membranes with 0.1 and 0.45 µm pores. This holds for particles filtrated separately as well as for the mixture of small and big particles. The retention behaviour of alginate layer and gel layers formed in a filterability set-up connected to a pilot scale MBR was similar. The retention of particles by gel layer fouled membranes was not influenced by the resistance of the gel layers (Table 3.2).

Filtration behaviour

The filtration data of the dead-end filtration experiments can be found in Table 3.3. For replicates, mean values are given including range of the measurements. Filtrations of particles from a water solution did not result in membrane fouling of the 0.45 µm pore membrane, as resistance did not increase with filtered volume and filtrations were finished within a few minutes. Fouling was observed for neither small and big particles filtered separately nor for the mixture of both particles when filtered through membranes with 0.45 µm pores. When applying membranes with 0.1 µm pores, only little fouling was observed: small fouling rates and short filtration times were obtained for these filtrations as compared with the other filtrations presented in Table 3.3. However, for the mix of small and big particles in water, considerable fouling was observed for the membrane with 0.1 µm pores.

Filtration of the sole alginate solution showed a higher fouling rate and longer filtration time than for the single particles in water. When particles were added to the alginate solution, increased fouling could clearly be observed from the filtration data: larger fouling rates and longer filtrations times than for the particles in water and the sole alginate solutions. For the small particles, big particles and the mixture in alginate, less fouling was found on 0.45 µm pore membranes than on 0.1 µm pore membranes. Comparing small and big particles in alginate solutions, the small particles fouled more than the big particles.

Filtering small particles using an alginate “pre-fouled” membrane took more time than simultaneous filtration of alginate and small particles. For gel layers formed in a filterability set-up connected to a pilot scale MBR, fouling development by particles was dependent on the resistance of the gel layer as determined in the filterability set-up. The membranes containing gel layers with different resistances were taken from the filterability set-up and applied in the dead-end filtration cell for particle filtrations. Higher resistance gel layers showed longer filtration times but no further fouling development. Filtration times and fouling rates for a mixture of particles on an alginate layer were in the same range as for all particles filtered in alginate solution. Small particles filtered on an alginate layer showed more severe fouling than the same particles filtered in alginate solutions.

Table 3.3 Filtration times and fouling rates obtained from dead-end filtrations of different solutions using membranes with 0.1 µm or 0.45 µm pores.

Name	Total resistance before particle filtration (m^{-1})	Pore size (µm)	Mean filtration time (min) & range	Mean ΔR/ΔV (10^8 m^{-1} ml^{-1}) & range
Water – SP (n=2)	n/a	0.1	6.00 (4.00-8.00)	6.88 (0.35-13.4)
Water – SP	n/a	0.45	4.47	0
Water – BP (n=2)	n/a	0.1	4.50 (4.50-4.50)	4.25 (4.25-4.25)
Water – BP	n/a	0.45	4.70	0
Water – mix (n=2)	n/a	0.1	14.00 (11.00-17.00)	19.9 (17.4-22.3)
Water – mix	n/a	0.45	4.60	0
Alg – SP (n=3)	n/a	0.1	23.6 (21.0-25.5)	38.1 (30.8-49.7)
Alg – SP (n=2)	n/a	0.45	17.5 (17.2-17.8)	22.0 (18.0-26.0)
Alg – BP (n=2)	n/a	0.1	18.4 (17.8-19.0)	25.0 (23.0-27.0)
Alg – BP (n=3)	n/a	0.45	11.5 (8.0-13.3)	15.4 (9.75-18.5)
Alg – mix (n=2)	n/a	0.1	18.5 (13.0-24.0)	21.8 (13.8-29.8)
Alg – mix (n=2)	n/a	0.45	16.2 (15.0-17.3)	10.8 (7.75-13.8)
Alginate	n/a	0.1	7.3	9.44
Alg layer – SP	n/a	0.1	52	47.5
Alg layer – mix	n/a	0.1	18	22.8
Gel layer – SP	$6.10*10^{12}$	0.1	130	0
	$4.55*10^{11}$	0.1	21	13.0
Gel layer – mix	$5.23*10^{12}$	0.1	135	0
	$1.21*10^{11}$	0.1	15.4	17.3

Particle distribution

The distribution of the fluorescent particles in both alginate and real gel layers was investigated by SEM and CLSM.

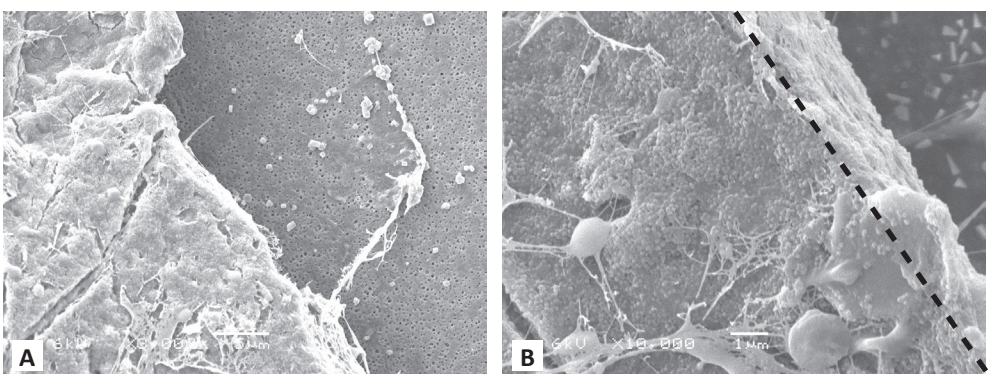

Figure 3.2 SEM images of a clean 0.1 µm pore size PVDF membrane (A) and a gel layer fouled 0.1 µm pore size PVDF membrane from the filterability set-up after filtration of SP and BP (total resistance before particle filtration R=1.57 $*10^{12}$ m^{-1}) (B), magnification: 10,000x. Left of the dashed line in B, particles are visible in the gel layer.

In Figure 3.2A, a clean 0.1 µm pore size PVDF membrane is shown. Figure 3.2B shows a gel layer formed in the filterability set-up on which small and big particles were filtered. Left of the dashed line in Figure 3.2B, the particles seem to be incorporated in the layer. The fibrillar structures are typical for the EPS matrix observed on biofouled membranes (Bereschenko et al., 2010).

Figure 3.3A shows the distribution of both small and big particles in a previously formed alginate layer and Figures 3.3B and 3.3C show the distribution of the separate particles in the alginate layer. The small particles are shown in green and the big particles in red. In the case both green and red particles are present in a certain area, the colour changed to orange/yellow. At the alginate layer-air interface, the majority of the particles seemed to be small. From 2D cross section images in the (z,y)- and (z,x)-directions that were constructed using the CLSM data, the average thickness of the particle layer was estimated at 7 µm (data not shown). Particles were in general homogeneously distributed, though differences between deposition of small and big particles were observed around the irregularities in the gel layer (Figure 3.3A).

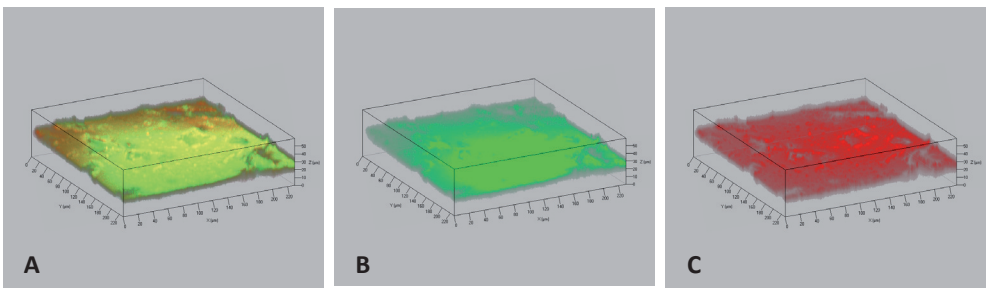

Figure 3.3 Distribution of SP and BP in a previously formed alginate layer on a 0.1 µm pore size PVDF membrane, magnification: 400x. Upper side (Z=60 µm): alginate layer-air interface, lower side (Z= 0 µm): alginate layer-membrane interface. A. Distribution of SP (green) and BP (red). B. Distribution of SP. C. Distribution of BP.

Figure 3.4A shows the distribution of both small and big particles in a gel layer formed in a filterability set-up connected to a pilot scale MBR and Figures 3.4B and 4C show the distribution of the separate particles in the same layer. The gel layer formed in a filterability set-up connected to a pilot scale MBR was rather rough due to sludge particles present in the layer and on the membrane. From 2D cross section images in the (z,y)- and (z,x)-directions that were constructed using the CLSM data, the average thickness of the particle layer was estimated at 6 µm (data not shown). The small particles seem to be more evenly distributed than the big particles (Figures 3.4B and 3.4C). Big particles are present in small groups while the small particles are dominantly present on one half of the sample, though

within that area they are evenly distributed. Looking at Figure 3.4A, in which the signals for both particles were combined, there are areas with either small or big particles and areas that contain both.

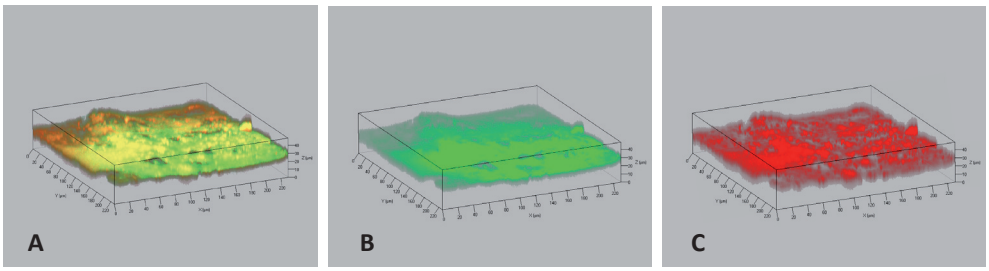

Figure 3.4 Distribution of SP and BP in a gel layer formed in the filterability set-up on a 0.1 µm pore size PVDF membrane (total resistance before particle filtration R=5.23 *10^{12} m^{-1}), magnification: 400x. Upper side (Z=50 µm): gel layer-air interface, lower side (Z= 0 µm): gel layer-membrane interface. A. Distribution of SP (green) and BP (red). B. Distribution of SP. C. Distribution of BP.

DISCUSSION

Particle retention during simultaneous filtration of alginate and particles

Particles that were passing the pores when filtered in a water solution were completely retained when filtered in alginate solution. This retention was observed directly at the start of filtration. The applied concentration of alginate is representative for the SMP (of which polysaccharides are a large fraction) concentration in MBR supernatant (Drews, 2010).

The applied mass ratio of particle and alginate was 0.2 when a single particle size was applied and 0.4 for the mixture. These ratios are similar to those applied during filtration of BSA on membranes “pre-fouled” with a Ca-alginate layer (Wang and Waite, 2008a). In these experiments the ratio BSA to alginate ranged from 0 to 0.5. At ratios of 0.2 or higher, retention of BSA was lower than 50%. This shows that, when the Ca-alginate layer is regarded as an adsorption medium, at high BSA to alginate ratios the Ca-alginate layer is not able to adsorb the BSA anymore resulting in BSA passing the membrane. In case retention behaviour of BSA and polystyrene particles is similar, the ratios particle to alginate applied in our experiments (0.2 and 0.4) are sufficiently high to measure possible column breakthrough and thereby to test whether the alginate indeed acted as an adsorption column. It should be taken into account that though the size of BSA and the small polystyrene particles are in the same order of magnitude, their interactions with alginate could differ due to their different physic-chemical nature.

While several researchers have explained increased retention of low molecular weight

compounds by the formation of a fouling layer during long-term MBR operation (Shin and Kang, 2003; Li and Chu, 2003), this can not directly be compared with the results presented in this study due to the differences in timescales of the experiments. In the experiments presented above, increased retention of particles was shown at the same time the alginate is fouling the membrane by gel layer formation. Retention of compounds smaller than the pore size by simultaneous formation of a fouling layer was found for constant pressure filtration of other substances, such as humic acids (Yuan and Zydney, 1999) and natural organic matter (NOM) (Taniguchi et al., 2003). Since the mean diameters of the small and big particles, 0.025 and 0.11 µm respectively, are similar to the different radii of gyration reported for the alginate molecule (0.050 ± 0.007 to 0.137 µm) (Wedlock et al., 1986; Bowen and Cooke, 1991; Windhues and Borchard, 2002), the hydrodynamic forces acting on the particles and alginate molecules are expected to be in the same order of magnitude (Bhattacharjee and Hong, 2005). This implies the particles and alginate molecules are approaching the membrane surface at the same time, possibly forming a fouling layer simultaneously as well.

Particle retention by previously formed layers

Alginate layers and gel layers formed in a filterability set-up connected to a pilot scale MBR showed increased retention for both particles up to 90-100%, compared to filtration of these particles in water using new membranes with 0.1 and 0.45 µm pores. These findings are partly in line with the retention of BSA (60 kDa) and catalase (250 kDa) by a Ca-alginate gel formed at different pressures (12.5 and 100 kPa) (Wang and Waite, 2008a). Single catalase molecules with a diameter of 0.0112 µm were found to pass the Ca-alginate gel, while larger aggregates were mostly retained. Apparent channel sizes of 0.005-0.025 µm (depending on applied pressure and the position in the gel) were estimated for the Ca-alginate gel. The retention of BSA (diameter 0.007 µm (Yohannes et al., 2010)) was explained by adsorption in the Ca-alginate gel which had a maximum capacity, after which breakthrough took place. This was observed as a decrease in retention upon increase of the mass ratio of BSA: alginate. Because in our experiments, retention stayed constant during filtration at values of 90-100 %, no breakthrough of particles was observed for the previously formed layers. As well as for the simultaneous filtration of alginate and particles, adsorption seems to be less suitable than other mechanisms to explain the high retention of previously formed layers.
Although the study of Wang and Waite (2008a) is similar to the experiments presented here, the alginate gels in our study were prepared from a 50 mg L^{-1} solution instead of 1 g L^{-1}. 50 mg L^{-1} is more representative to concentrations found in MBR supernatant (Drews, 2010).

To see whether the retention of the tested alginate layers was similar to that of gel layers from a filterability set-up connected to a pilot scale MBR, the latter were also checked for

their retention of small particles and of the mixture of particles. The retention behaviour was found to be similar for both types of layers. Although model polymers are not representative for MBR foulants concerning several aspects (sources, different chemical structure, absence of solid matrix, pH and ionic strength often not representative, MBR foulants are a mixture of compounds, aggregate size may change during experiment) (Drews, 2010), alginate gel layers seemed suitable to mimic MBR gel layers concerning particle retention. Microscopic investigation of particle distribution in previously formed alginate layers and in gel layers formed in a filterability set-up connected to a pilot scale MBR revealed similar distribution patterns and average particle layer thicknesses of 7 and 6 µm. This also pleads for the representativeness of alginate gel layers in the here presented experiments on retention of particles.

The retention of small particles by gel layer fouled membranes was not influenced by the resistance of the gel layers. Although Wang and Waite do not report filtration resistances in their colloid retention experiments (2008a), the pressure at which the Ca-alginate was formed was variable in these experiments. This pressure could be related to filtration resistance, with higher pressures possibly leading to higher resistances due to compression. No differences were found in retention of BSA and single catalase molecules for Ca-alginate gels prepared at different pressures, which is similar to what was found in our experiments. In contrast to these findings, higher removal efficiencies of bacteriophages (mean size 0.2 µm) at increased filtration resistances were reported for a MBR treating domestic sewage, while the membrane alone (pore size 0.4 µm) demonstrated poor removal efficiency (Ueda and Horan, 2000). This was explained by biofilm accumulation on the membrane surface, which could increase the removal in the following three manners: (1) reduction of the effective pore size by fouling development, (2) adsorption of viruses to bacterial cells and (3) predation of viruses by microorganisms. The first mechanism could hold for our experiments as well. The other two were less likely to have played a role as the only gel layers that possibly contained bacteria were the ones from the filterability set-up. Further on, the focus will be on mechanisms of fouling and retention.

Contribution of alginate to membrane fouling

Although retention for the membranes with 0.1 µm pores was 100% already at the start (big particles) or at the end of filtration (small particles), little or no fouling was observed for filtrations of particles from a water solution. Apparently, fouling can not be directly related to particle retention. For the mix of small and big particles in water, fouling was observed for the membrane with 0.1 µm pores. Binary mixtures of particles are more likely to form a less permeable cake on the membrane than single particles, as the voids between the big particles can be filled with small particles (Lee and Koo, 2013). Binary mixtures of particles

are more comparable to MBR supernatants than solutions containing a single particle size, as the supernatants typically have a particle size distribution (van den Brink et al., 2011).

The applied fluorescent particles are made of polystyrene, to which surfactants have been added to suspend them in efficiently in the liquid. This makes their surfaces hydrophilic. The PVDF membrane surface is also hydrophilic. Due to the hydrophilicity of both surfaces, little adsorption of particles on the outer or inner surface of the membrane could be expected. While in some particle in water filtrations the particles are retained on or in the membrane (in the case of BP-0.1 µm pores there was 100% retention), this apparently adds little fouling resistance to the membrane resistance. This can be explained by the low compressibility of the particles. Lower resistance cake layers can be expected during filtration of polystyrene particles of which the deposits were reported to be non-compressible at a pressure range of 0.5-1.0 bar (Teychene et al., 2011), compared to highly compressible material such as flocculated clays and microbial cells (Belfort et al., 1994).

When alginate was added to the particles, fouling could clearly be observed from the fouling rate and filtration times. The filtration times of particles in alginate using membranes with 0.45 µm pores were 2 to 3 times longer than for particles in water filtrations. It can be stated that, for the tested alginate concentration of 50 mg L^{-1} and mass ratio of particle and alginate of 0.2, increased retention comes at the cost of flux decline. In light of practical applicability, it would be interesting to know what is the minimum alginate concentration or highest mass ratio of particle and alginate that would still show full retention.
Fouling rates for particles in alginate solutions were in the same range as for the same particles on pre-made (alginate) gel layers. Both types of filtrations are relevant for practice: the alginate solution with particles can be compared with the start-up of a MBR, while the pre-made layers are comparable to gel layers that are often present on membranes during long-term sub-critical flux operation of MBRs (Wang et al., 2008; van der Marel et al., 2010).

For the particle in alginate solutions, less fouling was found on 0.45 µm pore membranes than on 0.1 µm pore membranes. This could be explained by formation of channels in the alginate gel layer as described earlier (Wang and Waite, 2008b), causing a more open fouling layer. Larger channel sizes may form on 0.45 µm pore membranes than on 0.1 µm pore membranes due to higher fluxes through the larger pores. The difference in fouling behaviour of these two membranes could be of importance when forming a dynamic membrane layer that increases retention but causes an acceptable flux decline. Also, when comparing small and big particles in alginate solutions, small particles foul more than the big particles. Faster initial flux decline for a decrease in the particle size of the suspension has been also observed experimentally (Hong et al., 1997). For binary mixtures, lower permeability was

observed for a relatively high fraction of small particles (Lee and Koo, 2013).

Gel layers formed in the filterability set-up connected to a pilot scale MBR showed different fouling rates depending on their resistance at the start of the particle filtration. The high resistance gel layers showed no additional fouling development when small particles or the mixture of both particles were filtered, while the low resistance gel layers did foul upon filtration of these particles. Apparently, small particles and the mixture of both particles did not add any resistance to existing high resistance gel layers, while still resistance could be added to low resistance gel layers.

Retention and fouling mechanisms

In literature, several mechanisms were suggested for increasing retention of compounds smaller than the pore size by fouling layers:

1. Lowering the apparent pore channel size and thereby causing steric hindrance (Wang and Waite, 2008a; Taniguchi et al., 2003; Chang et al., 2001)
2. Adsorption of these compounds in the fouling layer (Wang and Waite, 2008a; Taniguchi et al., 2003; Ognier et al., 2002)
3. Biodegradation of these compounds in the fouling layer (in case the fouling layer is a biofilm) (Ueda and Horan, 2000; Park and Lee, 2005)

As explained above, the second and third mechanism were less likely to have played a role in our experiments. The mechanisms mentioned above are all assuming the existence of a fouling layer on the membrane. As mentioned before, the hydrodynamic forces acting on the particles and alginate molecules were expected to be in the same order of magnitude. This would mean the particles and alginate molecules were approaching the membrane surface simultaneously, forming a fouling layer at that moment. In that case there would not have been an alginate gel layer at the start of filtration, by which the particles could have been hindered. Therefore, at least one other mechanism should be considered to explain the high retention at the start of these filtrations. A possible explanation could be the interaction of the particles with the soluble alginate, followed by formation of alginate-particle aggregates (which could not pass the membrane pore) or followed by gel formation on the membrane. Based on the performed experiments it is not possible to determine which mechanisms were most important. Further experiments should focus on retention mechanisms that play a role here.

From model compounds to practice

The experiments presented in this paper were performed with model compounds. In this Paragraph, an outlook is given to the practical relevance of the experimental results. Sodium alginate is the most commonly used model compound for polysaccharides, because it is

an important microbial polysaccharide and it was extensively studied (Mayer et al., 1999; Katsoufidou et al., 2007; Davis et al., 2008). A recent study that compared the alginate-like exopolysaccharides of aerobic granular sludge and aerobic flocculent sludge shows the importance of these exopolysaccharides for the sludge performance (Lin et al., 2013). The retention behaviour of pre-made alginate layers and gel layers from a filterability set-up connected to a pilot scale MBR was found to be similar for both types of layers. Therefore, the results obtained here can be used to predict particle retention by SMP in a MBR.
The mean diameter of the small particles (0.025 µm) is in the same range as those of noroviruses (0.027-0.038 µm) (Prasad et al., 2001), causing diarrhea by transmission via contaminated water and food (Patel et al., 2009). The mean diameter of the big particles (0.11 µm) is comparable to those of adenoviruses (0.110-0.118 µm) (Stewart et al., 1991; Cotton and Weber, 1995), which cause a wide range of illnesses and are spread via respiratory droplets and via fecal routes. Both small and big particles can be considered as nanoparticles. Virus and nanoparticle retention would greatly improve effluent quality of MBRs. In case MBR effluent is to be reused (either without or with further treatment), the effluent without viruses and nanoparticles is more attractive for direct reuse and saves on further treatment costs.

Virus retention or removal in MBRs has been extensively described (Ueda and Horan, 2000; Marti et al., 2011; Sima et al., 2011; Simmons et al., 2011). These studies report long term operation of pilot or full scale MBRs. Because of the complexity of the mixed liquor present in these systems and the limited data on the start-up of filtration, the mechanisms of virus retention or removal cannot easily be deducted from this type of research.

Some researchers explain enhanced virus retention or removal in MBRs as blockage or entrapment by a gel layer (Ueda and Horan, 2000; Zheng and Liu, 2007; Wu et al., 2010), adsorption to bacterial cells and EPS or biodegradation of these compounds in the fouling layer (Ueda and Horan, 2000). Ueda and Horan suggested long term operation of a MBR to allow development of a biofilm and thereby enhancing virus removal (2000). Virus retention or removal during start-up of a MBR was not considered in the mentioned MBR studies. Gel layer formation by polysaccharides present in MBR supernatant, or in case the concentration of polysaccharides is not sufficiently high, by addition of extra alginate, could be a strategy to obtain nanoparticle and virus retention or removal from the start of filtration. From our experimental results, in which alginate increased retention for particles smaller than the pore size, alginate seemed to be a suitable compound to create a dynamic membrane layer. Because gel layers formed in a filterability set-up connected to a pilot scale MBR were also found to increase retention for particles smaller than the pore size, these gel layers could act as dynamic membrane layers as well. Removal of the (alginate) gel layer when it

gives too much resistance could be achieved by adding sodium ions to the feed solution or, preferably, performing a backwash with a solution containing a high sodium concentration. Sodium competes with calcium for carboxyl groups on the alginate polymer and at high ionic strengths, ion exchange may take place (Martinsen et al., 1989; Draget et al., 1998; Neiser et al., 1999; de Kerchove and Elimelech, 2006). When the calcium ion is exchanged for sodium, the bridging effect of divalent cations with alginate is abolished, thereby releasing alginate molecules back into the solution and diminishing the gel layer. Another option would be to use deionised water instead of a sodium solution, which could force the leakage of calcium ions out of the alginate layer due to its low ionic strength. This strategy has been proven for a membrane fouling layer consisting of alginate and humic acid (Resosudarmo et al., 2013) and for fouling layers developed during seawater or natural surface water filtration (Li et al., 2011; Li et al., 2009).
Other strategies for creating a secondary of dynamic membrane layer with different rejection capacities are starting up at a high flux (60 L m^{-2} h^{-1}) for 1-2 min, followed by a lower flux (Wu et al., 2008b) and applying a 100 µm mesh instead of a microfiltration membrane (Fan and Huang, 2002).

Retention data presented in this paper showed full retention of particles from the start of filtration. These experiments were performed with 50 mg L^{-1} alginate and a mass ratio particle: alginate of 0.2. Further research should be performed to know how much higher mass ratio of particle and alginate would still show the same retention values. Less fouling could be expected at lower alginate concentrations, because less alginate is available to foul the membrane.
Moreover, experiments presented here should be repeated in a filtration system with shear force, as this is more representative for MBR operation. Finally, membrane selection is crucial for a proper balance between retention of particles while keeping a sustainable flux value. Pore size, porosity and morphology of the membrane would be most important here.

CONCLUSIONS

Studying the interaction of alginate and particles in dead-end filtration led to the following conclusions:

1. Gel layer formation increases particle retention.
2. Simultaneous filtration of alginate and particles shows a higher fouling rate than filtration of the solutions containing only alginate or particles.

Diameters of the applied particles were similar to those of viruses and nanoparticles. Therefore, the information obtained in this research could be useful for virus and

nanoparticle retention or removal in MBRs. More research should be performed to evaluate whether the findings of this research also hold for viruses and nanoparticles. Gel layer formation by polysaccharides present in MBR supernatant, or in case the concentration of polysaccharides is not sufficiently high, by addition of extra alginate, could be a strategy to obtain virus and nanoparticle retention or removal from the start of filtration.

ACKNOWLEDGEMENTS

This work was performed in the cooperation framework of Wetsus, centre of excellence for sustainable water technology (www.wetsus.nl). Wetsus is co-funded by the Dutch Ministry of Economic Affairs and Ministry of Infrastructure and Enviroµent, the European Union Regional Development Fund, the Province of Fryslân and the Northern Netherlands Provinces. The authors like to thank the participants of the research theme "Membrane processes and operation for wastewater treatment and reuse" for the fruitful discussions and their financial support. Witold Michalowski from the Biofilm Centre at the University of Duisburg-Essen is acknowledged for valuable help concerning the CLSM analyses. Special thanks also to Lena Faust and Lucie Averlant for their contributions to this work.

REFERENCES

Alhadidi A, Kemperman AJB, Blankert B, Schippers JC, Wessling M, van der Meer WGJ (2011) Silt Density Index and Modified Fouling Index relation, and effect of pressure, temperature and membrane resistance *Desalination* **273** (1), 48-56

Belfort G, Davis RH, Zydney AL (1994) The behavior of suspensions and macromolecular solutions in crossflow microfiltration *J. Membrane Sci.* **96** (1-2), 1-58

Bereschenko LA, Stams AJM, Euverink GJW, van Loosdrecht MCM (2010) Biofilm formation on reverse osmosis membranes is initiated and dominated by Sphingomonas spp. *Appl. Environ. Microbiol.* **76** (8), 2623-2632

Bhattacharjee S, Hong S (2005) Fundamentals of particle fouling in membrane processes *Korean Membrane J.* **7** (1), 1-18

Blanpain-Avet P, Fillaudeau L, Lalande M (1999) Investigation of mechanisms governing membrane fouling and protein rejection in the sterile microfiltration of beer with an organic membrane *Food Bioprod. Process.* **77** (2), 75-89

Bowen WR, Cooke RJ (1991) Properties of microfiltration membranes: computer automated determination of the electrokinetic properties of polycarbonate membranes *J. Colloid Interf. Sci.* **141**, 280-287

Chang IS, Bag SO, Lee CH (2001) Effects of membrane fouling on solute rejection during membrane filtration of activated sludge *Process Biochem.* **36** (8-9), 855-860

Chang IS, Le-Clech P, Jefferson B, Judd SJ (2002) Membrane fouling in membrane bioreactors for wastewater treatment *J. Environ. Eng.* **128** (11), 1018-1029

Choi H, Zhang K, Dionysiou DD, Oerther DB, Sorial GA (2006) Effect of activated sludge properties and membrane operation conditions on fouling characteristics in membrane bioreactors *Chemosphere* **63** (10), 1699-1708

Chu HP, Li XY (2004) Membrane fouling in a membrane bioreactor (MBR): sludge cake formation and fouling characteristics *Biotechnol. Bioeng.* **90** (3), 323-331

Cotton M, Weber JM (1995) The adenovirus protease is required for virus entry into host cells *Virology* 213 (2), 494-502

Davis TA, Pinheiro JP, Grasdalen H, Smidsrød O, van Leeuwen HP (2008) Stability of lead(II) complexes of alginate oligomers *Environ. Sci. Technol.* **42** (5), 1673-1679

de Kerchove AJ, Elimelech M (2006) Structural growth and viscoelastic properties of adsorbed alginate layers in monovalent and divalent salts *Macromolecules* **39**, 6558-6564

Draget KI, Steinsvåg K, Onsøyen E, Smidsrød O (1998) Na- and K-alginate; effect on Ca^{2+} gelation, *Carbohyd. Polym.* **35** (1-2), 1-6

Drews A (2010) Membrane fouling in membrane bioreactors - Characterisation, contradictions, cause and cures *J. Membrane Sci.* **363** (1-2), 1-28

Ersahin ME, Ozgun H, Dereli RK, Ozturk I, Roest K, van Lier J (2012) A review on dynamic membrane filtration: Materials, applications and future perspectives *Bioresource Technol.* **122**, 196-206

Hong S, Faibish RS, Elimelech M (1997) Kinetics of permeate flux decline in crossflow membrane filtration of colloidal suspensions *J. Colloid Interf. Sci.* **196** (2), 267-277

Fan B, Huang X (2002) Characteristics of a self-forming dynamic membrane coupled with a bioreactor for municipal wastewater treatment *Environ. Sci. Technol.* **36** (23), 4245-4251

Jermann D, Pronk W, Boller M, Schäfer AI (2009) The role of NOM fouling for the retention of estradiol and ibuprofen during ultrafiltration *J. Membrane Sci.* **329** (1-2), 75-84

Katsoufidou K, Yiantsios SG, Karabelas AJ (2007) Experimental study of ultrafiltration membrane fouling by sodium alginate and flux recovery by backwashing *J. Membrane Sci.* **300** (1-2), 137-146

Khor SL, Sun DD, Liu Y, Leckie JO (2007) Biofouling development and rejection enhancement in long SRT MF membrane bioreactor *Process Biochem.* **42** (12), 1641-1648

Lee H, Koo S (2013) Liquid permeability of packed bed with binary mixture of particles *J. Ind. Eng. Chem.*

Li XY, Chu HP (2003) Membrane bioreactor for the drinking water treatment of polluted surface water supplies *Water Res.* **37** (19), 4781-4791

Li S, Heijman SGJ, van Dijk JC (2011) Application of backwashing with demineralized water for UF fouling control in UF-RO desalination *Water Sci. Technol.: Water Supply* **11** (3), 364-369

Li S, Heijman SGJ, Verberk JQJC, Verliefde ARD, Kemperman AJB, van Dijk JC, Amy G (2009) Impact of backwash water composition on ultrafiltration fouling control *J. Membrane Sci.* **344** (1-2), 17-25

Lin YM, Sharma PK, van Loosdrecht MCM (2013) The chemical and mechanical differences between alginate-like exopolysaccharides isolated from aerobic flocculent sludge and aerobic granular sludge *Water Res.* **47** (1), 57-65

Marti E, Monclús H, Jofre J, Rodriguez-Roda I, Comas J, Balcázar JL (2011) Removal of microbial indicators from municipal wastewater by a membrane bioreactor (MBR) *Bioresource Technol.* **102** (8), 5004-5009

Martinsen A, Skjåk-Bræk G, Smidsrød O (1989) Alginate as immobilization material I: correlation between chemical and physical properties of alginate gel beads *Biotechnol. Bioeng.* **33** (1), 79-89

Mayer C, Moritz R, Kirschner C, Borchard W, Maibaum R, Wingender J, Flemming HC (1999) The role of intermolecular interactions: studies on model systems for bacterial biofilms *Int J. Biol. Macromol.* **26** (1) 3-16

Meng F, Chae SR, Drews A, Kraume M, Shin HS, Yang F (2009) Recent advances in membrane bioreactors (MBRs): Membrane fouling and membrane material *Water Res.* **43** (6), 1489-1512

Metzger U, Le-Clech P, Stuetz RM, Frimmel FH, Chen V (2007) Characterisation of polymeric fouling in membrane bioreactors and the effect of different filtration modes *J. Membrane Sci.* **301** (1-2), 180-189

Mulder M (2002) Basic Principles of Membrane Technology, Kluwers Academic Publisher, Dordrecht

Neiser S, Draget KI, Smidsrød O (1999) Interactions in bovine serum albumin-calcium alginate gel systems *Food Hydrocolloid.* **13** (6), 445-458

Ognier S, Wisniewski C, Grasmick A (2002) Influence of macromolecule adsorption during filtration of a membrane bioreactor mixed liquor suspension *J. Membrane Sci.* **209** (1), 27-37

Park JS, Lee CH (2005) Removal of soluble COD by a biofilm formed on a membrane in a jet loop type membrane bioreactor *Water Res.* **39** (19), 4609-4622

Patel MM, Hall AJ, Vinje J, Parashar UD (2009) Noroviruses: a comprehensive review *J. Clin. Virol.* **44** (1), 1-8

Pollice A, Brookes A, Jefferson B, Judd S (2005) Sub-critical flux fouling in membrane bioreactors–a review of recent literature *Desalination* **174** (3), 221-230

Prasad BV, Crawford S, Lawton JA, Pesavento J, Hardy M, Estes MK (2001) Structural studies on gastroenteritis viruses *Novart. Fdn. Symp.* **238**, 26-37; discussion 37-46

Resosudarmo A, Ye Y, Le-Clech P, Chen V (2013) Analysis of UF membrane fouling mechanisms caused by organic interactions in seawater *Water Res.* **47** (2), 911-921

Shannon MA, Bohn PW, Elimelech M, Georgiades JG, Mariñas BJ, Mayes AM (2008) Science and technology for water purification in the coming decades *Nature* **452** (7185) 301-310

Shin HS, Kang ST (2003) Characteristics and fates of soluble microbial products in ceramic membrane bioreactor at various sludge retention times *Water Res.* **37** (1), 121-127

Sima LC, Schaeffer J, Le Saux JC, Parnaudeau S, Elimelech M, Le Guyader FS (2011) Calicivirus removal in a membrane bioreactor wastewater treatment plant *Appl. Environ. Microbiol.* **77** (15), 5170-5177

Simmons FJ, Kuo DH, Xagoraraki I (2011) Removal of human enteric viruses by a full-scale membrane bioreactor during municipal wastewater processing *Water Res.* **45** (9), 2739-2750

Stewart P, Burnett R, Cyrklaff M, Fuller S (1991) Image reconstruction reveals the complex molecular organization of adenovirus *Cell* **67** (1), 145-154

Taniguchi M, Kilduff JE, Belfort G (2003) Modes of natural organic matter fouling during ultrafiltration *Environ. Sci. Technol.* **37** (8), 1676-1683

Teychene B, Guigui C, Cabassud C (2011) Engineering of an MBR supernatant fouling layer by fine particles addition: A possible way to control cake compressibility *Water Res.* **45** (5), 2060-2072

Ueda T, Horan NJ (2000) Fate of indigenous bacteriophage in a membrane bioreactor *Water Res.* **34** (7), 2151-2159

van den Brink P, Satpradit OA, van Bentem A, Zwijnenburg A, Temmink H, van Loosdrecht MCM (2011) Effect of temperature shocks on membrane fouling in membrane bioreactors *Water Res.* **45** (15), 4491-4500

van den Brink P, Vergeldt F, van As H, Zwijnenburg A, Temmink H, van Loosdrecht MCM (2013) Potential of mechanical cleaning of membranes from a membrane bioreactor *J. Membrane Sci.* **429**, 259-267

van den Brink P, Zwijnenburg A, Smith G, Temmink H, van Loosdrecht MCM (2009) Effect of free calcium concentration and ionic strength on alginate fouling in cross-flow membrane filtration *J. Membrane Sci.* **345** (1-2), 207-216

van der Marel P, Zwijnenburg A, Kemperman A, Wessling M, Temmink H, van der Meer W (2010) Influence of membrane properties on fouling in submerged membrane bioreactors J. Membrane Sci. **348** (1-2), 66-74

van de Ven WJC, van't Sant K, Pünt IGM, Zwijnenburg A, Kemperman AJB, van der Meer WGJ, Wessling M (2007) Hollow fiber dead-end ultrafiltration: Influence of ionic environment on filtration of alginates *J. Membrane Sci.* **308** (1-2), 218-229

Wang XM, Waite TD (2008a) Impact of gel layer formation on colloid retention in membrane filtration processes *J. Membrane Sci.* **325** (1), 486-494

Wang XM, Waite TD (2008b) Gel layer formation and hollow fiber membrane filterability of polysaccharide dispersions *J. Membrane Sci.* **322** (1), 204-213

Wang Z, Wu Z, Yin X, Tian L (2008) Membrane fouling in a submerged membrane bioreactor (MBR) under sub-critical flux operation: Membrane foulant and gel layer characterization *J. Membrane Sci.* **325** (1) 238-244

Wedlock DJ, Fasihuddin BA, Phillips GO (1986) Comparison of molecular weight determination of sodium alginate by sedimentation-diffusion and light scattering *Int. J. Biol. Macromol.* **8** (1), 57-61

Wei CH, Huang X, Ben Aim R, Yamamoto K, Amy G (2011) Critical flux and chemical cleaning-in-place during the long-term operation of a pilot-scale submerged membrane bioreactor for municipal wastewater treatment *Water Res.* **45** (2), 863-871

Windhues T, Borchard W (2002) Temperature depending light scattering measurements of aqueous gelatin and alginate solutions and their mixtures *Eur. Polym. J.* **38** (6), 1219-1227

Wu J, Le-Clech P, Stuetz RM, Fane AG, Chen V (2008a) Effects of relaxation and backwashing conditions on fouling in membrane bioreactors *J. Membrane Sci.* **324** (1-2), 26-32

Wu J, Le-Clech P, Stuetz RM, Fane AG, Chen V (2008b) Novel filtration mode for fouling limitation in membrane bioreactors *Water Res.* **42** (14), 3677-3684

Wu J, Li H, Huang X (2010) Indigenous somatic coliphage removal from a real municipal wastewater by a submerged membrane bioreactor *Water Res.* **44**, 1853-1862

Ye Y, Le-Clech P, Chen V, Fane AG, Jefferson B (2005) Fouling mechanisms of alginate solutions as model extracellular polymeric substances *Desalination* **175** (1), 7-20

Yohannes G, Wiedmer SK, Elomaa M, Jussila M, Aseyev V, Riekkola ML (2010) Thermal aggregation of bovine serum albumin studied by asymmetrical flow field-flow fractionation *Anal. Chim. Acta* **675** (2), 191-198

Yuan W, Zydney AL (1999) Humic acid fouling during microfiltration *J. Membrane Sci.* **157** (1), 1-12

Zhang J, Chua HC, Zhou J, Fane AG (2006) Factors affecting the membrane performance in submerged membrane bioreactors *J. Membrane Sci.* **284** (1-2), 54-66

Zhang X, Wang Z, Wu Z, Lu F, Tong J, Zang L (2010) Formation of dynamic membrane in an anaerobic membrane bioreactor for municipal wastewater treatment *Chem. Eng. J.* **165** (1), 175-183

Zheng X, Liu J (2007) Virus rejection with two model human enteric viruses in membrane bioreactor system *Sci. China Ser. B* **50** (3), 397-404

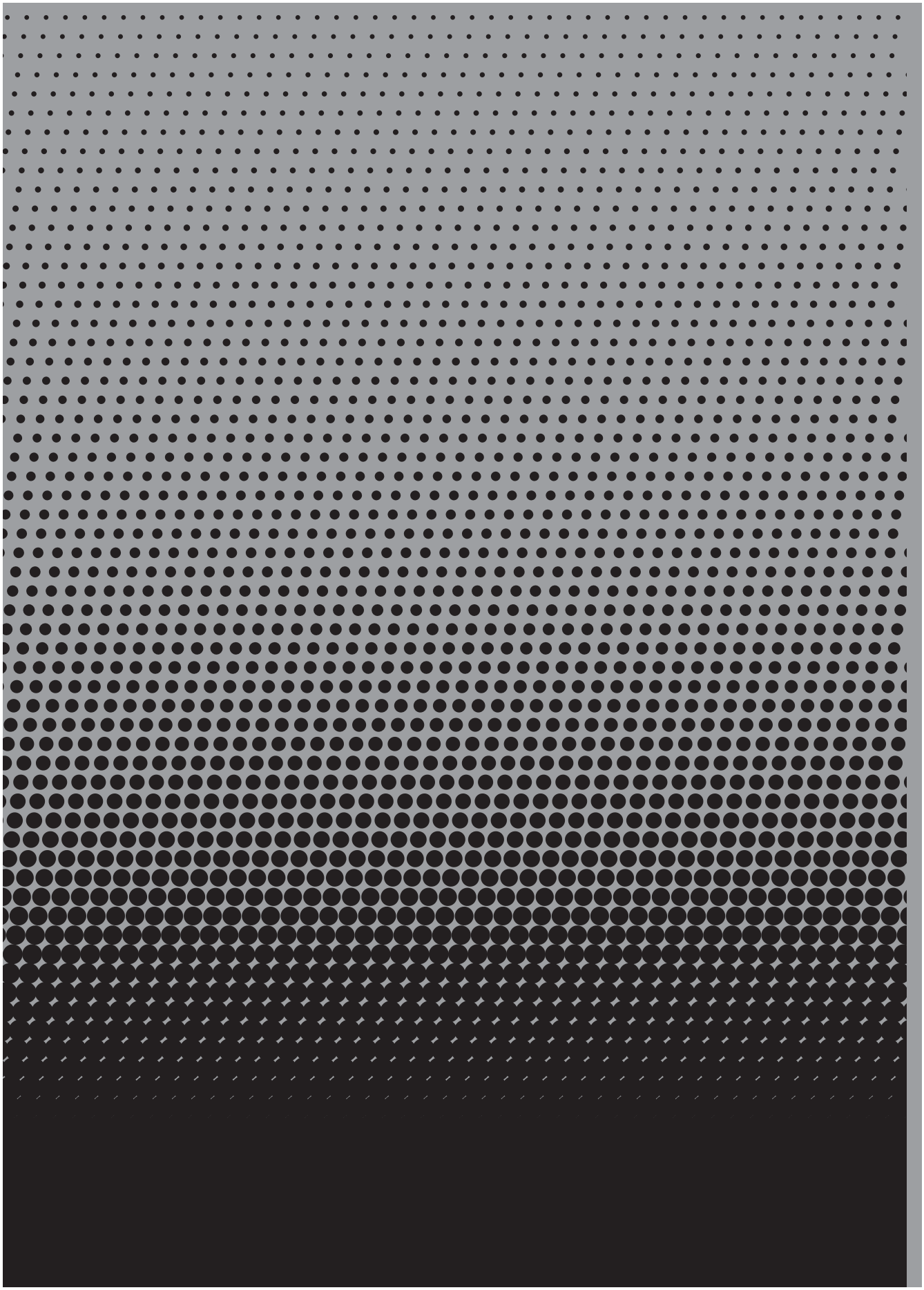

Chapter 4

POTENTIAL OF MECHANICAL CLEANING OF MEMBRANES FROM A MEMBRANE BIOREACTOR

This chapter has been published as:

van den Brink P, Vergeldt F, van As H, Zwijnenburg A, Temmink H, van Loosdrecht MCM (2013) Potential of mechanical cleaning of membranes from a membrane bioreactor *J. Membrane Sci.* **429**, 259-267

ABSTRACT

Several membrane fouling mechanisms have been identified in membrane bioreactors. While cake layers can be removed by physical cleaning, irreversible fouling such as a gel layer is difficult to remove by physical cleaning during filtration. Harsh mechanical cleaning was applied in this study to evaluate how much fouling could be maximally removed and distribution of remaining fouling was investigated. The fouling resistance of several membranes operated at different relatively low fluxes was followed during long term continuous flux operation. Remaining fouling was observed with scanning electron microscopy (SEM) and magnetic resonance imaging (MRI). Dead-end filtration tests with mechanically cleaned membranes showed a decreased permeability. To determine whether bacteria were present in the remaining fouling, oxygen consumption was quantified. Even after harsh mechanical cleaning, membrane samples showed considerable oxygen consumption. SEM did not show fouling inside the membrane. Of several membranes operated for at least 1 year, the permeate side was covered with bacteria and extracellular polymeric substances (EPS). These results show that fouling can not be removed completely by harsh mechanical cleaning and that both feed and permeate side of the membrane contains biofouling. This fouling on the permeate side should not be neglected when designing membrane cleaning.

Key words: biofilm, remaining fouling, membrane bioreactors, MRI measurements, permeate side.

INTRODUCTION

Several membrane fouling mechanisms have been identified in membrane bioreactors (Le-Clech et al., 2006). Prevalence of certain fouling mechanisms is partly dependent on operating conditions of the bioreactor, such as hydraulic retention time (HRT), solids retention time (SRT), mixed liquor suspended solids (MLSS) concentration, or of the membrane, such as operational flux, membrane surface area, aeration rate, and relaxation or backwashing frequency (Le-Clech et al., 2006). The applied flux is an important design parameter, because it relates directly to effluent production and thereby to plant capacity and size. Also, fouling mechanisms are dependent on the applied flux. At elevated fluxes, cake layer formation is generally accepted to be the dominant fouling mechanism (Wu et al., 2008). At sub-critical fluxes, which are closer to fluxes applied in practice, gel layer formation was found to prevail (Wang et al., 2008; van der Marel et al., 2010). In this case, fouling manifests itself as a two-stage process. The so-called "trans-membrane pressure (TMP) jump" is characteristic for this process, i.e. a gradual increase of TMP is followed by a quick exponential increase (Wang et al., 2008; Ognier et al., 2004).
Physical cleaning techniques for membrane bioreactors (MBRs) include mainly relaxation (where filtration is paused) and backwashing (where permeate is pumped in the reverse direction through the membrane) (Le-Clech et al., 2006). The main advantage of physical cleaning compared to chemical cleaning is the fact that no chemicals are needed. While cake layers, considered as reversible fouling, can be removed by relaxation or backwashing (Le-Clech et al., 2006; van der Marel et al., 2010), irreversible fouling such as a gel layer, is difficult to remove by physical cleaning (Wang et al., 2008; van der Marel et al., 2010; van den Brink et al., 2009). This results in an increase of irreversible fouling in time, as observed in flux step experiments (van der Marel et al., 2010).

In order to control irreversible fouling, it is necessary to know its characteristics and distribution over the different parts of the membrane: feed side, internal pore structure and permeate side. Fouling that remains after cleaning may deteriorate membrane performance in at least three ways:

1. It adds an additional resistance to the membrane resistance causing increased energy consumption during filtration.
2. It increases the flux through the areas of the membrane that are still permeable, according to the local flux concept (Ognier et al., 2004), causing exponential fouling development.
3. It might promote further fouling by creating the right conditions for specific fouling mechanisms, such as a local high pH inducing scaling (Arvin, 1983). A pH increase was shown in biofilms for the dissimilatory reduction of NO_3^- to N_2 (denitrification) (Arvin

and Kristensen, 1982; Lee and Rittmann, 2003). Another example is the production of extracellular polymeric substances (EPS) by bacteria during biofilm formation (Flemming and Wingender, 2001).

This study focuses on the fouling that remains after mechanical cleaning by scraping. Scraping is used as a research tool to remove as much fouling as possible and not as a way to clean membranes in practice. Several techniques have been applied to characterise the remaining fouling, such as determining resistance by dead-end filtration, scanning electron microscopy, magnetic resonance imaging and oxygen consumption measurements. With the latter technique, biological activity of the (remaining) fouling layer was quantified.
The main objectives of this study were to investigate the characteristics (resistance and biological activity) and the distribution of remaining fouling, to predict further fouling development.

EXPERIMENTAL

Experimental set-up

A pilot-scale MBR (Figure 4.1) with a working volume of 85 L and fed with municipal wastewater was used as a source of activated sludge for the experiments. The design of the pilot scale MBR has been extensively described in Remy et al. (2009). Operating conditions of the pilot reactor can be found in Table 4.1.

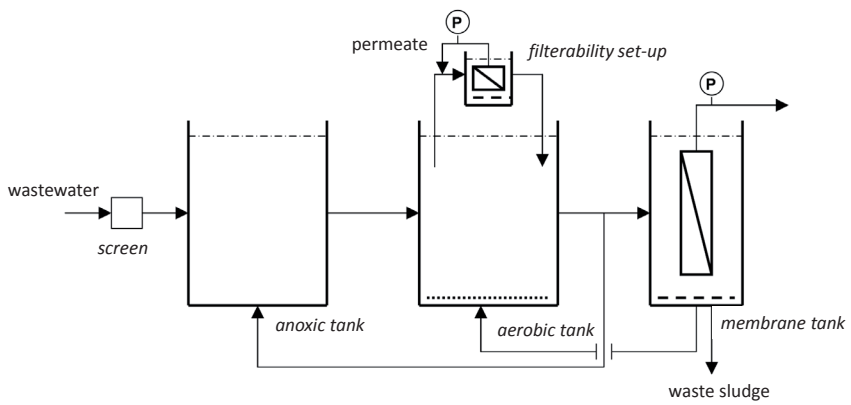

Figure 4.1 Pilot-scale MBR and filterability set-up (Remy et al., 2009).

The membrane tank was equipped with 5 polyethylene (PE) flat sheet membranes with a nominal pore size of 0.3 µm and a surface area of 0.063 m^2 each (Kubota, Japan). The

channel width between the membranes was 7 mm. The relatively low MLSS concentration was due to the low strength of the municipal wastewater. The MBR pilot had a COD removal of 85-90% and full nitrification.

Table 4.1 Operating conditions pilot MBR.

Operating condition	Value
Hydraulic Retention Time (HRT)	6 h
Sludge Retention Time (SRT)	25 d
Specific Aeration Demand (SAD)	1.4 m^3 m^{-2} h^{-1}
Flux	47.9 L m^{-2} h^{-1}
COD concentration influent	350 ± 200 mg L^{-1}
MLSS	4.0 g L^{-1}
DO concentration aerobic tank (controlled)	1.5 mg L^{-1}

To measure sludge filterability, sludge from the aerobic reactors of the MBR was continuously recirculated over a vessel with a volume of 5 L and a retention time of 1 h (Figure 4.1). The vessel contained two homemade submerged flat-sheet polyvinylidene fluoride (PVDF) membranes, with a surface area of 0.014 m^2. The temperature in the aerated tank of the pilot and filterability set-ups was continuously monitored.
The filterability set-ups (also called “experimental systems”) were equipped with a coarse bubble aerator to scour the membrane surface at a flow rate of about 28 m^3 m^{-2} h^{-1} (equivalent to 2.1 cm s^{-1}). This SAD was very high compared to practice to compensate for the broad channel width of 4.1 cm between the membrane sheets. Also, the air flow was divided by a relatively small surface area of the membranes used in these tests, resulting in a high specific air flow. The trans-membrane pressure (TMP) was monitored on-line (Endress + Hauser, Cerabar M PMC 41), both in the pilot and in the filterability set-ups.

Membranes

Two types of membranes were used in the experiments. A standard 0.1 µm PVDF membrane, casted from a PVDF/PVP/NMP solution (van der Marel et al., 2004), was applied in most experiments (Table 4.2, code P3). For oxygen consumption measurements, also PVDF membranes with larger pore sizes (0.2 µm) were prepared with a modified casting solution (Table 4.2, code A1). 200 µm thick films were casted on Freudenberg FO 2406 polyester non-woven. Tap water was used for coagulation via the phase inversion process. The different pore sizes were obtained by changing the temperature of the coagulation bath. After production, the membrane sheets were glued on PVC plates for the experiments. Because for preparation of all listed membranes, the same casting solution was used and the applied procedure was the same, their hydrophobicity and zeta potential are expected to be similar. The membranes are hydrophilic due to the presence of PVP. Because the casting

solution contains neutral polymers, the membranes are rather neutral at the applied pH range. Membranes were handmade, which could result in small changes in pore size due to the discontinuity of the production process. The pore size of all applied membranes was checked by performing scanning electron microscopy (SEM).

Experiments

Constant flux filtrations were performed in the filterability set-ups at fluxes between 11 and 36 L m^{-2} h^{-1} for 6-64 days (Table 4.2). Membrane fluxes were measured manually every day. At several points in time, membrane samples were taken for further analyses. Membranes were sampled by cutting pieces out of the membrane material with a scalpel. For scraping the fouling layer off the membrane, a spatula was applied. Analyses were performed on the fouled and scraped membrane samples. Depending on the type of analysis performed, the membrane was either sacrificed or repaired with duct tape and used to continue filtration. Table 4.2 gives an overview of the applied membranes, the average operating flux, operation time, resistance at time of sampling and performed analysis.

Table 4.2 Overview of applied membranes. Membrane coding represents the applied casting solution (P3 or A1) and a lab specific coding (the number).

Membrane	Average flux (L m^{-2} h^{-1})	Operation time (d)	Resistance (10^{12} m^{-1})	Analysis
P3-139	24.70	11	4.36	MRI
P3-123	24.48	11	n/a	Continuous filtration
P3-119a	20.63	11	0.754	MRI
	16.17	41	40.0	O_2
P3-131a	20.19	20	n/a	Continuous filtration
P3-131b	14.74	27	1.30	Dead-end filtration, SEM
P3-126	15.07	31	1.38	O_2
A1-01	15.57	16	0.231	O_2
	11.93	64	3.33	SEM
A1-03	29.28	17	2.41	O_2
A1-04	18.67	13	2.49	O_2
A1-08	18.16	12	6.12	O_2
A1-09	36.52	6	6.52	O_2
	26.01	8	6.52	O_2

Oxygen consumption measurements

The oxygen consumption rate is a measure for bacterial activity. To know whether bacterial activity was present on mechanically cleaned membrane samples, oxygen consumption measurements were performed.

Oxygen consumption of membrane samples was measured with a biological oxygen monitor

(BOM) (YSI 5300A, Yellow Springs Instr., OH, USA). The system consisted of a thermostat 10.0 mL glass chamber mounted on a magnetic stirrer to provide mixing and fitted with a piston holding a dissolved oxygen (DO) electrode. The piston contained a small opening to allow air to be removed from the chamber and to add reactants. A data acquisition system (Endress+Hauser, Germany) was used to record the oxygen concentration.

Synthetic wastewater (103 mg glucose, 77 mg $(NH_4)_2SO_4$, 15 mg KH_2PO_4, 19 mg $MgSO_4.7H_2O$, 2 mg $MnSO_4.7H_2O$, 0.1 mg $FeCl_3.6H_2O$, 1.9 mg $CaCl_2.2H_2O$, 12 mg $NaHCO_3$ per liter demineralised water) was saturated with oxygen by bubbling with air for at least 5 min. Measurements started by placing the sample in the chamber and plugging in the oxygen electrode. Glucose was used as a carbon source as reported in literature (Chen et al., 1994; Witzig et al., 2002; Guo et al., 2008). Because nutrients were present in excess, the measured oxygen uptake rate was a measure for the amount of active biomass in the sample.
The decrease of DO concentration in each experiment was measured in time. The oxygen level was decreasing during the measurement. From the initial slope (d(O2)/dt) the oxygen consumption rate (oxygen uptake rate) was estimated. Every measurement was made in duplicate by measuring the oxygen consumption of two similar samples. All experiments were performed at a temperature of 20 degrees Celsius.

Before measuring the oxygen consumption of membrane samples, first the specific oxygen consumption rate of the MBR sludge was determined. By combining this rate with the oxygen consumption rates of the membrane samples, an indication could be gained of the mass of volatile suspended solids (VSS) present on the surface of the membrane samples. To get to know the specific oxygen consumption of MBR sludge, a set of experiments was done with different amounts of biomass. Sludge samples from the MBR pilot were centrifuged from known volumes and the pellets were then introduced in the BOM chamber. The VSS concentration of the MBR sludge was measured three times per week and found to be rather constant with a value around 2.68 g L^{-1}.With that known VSS concentration, the amount of biomass in the pellets could be calculated. By obtaining the oxygen consumption rates and dividing these values by the VSS concentrations, the specific oxygen consumption rate of the sludge was determined.
The oxygen consumption measurement for membrane samples was carried out in the same way. Pieces of 2 cm^2 were cut from the fouled membranes and placed in air-saturated synthetic wastewater. The oxygen consumption was measured accordingly. Membrane fouling was scraped off from membrane pieces with the same size using a spatula, and oxygen consumption of these cleaned membrane samples was measured as well. Oxygen consumption of clean membrane pieces was also determined but was found to be insignificant.

Dead-end filtrations

Dead-end filtrations were performed to determine the total resistance before and after scraping off the fouling layer. Filtrations were performed with a dead-end filtration cell with a volume of 450 ml. Circular membrane pieces with an effective surface area of 0.0035 m^2 were cut from fouled membranes used in the filterability set-up. Tests were performed at a maximum of 2 bar pressure. To prevent osmotic shocks to the gel layer, permeate from the MBR pilot was used as feed solution for filtration. Permeate production was continuously measured with a mass balance (Kern, Germany). After running the dead-end filtration test cell with the fouled membranes from the filterability set-up, the fouling was scraped off the membrane surface and its resistance was determined again by a dead-end filtration at the same conditions. Permeabilities were calculated by dividing the flux at the beginning of filtration by the applied pressure difference.

Magnetic resonance imaging

Magnetic resonance imaging (MRI) was performed to obtain T_1-weighted contrast images to compare fouled and scraped off surfaces. T_1 is a time constant characterizing spin-lattice or longitudinal relaxation, the restoration of the thermal equilibrium distribution of the proton spins in water after disturbance by a radiofrequency pulse. T_1 of water deviates from that of bulk water due to local environment or different dynamics of the water molecules (Haacke et al., 1999). For the MRI measurements a special flow cell was designed that fitted into the MRI probe (see supporting information). The diameter of the flow cell was 4 cm, and of the applied membrane 2.6 cm. The bottom plate of the flow cell contained a grid for permeate removal. Fouled membrane samples were cut in the right shape and placed on the bottom plate of the probe. The probe was filled with tap water before placing it into the MRI probe.

All measurements were performed on a 3 T (128 MHz for protons) MRI system (Bruker, Karlsruhe, Germany), consisting of an Avance 200 console, a superconducting magnet with a a vertical bore (Magnex, Oxford, UK), a 1 T/m gradient coil, and a birdcage RF coil with an inner diameter of 4 cm.

Two and three dimensional T_1-weighted images were obtained using a Turbo Spin Echo (TSE) MRI sequence (Scheenen et al., 2000), with a repetition time of 1 s and a spectral bandwidth of 50 kHz. The images were measured with an effective echo time of 7.192 ms to avoid T_2 weighting. Per scan 16 echoes were measured for image formation to speed up the measurements. Odd and even echoes were separately phase encoded forming two different images to avoid Nyquist ghost artifacts, so the speed up or turbo factor was 8. Two acquisitions were averaged to improve image quality. The Field-Of-View (FOV) for the 2D images was 12.5 x 25 mm^2 with a matrix size of 256 x 256 resulting in an in-plane spatial

resolution of 49 x 98 μm^2. The slice thickness was 3 mm. These experiments lasted 6 minutes and 24 seconds. The FOV for 3D images was 12.5 x 25 x 25 mm^3 with a matrix size of 256 x 64 x 64 resulting in a spatial resolution of 49 x 391 x 391 μm^3. In this case the experimental time was 17 minutes and 4 seconds. In both experiments the axis of highest spatial resolution was chosen normal to the plane of the membrane.

All data handling and analysis was performed with home-built software written in IDL (RSI, Boulder, CO).

Scanning electron microscopy

Scanning electron microscopy (SEM) was performed to visualise the effectivity of scraping to remove the fouling layer and to check for fouling inside the membrane and on the permeate side of the membrane. Cross-sections and surfaces of the fouled membranes were investigated with a JEOL-6480LV SEM (Japan). Cryo observation under low vacuum (LV) was used to determine the cross-section and structure of the fouling. Samples were broken in liquid nitrogen and placed in a special clamp. The clamp was placed in a JEOL LV cooling holder and the clamp with holder was cooled during 10 minutes in liquid nitrogen. After freezing, the clamp and holder were placed in the SEM and the frozen sample could be observed for about 60 minutes. The SEM was operated at 50 Pa, 6 or 8 kV, Working Distance (WD) 10 mm and Spot Size (SS) 60. During observation under LV, the frozen water in the sample sublimates and the sample is freeze dried.

After LV observation, samples were coated in a JEOL JFC-1200 fine coater with a thin (10 nm) Au (gold) layer for observation under high vacuum (HV). Au coated samples were investigated at 6 kV, WD 10 mm and SS 20.

For more careful observation of the bacteria in the gel layer, fresh wet samples were fixated in a solution of 2 w% glutaraldehyde in PBS buffer during 2 hours. After washing with the buffer solution, samples were dehydrated with a series of ethanol/water solutions with increasing ethanol concentrations (10, 25, 50, 75, 90, 100 v/v %; 20 min for each step). Finally, samples were dried a few days in a desiccator and coated with a thin Au layer before observation under HV in the SEM.

RESULTS

Membrane fouling

The fouling resistance of several membranes operated at different relatively low fluxes (Table 4.1) was followed during long term continuous flux operation. Figure 4.2 shows representative filtration curves for continuous operation of two different membranes. In

both filtrations, the "TMP jump" can be clearly observed. Even though the difference in flux was relatively small, i.e. 24.5 compared to 20.2 L m^{-2} h^{-1}, the TMP jump started earlier in the course of filtration for the membrane operated at the higher flux. After sampling, the membrane was started-up at the same flux within one hour. These moments can be identified by breaks in the filtration curve: when membrane filtration was stopped, resistance dropped to zero. After starting up again after sampling, it took several minutes before the resistance was back at its original level. This delay in stabilisation of TMP upon intervention of the system was also observed when performing filtration according to the flux step method (van der Marel et al., 2009). Filtration with membrane P3-123 was stopped after 11 days, while membrane P3-131a was operated for 20 days.

To test the resistance of the remaining membrane fouling after scraping, permeabilities were determined for a clean and fouled membrane (P3-131b) and for this fouled membrane after scraping. The clean membrane had a permeability of $6.6*10^3$ L m^{-2} h^{-1} bar^{-1}, while the membrane fouled during continuous flux filtration (R = $1.30 * 10^{12}$ m^{-1}) had a tenfold lower permeability of $6.7*10^2$ L m^{-2} h^{-1} bar^{-1} (determined by dead-end filtration). After scraping off the fouling, the clean water permeability could only be partially restored to $1.6*10^3$ L m^{-2} h^{-1} bar^{-1}, i.e. to 24%.

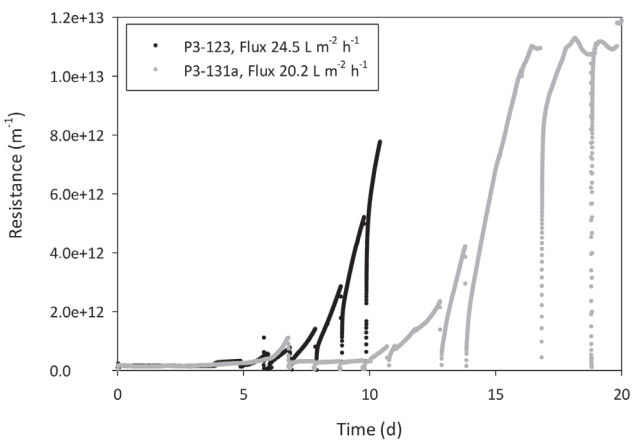

Figure 4.2 Resistance curves of two different membranes operated in continuous mode. Sampling points can be recognised by breaks in the curves.

Scanning electron microscopy was applied to check the effectivity of removing the fouling layer by scraping (Figure 4.3). Membrane P3-131b, with a low fouling resistance of R=$1.30*10^{12}$ m^{-1} after 27 days of operation, was found to be for a large part covered with fouling.

Removal of the fouling layer by scraping seemed to be rather effective, although the membrane skin was damaged by the force of the scraping action. However, while the fouling layer seemed to be removed for large part by scraping, permeability was not restored accordingly by scraping as mentioned above. Apparently, after scraping off the fouling layer, there was still "remaining fouling". The characteristics of this remaining fouling are presented further on.

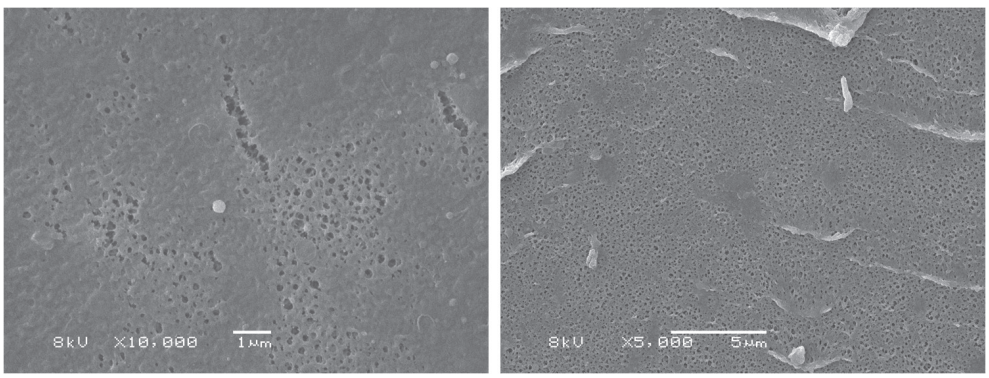

Figure 4.3 SEM images of a slightly fouled membrane (P3-131b) before scraping (R=1.30 $*10^{12}$ m^{-1}) (left) and after scraping (right).

Oxygen consumption measurements

Oxygen consumption of membrane samples from several filtrations was measured and compared to oxygen consumption of activated sludge from the MBR pilot. The specific oxygen consumption rate of the MBR sludge was found to be on average 11.8 ± 0.66 mg O_2 g^{-1} VSS h^{-1}.

Oxygen consumption rates of fouled membranes as a function of total resistance are shown in Figure 4.4. There seems to be no consistent relation between fouling layer resistance and oxygen consumption rate. Most duplicates showed a relatively small standard deviation, except for one (R=6.12*10^{12} m^{-1}). This data point is the average of the values 3.28 *10^{-4} and 1.24 *10^{-3} mg O_2 min^{-1} cm^{-2}. While the first value is in line with the other values presented in Figure 4.4, the last one (which equals 17.9 g O_2 m^{-2} d^{-1}) seems to be unrealistically high when comparing with maximum oxygen transfer rates modelled for trickling filters (5-15 g O_2 m^{-2} d^{-1}) (Logan, 1993) and measured for a membrane-aerated biofilm reactor in which the biofilm grew very fast at a rate of 300 µm d^{-1} (16 g O_2 m^{-2} d^{-1}) (Rishell et al., 2004).

Because the mass of sludge deposited on the membrane samples could not be determined by VSS measurements due to the small sample size, oxygen consumption rates of the membrane samples can be used to get an indication.

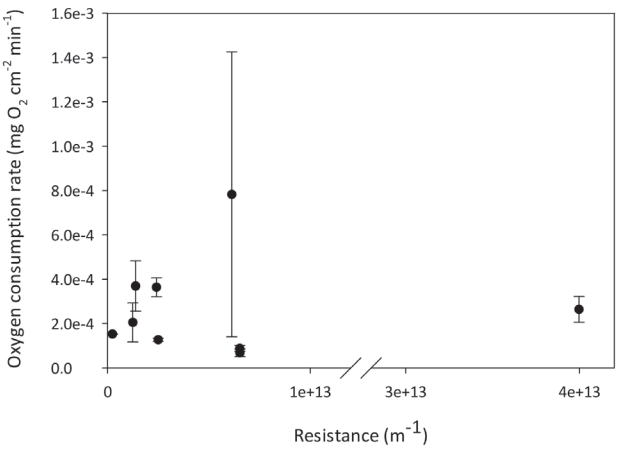

Figure 4.4 Oxygen consumption rates of several fouled membranes.

Assuming similar biomass composition of the MBR sludge and the fouling layer, dividing these rates with the specific oxygen consumption rate of MBR sludge gives an indication of the average mass of sludge present on the membranes: 1.04 ± 0.60 mg VSS cm^{-2}.

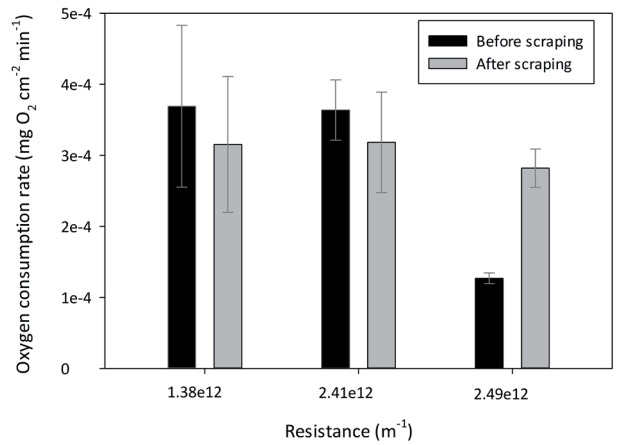

Figure 4.5 Oxygen consumption rates before and after removing the fouling layer by scraping.

After measuring the oxygen consumption rates of fouled membrane pieces, the fouling layer was scraped off with a spatula and oxygen consumption was measured again. The oxygen measurements were performed in duplicate. No consistent effect of scraping on oxygen

consumption could be observed after removing the fouling layer at different resistance values (Figure 4.5). For two samples, oxygen consumption decreased slightly after scraping, while for one sample, oxygen consumption increased drastically after scraping. This seems strange and no sound explanation was found for it.
Considering the slight decrease in oxygen consumption for the other two resistance values, apparently the part of the fouling layer that consumed oxygen was not removed by scraping the layer off and therefore the bacteria are still present after scraping. The "remaining fouling", as introduced above, could be located partly on the feed side of the membrane, but also inside the membrane or on the permeate side.

It is of interest to know whether the oxygen consumption rates are in the same range as the supply of oxygen into the fouling layer during filtration by convective flow. By comparing the oxygen consumption rates with the convective flux of oxygen through the fouling layer and the membrane, it will be known whether the oxygen consumption in the biofilm is transport limited. In this case, the biofilm will be partly anaerobic, which could influence biofilm growth and EPS production rates. Thereby, it could influence fouling behaviour.
With an average measured oxygen concentration of 5 mg L^{-1} in the membrane tank mixed liquor, the convective flux of oxygen through a membrane running at a flux of 22.35 L m^{-2} h^{-1} (average applied flux of the filtration, see Figure 4.2) becomes 112 mg O_2 m^{-2} h^{-1}. This value is in the same range as the average oxygen consumption rate measured in the fouling layers in the presence of easily biodegradable substrate of 2.05 * 10^{-4} mg O_2 min^{-1} cm^{-2} which is equal to 123 mg O_2 m^{-2} h^{-1}. These similar values for oxygen consumption rate and convective flux could mean that during filtration, the oxygen was depleted in the fouling layer. However, in the oxygen consumption measurement, nutrients were easily biodegraded and supplied in excess, which was not the case in the MBR. The oxygen consumption rate in the MBR was probably lower, and the biofilms on the membranes in the MBR were therefore most likely not transport limited. To verify this conclusion, the oxygen concentration in the permeate was measured for the MBR pilot and it was on average 3,73 mg L^{-1}. This shows that oxygen limitation is not of importance in these biofilms. By comparing this concentration with the 5 mg L^{-1} that was measured for the membrane tank it can be concluded that oxygen is indeed consumed during the membrane filtration. Knowing this, lowering the oxygen concentration in the membrane tank could be a way to limit the biofilm growth and thereby control membrane fouling.

MRI measurements

To further characterise the remaining fouling, T_1-weighted MRI measurements were performed on severely and lightly fouled membranes (as indicated by resistance values), as well as on scraped samples (Figures 4.6, 4.7). Fouled membranes were cut in a circular

shape and fouling was scraped off with a spatula from one part of the circle. Figure 4.6 shows a cross section through the flow cell. The membrane is represented by a bright layer on top of a black line (non-woven support layer). The O-rings holding the membrane in place can be clearly seen as two black circles on the complete left and right of the Figure. MRI measurements show lower intensity on the left part of the membrane, which is the part where the fouling is removed. Higher intensity can be observed for the area where fouling is still present on top of the membrane. The transition from the scraped off surface to the fouled surface is indicated by an arrow.

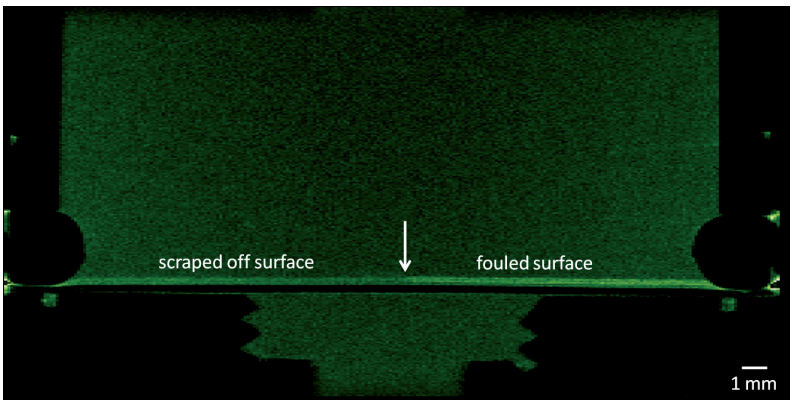

Figure 4.6 Cross section (x,z) through membrane and fouling layer of severely fouled membrane P3-139 (R=4.36*10^{12} m^{-1}), left part scraped off. The arrow indicates the transition point. Field of view (FOV) was 12.5 x 25 x 25 mm^3, repetition time was 1 s.

To compare clean, slightly fouled and severely fouled membranes, maximum intensity projections (MIP) were made of the original 3-dimensional plots: for all (x,y)-data points, the maximum along the z-axis was selected and plotted (Figure 4.7). For a better interpretation of the images in Figure 4.7, a cross section was drawn through these images along the x-axis and the intensities were plotted in a graph. The clean membrane (Figure 4.7A) shows low intensity on the entire x-axis. The slightly fouled membrane (Figure 4.7B) shows a higher intensity than the severely fouled membrane (Figure 4.7C). A transition can be observed from high intensities for the fouled parts to low intensities for the scraped parts of the membranes. The intensity of the scraped off surfaces was however not as low as for the clean membrane, indicating that not all fouling is removed by scraping. The transition from fouled to scraped surface is gradual for the slightly fouled membrane, while it is sudden for the severely fouled membrane.

The differences in intensity between the slightly and severely fouled membrane samples could possibly be explained by the different operating conditions of the two membranes:

although both membranes were operated for 11 days, the slightly fouled membrane P3-119a run at a lower flux (20.63 L m^{-2} h^{-1}) than the severely fouled membrane P3-139 (24.70 L m^{-2} h^{-1}) (Table 4.2). Operation time of both membranes being the same, fouling developed quicker on the severely fouled membrane. It is known that higher fluxes result in cake layer formation, while at lower fluxes (sub-critical fluxes), a gel layer develops (3). As mentioned above, cake layers are more easily removed by physical cleaning than gel layers (1,3,4,6). This could explain the effectivity of mechanical cleaning for the severely fouled membrane as shown in Figure 4.7.

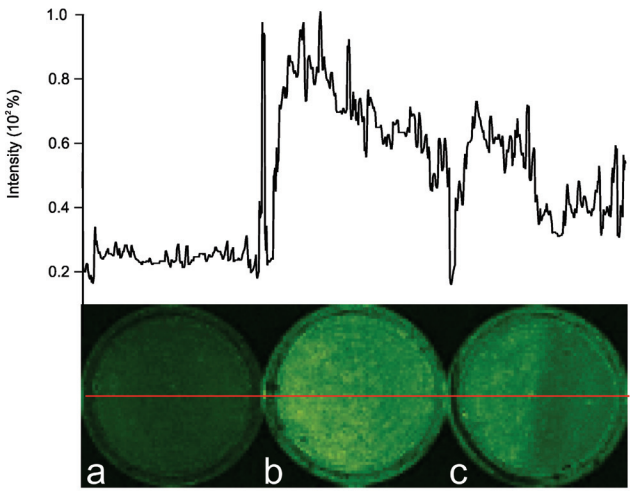

Figure 4.7 Maximum intensity projections (x,y) of the 3D plots (A: clean membrane, B: slightly fouled membrane P3-119a (R=7.54*10^{11} m^{-1}), right half scraped off, C: severely fouled membrane P3-139 (R=4.36*10^{12} m^{-1}), right half scraped off. The red line shows the y-position for which the intensity was plotted in the graph.

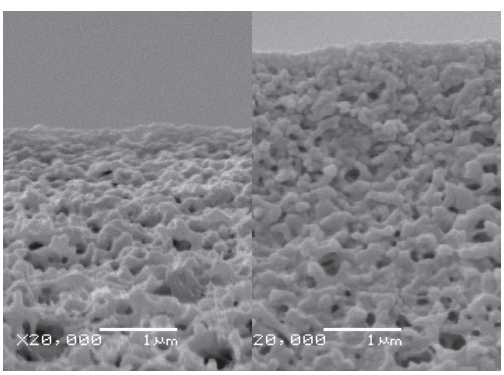

Figure 4.8 Cross section SEM images of a clean (left) and a moderately fouled membrane A1-01 (R=3.33*10^{12} m^{-1}) (right).

SEM

Membranes were analysed by SEM for fouling in the membrane pores, or "internal fouling". To visualise cross sections of the membranes, membrane samples were placed in liquid nitrogen followed by breaking of the membrane and fouling layer. No internal fouling could be observed when a clean membrane was compared with a moderately fouled membrane (Figure 4.8).

DISCUSSION

Membrane fouling

From the different analyses presented above (permeability testing, oxygen consumption, MRI measurements, SEM), it can be concluded that, although a harsh mechanical cleaning such as scraping removed the visible fouling on top of the membrane (Figure 4.3), some fouling remained on the membrane. This remaining fouling might have been located partly on the feed side of the membrane, but also inside the membrane or on the permeate side. It added to the total resistance, consumed oxygen and accounted for the remaining intensity in the T_1-weighted MRI measurement.

As mentioned in the introduction, remaining fouling after harsh mechanical cleaning can deteriorate the filtration process in at least three ways. To develop a strategy to minimise remaining fouling, it is necessary to know where this fouling is located. From Figure 4.3 we can conclude that only little remaining fouling was present on the feed side of the membrane. Internal fouling could also not be observed in these membranes (Figure 4.8), which suggests the remaining fouling was located at the permeate side of the membrane.
To test this hypothesis, the permeate sides of several membranes were studied with SEM: a double A4 plate with homemade PVDF (on FO support), operated for 6 days at a net flux of 29 L m^2 h^{-1} in a pilot scale MBR, and two double A4 Kubota plates, operated for at least 1 year at a net flux of 15.8 L m^2 h^{-1} in the same pilot scale MBR. All membranes were operated at an 8 min on, 2 min off (relaxation) regime. After stopping the filtration, the membranes were tested for leaks by applying 100 mbar over pressure on the permeate side of the membrane. No leakages were found at this pressure. A comparison between the permeate side of a clean PVDF membrane and one that ran for 6 days showed no fouling (data not shown).

The Kubota plates operated for at least 1 year at a net flux of 15.8 L m^2 h^{-1} in a pilot scale MBR showed a diverse fouling pattern on the feed side (Figure 4.9A). Samples were taken at different locations on the membrane sheets. The permeate side of the membranes was also covered with fouling, as was the support layer (Figure 4.9B).

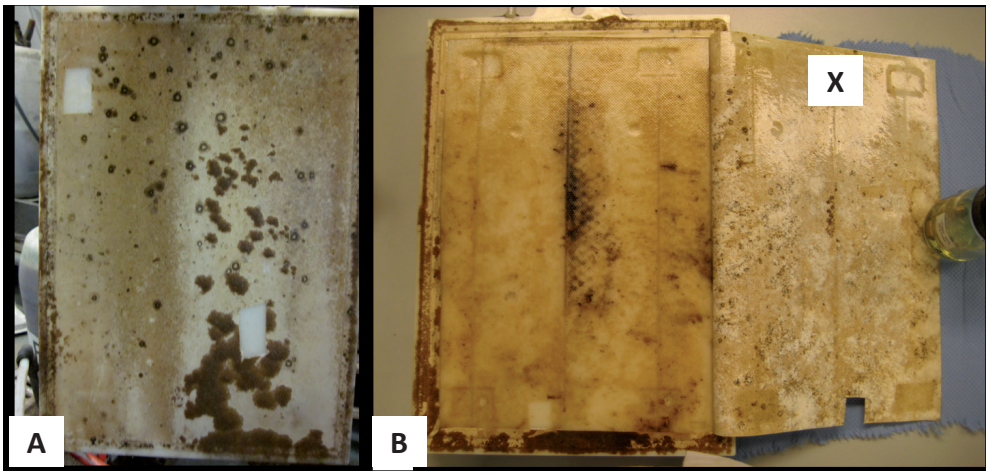

Figure 4.9 Kubota membrane plates operated for at least 1 year at a net flux of 15.8 L m^2 h^{-1}, with sampling position on membrane B.

Figure 4.10 shows the permeate side of the sample taken from membrane B. This sample is representative for permeate side samples from other membrane plates. Considerable fouling is observed for the permeate side of this sample. Apart from (groups of) bacteria, also protozoa can be seen, as well as patches of EPS. From the SEM images it can be concluded that, while running a membrane for a long time at a low flux, fouling on the permeate side cannot be prevented. The bacteria are embedded in an EPS layer, which may give additional resistance during filtration. It should be noted that fouling on the permeate side was observed for two Kubota plates running for at least 1 year, while the PVDF membranes used

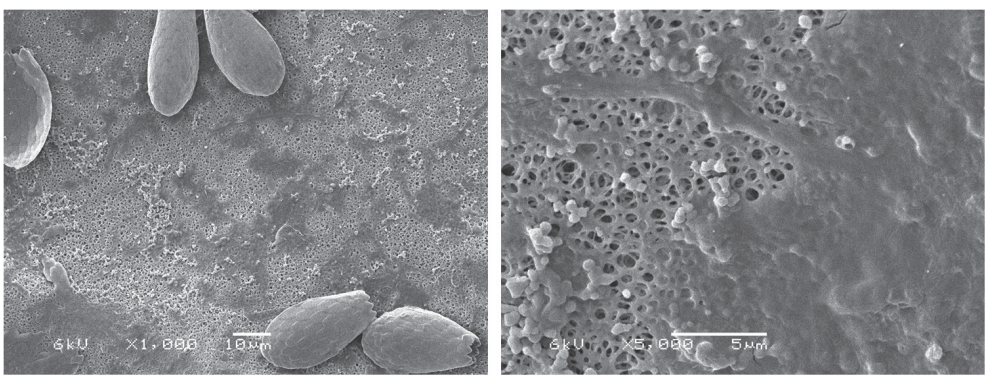

Figure 4.10 Permeate side of a representative sample from a Kubota membrane operated for 1.5 year (magnifications: 1,000x (left) and 5,000x (right)).

in the other experiments were not checked for permeate side fouling. Although the PVDF membranes had a smaller pore size than the Kubota membranes, their pore size distributions could have been rather wide and a fraction of the pores of the PVDF membranes was in the same range as those of the Kubota membranes. Therefore, fouling on the permeate side could also have been of importance in the experiments with PVDF membranes.

Applied imaging methods

Several techniques have been applied in these experiments for imaging of the fouling layer. Both feed side and permeate side of the membrane were imaged with scanning electron microscopy. Also, SEM was applied to look at cross sections of the membrane to check for internal fouling. Apart from breaking membrane samples in liquid nitrogen for creating cross section images, embedding of the membrane samples followed by cutting slices has been considered as well. The embedding technique is limited by the resin that needs to be etched away from the slices before observation by SEM. This is difficult because of the limited strength of the slices and will probably create artefacts in the image as well. Overall, SEM was not the most suitable technique for studying internal fouling.

T_1-weighted MRI measurements provided different information than SEM, as 3D images were constructed and cross sections along one of the three axes could be made. T_1 intensity gives an indication of the matrix the water is incorporated, which could be very useful information. In order to use this technique in fouling research, more studies need to be performed studying samples of known composition and water content.

Oxygen consumption

The fouling layer on the membrane samples of the constant flux filtrations consumed oxygen at a rate which was independent of its resistance (Figure 4.4). These rates represent the total of the feed side fouling, internal fouling and permeate side fouling. After scraping off the feed side fouling, oxygen consumption was not much lower.

Using an average composition of biomass of $C_5H_7NO_2$, the estimated average biomass on the membranes of 1.04 mg VSS cm^{-2} was recalculated to 0.552 mg organic carbon per $cm^{2.}$ This value is eight times higher than the average mass of TOC found before on membranes run at similar fluxes (data not shown). However, these measured TOC values are probably underestimating the real masses because dissolving a biofilm sample for subsequent TOC analysis is very difficult. An explanation for the independence of oxygen consumption on fouling layer resistance could be that the bacteria, which are responsible for oxygen consumption, are not the main contributors to the fouling resistance. It has been reported that the EPS produced by the bacteria can be more directly linked to membrane fouling (Chang and Lee, 1998) and type and amount of EPS production can be very different between bacterial species (Skillman et al., 1999; Sutherland, 2001).

Both oxygen consumption measurements and MRI measurements show that removal of the fouling layer from the feed side of the membrane does only partly decrease the oxygen consumption of the membrane sample (Figure 4.5), respectively the T_1-weighted intensity (Figures 4.6, 4.7). Also, internal fouling could not be observed by SEM (Figure 4.8). Therefore, the oxygen consumption and T_1-weighted intensity was at least partly caused by the fouling on the permeate side of the membrane, which shows the importance of the permeate side in fouling distribution.

Biofilm growth

It would be interesting to know how the permeate side of the membrane got inoculated. MBR systems in general are not sterilised at the start-up, which would allow bacteria to be present at the permeate side of the membrane when a filtration run is started up. Moreover, *B. subtilis* and *E. coli* were shown to grow, move, and penetrate very narrow constrictions, with *E. coli* even passing channels which are 2 times more narrow than its diameter (Männik et al., 2009), which would allow these bacteria to pass through the membrane pores. It was also recently shown that a wide range of bacteria is able to pass 0.45, 0.22 and 0.1 µm filters and regrow after the passage (Hahn, 2004; Wang et al., 2007). In case a membrane is damaged or not pasted properly to the support plate, this would be a way for bacteria to pass through easily. Another option would be growth on the permeate tube or at the connections between membrane plates and tubing.

Because usually not all the wastewater BOD is degraded in biological waste water treatment systems, remaining BOD can serve as substrate for the bacteria on the permeate side of the membrane. Growth of heterotrophs has been shown on concentrations of assimilable organic carbon (AOC) as low as 10 µg-C L^{-1} (van der Kooij et al., 1995; Srinivasan and Harrington, 2007). AOC was shown to have a significant correlation with bacteria regrowth (Escobar and Randall, 2001). While the front side of the membrane is usually exposed to high shear stress created for cleaning the membrane, the permeate side is more protected, allowing bacteria to attach and replicate in an undisturbed manner.

Practical implications

Harsh mechanical cleaning was applied in this study to know how much fouling could be maximally removed. This remaining fouling had a resistance to flow, was observed in MRI measurements and consumed oxygen. Because the remaining fouling has biological activity and can grow on low concentrations of dissolved substrates present in the mixed liquor, it is a type of fouling that can not easily be predicted or prevented. Unless even smaller pore size membranes (nanofiltration) are being applied, passage of bacteria through the membrane will occur. For any membrane, damage of the membrane or imperfections in the pasting allows bacteria to pass through to the permeate side. Moreover, membranes are

not sterilised before filtration is started up. Therefore, it does not seem feasible to focus on prevention of biofilm formation.
However, both for effluent discharge and reuse, permeate quality concerning microbial safety is essential, and biofilm growth on the permeate side of the membrane should be taken seriously when designing and operating membrane bioreactors. Permeate quality could actually improve by the biofilm on the permeate side because it can use the remaining organic carbon as a substrate. It is thereby important that the bacteria are not released into the permeate as this would decrease its microbiological quality.

Instead of prevention of biofilm formation, the focus should be on managing the biofilm growth and detachment. Important measures in this respect could be:

1. Decreasing organic carbon concentrations in the MBR mixed liquor by optimising the biological processes in the bioreactor, as this would result in low substrate availability for the biofilm, also on the permeate side. This also includes placing the membranes in a separate tank from the bioreactor and preventing shortcut streams so that peak loads in the wastewater can not reach the membrane. To prevent biofilm formation, AOC concentrations as low as 10 µg-C L^{-1} should be reached (van der Kooij et al., 1995; Srinivasan and Harrington, 2007). Ultrafiltration permeate (pore size approximately 40 nm) was reported to foul the subsequent candle filter that was placed before the reverse osmosis membrane modules (Bereschenko et al., 2007). This would mean additional treatment is needed after the membrane bioreactor.
2. Using proper cleaning procedures based on the type of membrane applied. For example, applying a backwash can cause the biofilm to be "pushed" in the membrane in case the smallest pores are located at the feed side of the membrane. On the longer term, this could possibly deteriorate the filtration performance.
3. Limiting the biofilm growth in the permeate tubes. Bacteria present in biofilms are known to survive even high-turbulence flow (Lehtola et al., 2007). In permeate tubes, shear values are rather low, which could allow bacteria to grow towards the membrane surface and contribute to the biofilm formation on the membrane permeate side.

CONCLUSIONS

Even though harsh mechanical cleaning was applied on membranes fouled during long term continuous flux operation, remaining fouling was present on the membrane. This remaining fouling had a resistance to flow, was observed in MRI measurements and consumed oxygen. Subsequently, the location of this remaining fouling was studied. While fouling inside the

membrane could not be observed with the applied techniques, the permeate side was found to be covered with bacteria, protozoa and EPS. This fouling on the permeate side should not be neglected when designing membrane cleaning strategies.

ACKNOWLEDGEMENTS

This work was performed in the TTIW-cooperation framework of Wetsus, Centre of Excellence for Sustainable Water Technology (www.wetsus.nl). Wetsus is funded by the Dutch Ministry of Economic Affairs, the European Union Regional Development Fund, the Province of Fryslân, the City of Leeuwarden and the EZ/Kompas program of the 'Samenwerkingsverband Noord-Nederland". The authors like to thank the participants of the research theme "Membrane Bioreactors" for the fruitful discussions and their financial support.

APPENDIX A. SUPPORTING INFORMATION

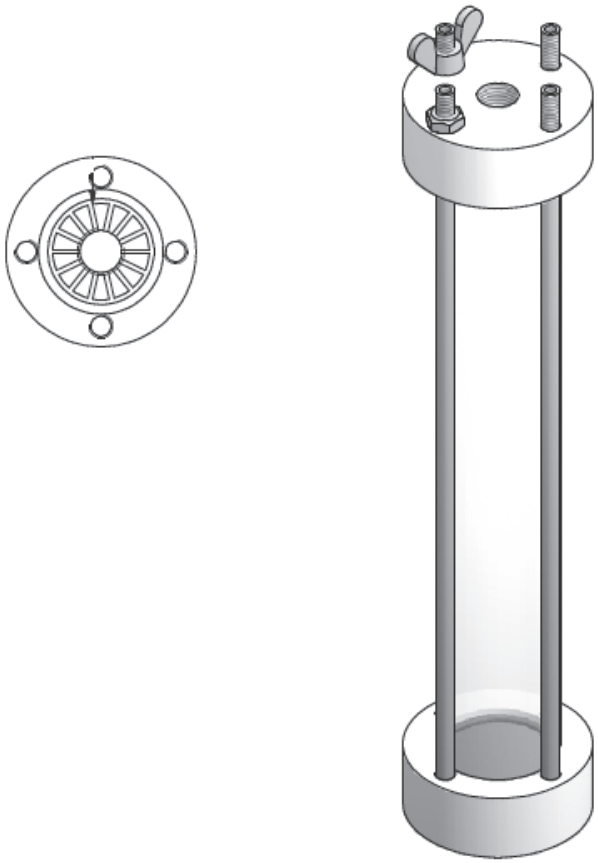

Figure S4.1 Flow cell designed for MRI measurements

REFERENCES

Arvin E (1983) Observations supporting phosphate removal by biologically mediated chemical precipitation - a review *Water Sci. Technol.* **15** (3-4), 43-63

Arvin E, Kristensen GH (1982) Effect of denitrification on the pH in biofilms *Water Sci. Technol.* **14** (8), 833-848

Bereschenko LA, Stams AJM, Heilig GHJ, Euverink GJW, Nederlof MM, van Loosdrecht MCM (2007) Investigation of microbial communities on reverse osmosis membranes used for process water production *Water Sci. Technol.* **55** (8-9), 181-190

Chang IS, Lee CH (1998) Membrane filtration characteristics in membrane coupled activated sludge system—the effect of physiological states of activated sludge on membrane fouling *Desalination* **120** (3), 221-233

Chen GH, Ng WJ, Ozaki H, Terashima Y (1994) Determination of dissolved oxygen limitation in aerobic biofilm reactors *Resour. Conserv. Recy.* **11** (1-4), 73-81

Escobar IC, Randall AA (2001) Assimilable organic carbon (AOC) and biodegradable dissolved organic carbon (BDOC): complementary measurements *Water Res.* **35** (18), 4444-4454

Flemming HC, Wingender J (2001) Relevance of microbial extracellular polymeric substances (EPSs) – part I: Structural and ecological aspects *Water Sci. Technol.* **43** (6), 1-8

Guo W, Vigneswaran S, Ngo HH, Xing W, Goteti P (2008) Comparison of the performance of submerged membrane bioreactor (SMBR) and submerged membrane adsorption bioreactor (SMABR) *Bioresource Technol.* **99** (5), 1012-1017

Haacke EM, Brown RW, Thompson MR, Venkatesan R (1999) Magnetic resonance imaging: Physical principles and sequence design, 1st ed., Wiley-Liss, New York

Hahn MW (2004) Broad diversity of viable bacteria in 'sterile' (0.2 µm) filtered water *Res. Microbiol.* **155** (8), 688-691

Le-Clech P, Chen V, Fane AG (2006) Fouling in membrane bioreactors used in wastewater treatment – A review *J. Membrane Sci.* **284** (1-2), 17-53

Lee KC, Rittmann BE (2003) Effects of pH and precipitation on autohydrogenotrophic denitrification using the hollow-fiber membrane-biofilm reactor *Water Res.* **37** (7), 1551- 1556

Lehtola MJ, Torvinen E, Kusnetsov J, Pitkänen T, Maunula L, von Bonsdorff CH, Martikainen PJ, Wilks SA, Keevil CW, Miettinen IT (2007) Survival of *Mycobacterium avium*, *Legionella pneumophila*, *Escherichia coli*, and Caliciviruses in drinking water-associated biofilms grown under high-shear turbulent flow *Appl. Environ. Microbiol.* **73** (9), 2854-2859

Logan BE (1993) Oxygen transfer in trickling filters *J. Environ. Eng.* **119** (6), 1059-1076

Männik J, Driessen R, Galajda P, Keymer JE, Dekker C (2009) Bacterial growth and motility in sub-micron constrictions *P. Natl. Acad. Sci. USA* **106** (35), 14861-14866

Ognier S, Wisniewski C, Grasmick A (2004) Membrane bioreactor fouling in sub-critical filtration conditions: a local critical flux concept *J. Membrane Sci.* **229** (1-2), 171-177

Remy M, van der Marel P, Zwijnenburg A, Rulkens W, Temmink H (2009 Low dose powdered activated carbon addition at high sludge retention times to reduce fouling in membrane bioreactors *Water Res.* **43** (2), 345-350

Rishell S, Casey E, Glennon B, Hamer G (2004) Characteristics of a methanotrophic culture in a membrane-aerated biofilm reactor *Biotechnol. Progr.* **20** (4), 1082-1090

Scheenen TWJ, van Dusschoten D, de Jager PA, van As H (2000) Microscopic displacement imaging with pulsed field gradient turbo spin-echo NMR *J. Magn. Reson.* **142**, 207-215

Skillman L, Sutherland IW, Jonse MV (1999) The role of exopolysaccharides in dual species biofilm development *J. Appl. Microbiol*. **85** (28), 13S-18S

Srinivasan S, Harrington GW (2007) Biostability analysis for drinking water distribution systems *Water Res.* **41** (10), 2127-2138

Sutherland IW (2001) Exopolysaccharides in biofilms, flocs and related structures *Water Sci. Technol.* **43** (6), 77–86

van den Brink P, Zwijnenburg A, Smith G, Temmink H, van Loosdrecht MCM (2009) Effect of free calcium concentration and ionic strength on alginate fouling in cross-flow membrane filtration *J. Membrane Sci.* **345** (1-2), 207-216

van der Kooij D, Vrouwenvelder HS, Veenendaal HR (1995) Kinetic aspects of biofilm formation on surfaces exposed to drinking water *Water Sci.Technol.* **32** (8), 61-65

van der Marel P, Zwijnenburg A, Kemperman AJB, Wessling M, Temmink H, van der Meer WGJ (2009) An improved flux-step method to determine the critical flux and the critical flux for irreversibility in a membrane bioreactor *J. Membrane Sci.* **332** (1-2) 24-29

van der Marel P, Zwijnenburg A, Kemperman A, Wessling M, Temmink H, van der Meer W (2010) Influence of membrane properties on fouling in submerged membrane bioreactors J. Membrane Sci. **348** (1-2), 66-74

Wang Y, Hammes F, Boon N, Egli T (2007) Quantification of the filterability of freshwater bacteria through 0.45, 0.22, and 0.1 µm pore size filters and shape-dependent enrichment of filterable bacterial communities *Environ. Sci. Technol.* **41** (20), 7080-7086

Wang Z, Wu Z, Yin X, Tian L (2008) Membrane fouling in a submerged membrane bioreactor (MBR) under sub-critical flux operation: Membrane foulant and gel layer characterization *J. Membrane Sci.* **325** (1) 238-244

Witzig R, Manz W, Rosenberger S, Krüger U, Kraume M, Szewzyk U (2002) Microbiological aspects of a bioreactor with submerged membranes for aerobic treatment of municipal wastewater *Water Res.* **36** (2), 394-402

Wu J, Le-Clech P, Stuetz RM, Fane AG, Chen V (2008) Novel filtration mode for fouling limitation in membrane bioreactors *Water Res.* **42** (14), 3677-3684

Chapter 5

BACTERIAL COMMUNITIES IN SLUDGE FRACTIONS AND MEMBRANE BIOFILMS IN A MEMBRANE BIOREACTOR

This chapter has been submitted as:

van den Brink P, Faust L, Zwijnenburg A, Temmink H, van Loosdrecht MCM (2014) Bacterial communities in sludge fractions and membrane biofilms in a membrane bioreactor

ABSTRACT

The contribution of wastewater and different sludge fractions in membrane bioreactors (mixed liquor, mixed liquor supernatant) to bacterial community structure of the membrane biofilm is limited characterised to date. The community structure and dynamics of sludge fractions in an MBR treating municipal wastewater were compared with those of the wastewater and membrane biofilms using cultivation independent molecular techniques. Constant flux filtrations were performed and samples were taken at three different dates. Total genomic DNA was extracted and the bacterial 16S rDNA genes were amplified. Denaturating gradient gel electrophoreses (DGGE) and sequence analysis of excised bands revealed a high bacterial diversity in the wastewater, sludge fractions and membrane biofilms. The reciprocal of Simpson's index of diversity (1/D) and Shannon-Wiener index showed an increase in diversity in the following order: wastewater < mixed liquor supernatant < mixed liquor < membrane biofilm. No higher similarity of biofilm communities with one specific other MBR fraction was observed. The bacterial communities in the wastewater, sludge fractions and membrane biofilms were time variable. Only at higher biofilms ages, a clear effect of biofilm age on biofilm communities was observed: communities, distinct from those in wastewater and sludge fractions, developed at higher biofilm ages. This indicates occurrence of active bacterial growth on the membrane. No effect of flux on bacterial diversity of the biofilms could be observed and few bacterial genera could be removed by harsh mechanical cleaning. Further research should focus on the relationship between bacterial community structure and function, such as EPS production.

Key words: biofilm formation, bacterial community, membrane bioreactors, biofilm age, community dynamics.

INTRODUCTION

The widespread application of membrane bioreactors (MBRs) for municipal wastewater treatment is hampered by membrane fouling, which increases energy costs, reduces performance and creates the need for more frequent membrane cleaning or replacement. Membrane fouling in MBRs is known to be caused by several membrane fouling mechanisms and many publications indicate that extracellular polymeric substances (EPS) play a major role during fouling development (Le-Clech et al. 2006). EPS can be produced by biofilm bacteria or deposited from the mixed liquor. The relative contributions of these fouling mechanisms to total fouling resistance are unclear and likely case specific. There are currently however no good methods to differentiate the different fouling mechanisms in practical situations.
The membrane surface is a suitable environment for biofilm formation (Bereschenko et al. 2007, Miura et al. 2007b, Huang et al. 2008) and biofilm formation, and associated EPS production, therefore recently has gained attention as an important fouling mechanism in MBRs (Ng et al. 2006, Zhang et al. 2006, Miura et al. 2007b, Huang et al. 2008). In MBRs, biofilms were shown to develop on the feed side of membranes as well as on their permeate sides (van den Brink et al. 2013). These biofilms could not be removed by harsh mechanical cleaning. Substrates and oxygen are provided to the biofilm bacteria by the diffusive flux towards and convective flux through the membrane.

While the few studies which have contributed to the characterisation of bacterial communities in MBRs and on the membranes in these reactors are well executed and quite extensive, the contribution of wastewater and different sludge fractions (mixed liquor, mixed liquor supernatant) in the MBRs to community structure of the membrane biofilm is not understood to date. Knowledge on the origin of bacterial species in the biofilm (wastewater, the mixed liquor or mixed liquor supernatant) can help to prevent biofouling by targeting fouling control techniques on this origin. The similarity between the microbial community on the membrane and in the wastewater and sludge fractions gives insight on whether bacteria just accumulate on the membrane surface or are actively growing or screened out at the membrane surface. Also the time variance of the microbial community on the membrane is relevant and as yet not investigated. Filtration flux could affect the bacterial community, as the convective force that acts on the bacteria is larger at higher flux values. A larger variety of bacteria in the biofilm therefore can be expected for membranes that are operated at higher fluxes. The convective force that drags particles towards the membrane surface increases with particle size, but the lift force, induced by shear flow and causing back transport away from the surface, increases even more with particle size (Altmann and Ripperger, 1997). This could result in a higher similarity of the bacterial community between the mixed liquor supernatant and the biofilm on the membrane as compared to the mixed

liquor and the biofilm. Removability of the biofilm by mechanical cleaning is relevant for practice. It is known that the bacteria remaining after a cleaning will quickly develop a new biofilm if sufficient nutrients are available (Flemming, 2002). As the membrane biofilms in a MBR are directly positioned in the mixed liquor, nutrient limitation does not occur unless the MBR removes all nutrients very efficiently. Mechanical cleaning to remove biofilms would therefore be most effective when all bacteria can be removed.
Ultimately, it would be the goal to identify potential key players in the biofilms. By studying bacterial community structure and dynamics of different fractions in MBRs treating municipal wastewater using cultivation independent molecular techniques, information can be gained that is useful to engineers designing new membrane bioreactors. Although active growth of bacteria can not be proven for all biofilms referred to in this manuscript, they do meet the definition by Costerton and co-workers: "Biofilms are defined as matrix-enclosed bacterial populations adherent to each other and/or to surfaces or interfaces" (1995).

The main objectives of this study were to find out whether

1. the bacterial communities in the biofilm are different from those in the wastewater, mixed liquor or mixed liquor supernatant
2. there are dominant bacterial species in the biofilm and if so, to identify them
3. the bacterial community in the biofilm is changing in time
4. the applied flux during filtration affects the bacterial community in the biofilm
5. bacteria can be removed from the membrane by harsh mechanical cleaning

Samples were taken from a pilot-scale MBR treating municipal wastewater of which the performance in terms of COD removal, nitrification and transmembrane pressure (TMP) development was monitored. In a filterability set-up connected to the pilot-scale MBR, different fluxes were applied and TMP development was monitored for each membrane. In this way, the dynamics of the bacterial communities of wastewater, different sludge fractions and the membrane biofilm and their relation could be obtained and linked to membrane performance in the MBR.

MATERIALS AND METHODS

Experimental set-up

A pilot-scale MBR (Figure 5.1) with a total working volume of 85 L and fed with municipal wastewater was used as a source of activated sludge for the experiments. The wastewater was screened (5 mm) before entering the biological reactors. The COD of the wastewater was 395 mg L^{-1} on average, but fluctuated between 150 and 600 mg L^{-1}. The pilot-scale MBR

was operated at an HRT of 6.3 h and SRT of 25 days and an average temperature of 20.6 degrees Celsius. The oxygen concentration in the aerobic tank was measured on-line and controlled at 1.5 mg L^{-1} with a fine-bubble diffuser.

The membrane tank was equipped with 5 PE flat sheet membranes with a nominal pore size of 0.3 µm and a surface area of 0.063 m^2 each (Kubota, Japan). The channel width between the membranes was 7 mm. Coarse bubble aerators placed below the membranes provided a specific aeration demand (SAD) of 1.4 m^3 m^{-2} h^{-1} (equivalent to 0.1 cm s^{-1}) to scour the membrane surface and in this manner reduce fouling. With a peristaltic pump, permeate was continuously extracted at a flux of 47.9 L m^{-2} h^{-1}.

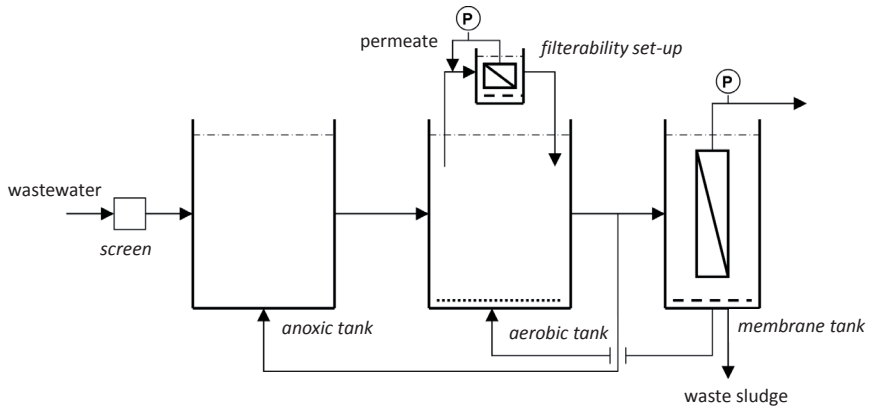

Figure 5.1 Pilot-scale MBR and filterability set-up (Remy et al., 2010).

To measure sludge filterability, sludge from the aerobic reactor of the MBR was continuously recirculated over two vessels with volumes of 5 L each and retention times of 1 h (Figure 5.1). The vessels contained homemade submerged flat-sheet polyvinylidene fluoride (PVDF) membranes with a surface area of 0.014 m^2, casted from a PVDF/PVP/NMP solution (van der Marel et al. 2010). The temperature in the aerated tank of the pilot and filterability set-ups was continuously monitored. The trans-membrane pressure (TMP) was monitored on-line (Endress + Hauser, Cerabar M PMC 41), both in the pilot and in the filterability set-ups.

Experiments and sampling

Constant flux filtrations were performed in the filterability set-ups at fluxes between 10.7 and 29.4 L m^{-2} h^{-1} for 15-111 days (Table 5.1). Membrane fluxes were measured manually every day. Pre-screened wastewater, MBR mixed liquor samples and membrane biofilm samples were taken at three different dates (21-7 (A), 24-8 (B) and 15-10 (C)). Mixed liquor samples were splitted, and half of the samples were allowed to settle for 30 minutes, after which their

supernatants were collected. Membrane biofilms were sampled by cutting pieces of 8 cm^2 out of the fouled membrane material with a sterile scalpel. Samples were taken at different positions on the membrane (left (L, middle (M), or right (R)). On 29-7, membranes 1 and 3 were replaced with clean membranes and on 20-8, membrane 1 was replaced again with a clean membrane, as too little membrane surface was left over after several membrane samplings (including samplings for other studies). At the last sampling date (15-10), biofilm material was also scraped from the membrane surface with a sterile spatula after rinsing the surface thoroughly with MBR permeate (to remove loosely attached sludge), yielding 2 additional samples: a scraped off biofilm and a scraped membrane surface. Scraped off biofilm was put in 0.5 ml DNAse free water prior to further treatment.

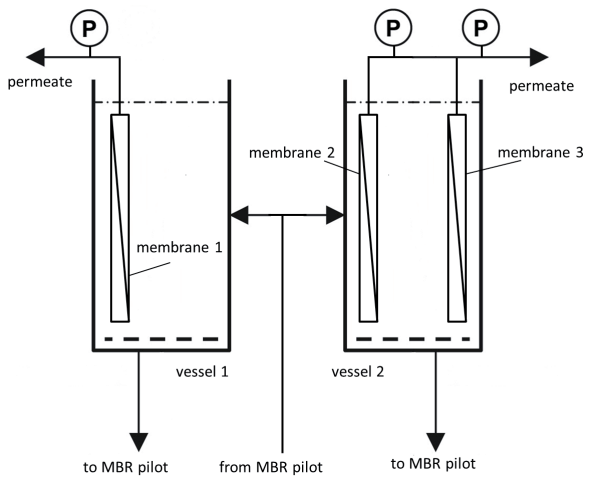

Figure 5.2 Filterability set-up containing 2 vessels. Vessel 1 contains membrane 1, vessel 2 contains membrane 2 and 3. There is a continuous recirculation of sludge from the aerobic reactor of the MBR pilot.

Figure 5.2 gives a description of the vessels from the filterability set-up. An explanation on the source of the samples can be found in Table 5.1. Vessel 1 in the filterability set-up contained membrane plate 1, while membrane plates 2 and 3 were placed in the other vessel. Therefore, the wastewater and sludge fractions of vessel 1 and the membrane samples of plate 1 are grouped in Table 5.1, as well as wastewater and sludge fractions of vessel 2 and membrane samples of plates 2 and 3. For the biofilm samples, flux values before sampling are given in Table 5.1. The residence time of the membrane plates in the vessels is expressed as biofilm age and can differ among membrane plates sampled at the same date. Biofilm age is counted from the day at which a clean membrane is placed in the vessel.

Table 5.1 Source of MBR samples, including sampling date (A = 21-7, B = 24-8, C = 15-10) and flux at sampling date (for biofilm samples). L (left), M (middle), and R (right) refer to positions on membrane where sample is taken.

Sample name	Source of sample	Flux (L m^{-2} h^{-1})	Sampling dates	Biofilm age (days)
WW	Screened wastewater	n/a	21-7, 24-8, 15-10	n/a
ML1	Mixed liquor vessel 1	n/a	21-7, 24-8, 15-10	n/a
S1	Supernatant vessel 1	n/a	21-7, 24-8, 15-10	n/a
1R-A	Biofilm membrane 1	29.4	21-7	15
1L-A	Biofilm membrane 1	29.4	21-7	15
1L-B	Biofilm membrane 1	24.4	24-8	4
1M-B	Biofilm membrane 1	24.4	24-8	4
1A-C	Biofilm membrane 1	22.1	15-10	56
1B-C	Biofilm membrane 1	22.1	15-10	56
1S-C	Scraped membrane 1	22.1	15-10	56
Sc1-C	Scrapings membrane 1	22.1	15-10	56
ML2	Mixed liquor vessel 2	n/a	21-7, 24-8, 15-10	n/a
S2	Supernatant vessel 2	n/a	21-7, 24-8, 15-10	n/a
2L-B	Biofilm membrane 2	10.7	24-8	69
2R-B	Biofilm membrane 2	10.7	24-8	69
2A-C	Biofilm membrane 2	10.1	15-10	111
2B-C	Biofilm membrane 2	10.1	15-10	111
2S-C	Scraped membrane 2	10.1	15-10	111
Sc2-C	Scrapings membrane 2	10.1	15-10	111
3R-A	Biofilm membrane 3	15.1	21-7	30
3M-A	Biofilm membrane 3	15.1	21-7	30
3L-B	Biofilm membrane 3	15.4	24-8	41
3R-B	Biofilm membrane 3	15.4	24-8	41
3A-C	Biofilm membrane 3	13.5	15-10	93
3B-C	Biofilm membrane 3	13.5	15-10	93
3S-C	Scraped membrane 3	13.5	15-10	93
Sc3-C	Scrapings membrane 3	13.5	15-10	93

Total DNA extraction and PCR amplification

Total DNA was extracted from liquid and membrane samples using a mini bead beater (Biospec Products Inc., Bartlesville, OK) and a FastDNA Spin kit for soil (MP Biomedicals, Illkirch, France) in accordance with the manufacturer's instructions. For liquid samples (wastewater, bioreactor mixed liquor, scraped biofilm in DNAse free water), a sample volume of 0.5 ml was put in a lysing tube. To obtain sufficient material for this sample type, mixed liquor supernatants were filtered through a 0.22 µm disc filter (Millipore, Ireland) and the filter was added to a lysing tube. Membrane samples were also added to a lysing tube. In order to reach the same total volume in all lysing tubes, 0.5 ml of DNAse free water was added to the lysing tubes containing the filters and membranes.

Fragments (433 bp) of bacterial 16S rRNA genes were amplified from total genomic DNA by PCR using *Taq* polymerase (Invitrogen, the Netherlands) with eubacterial primers 968f and

1401r (Nübel et al., 1996). For denaturing gradient gel electrophoresis (DGGE) analysis, the same fragment was amplified, and a GC clamp was attached to the forward primer at the 5' end (Nübel et al., 1996).

The thermocycling parameters were as follows: predenaturation at 94°C for 5 min, followed by 30 cycles of denaturation at 94°C for 1 min, primer annealing at 56°C for 40 s, and elongation at 72°C for 1 min. The thermocycling postelongation step was held at 72°C for 30 min to avoid artifactual double bands (Janse et al., 1994), followed by cooling at 4°C. Size and yield of the PCR products were estimated by electrophoresis on a 1% (wt/vol) agarose gel. All primers were purchased from MWG-Biotech (Ebersberg, Germany), and PCR buffer, $MgCl_2$ solution, deoxynucleotides, and *Taq* polymerase were purchased from Invitrogen (Breda, the Netherlands).

DGGE analysis of amplified 16S rRNA genes and sequencing

Amplicons were run on 8% (wt/vol) polyacrylamide gels containing a 30 to 60% denaturant gradient of formamide and urea, as previously described (Muyzer et al., 1993). Bands were visualized by silver nitrate staining (Sanguinetti et al., 1994). DGGE profiles were analysed using Bionumerics 7.1 software (Applied Maths). Band-independent, whole-densitometric curve-based Pearson correlation analysis was performed followed by UPGMA (unweighted pair group method using arithmetic average) clustering. The reciprocal of Simpson's index of diversity (1/D) and Shannon-Wiener index were determined. Average values were calculated for wastewater, sludge fractions and membrane biofilms based on the DGGE fingerprints of the three sampling dates as well as averages for membrane biofilm samples which were operated at the same flux.

All amplicons except for duplicates, were run on 8% (wt/vol) polyacrylamide gels again to excise the bands for sequencing. For band excision, the DGGE gel was stained with SYBR green solution (SigmaAldrich, the Netherlands). Individual bands were excised, placed in 10 mM Tris buffer, incubated for 2 nights at 4°C, and re-amplified. PCR products were purified and sequenced by a commercial company (Baseclear, the Netherlands). For bands that gave double signal during sequencing, the PCR products were run again on 8% (wt/vol) polyacrylamide gels to obtain a better separation. The bands of these gels were processed and sequenced as explained above.

Sequences were processed using Chromas Pro 1.7.5 (Technelysium Pty Ltd, Australia) before analysing the sequence similarity using the NCBI BLAST search tool at http://ncbi.nlm.nih.gov/BLAST (Altschul et al., 1997).

The 16S rRNA gene sequences from this study have been deposited in the European Molecular Biology Laboratory nucleotide sequence database under accession numbers HG942394 to HG942425.

RESULTS

MBR performance and membrane fouling

The pilot-scale MBR was operated at an HRT of 6.3 h and SRT of 25 days and an average temperature of 20.6 degrees Celsius. The mixed liquor suspended solid (MLSS) concentration was on average 3.9 g L^{-1} (ranging from 2.9 - 5.2 g L^{-1}) in the aerobic tank of the MBR. This relatively low MLSS concentration was due to the fluctuations in strength of the municipal wastewater (150-600 mg COD L^{-1}). The pilot-scale MBR showed good COD removal (around 90%) and full nitrification (99%).

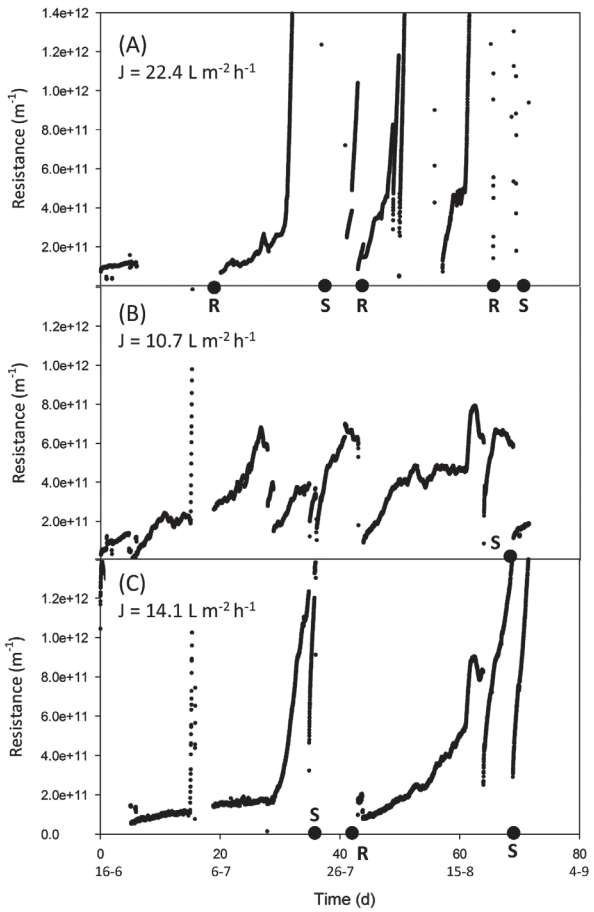

Figure 5.3 Resistance curves of the three different membranes operated in continuous mode. (A) Membrane 1 run at an average flux of 22,4 L m^{-2} h^{-1}, (B) Membrane 2 run at an average flux of 10,7 L m^{-2} h^{-1} and (C) Membrane 3 run at an average flux of 14,1 L m^{-2} h^{-1}. Sampling points (S) and membrane replacements (R) can be recognised by dots.

Figure 5.3 shows the resistance curves of the membranes in the filterability set-up, run at different continuous fluxes, for the first 71 days of filtration. Sampling (S) and membrane replacement (R) is indicated with dots and is always associated with a hitch in the filtration curve. Exponential increase of resistance can be observed at several points in time during filtration. Membrane 1, which was run at the highest average flux, shows a faster increase of resistance than membranes 2 and 3. For membrane 2, filtration resistance stayed below $8*10^{11}$ m^{-1} during the entire course of filtration.

General impression DGGE fingerprints

All tested samples showed many distinct bands, indicating multiple genera and thus a high microbial diversity. Two diversity indices are given in Table 5.2 for wastewater, sludge fractions and membrane biofilms: the reciprocal of Simpson's index of diversity (1/D) and Shannon-Wiener. Average values were calculated based on the DGGE fingerprints of the three sampling dates. These indices clearly show an increase in diversity in the following order: wastewater < mixed liquor supernatant < mixed liquor < membrane biofilm. DGGE fingerprints of duplicate samples had similar banding patterns with cophenetic correlation values ranging from 78.2-96.9% (from Pearson correlation analysis and clustering analysis based on UPGMA algorithm). This proves the reproducibility of DNA extraction, PCR amplification and DGGE analysis. In most cases, the banding patterns of membrane biofilms of different sampling positions on the same membrane were similar. This shows that, although fouling was mostly not evenly distributed by visual observation, the bacterial diversity did not markedly differ over the membrane surface.

Table 5.2 Average diversity values for wastewater, sludge fractions and membrane biofilms based on DGGE fingerprints of the three different sampling dates.

Source of sample	1/D	Shannon-Wiener
Screened wastewater	6,39	2,00
Mixed liquor	11,7	2,62
Mixed liquor supernatant	10,6	2,44
Membrane biofilm	13,1	2,74

Fingerprints of wastewater, sludge fractions and membrane biofilm communities

Although Figure 5.4 only shows the DGGE gel of samples taken at 21-7, it is representative for DGGE gels containing samples taken at the other time points. DGGE patterns of wastewater, sludge fractions and membrane biofilm samples were compared to assess the distribution of bacteria over these fractions. Although the intensity of bands in some lanes (especially for the ML samples and 3R) is low, the dominant (intense) bands are still visible. In total, approximately fourteen different DGGE bands could be identified for all samples. At least five dominant bands could be clearly discriminated for each sample (Figure 5.4).

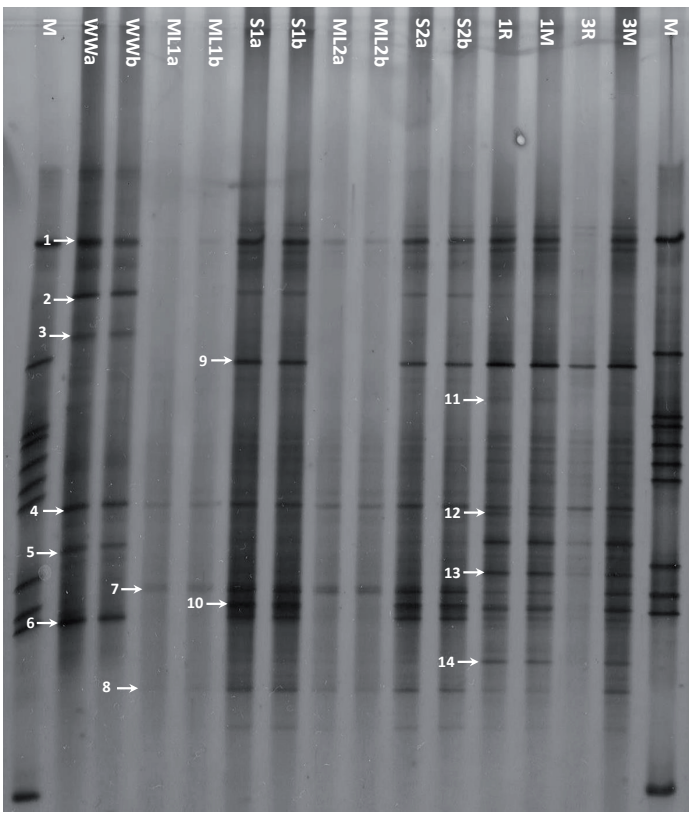

Figure 5.4 DGGE band profiles of amplified 16S rDNA fragments from different MBR fractions (samples taken at 21-7). M = synthetic marker, WW = wastewater, ML = mixed liquor, S = mixed liquor supernatant, Number = biofilm sample from that membrane, R = right side of membrane, M = middle of membrane, a, b = duplicates. Band position was highlighted with a numbered arrow.

When the banding patterns of the samples shown in Figure 5.4 are compared, bands with different abundance were found. Some bands were abundant in all samples (bands 1,4). Others were not present in the mixed liquor samples, while they were present in the other samples (bands 2,5,6). This can be explained by the low intensity of banding patterns of the mixed liquor samples, which decreases the visibility of some bands. Biases to take into account when applying traditional cultivation independent molecular techniques to study bacterial diversity are treated in the Discussion section. One band was only observed in the wastewater samples (band 3). Several bands were not present in the wastewater samples, while in both sludge fractions and membrane biofilms (bands 7,8) or in mixed liquor supernatants and membrane biofilms (bands 9,10) they could be seen. A considerable part of the fourteen distinct bands were only found in the biofilm samples (bands 11-14), indicating that enrichment of bacteria is taking place at the membrane surface. Comparing

banding patterns of the biofilm samples with those of wastewater and sludge fractions for all three sampling dates, similarities between biofilm communities and those of wastewater and sludge fractions were found to be identical: no higher similarity of biofilm communities with one specific other MBR fraction (wastewater, mixed liquor, mixed liquor supernatant) was observed.

To see whether there are bacteria specifically present in the biofilm, DGGE patterns of biofilm samples were compared with those of the wastewater and sludge fractions sampled at the same day for all three sampling dates. Bands that are only observed for the biofilm samples, specific biofilm bands (e.g. Figure 5.4, bands 11-14), are in general the same for different positions on the same membrane, but also for different membrane plates (2 and 3) which were operated in the same vessel (that contained the same mixed liquor). Development of bacterial communities on the membranes in time will be further discussed below.

Community dynamics

To evaluate the development of bacterial communities in wastewater and sludge fractions in time (community dynamics), the band profiles of wastewater, mixed liquor and supernatant samples taken at different time points were compared (data not shown). For all these samples holds that, although there are some bands appearing at two or three time points, the majority of the bands in the banding patterns appear only once in time. This means that the wastewater, sludge fractions and membrane biofilms contain very dynamic bacterial communities.

The community dynamics of the membrane biofilms was studied in detail by running all membrane biofilm samples on one DGGE gel. Comparing the DGGE band profiles of biofilm samples taken at different time points, several patterns could be identified (Figure 5.5). Some bands were only observed at one time point (21-7: bands 1-3; 24-8: bands 9, 11; 15-10: bands 14-17), while others are present for two time points (21-7 & 24-8: bands 4, 6; 24-8 & 15-10: bands 10, 12, 13) or even all three time points (bands 5, 7, 8).
As described in Materials and Methods, on 29-7 the membranes were replaced by other membranes that already contained biofilms (see Table 5.1 for their respective biofilm ages). Because of this, only the biofilm communities sampled at 24-8 and 15-10 can be compared. Despite of this, it is interesting to see several bands appearing in the biofilm samples of 21-7 as well as in those of 24-8 (bands 4-8). Similar communities seem to develop on membrane plates run at different fluxes and placed in different vessels. The mixed liquor exposed to the membrane is the same in both vessels, because the residence time in the vessels is very small compared to that of the pilot-scale MBR. Figure 5.4 also shows similar banding patterns for ML1 and ML2 samples and for S1 and S2 samples. Altogether, mixed liquor,

mixed liquor supernatant and biofilm samples from different vessels show similar bacterial communities.

When discussing community dynamics, it is also important to take into account the operational time of the membrane plates in the vessels, expressed in Table 5.1 as biofilm age. Comparing the banding patterns of membranes that were operated in different vessels, a difference is observed between the samples taken at 21-7 and 24-8 and the samples taken at 15-10 (Figure 5.5). For biofilms from different vessels sampled at the same date, no large differences can be found in the banding patterns, while their biofilm ages are rather different (15 and 30 days for 21-7, and 4-69 days for 24-8). This would indicate no large effect of biofilm age on biofilm community at these relatively short biofilm ages. For the samples taken at 15-10, there are some common bands, but also many different bands (for example bands 15 and 17).

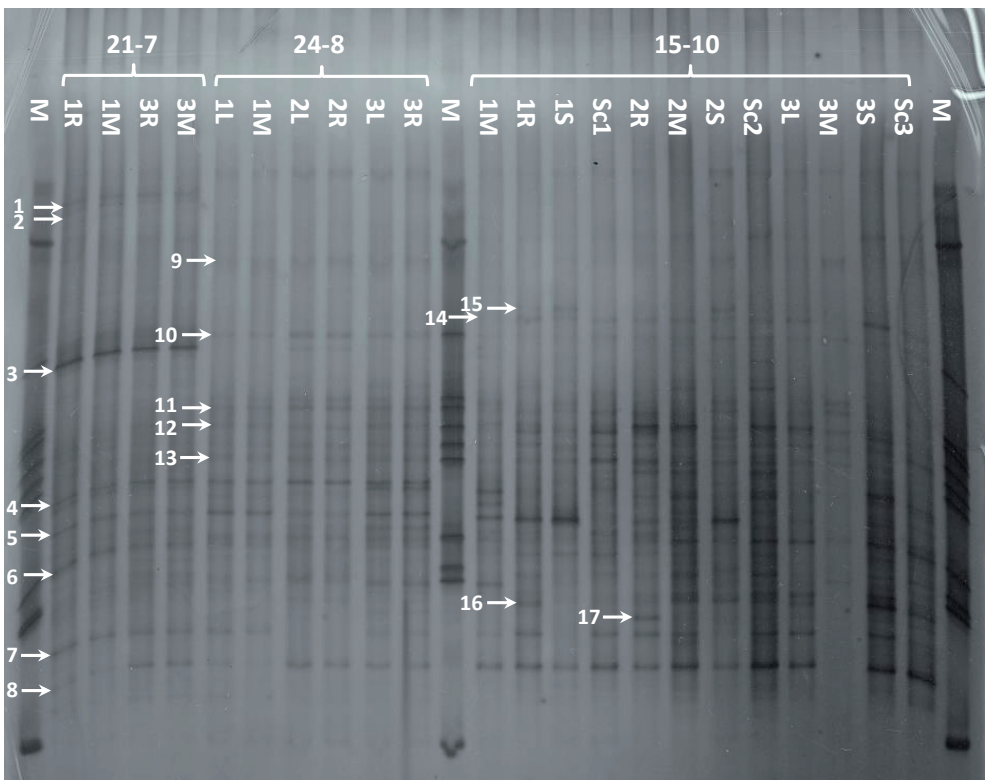

Figure 5.5 DGGE band profiles of amplified 16S rDNA fragments from biofilm samples taken at different time points. M = synthetic marker, Number = biofilm sample from that membrane, R = right side of membrane, M = middle of membrane, L = left side of membrane, Sc = scrapings, S = scraped off surface, a, b = duplicates. Band position was highlighted with a numbered arrow.

As these bands were not observed for the wastewater and sludge fractions at 15-10, the genera represented by these bands must have deposited on the membranes during filtration before 15-10. The difference between banding patterns of the membrane biofilms and the other samples was higher for membranes 2 and 3, which had biofilm ages of 93 and 111 days, respectively, as compared to membrane 1 with biofilm age 56 days (see Table 5.1). Membranes 2 and 3 were exposed to the wastewater and sludge fractions for the longest time of all samples. The biofilms on these two membranes had higher chances to develop towards more distinct communities. Long-term experiments should be performed to test this hypothesis.

Looking at the complexity of the banding patterns of the biofilm samples and taking into account the diversity indices as shown in Table 5.2, it can be concluded that the diversity of the membrane biofilms is high compared to the wastewater and sludge fractions. No dominant genera were identified in the membrane biofilms. At higher biofilm ages, more distinct communities form on the membranes, indicating that active bacterial growth is taking place at the membrane surface. The high dynamics of the membrane biofilm samples seems to be in line with the observations made for the wastewater and sludge fractions, which also vary a lot in time.

To conclude, there is quite some similarity between communities in the membrane biofilms and the wastewater and sludge fractions (Figure 5.4). The dynamics of the biofilm community is high with several genera coming up and disappearing in time (Figure 5.5). Distinct biofilm communities form at higher biofilm ages.

Effect of mechanical cleaning

At the third sampling date (15-10), the effect of mechanical cleaning on the presence of bacteria was also investigated. Next to taking regular biofilm samples, biofilm material was scraped from the membrane surfaces, yielding 2 additional sample types: scraped off biofilms and scraped membrane surfaces. Figure 5.5 shows the banding patterns of the scraped off membranes (1S, 2S, 3S) and the scrapings (Sc1, Sc2, Sc3). In general, the banding patterns of the membrane biofilm samples are similar to those of the scrapings (for example 2R, 2M and Sc2) and also mostly to those of the scraped off membrane surfaces. As after scraping most community members are still present on the membrane surface, scraping causes little selective removal of bacteria.

Effect flux

A larger variety of bacteria in the biofilm was expected for membranes that are operated at higher fluxes. Filtrations were performed at different average flux values (10.7 (membrane

2), 14.1 (membrane 3) and 22.4 (membrane 1) L m^{-2} h^{-1}). DGGE banding patterns of the different biofilm samples (Figure 5.5) were compared to check whether a larger diversity of bacteria in the biofilm was found for the membranes that were operated at higher fluxes. No differences in bacterial diversity were observed for the biofilm samples obtained at different fluxes. This was confirmed by calculation of the reciprocal of Simpson's index of diversity (1/D) and Shannon-Wiener index for the three flux values. These values were very similar for all three flux values: 12,71 (1/D) and 2.73 (SW) for 22,4 L m^{-2} h^{-1}, 12,59 (1/D) and 2,68 (SW) for 14,1 L m^{-2} h^{-1} and 12,79 (1/D) and 2,72 (SW) for 10,7 L m^{-2} h^{-1}. Perhaps the flux differences applied were too small to test the hypothesis of larger bacterial diversity at higher fluxes. However, as the applied fluxes are relevant for practical MBR operation, it can be concluded that in the operationally relevant flux range no differences in bacterial diversity can be expected in the membrane biofilms. Another explanation could be that there are differences in diversity being more evident for the taxa below the detection limit.

Apart from the larger variety biofilm communities that were expected for the high flux biofilms, another hypothesis was tested for the effect of flux on biofilm community development. Because lift forces and associated back transport increase with particle size (Altmann and Ripperger, 1997), the balance between permeation drag and back transport was expected to cause preferential deposition of smaller particles on the membrane surface. Therefore, a higher similarity of bacterial community between the mixed liquor supernatant (having a smaller average particle size) and the membrane biofilm was expected than between the mixed liquor and the membrane biofilm. This effect should be most clear for the high flux biofilms. From the DGGE banding patterns of two sampling dates (21-7 and 24-8), no clear correlation was obtained concerning similarity between mixed liquor, mixed liquor supernatant and membrane biofilm samples run at different flux values. For the samples taken at 15-10, which have biofilm ages of 56-111 days (Table 5.1), the banding patterns of the higher flux biofilm samples (membrane 1) show a higher similarity to both mixed liquor and mixed liquor supernatant samples than for the lower flux biofilms (membrane 2 and 3). This suggests that the higher flux biofilm has a more dynamic bacterial community that is influenced by the mixed liquor and supernatant bacteria, while the lower flux biofilms contain a more independent community. This would be in agreement with active bacterial growth on the membrane. It should be noted that the membranes with the lower fluxes were also the ones with the highest biofilm ages. Longer term MBR operation with regular sampling should be performed to test the importance of applied flux and biofilm age on community development.

Sequencing

Sequencing was performed to find out which bacterial species were present in the wastewater, sludge fractions and membrane biofilm. The 16S rRNA amplicons were run

on DGGE gels again prior to band excision and sequencing. Sequence similarity of these amplicons with their closest relative in the NCBI database is shown in Table 5.3.
Only 30% of all excised and sequenced bands gave a single signal. This is probably due to the high diversity in the wastewater, sludge fractions and membrane biofilms. Next generation sequencing would be a better option for future studies with these types of samples. Despite the low success rate of the applied procedure, interesting information was obtained from the sequenced amplicons. A clear difference was found between the closest relatives found for the 24-8 samples compared to the samples of the other two dates. *Pseudomonas* was the only cultured genus encountered on 24-8, and it was found in the wastewater and sludge fractions but not in the biofilm. In the samples of other two sampling dates, *Pseudomonas* was not detected at all. A strain of *Arcobacter cibarius* was detected in the wastewater and mixed liquor at 15-10. In case the same closest relatives were found in different samples, these samples were never biofilm samples and the samples were mostly taken at the same date. Most of the closest relatives were uncultured bacterium clones of various sources, such as salt and fresh water, soils and various wastewater treatment plants. Few bacterium clones were specifically found in the biofilm samples, of which only clone GRF1171d09 was isolated from a biofilm-type of source: a microbial mat found in caves. A few different bacterium clones, isolated from high N-amended soils, were found in the biofilm samples of 21-7 and the mixed liquor of 15-10. No bacterial species or uncultured bacterium clones were found in the biofilms at more than one time point. This is in line with what was concluded before, that the bacterial diversity in the biofilms is very high, and no dominant species can be identified.

DISCUSSION

Bacterial diversity in the MBR

The high diversity as found for the MBR samples is common for municipal wastewater (McLellan et al. 2010) and activated sludge samples (Snaidr et al. 1997; Wagner and Loy, 2002; Zhang et al. 2012). In most literature on bacterial communities in MBRs, diversity is linked to biological process performance (Miura et al. 2007a; Wan et al. 2011). In our study, the performance of the membrane filtration and the origin of membrane fouling were of interest rather than the biological process performance. Insight in the structure and dynamics of bacterial communities in MBR fractions may help us to understand biofilm formation and biofouling in MBRs in a better way.

Comparing banding patterns of the biofilm samples with those of the wastewater and sludge fractions (Figure 5.4), almost all bands identified on this DGGE gel can be found in

the biofilm samples. The biofilm communities were are suggested to be more diverse than the wastewater and sludge fractions, which is confirmed by the diversity indices which were found (Table 5.2). Four out of 14 bands were only observed for the biofilm samples. This indicates that enrichment of bacteria is taking place on the membrane. Apparently, for some bacteria, the biofilm is their preferred niche. Specific groups of bacteria were also found to preferentially grow on membranes in MBRs by Huang and others (2008). Biofilm communities found by these researchers were both diverse and distinct from those in the planktonic biomass. Comparing banding patterns of the biofilm samples with those of wastewater and sludge fractions for all three sampling dates, similarities between biofilm communities and those of wastewater and MBR sludge fractions were found to be identical: no higher similarity of biofilm communities with one specific other MBR fraction (wastewater, mixed liquor, mixed liquor supernatant) was observed. One should realise that biases may occur in several of the applied steps in the cultivation independent molecular approaches developed and used nowadays to study bacterial diversity in WWTPs, such as in cell lysis (Picard et al. 1992), during DNA extraction and purification (Liesack et al. 1991; Ogram et al. 1987; Tebbe and Vahjen, 1993), during PCR amplification (Cariello et al. 1991; Meyerhans et al. 1990; Reysenbach et al. 1992; Weller et al. 1991), or in cloning (Rainey et al. 1994).

No differences in bacterial diversity were found over the membrane surface as seen from the DGGE banding patterns of samples taken at different positions on the same membrane plate (for example 1R and 1M Figure 5.4), proving the reproducibility of DNA extraction, PCR amplification and DGGE analysis. Concerning the different MBR fractions, it should be noted that the MBR mixed liquor and mixed liquor supernatant are not entirely different as the mixed liquor also contains the mixed liquor supernatant bacterial community. However, the species richness (number of bacteria) of the mixed liquor supernatant is expected to be much lower than that of the mixed liquor and will not have a large influence on the mixed liquor bacterial community.

Though the process of band excision followed by re-amplification and purification resulted in a double signal during sequencing for most bands, 30% of all excised bands were successfully sequenced. Closest relatives of bacterial 16S rRNA gene amplicons retrieved from the different samples shown in Table 5.3 are given with their percentage of similarity. 16S rRNA sequence similarity of ≥ 97% was found to be a good threshold for grouping bacteria into species (Madigan et al. 2000; Hagström et al. 2002). Most of the closest relatives are uncultured bacterium clones, which is in line with the general understanding that uncultured bacteria are responsible for most key processes in WWTPs (Wagner and Loy, 2002). The closest cultured relatives with ≥ 97% similarity will be discussed below, as well as

Table 5.3 Closest relatives of bacterial 16S rRNA gene amplicons (approximately 433 bp) retrieved from wastewater, sludge fractions and membrane biofilms at several time points (see Table 5.1).

Source	Date	Accession number	Closest relative in GenBank (taxon, source, accession number)			%*
WW	21-7	HG942394	Uncultured bacterium clone BF2010_May_21m_G2	21m depth, Gulf of Trieste	JX864422.1	99
WW	21-7	HG942395	Uncultured *Arcobacter* sp. clone ATB-KS-13874	Wash water from spinach-processing plant	JQ845781.1	98
WW	21-7	HG942396	Uncultured bacterium clone H3	Sludge from wastewater treatment plant	KC352323.1	99
S1	21-7	HG942397	Uncultured bacterium clone C-84	Dianchi Lake, China	HQ860591.1	99
S2	21-7	HG942398	Uncultured bacterium clone FHINOA10/1-7682	Activated sludge	FJ430167.1	98
1M	21-7	HG942399	Uncultured bacterium clone H-LN-F2-Min_23388	Chronic N-amended soils	JQ055739.1	96
3M	21-7	HG942400	Uncultured bacterium clone H-Con-B2-Org_418021	Chronic N-amended soils	JQ054584.1	97
WW	24-8	HG942401	*Pseudomonas* sp. OOS114	Apple trees	KF448057.1	100
WW	24-8	HG942402	Uncultured bacterium clone AMD-H77	Pyrite mine acid mine drainage samples	KC749417.1	99
WW	24-8	HG942403	Uncultured bacterium clone 6C233145	Aquatic bacterial communities 250 miles from Panama City	EU805154.1	99
ML1	24-8	HG942404	Uncultured Unclassified bacterium 16S rRNA gene from clone QEDR3CD10	Mesophilic anaerobic digester treating municipal wastewater sludge	CU922371.1	99
ML1	24-8	HG942405	Uncultured bacterium clone 6C233145	Aquatic bacterial communities 250 miles from Panama City	EU805154.1	99
ML1	24-8	HG942406	Uncultured bacterium isolate DGGE gel band 25	Membrane bioreactor treating acetone, toluene, limonene and hexane	JX627839.1	95
S1	24-8	HG942407	*Pseudomonas* sp. OOS114	Apple trees	KF448057.1	99
ML2	24-8	HG942408	*Pseudomonas* sp. OOS114	Apple trees	KF448057.1	98
ML2	24-8	HG942409	Uncultured bacterium clone FHINOA10/1-7682	Activated sludge	FJ430167.1	98
ML2	24-8	HG942410	Uncultured bacterium isolate DGGE gel band BS112	Baltic Sea surface water	EU000891.1	99
S2	24-8	HG942411	*Pseudomonas* sp. OOS114	Apple trees	KF448057.1	99
1M	24-8	HG942412	Uncultured bacterium clone T0-Ps-25C-23	Ornamental fish aquaria	JX105655.1	97
1M	24-8	HG942413	Uncultured bacterium clone DPYIY	Atta colombica colony N12 fungus garden bottom	HM553768.2	99
2L	24-8	HG942414	Uncultured bacterium clone DPYIY	Atta colombica colony N12 fungus garden bottom	HM553768.2	99

Table 5.3 Continued.

Source	Date	Accession number	Closest relative in GenBank (taxon, source, accession number)			%*
WW	15-10	HG942415	*Arcobacter cibarius* strain AT1103	Bacteria isolated from fish processing wastewater treatment plant	KC161908.1	99
ML1	15-10	HG942416	Uncultured bacterium clone z37	Archeological complexes of the Pazyryk culture (IV-III centuries BC) in the north-west of Mongolia	JQ012230.1	95
ML1	15-10	HG942417	Uncultured bacterium clone H-LN-A3-Org_110017	Chronic N-amended soils	JQ049304.1	94
S1	15-10	HG942418	Uncultured bacterium clone b2	Rumen fluid	GQ301546.1	100
ML2	15-10	HG942419	Uncultured bacterium clone B22	Sewage of Da Qing Oil field	DQ452478.1	99
ML2	15-10	HG942420	Uncultured bacterium clone b2	Rumen fluid	GQ301546.1	99
ML2	15-10	HG942421	Uncultured *Acinetobacter* sp. clone SS38B102	South Shore wastewater treatment plant influent	GU356319.1	98
ML2	15-10	HG942422	*Arcobacter cibarius* strain AT1103	Bacteria isolated from fish processing wastewater treatment plant	KC161908.1	99
S2	15-10	HG942423	Uncultured bacterium clone b2	Rumen fluid	GQ301546.1	100
2M	15-10	HG942424	Uncultured bacterium clone YZ719	Soil	KF037537.1	97
Sc2	15-10	HG942425	Uncultured bacterium clone GRF1171d09	White microbial mat lava tube wall	JF266296.1	98

some sources of uncultured bacterium clones with ≥ 97% similarity that could be relevant.

Pseudomonas was the only cultured genus encountered on 24-8, and it was found in the wastewater and sludge fractions. In the samples of other two sampling dates, Pseudomonas was not detected. Pseudomonads are Gram-negative aerobic gammaproteobacteria and they belong to the family Pseudomonadaceae containing 191 validly described species (Euzéby, 1997). Many pseudomonads are able to degrade a very wide variety of organic molecules. They are therefore important in the mineralisation process in nature and in sewage treatment (Prescott et al. 1996). Their ability to degrade a wide range of carbon sources is in agreement with their abundance among the wastewater and sludge fractions. A strain of Arcobacter cibarius was detected in the wastewater and mixed liquor at 15-10. Arcobacter is considered an emerging, potential food and waterborne pathogen (Ho et al. 2006; Samie et al. 2006). A. Cibarius has been detected worldwide in products of animal origin (Ho et al. 2006).

In case the same closest relatives were found in different samples, these samples were always liquid samples and mostly taken at the same date. This can be explained by the small residence time in the vessels compared to that of the pilot-scale MBR, which does not allow distinct communities to be formed. Uncultured bacterium clones had various sources, such as salt and fresh water, soils and various wastewater treatment plants. At the first sight, salt water (Gulf of Trieste) as a source for bacterium clones encountered in the wastewater of 21-7 seems rather strange. However, the Gulf of Trieste is the shallowest (<60 m) part of the Adriatic Sea and has a high freshwater and nutrient discharge of the Po and other rivers (Giani et al. 2012), which does not make it a typical marine environment and allows for some species similarities with freshwater. Few bacterium clones were specifically found in the biofilm samples, of which only clone GRF1171d09 was isolated from a biofilm-type of source: a microbial mat found in caves. A few different bacterium clones, isolated from high N-amended soils, were found in the biofilm samples of 21-7 and the mixed liquor of 15-10. No bacterial species or uncultured bacterium clones were found in the biofilms at more than one time point. The overall impression from the DGGE gels and the sequencing data is that the bacterial diversity in the wastewater, sludge fractions and membrane biofilms is high and no dominant species can be identified.

Community dynamics

Apart from being diverse, the bacterial communities in the wastewater, sludge fractions and membrane biofilms were also found to be dynamic. High dynamics was suggested to be important for flexibility of a reactor to adapt to changing environmental conditions (Miura et al. 2007a). Though their positive correlation with bacterial community changes were

recently reported (Winkler et al. 2013), temperature shifts were not influencing the bacterial communities in our pilot-scale MBR as the temperature in the aerated tank was rather constant during operation. While the pilot-scale MBR was operated without disturbances and showed good COD removal (around 90%) and full nitrification (99%), stable performance is not necessarily linked to a stable bacterial community (Carrero-Colon et al. 2006; Fernandez et al. 1999; Lee et al. 2002; Wan et al. 2011). Fluctuations of nutrient levels in the influent could be a cause of the high diversity and dynamics of the bacterial community in the sludge fractions, as shown before in nutrient-pulsed chemostats (Carrero-Colon et al. 2006).

Membrane biofilms can be considered ecological niches compared to the wastewater and sludge fractions due to substrate gradients, different shear stress and perhaps the presence of slower-growing organisms, as was described for granular sludge (Winkler et al. 2013). One could therefore expect different bacterial diversity and less dynamics in the membrane biofilm as compared to the wastewater and sludge fractions. The reciprocal of Simpson's index of diversity (1/D) and Shannon-Wiener index were calculated and showed an increase in diversity in the following order: wastewater < mixed liquor supernatant < mixed liquor < membrane biofilm. The highest diversity of the membrane biofilms indicates that for many bacteria the biofilm is a suitable habitat. 4 out of 14 bands observed in Figure 5.4 were only found for the membrane biofilm samples. Comparing the DGGE banding patterns of all biofilm samples as shown in Figure 5.5, 8 out of 17 bands were identified at least at two different sampling dates. The composition of the bacterial communities in the membrane biofilms does change in time, but some bacteria stay for a certain time, or keep coming back to the membrane biofilm.

Biofilm age was also considered in the sense of community dynamics. No large effect of biofilm age on biofilm community was found at the first two sampling dates with relatively short biofilm ages of 4 to 69 days. For the 15-10 samples, biofilm ages ranged from 56 to 111 days. Different banding patterns were found for these different biofilm ages, with those of the highest biofilm ages (93 and 111 days) being more distinct from those of the wastewater and sludge fractions than was the case for the membrane biofilm of 56 days. Increasing biofilm age might induce the biofilm to become a distinct community, getting more mature by growing in cell numbers and being less influenced by their environment. This is in agreement with active bacterial growth on the membrane. Biofilms developed in a model drinking water distribution system according to three stages: (1) attachment of single cells to the surface that originated from the planktonic population, followed by (2) biofilm growth that is defined by high cell numbers and decreasing species richness, and finally (3) maturation of the biofilm forming a distinct bacterial community with a higher species richness than during biofilm growth (Martiny et al. 2003). This also agrees with the conceptual model for biofilm development of Jackson and co-workers (2001). Because in

our experiments, the biofilm age was at maximum 111 days, and much longer periods were reported by the researchers quoted above, long-term experiments should be performed to test the effect of biofilm age on community development in our system.

Membrane fouling and cleaning

An important question to ask ourselves in the context of membrane fouling prevention and control is: does this knowledge on biofilm composition and dynamics help us to prevent or minimize membrane fouling? While higher fluxes in MBRs undoubtedly lead to increased membrane fouling (Drews, 2010), no clear differences in bacterial diversity have been observed for membranes run at different fluxes in our experiments. This was confirmed by the diversity indices which were very similar for all three flux values (see Results). This is in contrast with the results obtained by Huang and co-workers, that membrane flux had great impact on the predominant populations selected in the fouling biofilms (2008). Their work also indicated that specific groups of bacteria were preferentially growing in the membrane habitats. However, biofilm growth is not directly linked to membrane fouling, and it is likely that not the presence of certain bacterial species in the biofilm is of greatest importance, but rather their physiological state. Biofilm resistance was suggested to be mostly determined by the extracellular polymeric substances (EPS) (Dreszer et al. 2013) and gel layer formation was found to be the dominant fouling mechanism in MBRs at sub-critical fluxes (Wang et al. 2008; van der Marel et al. 2010). For a long time it has been known that several factors, other than the bacterial species themselves, influence EPS production by bacteria: growth phase, the type of limiting substrate (carbon, nitrogen and phosphorus), feeding pattern, oxygen availability, ionic strength, culture temperature, shear force and other stressful culture conditions (Nielsen et al. 1997; Tay et al. 2001; Liu et al. 2004; Nichols et al. 2004). In further studies on the relation of MBR operation and fouling with bacterial diversity, the EPS production capability of bacteria and the conditions at which they actually produce EPS in the MBR system should be integrated. Moreover, the contribution of EPS production by biofilm bacteria to the total fouling resistance should be compared with that of other fouling mechanisms such as transport of EPS from the mixed liquor towards, and followed by deposition onto the membrane surface.

Few bacterial genera were removed by scraping while most stayed to some extent attached to the membrane surface. This is in line with research by Miura and co-workers, who found microorganisms firmly attached on hollow fiber membrane surfaces with anchor-like structures even after physical washing (spraying pressurized water) (2007b). Therefore, mechanical cleaning does not seem very effective in removing the biofilm. Moreover, little difference in bacterial community was found between the scrapings and scraped off membrane samples. Apparently, there was neither a specific group of loosely attached

bacteria on the outside of the biofilm that can be easily removed nor a group that is more firmly attached on the inside of the biofilm. Is it a problem when some bacteria stay behind on the membrane surface after (mechanical) cleaning? As mentioned above, the presence of bacteria on the membrane surface does not directly lead to a high fouling resistance. Apart from bacteria that are still present after (mechanical) cleaning, usually not all EPS is removed either. Remaining fouling after harsh mechanical cleaning was reported to consume oxygen and to cause a resistance to flow (van den Brink, et al. 2013). Moreover, the fact that the bacteria that survived the cleaning can initiate new biofilm formation is of great importance. In that case, the crucial first step in biofilm formation of initial adhesion of bacteria (Dunne, 2002; Palmer et al. 2007) is not needed anymore. It is known that the remaining bacteria after a cleaning will quickly develop a new biofilm if sufficient nutrients are available (Flemming, 2002). Control of the biofilm growth is within better reach than complete removal of the biofilm from the membrane surface and, therefore, efforts should be focused on biofilm control rather than on complete biofilm removal. As mentioned before, the contribution of biofilm growth and associated EPS production to the total fouling resistance compared to the contribution of other fouling mechanisms is not known yet. In case other fouling mechanisms such as transport of EPS from the mixed liquor towards the membrane surface followed by deposition cause a much higher fouling resistance, biofilm control will be of less importance and other measures should be taken.

Future studies

Although yielding relevant information about the bacterial community composition in the MBR fractions, the techniques applied in this study do have some biases and shortcomings. Smaller bacterial populations are not detected with the PCR – DGGE approach due to the low sequencing depth obtained (Zhang et al. 2012). DGGE fingerprints underestimate the diversity of the bacterial communities because of overlapping bands and co-migration of different 16S rRNS fragments (Muyzer et al. 1993; Murray et al. 1996; Nübel, et al. 1999). For complex communities as present in MBRs, high throughput screening could be a suitable method (Shendure and Ji, 2008). However, noticing recent efforts to study bacterial communities with high throughput screening (Zhang et al. 2012), the question rises whether detailed information on the composition of bacterial communities alone can help us to reach better process performance. To elucidate also the functions and interactions of bacterial communities and to link these to environmental processes, one should combine DNA-based, mRNA-based, and protein-based analyses of bacterial communities in the environment of interest (Simon and Daniel, 2011). This detailed information should then be linked with performance and fouling data, as well as with the physiological state of the bacteria to be useful for optimisation of the MBR process.

CONCLUSIONS

The bacterial communities showed an increase in diversity in the following order: wastewater < mixed liquor supernatant < mixed liquor < membrane biofilm. No dominant species was identified. A considerable part of the DGGE bands were only observed for the biofilm samples, indicating that enrichment of bacteria is taking place at the membrane surface. The bacterial communities in wastewater, sludge fractions and membrane biofilms in MBRs were time variable. Biofilm age only affected biofilm community at higher biofilm ages, developing communities that were more distinct from the wastewater and sludge fractions. This indicates occurrence of active bacterial growth on the membrane. No effect of flux on bacterial diversity of the biofilms could be observed and few bacterial genera can be removed by harsh mechanical cleaning while most will stay to some extent attached to the membrane surface. Further research should be focussed on the relationship between bacterial community structure and function. Therefore, one should combine DNA-based, mRNA-based, and protein-based analyses of bacterial communities and link this with performance and fouling data, as well as with the physiological state of the bacteria.

ACKNOWLEDGEMENTS

This work was performed in the cooperation framework of Wetsus, centre of excellence for sustainable water technology (www.wetsus.nl). Wetsus is co-funded by the Dutch Ministry of Economic Affairs and Ministry of Infrastructure and Environment, the European Union Regional Development Fund, the Province of Fryslân and the Northern Netherlands Provinces. The authors like to thank the participants of the research theme “Membrane processes and operation for wastewater treatment and reuse” for the fruitful discussions and their financial support.

REFERENCES

Altmann J, Ripperger, S (1997) Particle deposition and layer formation at the crossflow microfiltration *J. Membrane Sci.* **124** (1), 119-128

Altschul SF, Madden TL, Schaffer AA, Zhang J, Zhang Z, Miller W, Lipman DJ (1997) Gapped BLAST and PSI-BLAST: a new generation of protein database search programs *Nucleic Acids Res.* **25** (17), 3389-3402

Bereschenko LA, Stams AJM, Heilig GHJ, Euverink GJW, Nederlof MM, Van Loosdrecht MCM (2007) Investigation of microbial communities on reverse osmosis membranes used for process water production *Water Sci. Technol.* **55** (8-9), 181-190

Cariello NF, Thilly WG, Swenberg JA, Skopek TR (1991) Deletion mutagenesis during polymerase chain reaction: dependence on DNA polymerase *Gene* **99** (1), 105-108.

Carrero-Colon M, Nakatsu CH, Konopka A (2006) Microbial community dynamics in nutrient-pulsed chemostats *FEMS Microbiol. Ecol.* **57** (1), 1–8

Costerton JW, Lewandowski Z, Caldwell DE, Korber DR, Lappin-Scott HM (1995) Microbial biofilms *Annu. Rev. Microbiol.* **49**, 711-745

Dreszer C, Vrouwenvelder JS, Paulitsch-Fuchs AH, Zwijnenburg A, Kruithof JC, Flemming HC (2013) Hydraulic resistance of biofilms *J. Membrane Sci.* **429**, 436-447

Drews A (2010) Membrane fouling in membrane bioreactors - Characterisation, contradictions, cause and cures *J. Membrane Sci.* **363**, 1-28

Dunne WM (2002) Bacterial adhesion: Seen any good biofilms lately? *Clin. Microbiol. Rev.* **15** (2), 155-166

Euzéby JP (1997) List of bacterial names with standing in nomenclature: a folder available on the internet *Int. J. Syst. Bacteriol.* **47** (2), 590-592

Fernandez A, Huang SY, Seston S, Xing J, Hickey R, Criddle C, Tiedje J (1999) How stable is stable? Function versus community composition *Appl. Environ. Microbiol.* **65** (8), 3697-3704

Flemming HC (2002) Biofouling in water systems – cases, causes and countermeasures *Appl. Microbiol. Biotechnol.* **59**, 629-640

Giani M, Djakovac T, Degobbis D, Cozzi S, Solidoro C, Umani SF (2012) Recent changes in the marine ecosystems of the northern Adriatic Sea *Estuar. Coast. Shelf. Sci*. **115**, 1-13

Hagström Å, Pommier T, Rohwer F, Simu K, Stolte W, Svensson D, Zweifel UL (2002) Use of 16S ribosomal DNA for delineation of marine bacterioplankton species *Appl. Environ. Microbiol.* **68** (7), 3628–3633

Ho HTK, Lipman LJA, Gaastra W (2006) *Arcobacter*, what is known about a potential foodborne zoonotic agent! *Vet. Microbiol.* **115** (1-3), 1-13

Huang LN, de Wever H, Diels L (2008) Diverse and distinct bacterial communities induced biofilm fouling in membrane bioreactors operated under different conditions *Environ. Sci. Technol.* **42** (22), 8360-8366

Jackson CR, Churchill PF, Roden EE (2001) Successional changes in bacterial assemblage structure during epilithic biofilm development *Ecology* **82** (2), 555-566

Janse I, Bok J, Zwart G **(**2004) A simple remedy against artifactual double bands in denaturing gradient gel electrophoresis *J. Microbiol. Meth.* **57** (2), 279-281

Le-Clech P, Chen V, Fane AG (2006) Fouling in membrane bioreactors used in wastewater treatment – A review *J. Membrane Sci.* **284** (1-2), 17-53

Lee N, Jansen JL, Aspegren H, Henze M, Nielsen PH, Wagner M (2002) Population dynamics in wastewater treatment plants with enhanced biological phosphorus removal operated with and without nitrogen removal *Water Sci. Technol.* **46** (1-2), 163-170

Liesack W, Weyland H, Stackebrandt E (1991) Potential risks of gene amplification by PCR as determined by 16S rDNA analysis of a mixed culture of strict barophilic bacteria *Microbial Ecol.* **21** (1), 191-198

Liu YQ, Liu Y, Tay JH (2004) The effects of extracellular polymeric substances on the formation and stability of biogranules *Appl. Microbiol. Biotechnol.* **65** (2), 143-148

Madigan MT, Martinko JM, Parker J (2000) Biology of microorganisms, 9th ed. Prentice Hall International Editions, Englewood Cliffs, N.J.

Martiny AC, Jørgensen TM, Albrechtsen HJ, Arvin E, Molin S (2003) Long-term succession of structure and diversity of a biofilm formed in a model drinking water distribution system *Appl. Environ. Microbiol.* **69** (11), 6899-6907

McLellan SL, Huse SM, Mueller-Spitz SR, Andreishcheva EN, Sogin ML (2010) Diversity and population structure of sewage-derived microorganisms in wastewater treatment plant influent *Environ. Microbiol.* **12** (2), 378-392

Meyerhans A, Vartanian J, Wain-Hobson S (1990) DNA recombination during PCR *Nucleic Acids Res.* **18** (7), 1687-1691

Miura Y, Hiraiwa MN, Ito T, Itonaga T, Watanabe Y, Okabe S (2007a) Bacterial community structures in MBRs treating municipal wastewater: Relationship between community stability and reactor performance *Water Res.* **41**, 627-637

Miura Y, Watanabe Y, Okabe S (2007b) Membrane biofouling in pilot-scale membrane bioreactors (MBRs) treating municipal wastewater: impact of biofilm formation *Environ. Sci. Technol.* **41** (2), 632–638

Murray AE, Hollibaugh JT, Orrego C (1996) Phylogenetic compositions of bacterioplankton from two California estuaries compared by denaturating gradient gel electrophoresis of 16S rDNA fragments *Appl. Environ. Microbiol.* **62** (7), 2676-2680

Muyzer G, De Waal EC, Uitterlinden AG (1993) Profiling of complex microbial populations by denaturing gradient gel electrophoresis analysis of polymerase chain reaction-amplified genes coding for 16S rRNA *Appl. Environ. Microbiol.* **59** (3), 695-700

Ng HY, Tan TW, Ong SL (2006) Membrane fouling of submerged membrane bioreactors: impact of mean cell residence time and the contributing factors *Environ. Sci. Technol.* **40** (8), 2706-2713

Nichols CAM, Garon S, Bowman JP, Raguenes G, Guezennec J (2004) Production of exopolysaccharides by Antarctic marine bacterial isolates *J. Appl. Microbiol.* **96** (5), 1057-1066

Nielsen PH, Jahn A, Palmgren R (1997) Conceptual model for production and composition of exopolymers in biofilms *Water Sci. Technol.* **36** (1), 11-19

Nübel U, Engelen B, Felsre A, Snaidr J, Wieshuber A, Amann RI, Ludwig W, Backhaus H (1996) Sequence heterogeneities of genes encoding 16S rRNAs in *Paenibacillus polymyxa* detected by temperature gradient gel electrophoresis *J. Bacteriol.* **178** (19), 5636-5643

Nübel U, Garcia-Pichel F, Kühl M, Muyzer G (1999) Quantifying microbial diversity: morphotypes, 16 S rRNA genes, and carotenoids of oxygenic phototrophs in microbial mats *Appl. Environ. Microbiol.* **65** (2), 422-430

Ogram AV, Sayler GS, Barkay T (1987) The extraction and purification of microbial DNA from sediments *J. Microbiol. Meth.* **7**, 57-66

Palmer J, Flint S, Brooks J (2007) Bacterial cell attachment, the beginning of a biofilm *J. Ind. Microbiol. Biotechnol.* **34** (9), 577-588

Picard C, Ponsonnet C, Paget E, Nesme X, Simonet P (1992) Detection and enumeration of bacteria in soil by direct DNA extraction and polymerase chain reaction *Appl. Environ. Microbiol.* **58** (9), 2717-2722

Prescott LM, Harley JP, Klein DA (1996) Microbiology, 3rd ed. Wm. C. Brown Publishers, Dubuque, IA.

Rainey FA, Ward N, Sly LI, Stackebrandt E (1994) Dependence on the taxon composition of clone libraries for PCR amplified, naturally occurring 16S rDNA, on the primer pair and the cloning system used *Experientia* **50** (9), 796–797

Remy M, Potier V, Temmink H, Rulkens W (2010) Why low powdered activated carbon addition reduces membrane fouling in MBRs *Water Res.* **44** (3), 861-867

Reysenbach A, Giver LJ, Wickham GS, Pace NR (1992) Differential amplification of rRNA genes by polymerase chain reaction *Appl. Environ. Microbiol.* **58** (10), 3417-3418

Samie A, Obi CL, Barret LJ, Powell SM, Guerrant RL (2006) Prevalence of *Campylobacter* species, *Helicobacter pylori* and *Arcobacter* species in stool samples from the Venda region, Limpopo, South Africa: studies using molecular diagnostic methods *J. Infection* **54** (6), 558-566

Sanguinetti CJ, Dias Neto E, Simpson AJ (1994) Rapid silver staining and recovery of PCR products separated on polyacrylamide gels *Biotechniques* **17** (5), 914-921

Shendure J, Ji H (2008) Next-generation DNA sequencing *Nat. Biotechnol.* **26** (10), 1135-1145

Simon C, Daniel R (2011) Metagenomic analyses: Past and future trends *Appl. Environ. Microbiol.* **77** (4), 1153-1161

Snaidr J, Amann R, Huber I, Ludwig W, Schleifer KH (1997) Phylogenetic analysis and in situ identification of bacteria in activated sludge *Appl. Environ. Microbiol.* **63** (7), 2884-2896

Tay JH, Liu QS, Liu Y (2001) The effects of shear force on the formation, structure and metabolism of aerobic granules *Appl. Microbiol. Biotechnol.* **57** (1-2), 227-233

Tebbe CC, Vahjen W (1993) Interference of humic acids and DNA extracted directly from soil in detection and transformation of recombinant DNA from bacteria and a yeast *Appl. Environ. Microbiol.* **59** (8), 2657–2665

van den Brink P, Vergeldt F, van As H, Zwijnenburg A, Temmink H, van Loosdrecht MCM (2013) Potential of mechanical cleaning of membranes from a membrane bioreactor *J. Membrane Sci.* **429**, 259-267

van der Marel P, Zwijnenburg A, Kemperman A, Wessling M, Temmink H, van der Meer W (2010) Influence of membrane properties on fouling in submerged membrane bioreactors *J. Membrane Sci.* **348** (1-2), 66-74

Wagner M, Loy A (2002) Bacterial community composition and function in sewage treatment systems *Curr. Opin. Biotech.* **13** (3), 218-227

Wan CY, de Wever H, Diels L, Thoeye C, Liang JB, Huang LN (2011) Biodiversity and population dynamics of microorganisms in a full-scale membrane bioreactor for municipal wastewater treatment *Water Res.* **45** (1), 1129-1138

Wang Z, Wu Z, Yin X, Tian L (2008) Membrane fouling in a submerged membrane bioreactor (MBR) under sub-critical flux operation: membrane foulant and gel layer characterization *J. Membrane Sci.* **325** (1), 238-244

Weller R, Weller JW, Ward DM (1991) 16S rRNA sequences of uncultivated hot spring cyanobacterial mat inhabitants retrieved as randomly primed cDNA *Appl. Environ. Microbiol.* **57** (4), 1146-1151

Winkler MKH, Kleerebezem R, de Bruin LMM, Verheijen PJT, Abbas B, Habermacher J, van Loosdrecht MCM (2013) Microbial diversity differences within aerobic granular sludge and activated sludge flocs *Appl. Microbiol. Biotechnol.* **97** (16), 7447-7458

Zhang K, Choi H, Dionysiou DD, Sorial GA, Oerther DB (2006) Identifying pioneer bacterial species responsible for biofouling membrane bioreactors *Environ. Microbiol.* **8** (3), 433-440

Zhang T, Shao MF, Ye L (2012) 454 Pyrosequencing reveals bacterial diversity of activated sludge from 14 sewage treatment plants *ISME J.* **6** (6), 1137-1147

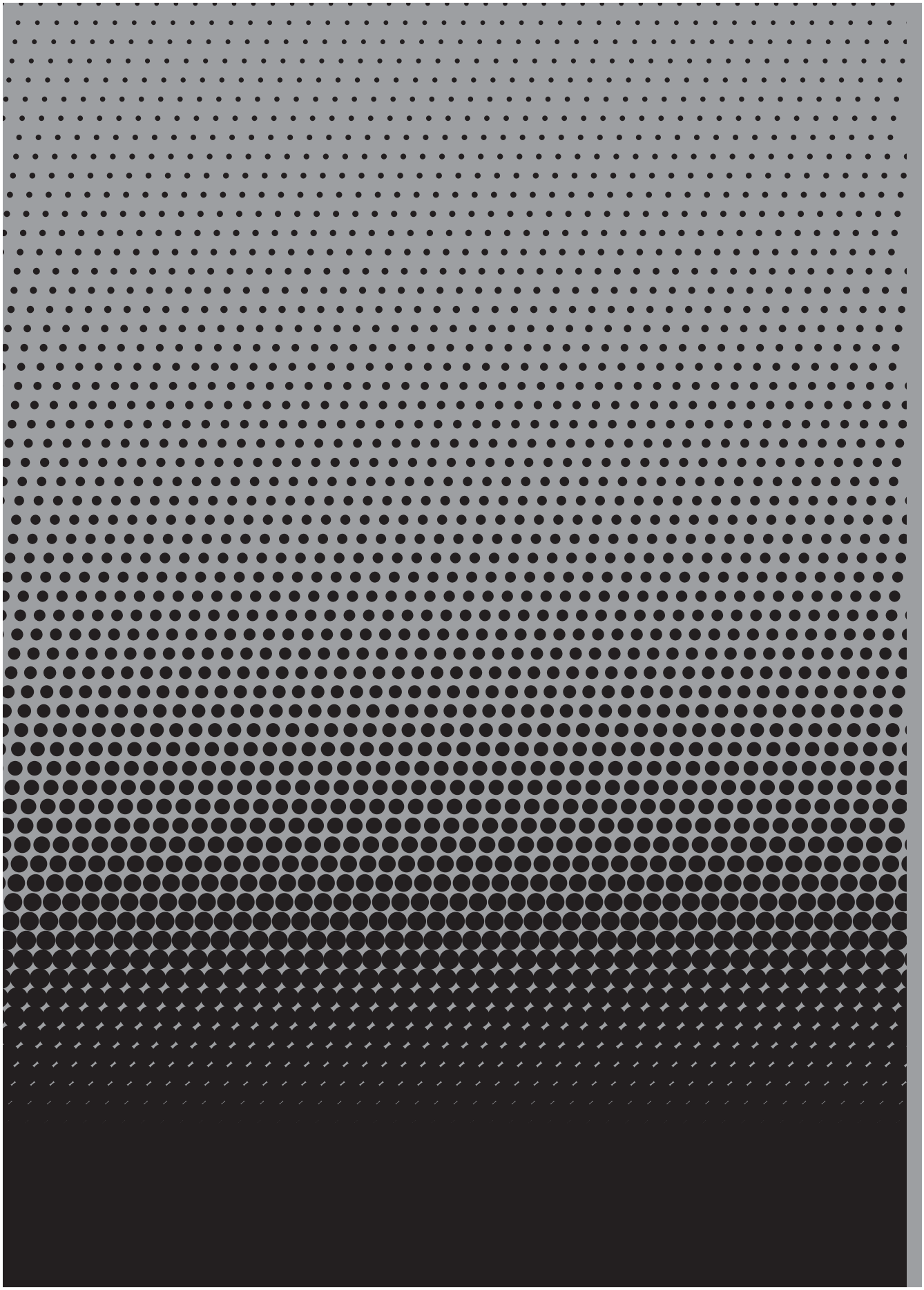

Chapter 6

EFFECT OF TEMPERATURE SHOCKS ON MEMBRANE FOULING IN MEMBRANE BIOREACTORS

This chapter has been published as:

van den Brink P, Satpradit OA, van Bentem A, Zwijnenburg A, Temmink H, van Loosdrecht MCM (2011) Effect of temperature shocks on membrane fouling in membrane bioreactors *Water Res.* **45** (15), 4491-4500

ABSTRACT

Temperature is known to influence the biological performance of conventional activated sludge systems. In membrane bioreactors (MBRs), temperature not only affects the bioconversion process but is also shown to have an effect on the membrane performance. Four phenomena are generally reported to explain the higher resistance for membrane filtration found at lower temperatures: (1) increased mixed liquor viscosity, reducing the shear stress generated by coarse bubbles, (2) intensified deflocculation, reducing biomass floc size and releasing EPS into the mixed liquor, (3) lower back transport velocity and (4) reduced biodegradation of COD. Although the higher resistance at low temperatures has been reported in several papers, the relation with supernatant composition has not been investigated before. In this paper, the composition of the soluble fraction of the mixed liquor is related to membrane performance after exposing the sludge to temperature shocks. Flux step experiments were performed in an experimental system at 7, 15, and 25° Celsius with sludge that was continuously recirculated from a pilot-scale MBR. After correcting the permeate viscosity for temperature, higher membrane fouling rates were obtained for the lower temperature in combination with low fouling reversibility. The soluble fraction of the MBR mixed liquor was analysed for polysaccharides, proteins and submicron particle size distribution. At low temperature, a high polysaccharide concentration was found in the experimental system as compared to the MBR pilot. Upon decreasing the temperature of the mixed liquor, a shift was found in particle size towards smaller particles. These results show that the release of polysaccharides and/or submicron particles from sludge flocs could explain the increased membrane fouling at low temperatures.

Key words: membrane fouling, temperature, membrane bioreactor, particle size, flux-step method, polysaccharides, fouling mechanisms.

INTRODUCTION

Temperature is known to influence the biological performance of conventional activated sludge systems (Farrell and Rose, 1967; McClintock et al., 1993; Metcalf and Eddy, 2004). Both the rate of treatment and the microbial composition are affected by temperature (Chiemchaisri and Yamamoto, 1994; Wilén et al., 2000a, 2000b). Temperature also influences the structure of sludge flocs, although conflicting results have been reported. Experiments in which the sludge settleability was studied at different temperatures, showed an increased tendency for sludge bulking at lower temperatures (5 °C) (Henry and Salenieks, 1980). Long-term monitoring of a full-scale municipal MBR revealed that settleability was positively influenced by higher temperatures (Lyko et al., 2008). In other studies, higher temperatures showed the opposite effect. An increase of sludge volume index (SVI) was found at higher temperatures (Sürücü and Çetin, 1990). Poor settling was also observed at elevated temperatures (35 °C as compared to 15 °C) for SBR reactors running at low SRTs (Krishna and van Loosdrecht, 1999).
In MBRs, temperature has a similar effect on the biological processes as in conventional activated sludge systems. However, because temperature also has an impact on sludge morphology, the membrane filtration process can be affected. Seasonal variations in membrane fouling, with increased membrane fouling at lower temperatures, have been mentioned for several full scale systems (Rosenberger et al., 2006; Lyko et al., 2008; Miyoshi et al., 2009; Moreau, 2010; Wang et al., 2010b). Temperature has an impact on membrane filtration because it determines permeate viscosity. However, even after correcting for this change in permeate viscosity, increased membrane fouling has been quantified before for a small temperature shift (17-18 °C to 13-14 °C) (Jiang et al., 2005). Four phenomena, induced by low temperatures, were mentioned that could explain this effect:

(1) increased mixed liquor viscosity, reducing the stress generated by coarse bubbles;
(2) more severe deflocculation, reducing biomass floc size and releasing extracellular polymeric substances (EPS) into the mixed liquor that may cause membrane fouling;
(3) lower particle back transport velocity because Brownian diffusion is linearly related to temperature;
(4) reduced biodegradation of COD, resulting in higher concentrations of soluble and particulate COD in the reactor (Tian et al., 1994; Lishman et al., 2000), including potential foulants.

Apart from these hypotheses, other explanations or phenomena could be of importance as well. Changes in the cake layer thickness and/or porosity were possible explanations for the increased membrane fouling found at low temperatures for a laboratory scale MBR treating domestic wastewater, in which the temperature was lowered every two weeks in steps

of 5 °C from 25 °C to 5 °C (Chiemchaisri and Yamamoto, 1994). Temperature also has an effect on bubble size: for pure water, bubble coalescence and consequently bubble size was increased as the liquid temperature was raised from 10 °C to 30 °C (Ribeiro jr. and Mewes, 2006). Coarse bubbles are generally accepted to be more effective in fouling mitigation than smaller bubbles (Li et al., 1997; Judd, 2005; Zhang et al., 2009). Therefore, low temperature might induce membrane fouling.

Although more severe membrane fouling at low temperatures has been reported in several papers, the relation with supernatant composition has not been investigated before. In the experiments presented in this paper, the composition of the supernatant with respect to organic carbon concentrations and submicron particle size distribution and its relation to membrane fouling was investigated in short term temperature experiments. The focus on submicron particle size was chosen, because these particles are more likely to cause irreversible fouling (Geilvoet, 2010). By changing the sludge temperature, while keeping the influent composition constant, the individual temperature experiments could be more properly compared than data from full scale MBRs run at different temperatures. Operational data from a full scale MBR were used to inventorise long term temperature effects on membrane fouling. A better understanding of both short and long term temperature effects on membrane fouling in MBRs can help to develop more effective membrane fouling control strategies.

MATERIALS AND METHODS

Experimental set-up

A pilot-scale MBR (Figure 6.1) with a working volume of 85 L and fed with municipal wastewater was used as a source of activated sludge for the experiments. The wastewater was screened (5 mm) before entering the biological reactors. The COD of the wastewater was 350 mg L^{-1} on average, but fluctuated between 150 and 600 mg L^{-1}. The overall hydraulic retention time (HRT) of the MBR was 6 h. The dissolved oxygen concentration in the aerobic tank was measured on-line and controlled at 1.5 mg L^{-1} with a fine-bubble diffuser.

The membrane tank was equipped with 5 PE flat sheet membranes with a nominal pore size of 0.3 µm and a surface area of 0.063 m^2 each (Kubota, Japan). The channel width between the membranes was 7 mm. Coarse bubble aerators placed below the membranes provided a specific aeration demand (SAD) of 1.4 m^3 m^{-2} h^{-1} (equivalent to 0.1 cm s^{-1}) to scour the membrane surface and in this manner reduce fouling. With a peristaltic pump, permeate was continuously extracted at a flux of 47.9 L m^{-2} h^{-1}.

The pilot reactor was operated at an HRT of 6.3 h and SRT of 25 days. The average mixed liquor suspended solid (MLSS) concentration was around 4.0 g L^{-1} in the aerobic tank of the

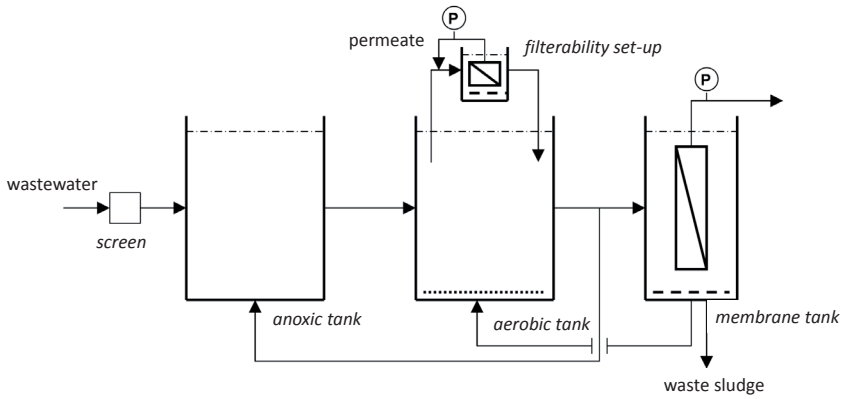

Figure 6.1 Pilot-scale MBR and filterability set-up (Remy et al., 2010).

MBR. This low MLSS concentration was due to the low strength of the municipal wastewater. The MBR pilot had good COD removal and full nitrification.

To measure filterability, sludge from the aerobic reactors of the MBR was continuously recirculated over a vessel with a volume of 5 L and a retention time of 1 h (Figure 6.1). The vessel contained two homemade submerged flat-sheet PVDF membranes, with a nominal pore size of 0.1 µm and a surface area of 0.014 m^2. The temperature in the aerated tank of the pilot was continuously monitored. For temperature control, a cooling spiral connected to a water bath (Thermo Haake DC30-K10, US) was placed in the vessel. The filterability set-up (also called "experimental system") was equipped with a coarse bubble aerator to scour the membrane surface at a flow rate of about 28 $m^3\ m^{-2}\ h^{-1}$ (equivalent to 2.1 cm s^{-1}). This SAD was very high compared to practice to compensate for the broad channel width between the membrane sheets. Also, the air flow was divided by a relatively small surface area of the membranes used in these tests, resulting in a high specific air flow. Although the applied membranes and hydrodynamics are not the same in the pilot reactor and the filterability set-up, the individual experiments performed in the filterability set-up can be properly compared. The transmembrane pressure (TMP) was monitored on-line (Endress + Hauser, Cerabar M PMC 41), both in the pilot MBR and in the experimental system.

Experimental procedure

Membrane fouling can be quantified using different methods. In the past few years, efforts have been made to quantify membrane fouling, and more specifically the critical flux, in a reproducible way by developing the so-called "flux step method" (Le-Clech et al., 2003). The critical flux concept was originally developed by Field et al. (1995) and described as such: "the critical flux hypothesis for microfiltration is that on start-up there exists a flux

below which a decline of flux with time does not occur; above it, fouling is observed". The improved flux step method gives, apart from the critical flux value, additional information on reversibility and irreversibility of the membrane fouling (van der Marel et al., 2009).
Flux step experiments were performed at three different temperatures in the filterability set-up: 7, 15 (reference temperature) and 25 °C. These temperatures were selected because they are representative for operating conditions in winter and summer times: values from 8.4 to 26.8 °C have been reported in an extensive report on filterability in pilot and full-scale MBRs all over Europe (Moreau, 2010). In order to properly compare the lower and higher temperatures with the reference temperature, experiments were performed in the following sequence: 15 - 7 - 15 - 25 - 15 °C, using the same membrane for all 5 experiments. The filtrations were performed in duplicate, i.e. two membrane sheets were filtering the same mixed liquor but had separate TMP measurements. The complete sequence of filtrations was carried out 3 times to minimise effects of varying wastewater composition. After reaching the required temperature (taking 1-3 h) in the filtration set-up, flux step experiments lasting 5 h were performed. Samples of the mixed liquor in both the filtration set-up and the aerated tank of the pilot were taken after the first flux step cycle, i.e. one filtration and one relaxation step.

The filtrations were performed according to the flux step method as described by van der Marel et al. (2009), applying 5 membrane fluxes for J_H: 20, 40, 60, 80, and 100 L m^{-2} h^{-1}. Each relaxation step of 15 min was followed by a filtration step of 45 min. Before starting the experiment, a clean water filtration was performed for 30 min to determine the clean water permeability of the membranes. After each experiment, the membranes were mechanically cleaned by thorough rinsing with a nozzle to remove all accumulated fouling.

The total filtration resistance was calculated from the TMP, membrane flux and permeate viscosity, according to the following expression:

$$R_t = TMP/(\eta J) \quad (1)$$

where R_t is total resistance (m^{-1}), η the permeate viscosity (Pa s) and J the membrane flux (m^3 m^{-2} s^{-1}). A temperature correction was performed on permeate viscosity, according to the following relation (Roorda et al., 2001)

$$\eta = 0.497(T+42.5)^{-1.5} \quad (2)$$

with temperature T in degrees Celsius. This relation agrees with the values as reported in the CRC Handbook of Chemistry and Physics and first published by Sengers and Watson (1986).

Total fouling rate, i.e. the increase of the total filtration resistance in time, was calculated at each flux step from the slope of the resistance in time (R(t)) after 30 minutes of filtration. Reversibility upon relaxation for 15 min at a membrane flux of 5 L m^{-2} h^{-1} was expressed as a percentage of the total resistance increase for one membrane flux step:

$$\% \text{ Reversibility} = (R_{high\ n} - R_{low\ n})/(R_{high\ n} - R_{low\ n-1})*100 \quad (3)$$

$R_{high,\ n}$ represents the resistance at the end of one filtration step, $R_{low,\ n}$ represents the average resistance at the corresponding relaxation step and $R_{low,\ n-1}$ represents the average resistance at the previous relaxation step. For the schematic representation of this calculation, the reader is referred to van den Brink et al. (2009).

Sampling and fractionation

As mentioned above, samples of the mixed liquors of the aerobic tank of the MBR pilot and of the experimental system were taken after the first flux step cycle. Mixed liquor supernatant was obtained with a centrifuge (Sigma, 2–16) at 3260 g for 10 min. After centrifugation, the supernatant was subsequently paper filtered (Whatman Black Ribbon 589/1, 12–25 µm) and membrane filtered (Cronus PTFE syringe filter, nominal pore size of 0.45 µm). The membrane filtrate, which is referred to as the soluble fraction of the supernatant, was used for all analyses.

Analyses

Concentrations of polysaccharides and proteins were measured according to the methods of Dubois et al. (1956) and Biorad based on Bradford (1976), respectively using glucose and bovine serum albumin (BSA) as standards.

Apart from chemical techniques, fouling potential can also be assessed by measuring the particle size distribution of the mixed liquor. Particle size measurements are often used in membrane fouling studies (Wisniewski and Grasmick, 1998; Wang et al., 2008, 2010a; Zhang et al., 2010; Remy et al., 2010). However, usually particle sizes of 1 µm and higher are measured, while this is not the interesting range for a direct relation to membrane fouling. Particle size measurements in the micrometer range could be interesting to, for example, study flocculation and deflocculation. For assessing the fouling potential of a solution, rather the submicron range should be considered.

Particle size distribution of the soluble fractions (<0.45 µm) was analysed with a particle size analyser based on dynamic light scattering (Coulter N4MD, US). This system is able to measure particle size down to 10 nm. Each sample was measured in three different size ranges in order to reach highest sensitivity over the entire measuring range. The minimum

measured intensity was 50.000 counts per second. These data were used by the particle size analyser to create a frequency distribution. From this distribution, a Gaussian curve was created.

RESULTS

Membrane fouling

Although also other parameters have varied considerably during this time period, full scale data on 6 years operation of the Varsseveld municipal wastewater treatment plant (the Netherlands) clearly indicate higher transmembrane pressures at lower temperatures (Figure 6.2A). This effect is still apparent after correcting the trendlines to a temperature of 15 °C (Figure 6.2B). It can also be observed that this effect is more distinct at higher flux values. Similarly, differences in permeability of 50 % were found between summer and winter periods in the full scale MBR Monheim, Germany (Wedi et al., 2009). The significant

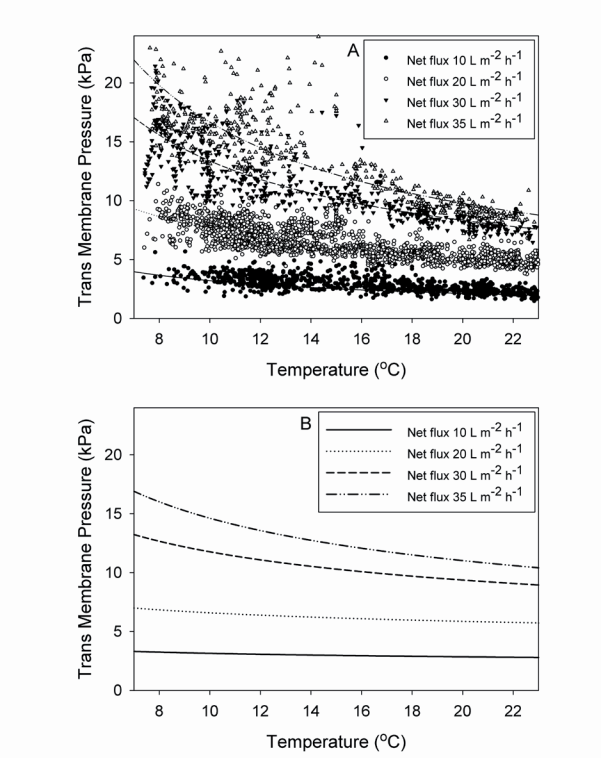

Figure 6.2 Effect of temperature on transmembrane pressure at different flux values in full scale MBR Varsseveld, NL (A) uncorrected data (B) data corrected for permeate viscosity.

changes in microbial composition detected during the year for this plant were suggested as an explanation for these permeability differences.

In order to uncouple temperature from seasonal variations, the effect of temperature on membrane fouling was tested with sludge from a pilot-scale MBR. In a test set-up the sludge of the pilot MBR was subjected to different temperatures and the impact on membrane fouling was assessed using the flux step method. After correcting the permeate viscosity for temperature, fouling resistance was observed to build up faster at lower temperatures. This effect was reproducible for each of the three sequences of filtrations that were carried out. A representative result of the filtrations performed according to the improved flux step method is provided in Figure 6.3. Resistance was building up faster at the higher fluxes. Resistance increased faster and to higher values at 7 °C, while the results for 15 and 25 °C were similar. The relaxation steps were not very effective for the first flux steps, as the resistance during relaxation stayed at the same level as for the filtration steps. At the higher flux steps, a part of the fouling was removed during relaxation.

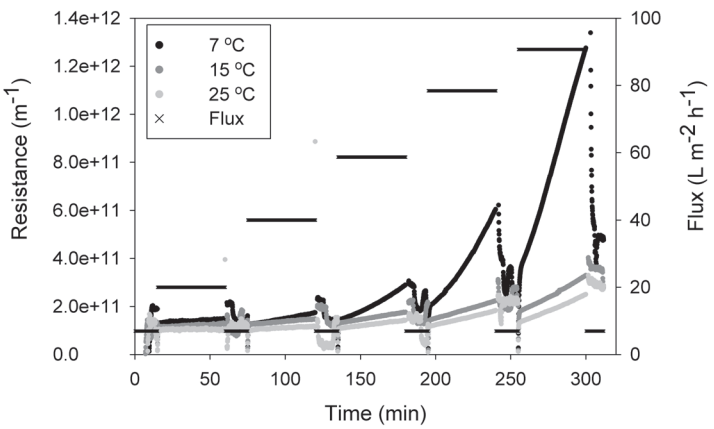

Figure 6.3 Membrane resistance for sludge filtration at three different temperatures in a flux step experiment. Permeate viscosity, used in the calculations, was corrected for temperature.

Average values for the fouling rate at every flux step and temperature were calculated from three independent experiments at 7 and 25 °C and from 7 experiments at 15 °C (Figure 6.4). The large standard deviation for the fouling rates can be explained by the sensitivity of the method as has been explained before (van den Brink et al., 2009). Fouling rates at each flux step were significantly higher when the temperature of the mixed liquor decreased from 15 to 7 °C, while an increase from 15 to 25 °C only gave a small decrease in fouling rate for most

flux steps. Differences in fouling rates between 15 and 5 °C were observed at all flux steps, but can be most clearly seen at the higher flux steps, starting at 60 L m^{-2} h^{-1}.

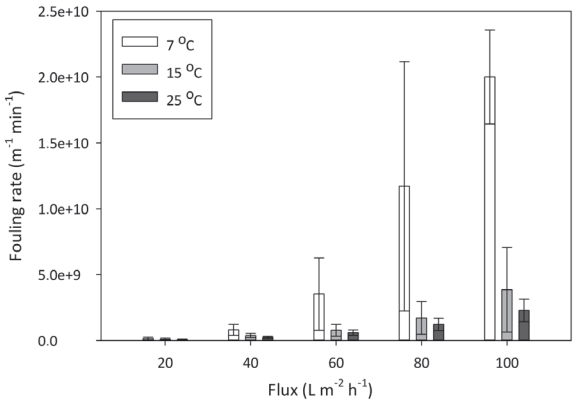

Figure 6.4 Average fouling rates for different flux steps at three different temperatures.

Apart from fouling rates, also end resistances after every filtration step, and fouling reversibilities were compared (Table 6.1). Average values for the end resistance at every flux step and temperature were determined from three independent experiments at 7 and 25 °C and from 7 experiments at 15 °C. End resistances showed the same trend as fouling rates: severe fouling at 7 °C, and only a small decrease in fouling when comparing 25 °C to 15 °C. Differences were most clearly observed at the higher flux steps from 60 L m^{-2} h^{-1}.

Fouling reversibility shows an interesting trend: the fouling obtained at 7 °C has an increasing reversibility at higher fluxes. The opposite seems to be true for the first three flux steps at 15 °C with decreasing reversibilities at increasing fluxes. At 25 °C, the little fouling that was measured is also very reversible for most flux steps.

Table 6.1 Average end resistances and reversibilities for different flux steps at three different temperatures.

Flux step (L m^{-2} h^{-1})	End resistance (10^{10} m^{-1})			Reversibility (%)		
	7 °C	15 °C	25 °C	7 °C	15 °C	25 °C
20	11.5	9.90	10.8	4.25	86.2	100
40	14.0	11.3	11.9	36.4	76.5	85.5
60	21.0	14.1	13.7	65.1	29.7	100
80	39.8	19.9	16.6	63.6	59.1	96.2
100	85.6	29.7	21.6	84.0	43.9	67.9

To test whether these effects of temperature on membrane fouling were not (partly) caused by differences in intrinsic membrane resistance, membrane resistances were measured in dead-end filtrations of MilliQ water using Amicon cells at different temperatures. Intrinsic membrane resistances of the homemade PVDF membranes were found not to change with temperature (data not shown), and could therefore not explain the temperature effect that was found when filtering sludge.

Particle size distribution

The average particle size for the sludge supernatant in the MBR pilot could have differed from day to day. Therefore, particle sizes in the experimental system were compared with the particle sizes of the sludge supernatant in the MBR pilot at the same time. Throughout

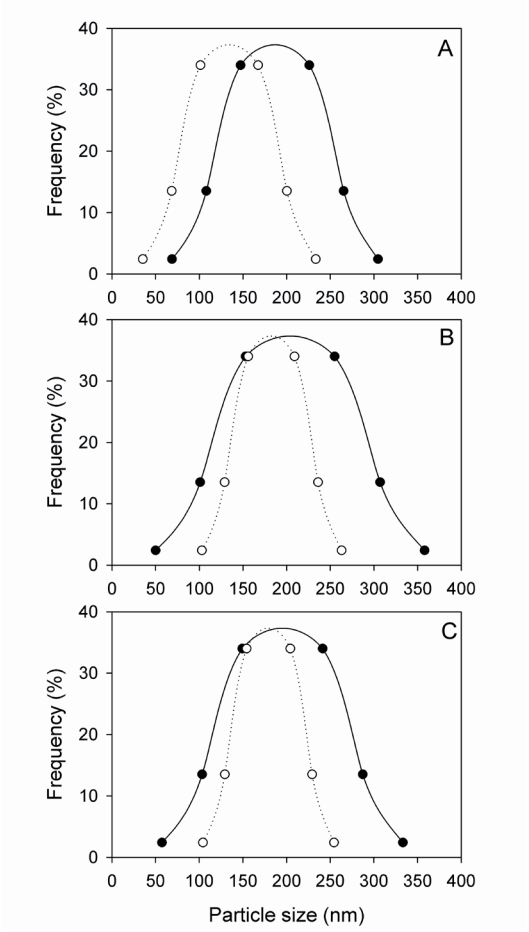

Figure 6.5 Particle size distribution in the soluble fraction of the MBR pilot (filled symbols) and experimental system (open symbols) at 7 °C (A), 15 °C (B) and 25 °C (C).

this article, the word "particle" is also used for the fraction 0-0.45 µm, although this fraction is referred to as the "soluble fraction". The presented graphs represent the trend found for all performed experiments. For the low temperature (7 °C) (Figure 6.5A), a shift can be observed from larger particles (average particle size 190 nm) to smaller particles (average particle size 130 nm) when comparing the soluble fractions of the MBR pilot (15 °C) and the experimental system mixed liquors. The average particle size in the experimental system at 7 °C was very close to the nominal pore size of the membranes (100 nm). Taking into account the higher membrane fouling at this low temperature, these smaller particles could be important foulants.

For the other temperatures (15 and 25 °C) (Figure 6.5B and C), the MBR pilot peak covers the peak for the experimental system. Average particle sizes of the MBR pilot and the experimental system were more similar for 15 and 25 °C than for 7 °C. In all Figures, the average particle size of the MBR pilot is similar.

Chemical analyses mixed liquor

The ratio between the polysaccharide concentration in the soluble fraction of the experimental system and the MBR pilot was high for 7 °C, while it was around 1 for the other two temperatures (Figure 6.6). For proteins, the ratios between the experimental system and the MBR pilot were around 1 for all tested temperatures. From these results, low temperature was shown to increase polysaccharide concentrations in the soluble fraction of the mixed liquor. Taking into account the higher membrane fouling at this low temperature,

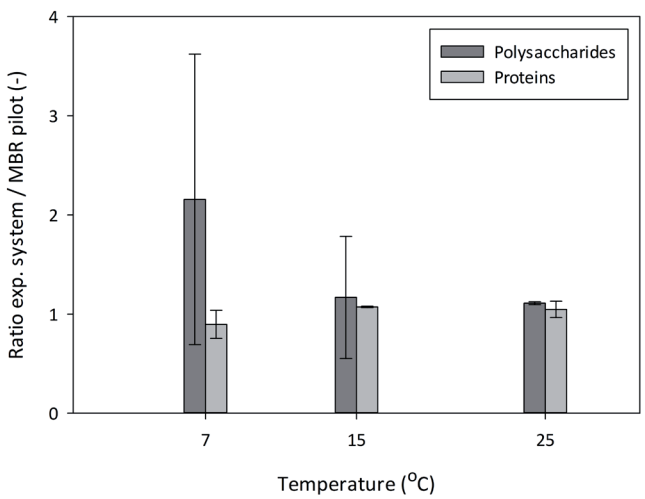

Figure 6.6 Ratio between organic carbon concentrations in the experimental system and MBR pilot at the following temperatures: 7 (n=3), 15 (n=7) and 25 (n=3) °C.

polysaccharides could play an important role here (Kimura et al., 2005; Rosenberger et al., 2005; Rosenberger et al., 2006). It should be noted that the standard deviations for the polysaccharide method were high, while the applied method is the best available one. More reliable methods should be developed to measure polysaccharides in order to more accurately draw conclusions on the relation between specific organic carbon groups and membrane fouling.

DISCUSSION

Temperature effect membrane fouling

Both full scale data shown in Figure 6.2 and experiments performed with the filterability set-up (Figures 6.3-6.6) give a strong indication of a negative effect of temperature on membrane fouling. In the filterability set-up, this effect was found separately from seasonal influences. Apart from fouling rates also reversibility was determined, which is important for identifying the membrane fouling mechanisms involved.

As mentioned in the introduction, four explanations for increased membrane fouling at low temperatures were mentioned by Jiang et al. (2005): (1) increased mixed liquor viscosity, reducing the stress generated by coarse bubbles; (2) more severe deflocculation, reducing biomass floc size and releasing extracellular polymeric substances (EPS) into the mixed liquor that may cause membrane fouling; (3) lower particle back transport velocity because Brownian diffusion is linearly related to temperature; (4) reduced biodegradation of COD, resulting in higher concentrations of soluble and particulate COD in the reactor.

Both reduced stress by coarse bubbles due to increased mixed liquor viscosity and smaller bubble size, and a lower particle back transport velocity at low temperatures could not be measured in the filterability set-up. Back transport by Brownian motion is not the only force acting on the foulants. In case fouling is controlled by bubble aeration, inertial lift forces and shear induced diffusion could be more important (Belfort et al., 1994). Techniques commonly used to study bubble size are mostly optical (Yeo et al., 2006; Yamanoi and Kageyama, 2010), which makes it difficult to measure in an activated sludge mixed liquor. Non-optical techniques include intrusive and non-intrusive techniques but are all quite advanced (Yang et al., 2007). Therefore, bubble size and back transport velocity unfortunately could not be tested.

Indications of stronger deflocculation were found in the short term temperature effect experiments, because of the release of EPS and submicron particles into the soluble fraction of the mixed liquor. Relatively high levels of polysaccharides were found at a low

temperature in the soluble fraction. Also, a shift towards smaller particles was observed at low temperature. Short term experiments, considered as shock experiments, were performed to rule out differences in biodegradation or population changes. Longer experiments would be required to capture these phenomena. A reduction
of strictly aerobic bacteria was found upon decreasing the temperature of the MBR from 25 °C down to 5 °C in two-week steps (Chiemchaisri and Yamamoto, 1994). A difference in microbial composition of the sludge was observed between summer and winter periods in the full scale MBR of Monheim, Germany (Wedi et al., 2009). Decreased concentrations of protozoa and metazoa were also found upon controlled temperature shifts, both from 35 °C to 45 °C and from 45 °C to 35 °C (Morgan-Sagastume and Allen, 2003). Therefore, it seems that temperature shocks in general might negatively influence microfauna. Although the effluent quality was still high, an absence of microfauna might induce membrane fouling, as the concentration of dispersed cells will increase and there might be an accumulation of certain substrates that can foul the membrane.

Particle size distribution soluble fraction

Apart from characterising the dissolved organic carbon in the mixed liquor, measuring the particle size distribution is of interest as well to get to know the fouling potential of this mixed liquor. When measuring particle size distribution, the aim of the measurement should always be taken into account. In case the floc size of the activated sludge is monitored, particle sizes in the order of (tens of) micrometers need to be measured. Because the cake layer that is formed by flocs is mostly reversible, focus has shifted to particles in the submicron range, which are more likely to cause irreversible fouling (Geilvoet, 2010). In order to relate particle size distribution of a solution to its fouling potential, measurements in this range are to be performed. Often, particle sizes are only measured accurately down to 0.4-0.45 µm, while these measured particles are then claimed to foul membranes with pore sizes that are several times smaller (Wisniewski et al., 2000; Jiang et al., 2007; Geilvoet, 2010). Reported particle size distributions and associated conclusions on membrane fouling potential of solutions should therefore be carefully evaluated for their validity.

Decreased temperature was reported to cause deflocculation (Wilén et al., 2000a). Also in our experiments, a shift in particle size distribution to smaller particles was observed upon a temperature decrease to 7 °C, while this was not the case for 15 and 25 °C (Figure 6.5). For non-interacting particles, smaller particles are known to cause a less permeable cake layer, because they reduce the void fraction of the cake and thereby increase the specific cake resistance according to the Carman-Kozeny equation (Carman, 1938). Small particles are also back transported less efficiently from the membrane surface (Lahoussine-Turcaud et al., 1990). In addition, the closer the particle size distribution of the mixed liquor

soluble fraction gets to the pore size distribution, the more likely it is that pore blocking and pore narrowing become important. Pore blocking and pore narrowing are known to be irreversible fouling mechanisms. This agrees with the low fouling reversibility values found for the first flux steps at low temperature (Table 6.1).
Apart from increased deflocculation at lower temperatures, also decreased (re)flocculation might be expected. For coagulation of kaolinite suspensions, especially the slow growth of small flocs was severely influenced by temperature: at 2 °C, the slow coagulation rate was greatly reduced as compared to 22 °C (Xiao et al., 2008). This was explained by reduced Brownian diffusion.

Organic carbon characterisation of soluble fractions

Protein and polysaccharide measurements showed different behaviour: low temperature was shown to increase polysaccharide concentrations in the soluble fraction of the mixed liquor, while no effect of temperature was observed on protein levels. This is in line with the smaller particles found at lower temperatures (Figure 6.5A). The nature of these submicron particles in the pore size range could well be polysaccharides. For example, for the alginate molecule radii of gyration have been reported ranging from 50 ± 7 to 137 nm (Wedlock et al., 1986; Bowen and Cooke, 1991; Windhues and Borchard, 2002). Increased membrane fouling was linked before to polysaccharide concentration in the mixed liquor (Kimura et al., 2005; Rosenberger et al., 2005; Rosenberger et al., 2006). Also, low temperature could be as an environmental stress factor to the sludge flocs, causing the release of EPS or SMP into the solution (Barker and Stuckey, 1999; Rosenberger et al., 2006).

It should be noted that the polysaccharide and protein methods are not very sensitive (Mehrez et al., 2007), which makes it hard to measure small differences in concentrations. Furthermore, the applied method (DuBois) is known to give a higher response to smaller polysaccharide molecules and monosaccharides.
It would be interesting to use more specific organic carbon analyses than polysaccharide and protein measurements in order to study the relation between mixed liquor composition and membrane fouling. This was also mentioned by Kimura et al. (2005) who performed more specific FTIR and ^{13}C NMR analyses on the organic carbon. While concentrations of dissolved organic matter in the reactors and mixed liquor viscosity did not show a clear relationship with membrane fouling in their study, the food-microorganisms ratio turned out to be important for membrane fouling because it influences the type of organic carbon molecules found in the membrane fouling layer.

Fouling mechanisms

In order to identify the fouling mechanisms that are playing a role in these experiments, it

is important to look at the reversibility values (Table 6.1). At a lower temperature, a higher amount of submicron particles in the pore size range was found (Figure 6.5A), in combination with a lower reversibility for the first number of fluxes. This indicates a fast and irreversible fouling at the start of filtration, caused by direct pore blocking or narrowing of the membrane pores (Belfort et al., 1994). Also adsorption of soluble compounds might play a role here. At the later (higher) flux steps, after the initial fouling, cake layer formation will become dominant as the membrane surface and pores are already fouled. Cake layer formation is generally regarded as a reversible fouling mechanism, removable by both relaxation and backwashing (van der Marel et al., 2010). This explains the higher reversibility at the later flux steps. Submicron particles influence cake layer formation in two ways:

(1) Because of their small size their backtransport velocity is smaller because the physical forces acting on the submicron particle during membrane filtration, such as inertial lift, are smaller than for larger particles (Altmann and Ripperger, 1997; Bhattacharjee and Hong, 2005). This results in a relatively high amount of small particles in the cake.
(2) The combination of smaller and bigger particles results in a less permeable cake as the void fraction of the cake decreases (Carman, 1938; Le-Clech et al., 2006).

As a result of these two phenomena, smaller particles are retained in the cake layer and thereby accumulate in the cake. Preferential deposition of the smaller particles in a polydisperse suspension was shown by theoretical work and experimentally (Baker et al., 1985; Lu and Ju, 1989). Moreover, the smallest particles in a poly-dispersed suspension often determine the filtration rate (Kim et al., 2002; Kromkamp et al., 2002).

For a temperature of 15 °C, reversibility was high at the beginning of filtration and decreased towards the highest fluxes. This information combined with the particle size distribution data would suggest the development of a cake or gel that is getting thicker during the filtration. Towards the last flux steps, compression of the cake might have taken place (van den Brink et al., 2009), explaining the decreasing reversibility. At 25 °C, very little fouling was observed with a reversibility of close to 100%. Because there is so little fouling at this temperature, compression could not have played a role here. Moreover, when there is little fouling the TMP stays low and the fouling can therefore be more easily back transported into the mixed liquor. This can explain the high fouling reversibility at 25 °C.

Practical relevance

Studying the effect of temperature on membrane fouling in MBRs is very relevant for practice. As shown in Figure 6.2, even after correction for permeate viscosity, lower temperatures caused higher TMPs and thus resistances at the full scale plant of Varsseveld,

the Netherlands. Similar results were obtained by the Delft Filtration Characterisation method that was applied in several pilot and full scale installations all over Europe (Moreau, 2010). Unfortunately, no full scale data were available of plants with a relatively constant temperature all year round. Perhaps, overall MBR performance would be higher in warmer countries. A pilot study with a submerged MBR in Singapore, run at an average mixed liquor temperature of 30 °C, showed stable operation at net fluxes of 25-29 L m^{-2} h^{-1} (Qin et al., 2009). The 5-mgd demo plant at Ulu Pandan (Singapore) has been in operation since December 2006 and had stable operation at membrane flux of 25.3 L m^{-2} h^{-1} (website PUB, 2008). When comparing a number of large scale pilot trials in which several MBR technologies were tested in Europe, USA and Singapore, net fluxes were found to be higher in the warmer countries (van der Roest et al., 2002; Adham et al., 2004; Tao et al., 2005). It should be noted that in many full scale systems conservative average fluxes are applied (Judd, 2006).
As shown in this study, temperature influences membrane fouling in MBRs. Therefore, temperature should be taken into account in the design of such systems. In countries with seasonal temperature variations, extra membrane area should be installed for the colder periods. By using the extra membrane area during winter time, fluxes can be lowered in order to control membrane fouling. In countries with constant temperature during the year, fewer membranes need to be installed. Higher and more constant fluxes should be reached in this case, and these places are favourable for applying MBRs.

In order to react on temperature shocks it is important to develop control strategies. Addition of low amounts of Powdered Activated Carbon (PAC) or other inert particles to the activated sludge was shown to make the sludge flocs stronger and less susceptible to factors that induce deflocculation such as shear (Lee et al., 2001; Remy et al., 2009, 2010). Perhaps PAC addition could also prevent the deflocculation of the sludge flocs when it is subjected to a temperature decrease. In winter periods, this could offer a rather straightforward solution to decreased filterability. Another option, focused on cleaning instead of fouling prevention, is to apply (chemically enhanced) backwashing, a method that is applied in both traditional membrane filtration processes and membrane bioreactor systems (MBR) (Teodosiu et al., 1999; Le-Clech et al., 2006). Backwashing is not applicable when flat sheet membranes are used. Other possibilities for controlling membrane fouling are for example decreasing the flux or increasing membrane aeration.

CONCLUSIONS

Flux step experiments showed increased membrane fouling at lower temperatures. Resistances calculated with a temperature corrected permeate viscosity gave increased

fouling rates at lower temperatures. The combination with low fouling reversibility yielded a detrimental effect of low temperature on permeability. Analyses of the mixed liquor soluble fraction showed a high polysaccharide concentration in the experimental system as compared to the MBR pilot. Upon decreasing the temperature of the mixed liquor, a shift was found in particle size distribution of the soluble fraction towards smaller particles. Because these smaller particles are very similar in size to the membrane pore size, fast pore narrowing or pore blocking could explain the low fouling reversibility.
The results showed that the release of polysaccharides or submicron particles from sludge flocs could explain the increased membrane fouling at low temperatures. Consequently, temperature should be taken into account when designing an MBR.

ACKNOWLEDGEMENTS

This work was performed in the TTIW-cooperation framework of Wetsus, Centre of Excellence for Sustainable Water Technology (www.wetsus.nl). Wetsus is funded by the Dutch Ministry of Economic Affairs, the European Union Regional Development Fund, the Province of Fryslân, the City of Leeuwarden and the EZ/Kompas program of the 'Samenwerkingsverband Noord-Nederland". The authors like to thank the participants of the research theme "Membrane Bioreactors" for the discussions and their financial support.

REFERENCES

Adham S, DeCarolis JF, Pearce W (2004) Optimisation of various MBR systems for water reclamation – phase II, Desalination and Water Purification Research and Development Program Final Report, No. 103

Altmann J, Ripperger S, (1997) Particle deposition and layer formation at the crossflow microfiltration *J. Membrane Sci.* **124** (1), 119-128

Baker RJ, Fane AG, Fell CJD, Yoo BH (1985) Factors affecting flux in crossflow filtration, *Desalination* **53** (1-3), 81-93

Barker DJ, Stuckey DC (1999) A review of soluble microbial products (SMP) in wastewater treatment systems *Water Res.* **33** (14), 3063-3082

Belfort G, Davis RH, Zydney AL (1994) The behavior of suspensions and macromolecular solutions in crossflow microfiltration *J. Membrane Sci.* **96** (1-2), 1-58

Bhattacharjee S, Hong S (2005) Fundamentals of particle fouling in membrane processes *Korean Membrane J.* **7** (1), 1-18

Bowen WR, Cooke RJ (1991) Properties of microfiltration membranes: computer automated determination of the electrokinetic properties of polycarbonate membranes, *J. Colloid Interf. Sci.* **141**, 280-287

Bradford M (1976) A rapid and sensitive method for the quantification of microgram quantities of protein utilizing the principle of protein-dye binding *Anal. Biochem.* **72** (1-2), 248-254

Carman PC (1938) Fundamental principles of industrial filtration *Trans. Inst. Chem. Eng.* **16**, 168-187

Chiemchaisri C, Yamamoto K (1994) Performance of membrane separation bioreactor at various temperatures for domestic wastewater treatment *J. Membrane Sci.* **87** (1-2), 119-129

Dubois M, Gilles KA, Hamilton JK, Rebers PA, Smith F (1956) Colorimetric method for determination of sugars and related substances *Anal. Chem.* **28** (3), 350-356

Farrell J, Rose AH (1967) Temperature effects on micro-organisms. Thermobiology, Ed. Rose A. H., pp. 147-218. Academic Press, London

Field RW, Wu D, Howell JA, Gupta BB (1995) Critical flux concept for microfiltration fouling *J. Membrane Sci.* **100** (3), 259-272

Geilvoet SP (2010) The Delft Filtration Characterisation method. Assessing membrane bioreactor activated sludge filterability. PhD Thesis, Delft University of Technology, Delft, the Netherlands

Henry JG, Salenieks EE (1980) Variation in sludge settleability with temperature *Water Poll. Res. J. Can.* **15** (1), 73-82

http://www.pub.gov.sg/research/Key_Projects/Pages/Membrane2.aspx, accessed 20 Jan 2011

Jiang T, Kennedy MD, Guinzbourg BF, Vanrolleghem PA, Schippers JC (2005) Optimising the operation of a MBR pilot plant by quantitative analysis of the membrane fouling mechanism *Water Sci. Technol.* **51** (6-7), 19-25

Jiang T, Kennedy MD, Yoo C, Nopens I, van der Meer W, Futselaar H, Schippers JC, Vanrolleghem, PA (2007) Controlling submicron particle deposition in a side-stream membrane bioreactor: A theoretical hydrodynamic modelling approach incorporating energy consumption *J. Membrane Sci.* **297** (1-2), 141-151

Judd S (2005) Fouling control in submerged membrane bioreactors *Water Sci. Technol.* **51** (6-7), 27-34

Judd S (2006) The MBR Book: Principles and Applications of Membrane Bioreactors for Water and Wastewater Treatment, Elsevier, Oxford

Kim S, Cho SH, Park H (2002) Effects of particle size distribution on the cake formation in crossflow microfiltration *Water Sci. Technol.: Water Supply* **2** (2), 305-311

Kimura K, Yamato N, Yamamura H, Watanabe Y (2005) Membrane fouling in pilot-scale membrane bioreactors (MBRs) treating municipal wastewater *Environ. Sci. Technol.* **39** (16), 6293-6299

Krishna C, van Loosdrecht MCM (1999) Effect of temperature on storage polymers and settleability of activated sludge *Water Res.* **33** (10), 2374-2382

Kromkamp J, van Domselaar M, Schroen K, van der Sman R, Boom R (2002) Shear-induced diffusion model for microfiltration of polydisperse suspensions *Desalination* **146** (1-3), 63-68

Lahoussine-Turcaud V, Wiesner MR, Bottero JY (1990) Fouling in tangential-flow ultrafiltration: The effect of colloid size and coagulation pretreatment *J. Membrane Sci.* **52** (2), 173-190

Le-Clech P, Chen V, Fane AG (2006) Fouling in membrane bioreactors used in wastewater treatment – A review *J. Membrane Sci.* **284** (1-2), 17-53

Le Clech P, Jefferson B, Chang IS, Judd SJ (2003) Critical flux determination by the flux-step method in a submerged membrane bioreactor *J. Membrane Sci.* 227 (1-2), 81-93

Lee JC, Kim JS, Kang IJ, Cho MH, Park PK, Lee CH (2001) Potential and limitations of alum or zeolite addition to improve the performance of a submerged membrane bioreactor *Water Sci. Technol.* **43** (11), 59-66

Li QY, Cui ZF, Pepper DS (1997) Effect of bubble size and frequency on the permeate flux of gas sparged ultrafiltration with tubular membranes *Chem. Eng. J.* **67** (1), 71-75

Lishman LA, Legge RL, Farquhar GJ (2000) Temperature effects on wastewater treatment under aerobic and anoxic conditions *Water Res.* **34** (8), 2263-2276

Lu WM, Ju SC (1989) Selective particle deposition in crossflow filtration *Sep. Sci. Technol.* **24** (7-8), 517-540

Lyko S, Wintgens T, Al-Halbouni D, Baumgarten S, Tacke D, Drensla K, Janot A, Dott W, Pinnekamp J, Melin T (2008) Long-term monitoring of a full-scale municipal membrane bioreactor-Characterisation of foulants and operational performance *J. Membrane Sci*. **317** (1-2), 78-87

McClintock SA, Randall CW, Pattarkine VM (1993) Effects of temperature and mean cell residence time on biological nutrient removal processes *Water Environ. Res.* **65** (5), 110-118

Mehrez R, Ernst M, Jekel M (2007) Development of a continuous protein and polysaccharide measurement method by sequential injection analysis for application in membrane bioreactor systems *Water Sci. Technol.* **56** (6), 163-171

Metcalf and Eddy (2004) Wastewater engineering: treatment and reuse, 4th int. ed. McGraw-Hill, New York, USA

Miyoshi T, Tsuyuhara T, Ogyu R, Kimura K, Watanabe Y (2009) Seasonal variation in membrane fouling in membrane bioreactors (MBRs) treating municipal wastewater *Water Res.* **43** (20), 5109-5118

Moreau AA (2010) Filterability assessment of membrane bioreactors at European scale. PhD Thesis, Delft University of Technology, Delft, the Netherlands

Morgan-Sagastume F, Allen DG (2003) Effects of temperature transient conditions on aerobic biological treatment of wastewater *Water Res.* **37** (15), 3590-3601

Qin JJ, Oo MH, Tao G, Kekre KA, Hashimoto T (2009) Pilot study of a submerged membrane bioreactor for water reclamation *Water Sci. Technol.* 60 (12), 3269-3274

Remy M, Potier V, Temmink H, Rulkens W (2010) Why low powdered activated carbon addition reduces membrane fouling in MBRs *Water Res.* **44** (3), 861-867

Remy M, van der Marel P, Zwijnenburg A, Rulkens W, Temmink H (2009) Low dose powdered activated carbon addition at high sludge retention times to reduce fouling in membrane bioreactors *Water Res.* **43** (2), 345-350

Ribeiro Jr. CP, Mewes D (2006) On the effect of liquid temperature upon bubble coalescence *Chem. Eng. Sci.* **61** (17), 5704-5716

Roorda JH, van der Graaf JHJM (2001) New parameter for monitoring fouling during ultrafiltration of WWTP effluent *Water Sci. Technol.* **43** (10), 241-248

Rosenberger S, Evenblij H, te Poele S, Wintgens T, Laabs C (2005) The importance of liquid phase analyses to understand fouling in membrane assisted activated sludge processes - six case studies of different European

research groups *J. Membrane Sci.* **263** (1-2), 113-126

Rosenberger S, Laabs C, Lesjean B, Gnirss R, Amy G, Jekel M, Schrotter JC (2006) Impact of colloidal and soluble organic material on membrane performance in membrane bioreactors for municipal wastewater treatment *Water Res*. **40** (4), 710-720

Sengers JV, Watson JTR (1986) Improved international formulations for the viscosity and thermal conductivity of water substance *J. Phys. Chem. Ref. Data* **15** (4), 1291-1314

Sürücü G, Çetin FD (1990) Effects of temperature, pH and D.O. concentration on settleability of activated sludge *Environ. Technol.* **11** (3), 205-212

Tao G, Kekre K, Wei Z, Lee TC, Viswanath B, Seah H (2005) Membrane bioreactors for water reclamation *Water Sci. Technol.* **51** (6-7), 431-440

Tian S, Lishman LA, Murphy KL (1994) Investigations into excess activated sludge accumulation at low temperatures *Water Res.* **28** (3), 501-509

van den Brink P, Zwijnenburg A, Smith G, Temmink H, van Loosdrecht MCM (2009) Effect of free calcium concentration and ionic strength on alginate fouling in cross-flow membrane filtration *J. Membrane Sci.* **345** (1-2), 207-216

van der Marel P, Zwijnenburg A, Kemperman AJB, Wessling M, Temmink H, van der Meer, WGJ (2009) An improved flux-step method to determine the critical flux and the critical flux for irreversibility in a membrane bioreactor *J. Membrane Sci.* **332** (1-2), 24-29

van der Marel P, Zwijnenburg A, Kemperman AJB, Wessling M, Temmink H, van der Meer WGJ (2010) Influence of membrane properties on fouling in submerged membrane bioreactors *J. Membrane Sci*. **348** (1-2), 66-74

van der Roest HF, Lawrence DP, van Bentem AGN (2002) Membrane bioreactors for municipal wastewater treatment. IWA Publishing.

Wang Z, Wang P, Wang Q, Wu Z, Zhou Q, Yang D (2010a) Effective control of membrane fouling by filamentous bacteria in a submerged membrane bioreactor *Chem. Eng. J.* **158** (3), 608-615

Wang Z, Wu Z, Tang S (2010b) Impact of temperature seasonal change on sludge characteristics and membrane fouling in a submerged membrane bioreactor *Separ. Sci. Technol.* **45** (7), 920-927

Wang Z, Wu Z, Yin X, Tian L (2008) Membrane fouling in a submerged membrane bioreactor (MBR) under sub-critical flux operation: Membrane foulant and gel layer characterization *J. Membrane Sci.* **325** (1), 238-244

Wedi D, Bleisteiner S, Wild W (2009) Seasonal changes in filterability and permeability shown by the example of MBR-Monheim. Proceedings of the 8. Aachener Tagung Wasser und Membranen, Aachen, Germany, pp. A26-1 - A26-11

Wedlock DJ, Fasihuddin BA, Phillips GO (1986) Comparison of molecular weight determination of sodium alginate by sedimentation-diffusion and light scattering *Int. J. Biol. Macromol.* **8** (1), 57-61

Wilén BM, Keiding K, Nielsen PH (2000a) Anaerobic deflocculation and aerobic reflocculation *Water Res.* **34** (16), 3933-3942

Wilén BM, Nielsen JL, Keiding K, Nielsen PH (2000b) Influence of microbial activity on the stability of activated sludge flocs *Colloid Surface B* **18** (2), 145-156

Windhues T, Borchard W (2002) Temperature depending light scattering measurements of aqueous gelatin and alginate solutions and their mixtures *Eur. Polym. J.* **38** (6), 1219-1227

Wisniewski C, Grasmick A (1998) Floc size distribution in a membrane bioreactor and consequences for membrane fouling *Colloid Surface A* **138** (2-3), 403-411

Wisniewski C, Grasmick A, Leon Cruz A (2000) Critical particle size in membrane bioreactors: Case of a denitrifying bacterial suspension *J. Membrane Sci.* **178** (1-2), 141-150

Xiao F, Ma J, Yi P, Huang JCH (2008) Effects of low temperature on coagulation of kaolinite suspensions *Water Res.* **42** (12), 2983-2992

Yamanoi I, Kageyama K (2010) Evaluation of bubble flow properties between flat sheet membranes in membrane bioreactor *J. Membrane Sci*. **360** (1-2), 102-108

Yang GQ, Du B, Fan LS (2007) Bubble formation and dynamics in gas-liquid-solid fluidization-A review *Chem. Eng. Sci.* **62** (1-2), 2-27

Yeo APS, Law AWK, Fane AG (2006) Factors affecting the performance of a submerged hollow fiber bundle *J. Membrane Sci.* **280** (1-2), 969-982

Zhang K, Cui Z, Field RW (2009) Effect of bubble size and frequency on mass transfer in flat sheet MBR *J. Membrane Sci.* **332** (1-2), 30-37

Zhang YP, Fane AG, Law AWK (2010) Critical flux and particle deposition of fractal flocs during crossflow microfiltration *J. Membrane Sci.* **353** (1-2), 28-35

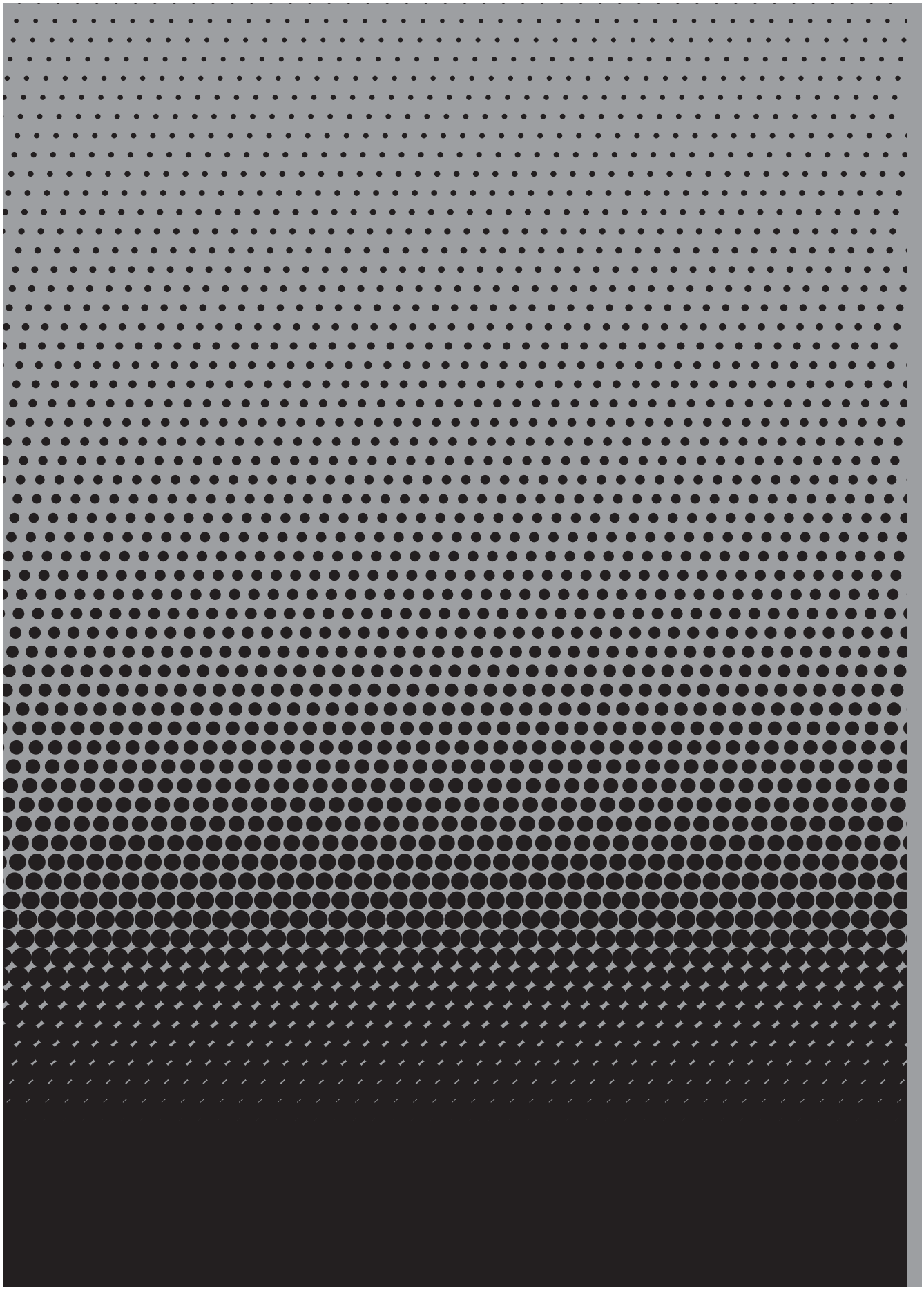

Chapter 7

CONCLUDING REMARKS

The widespread application of membrane bioreactors (MBRs) for municipal wastewater treatment is hampered by membrane fouling. Fouling increases energy demand, reduces process performance and creates the need for more frequent (chemical) membrane cleaning or replacement. Membrane fouling in MBRs is known to be caused by several membrane fouling mechanisms. Many publications, reviewed by Le-Clech and co-workers (2006) and Drews (2010), indicate that extracellular polymeric substances (EPS) play a major role during fouling development. However, EPS concentration in the bulk solution can not be generally used as an indicator for fouling propensity, because (among other reasons): EPS is a bulk parameter, the wide variety of applied measurement techniques for EPS yields incomparable information, EPS has complex interactions with other compounds and the EPS concentration in the bulk solution does not represent conditions at the membrane surface (Drews, 2010). From this thesis, several findings were obtained concerning the role and behaviour of EPS during membrane fouling in MBRs that aim to (partly) close these knowledge gaps:

(1) A strong positive relation between calcium concentration and fouling rate was found for alginate, a model compound for EPS. Reversibility of the fouling decreased with increasing calcium concentrations (Chapter 2).
(2) Increased concentrations of monovalent ions decreased the fouling rate for alginate with 66–72% at high calcium to alginate ratios (i.e., high fouling conditions) (Chapter 2).
(3) In an MBR pilot, increased membrane fouling rates were obtained at low temperature (7 °C) in combination with low fouling reversibility. This was accompanied by higher polysaccharide concentrations and a decrease in particle size. Increased membrane fouling at low temperatures therefore was explained by a release of polysaccharides and/or submicron particles from the sludge flocs (Chapter 6).
(4) Alginate fouling increased particle retention during simultaneous filtration of alginate and particles. Also for already existing alginate layers and for gel layers in a filterability set-up connected to a pilot scale MBR, extra particle retention was observed (Chapter 3).
(5) Gel layers could not be removed completely from membranes operated in a small scale filterability set-up by harsh mechanical cleaning. Both the feed and the permeate side of several membranes, operated for at least 1 year in a pilot scale MBR, contained a layer of bacteria and EPS (Chapter 4).
(6) Older biofilms showed a clear effect of biofilm age on the bacterial biofilm composition, as at higher biofilm ages communities distinct from those in wastewater and sludge fractions developed on the membrane surface in a pilot scale MBR (Chapter 5).

Some suggestions for further research to increase the understanding of the origin of EPS and their fate in MBRs will be highlighted below.

Origin of EPS in MBRs

Two main origins and associated fouling mechanisms of EPS can be identified in MBRs:

(1) EPS from the bulk solution of the MBR (mixed liquor and supernatant) that foul the membrane by depositing on the membrane
(2) Production of EPS during growth of the biofilm bacteria on the membrane surface

Biofilm resistance was suggested to be mainly determined by the EPS (Dreszer et al., 2013). At sub-critical fluxes, gel layer formation was found to be the dominant fouling mechanism in MBRs (Wang et al., 2008; van der Marel et al., 2010). For fouling control purposes, it is important to quantify the possible contributions of both fouling mechanisms to total fouling resistance.

Both scenarios (deposition from the bulk solution and production by biofilm bacteria) are compared below. It should be noted that these are rough calculations that show the maximal values for each scenario. These values are not representative for practice. Further experimental research should be performed to quantify the different scenarios more thoroughly.

Deposition

An EPS concentration of 10 mg L^{-1} is assumed in the calculations. 10 mg L^{-1} approximates polysaccharide concentration found in the activated sludge liquid phase of three MBR pilot plants fed with municipal wastewater (Evenblij et al., 2004; Rosenberger et al., 2005). Furthermore, a permeate flux of 15 L m^{-2} h^{-1} was assumed. This value is in the lower range of fluxes (15–25 L m^{-2} h^{-1}) applied in full-scale municipal MBRs equipped with submerged membranes (Remy et al., 2009). Using 15 L m^{-2} h^{-1}, the EPS deposition rate was 10 * 15 = 150 mg m^{-2} h^{-1}. So far, only the EPS concentration in the liquid phase and permeate flux were taken into account. The extent of back transport depends on particle or solute size (Belfort et al., 1994). Assuming that 99% of all EPS deposited on the membrane is transported back into the liquid phase, the final deposition rate becomes 1.5 mg m^{-2} h^{-1}.

EPS production by biofilm bacteria

For this calculation, the concentration of COD approaching the membrane biofilm needs to be assumed. This concentration is much lower than that of the influent, as most COD will be converted during the biological process. A reasonable assumption is 2 mg L^{-1}. Taking into account a flux of 15 L m^{-2} h^{-1} as mentioned above, the flux of COD towards the membrane surface is 30 mg m^{-2} h^{-1}. A yield of EPS on COD of 0.289 g g COD^{-1} is taken from Alpkvist et al. (2006), which leads to an EPS production rate of 8.7 mg m^{-2} h^{-1}.

The values calculated for EPS deposition and production rates are comparable to those found in continuous flux filtrations performed for 6 months in a filterability set-up (for description, see Chapter 6): an average value for total organic carbon (TOC) of 4.74 mg m^{-2} h^{-1} was deduced from gel layer analyses (expressed in mg m^{-2}) and total filtration time (h). From the calculations shown above, the contributions of both scenarios to the total mass of EPS ending up on the membrane surface are comparable. However, the outcome of the calculations depends highly on assumptions, such as the concentration of COD approaching the membrane surface and the percentage of EPS that actually stays on the membrane after deposition. Both scenarios are considered separately, but they could also influence each other. Some of the EPS depositing on the membrane surface could for example serve as substrate for the biofilm bacteria. As mentioned before, additional experiments to quantify the effect of both scenarios are needed to enable targeted control measures. Several model compounds for EPS (bacterial alginates (Remminghorst and Rehm, 2006), polyacrylic acid, polyvinyl alcohol (Mayer et al., 1999)) are available to study deposition of EPS from the bulk solution. Another option is to use EPS isolated from aerobic flocculent sludge or granular sludge (Lin et al., 2013; Faust, 2014).

EPS measuring methods

In order to quantify the contribution of EPS to membrane fouling and to assess the efficiency of fouling control measures, reliable and reproducible EPS measuring methods are essential. Two complicating factors are the complexity of the wastewater matrix and the requirement to extract EPS from sludge flocs or biofilms prior to the measurement of EPS. After extraction, an extra pre-treatment is often needed to re-dissolve the EPS into the solution.

Although usually EPS either tightly or loosely bound to the flocs (bound EPS) or freely suspended or dissolved in the supernatant (soluble microbial products (SMP)) (Nielsen and Jahn, 1999; Drews, 2010) are distinguished. In this chapter both groups together are referred to as “EPS”. EPS consist mainly of polysaccharides, proteins, lipids or nucleic acids. They originate from cell lysis, microbial metabolites or unmetabolised wastewater components (Flemming and Wingender, 2001).

Several methods are available to measure EPS concentration, chemical composition, morphology or spatial distribution of EPS on the membrane surface. Table 7.1 gives and overview of these methods and their restrictions.

Table 7.1 Methods to measure EPS concentration, chemical structure or morphology and spatial distribution of EPS, including limits of detection or resolution and most important restrictions. (TOC = total organic carbon, UV = ultraviolet, LC-OCD = liquid chromatography with organic carbon detection, GC-FID = gas chromatography with flame ionisation detection, NMR = nuclear magnetic resonance, GC-MS = gas chromatography–mass spectrometry, FT-IR = fourier transform infrared spectroscopy, (E)SEM = (environmental) scanning electron microscopy, TEM =transmission electron microscopy, CLSM = confocal laser scanning microscopy, AFM = atomic force microscopy, OCT = optical coherence tomography).

Method	Type of information	Limit of detection / resolution	Restrictions
TOC	Concentration (organic carbon)	1 mg L^{-1}	General method
Dubois method (phenol-sulphuric acid)	Concentration (polysaccharides)	4.5-9 mg L^{-1}	Laborious, high chemical use, difficulty measuring complex polysaccharides, interferences of humic acids
Sulphuric Acid–UV (modified Dubois)	Concentration (polysaccharides)	2 mg L^{-1}	Laborious (though less than original Dubois method)
Lowry/Bradford assay	Concentration (proteins)	1 mg L^{-1}	Laborious, high chemical use
LC-OCD	Concentration	5 µg L^{-1} (C) 10 µg L^{-1} (N)	Pre-filtration required
Pyro GC-FID	Concentration	100-150 nM	Difficult data interpretation
NMR spectroscopy	Chemical structure	n/a	Qualitative, data intensive
Pyro-GC-MS	Chemical structure	n/a	Qualitative, data intensive
FT-IR	Chemical structure	n/a	Qualitative, data intensive
Raman spectroscopy	Chemical structure	n/a	Qualitative, data intensive
NMR imaging	Morphology	Micrometers	Low resolution, laborious
SEM	Morphology	1-20 nm	Difficult to maintain structure
ESEM	Morphology	500 nm	Low resolution
TEM	Morphology	0.1 nm	Difficult to maintain structure
Epifluorescence microscopy	Morphology	Several hundred nanometres	Low penetration depth, staining with lectins needed (Strathmann et al., 2002)
CLSM	Morphology	Several hundred nanometres	Staining with lectins needed (Strathmann et al., 2002)
AFM	Morphology	Nanometers	Tip sticks to EPS gel
OCT	Morphology	Micrometers	Low resolution

It was not intended to give a complete overview of all available analytical and microscopic techniques for EPS characterization, but rather to evaluate the methods used or considered in this thesis. For the polysaccharide part of the EPS, refer to the review by Panagiotopoulos and Sempéré (2005), in which an excellent overview is provided of analytical methods (colorimetric and chromatographic techniques) available for sugar analyses in marine samples.

Because of the relevance of EPS for membrane fouling, the difficulty to compare results concerning EPS fouling obtained with different methods, and the restrictions of these methods (Table 7.1), there is a need for a reliable and reproducible EPS measuring method. One of the main issues complicating the measurement of EPS originating from MBR systems is the fact that most EPS is bound to either sludge flocs or fixed in a biofilm. Most EPS characterization studies therefore rely on the extraction of EPS components from biomass samples and subsequent analysis of the recovered extracts (Sheng et al., 2010). EPS extraction can be done with several methods, such as application of a cation exchange resin (Frølund et al., 1996), or using Na_2CO_3 at 80 °C for 1 h as described by Lin et al (2010). In addition, numerous other EPS extraction protocols have recently been published that aim to optimize the trade-off between high EPS recovery and low cell lysis. Despite extensive efforts, the results are often contradictory. A recent review assesses critically and rigorously the existing physical and chemical EPS extraction methods (Pellicer-Nàcher et al., 2013). Taking into account maximum EPS extraction yields and minimal biomass lysis, a sonication-based extraction method was considered the best to determine and compare tightly-bound EPS fractions in different biomass samples.
Recently, the colorimetric Dubois method for polysaccharides was adapted by replacing the coloration step with phenol by UV spectrophotometry (Albalasmeh et al., 2013). This adaptation avoids the use of the hazardous phenol and improves accuracy while reducing measurement time. Combined with the high simplicity and low costs of the method (Panagiotopoulos and Sempéré, 2005), it would be a suitable method for measuring EPS concentrations or amounts in sludge flocs, mixed liquor supernatants or biofilms.

Concerning spatial information on the biofilm structure, OCT could be a relatively cheap and simple method as an alternative for expensive and laborious methods such as (E)SEM/TEM and CLSM, that all require pre-treatment and skilful operators. OCT can offer in situ, non-destructive observation of fouling. The main disadvantage of OCT however is the low resolution, which could limit its application on biofilms. Moreover, in the MBR mixed liquor the optical techniques can not be applied, which makes in situ observation very difficult in MBRs.
As mentioned above for MBR systems, possible sources of EPS are the bulk solution or production by the biofilm bacteria. Although there are some extensive studies on bacterial communities in MBRs (Miura et al., 2007; Huang et al., 2008; Wan et al., 2011; van den Brink et al., 2014), their EPS production capabilities and the conditions at which they actually produce EPS are not yet known. Bacterial community structure in the biofilm should therefore be integrated with EPS production by the biofilm bacteria. The effect of operating conditions on EPS production such as substrate load or cross flow velocity could be tested using a model organism such as *Pseudomonas aeruginosa* (Remminghorst and Rehm, 2006).

Practical implications of EPS fouling for MBR performance and water reuse

Several issues concerning fouling by EPS are relevant for practice:

(1) Removability of EPS is low

As described in chapter 4, the gel layer could not completely be removed by harsh mechanical cleaning. Remaining fouling may deteriorate membrane performance and enhance further fouling (van den Brink et al., 2013). In case harsh mechanical cleaning is not effective, chemical cleaning might be applied. Chemical cleaning is often a combination of maintenance cleaning at a regular basis (e.g. weekly) and intensive or recovery cleaning once or twice a year (Le-Clech et al., 2006). These techniques result in lower net filtration efficiency, may cause membrane aging and the aggressive chemicals applied have a negative impact on the environment (Wintgens et al., 2003, Le-Clech et al., 2006; Brepols et al., 2008; Drews, 2010). Another option would be to clean with salt solutions, as high ionic strengths were shown to decrease fouling rates of Ca-alginate due to competition between mono- and divalent cations for binding sites on the alginates (chapter 2). Salt solutions were shown to be effective in cleaning organic-fouled reverse osmosis membranes (Lee and Elimelech, 2007) and BSA-fouled ultrafiltration membranes (Corbatón-Báguena et al., 2014)

(2) Preventing deposition of EPS

Referring to the two main origins and associated fouling mechanisms of EPS as mentioned above, prevention of EPS deposition and management of the biofilm are important strategies to reach stable MBR performance. As shown in the calculation on EPS deposition, the main factors influencing this deposition rate are: (1) the EPS concentration in the liquid phase, (2) the applied flux, and (3) the back transport of EPS into the bulk solution.

The EPS concentration in the liquid phase is influenced by many factors that may also interact and which cannot be changed independently (Drews, 2010). The most important operating and ambient conditions that influence (de)flocculation and thereby EPS concentration in the liquid phase are: sludge retention time (SRT), temperature, dissolved oxygen concentration (DO), nitrification and denitrification activity and sudden changes in operating and environmental conditions. Apart from these conditions, it is obvious that the origin of the wastewater and the residence time in the sewers also affect EPS concentration. The balance between permeate flux and back transport is the other main factor influencing the EPS deposition rate. Gel layers are formed at sub-critical fluxes (Wang et al., 2008, van der Marel et al., 2010). Back transport of EPS is provided by the crossflow or turbulence generated by imposed liquid flow and/or bubbling (Le-Clech et al., 2006). Size of the EPS molecules plays a significant role in determining whether the back transport is diffusive or induced by inertial lift (Chapter 1).

Many anti-fouling studies have been based on membrane surface modification (Le-Clech

et al., 2006). Having both polar and apolar groups (Flemming and Leis, 2002), EPS could deposit on both hydrophilic and hydrophobic surfaces. This does not give an unambiguous direction how to modify the membrane surface to prevent EPS deposition. Moreover, the effect of hydrophobicity of the membrane is most likely only playing a role during the first stages of filtration. Thereafter, a gel layer has formed on the membrane which is covering the membrane surface properties and governing the interactions with the bulk liquid (Le-Clech et al., 2006). Taking this into account, membrane surface modification is not an obvious solution to prevent EPS deposition.
Because of the many factors influencing EPS deposition, no straightforward measure can be suggested to prevent deposition of EPS on the membrane surface.

(3) Management of the biofilm
A trend in biofouling research is to manage the biofilm instead of focussing on complete removal of the biofilm. In this respect, it is of interest to keep the biofilm more "open" or porous with flux enhancers such as cationic polymers (Lee et al., 2007). Another way of managing the biofilm is trying to decrease EPS production by the biofilm bacteria. For total MBR performance however, it is important that the sludge bacteria still produce EPS, because EPS are essential to sludge floc formation (Morgan et al., 1990; Urbain et al., 1993). Factors that are known to influence EPS production by bacteria are: growth phase, type of limiting substrate (carbon, nitrogen and phosphorus), feeding pattern, oxygen availability, ionic strength, culture temperature, shear force and other stressful culture conditions (Nielsen et al., 1997; Tay et al., 2001; Liu et al., 2004; Nichols et al., 2004). Taking into account the performance of the biological processes in the MBR, these factors should be steered in order to decrease EPS production. For some factors, it is obviously difficult to apply different conditions in the bulk solution and on the membrane. On the other hand, diffusion limitation creates different conditions in the membrane biofilm and in the bulk solution (e.g. oxygen and substrate concentrations). Apart from managing the EPS production of the biofilm, the EPS layer could also be used as a secondary or dynamic membrane, taking advantage of its increased retention.

(4) Increased retention
A positive effect of EPS fouling is that it increases retention for particles, as shown in Chapter 3. Though this was not tested yet, increased permeate quality could perhaps be obtained concerning bacteria and viruses. Virus retention would be of importance in case the MBR effluent is to be reused for irrigation water or even drinking water. When using the EPS layer as a secondary or dynamic membrane, it is important to create and maintain gel layers that have a low resistance.
Obviously, there is a trade-off between retention and flux which should be optimised.

All these issues deserve further investigation. Increased permeate quality could make MBR technology advantageous for certain reuse applications, but the costs involved with the additional resistance caused by the EPS fouling should be taken into account when making a full comparison with other (combinations of) treatment technologies.

REFERENCES

Albalasmeh AA, Berhe AA, Ghezzehei TA (2013) A new method for rapid determination of carbohydrate and total carbon concentrations using UV spectrophotometry *Carbohyd. Polym.* **97** (2), 253-261

Alpkvist E, Picioreanu C, van Loosdrecht MCM, Heyden A (2006) Three-dimensional biofilm model with individual cells and continuum EPS matrix *Biotechnol. Bioeng.* 94 (5), 961-979

Belfort G, Davis RH, Zydney AL (1994) The behavior of suspensions and macromolecular solutions in crossflow microfiltration *J. Membrane Sci.* **96** (1-2), 1-58

Brepols C, Drensla K, Janot A, Trimborn M, Engelhardt N (2008) Strategies for chemical cleaning in large scale membrane bioreactors *Water Sci. Technol.* **57** (3), 457-463

Corbatón-Báguena MJ, Álvarez-Blanco S, Vincent-Vela MC (2014) Cleaning of ultrafiltration membranes fouled with BSA by means of saline solutions *Sep. Purif. Technol.* **125**, 1-10

Dreszer C, Vrouwenvelder JS, Paulitsch-Fuchs AH, Zwijnenburg A, Kruithof JC, Flemming HC (2013) Hydraulic resistance of biofilms *J. Membrane Sci.* **429**, 436-447

Drews A (2010) Membrane fouling in membrane bioreactors - Characterisation, contradictions, cause and cures *J. Membrane Sci.* **363** (1-2), 1-28

Evenblij H, van der Graaf JHJM (2004) Occurrence of EPS in activated sludge from a membrane bioreactor treating municipal wastewater *Water Sci. Technol.* **50** (13), 293-300

Faust L (2014) Personal communication

Flemming HC, Leis A (2002) Sorption properties of biofilms. In: Encyclopedia of Environmental Microbiology; Flemming HC, Bitton G, Eds. John Wiley & Sons, Inc.: New York, NY, USA **5**, 2958–2967

Flemming HC, Wingender J (2001) Relevance of microbial extracellular polymeric substances (EPSs) – part I: Structural and ecological aspects *Water Sci. Technol.* **43** (6), 1-8

Frølund B, Palmgren R, Keiding K, Nielsen P (1996) Extraction of extracellular polymers from activated sludge using a cation exchange resin *Water Res.* **30** (8), 1749-1758

Huang LN, de Wever H, Diels L (2008) Diverse and distinct bacterial communities induced biofilm fouling in membrane bioreactors operated under different conditions *Environ. Sci. Technol.* **42** (22), 8360-8366

Le-Clech P, Chen V, Fane AG (2006) Fouling in membrane bioreactors used in wastewater treatment - A review *J. Membrane Sci.* **284** (1-2), 17-53

Lee WN, Chang IS, Hwang BK, Park PK, Lee CH, Huang X (2007) Changes in biofilm architecture with addition of membrane fouling reducer in a membrane bioreactor *Process. Biochem.* **42** (4), 655-661

Lee S, Elimelech M (2007) Salt cleaning of organic-fouled reverse osmosis membranes *Water Res*. **41** (5), 1134-1142

Lin YM, de Kreuk M, van Loosdrecht MCM, Adin A (2010) Characterization of alginate-like exopolysaccharides isolated from aerobic granular sludge in pilot-plant *Water Res.* **44** (11), 3355-3364

Lin YM, Sharma PK, van Loosdrecht MCM (2013) The chemical and mechanical differences between alginate-like exopolysaccharides isolated from aerobic flocculent sludge and aerobic granular sludge *Water Res.* **47** (1), 57-65

Liu YQ, Liu Y, Tay JH (2004) The effects of extracellular polymeric substances on the formation and stability of biogranules *Appl. Microbiol. Biotechnol.* **65** (2), 143-148

Mayer C, Moritz R, Kirschner C, Borchard W, Maibaum R, Wingender J, Flemming HC (1999) The role of intermolecular interactions: studies on model systems for bacterial biofilms *Int J. Biol. Macromol.* **26** (1) 3-16

Miura Y, Watanabe Y, Okabe S (2007) Membrane biofouling in pilot-scale membrane bioreactors (MBRs) treating municipal wastewater: Impact of biofilm formation *Environ. Sci. Technol.* **41**, 632-638

Morgan JW, Forster CF, Evison L (1990) A comparative study of the nature of biopolymers extracted from anaerobic and activated sludge *Water Res.* **24** (6), 743-750

Nichols CAM, Garon S, Bowman JP, Raguenes G, Guezennec J (2004) Production of exopolysaccharides by Antarctic marine bacterial isolates *J. Appl. Microbiol.* **96** (5), 1057-1066

Nielsen PH, Jahn A (1999) Extraction of EPS Wingender J, Neu TR, Flemming HC (Eds.) Microbial Extracellular Polymeric Substances, Springer, Heidelberg

Nielsen PH, Jahn A, Palmgren R (1997) Conceptual model for production and composition of exopolymers in biofilms *Water Sci. Technol.* **36** (1), 11-19

Panagiotopoulos C, Sempéré R (2005) Analytical methods for determination of sugars in marine samples: A historical perspective and future directions *Limnol. Oceanogr.-Meth.* **3**, 419-454

Pellicer-Nàcher C, Domingo-Félez C, Mutlu AG, Smets BF (2013) Critical assessment of extracellular polymeric substances extraction methods from mixed culture biomass *Water Res.* **47** (15), 5564-5574

Remminghorst U, Rehm BHA (2006) Bacterial alginates: from biosynthesis to applications, *Biotechnol. Lett.* **28** (2006), 1701-1712

Remy M, van der Marel P, Zwijnenburg A, Rulkens W, Temmink H (2009 Low dose powdered activated carbon addition at high sludge retention times to reduce fouling in membrane bioreactors *Water Res.* **43** (2), 345-350

Rosenberger S, Evenblij H, te Poele S, Wintgens T, Laabs C (2005) The importance of liquid phase analyses to understand fouling in membrane assisted activated sludge processes - six case studies of different European research groups *J. Membrane Sci.* **263** (1-2), 113-126

Sheng GP, Yu HQ, Li XY (2010) Extracellular polymeric substances (EPS) of microbial aggregates in biological wastewater treatment systems: a review *Biotechnol. Adv.* **28** (6), 882-894

Strathmann M, Wingender J, Flemming HC (2002) Application of fluorescently labelled lectins for the visualization and biochemical characterization of polysaccharides in biofilms of Pseudomonas aeruginosa *J. Microbiol. Meth.* **50** (3), 237-248

Tay JH, Liu QS, Liu Y (2001) The effects of shear force on the formation, structure and metabolism of aerobic granules *Appl. Microbiol. Biotechnol.* **57** (1-2), 227-233

Urbain V, Block JC, Manem J (1993) Bioflocculation in activated sludge: An analytical approach *Water Res.* **27** (5), 829-838

van den Brink P, Faust L, Zwijnenburg A, Temmink H, van Loosdrecht MCM (2014) Bacterial communities in sludge fractions and membrane biofilms in a membrane bioreactor *submitted for publication*

van den Brink P, Vergeldt F, van As H, Zwijnenburg A, Temmink H, van Loosdrecht MCM (2013) Potential of mechanical cleaning of membranes from a membrane bioreactor *J. Membrane Sci.* **429**, 259-267

van der Marel P, Zwijnenburg A, Kemperman A, Wessling M, Temmink H, van der Meer W (2010) Influence of membrane properties on fouling in submerged membrane bioreactors *J. Membrane Sci.* **348** (1-2), 66-74

Wan CY, de Wever H, Diels L, Thoeye C, Liang JB, Huang LN (2011) Biodiversity and population dynamics of microorganisms in a full-scale membrane bioreactor for municipal wastewater treatment *Water Res.* **45** (1), 1129-1138

Wang Z, Wu Z, Yin X, Tian L (2008) Membrane fouling in a submerged membrane bioreactor (MBR) under sub-critical flux operation: membrane foulant and gel layer characterization *J. Membrane Sci.* **325** (1), 238-244

Wintgens T, Rosen J, Melin T, Brepols C, Drensla K, Engelhardt N (2003) Modelling of a membrane bioreactor system for municipal wastewater treatment *J. Membrane Sci.* **216** (1-2), 55-65

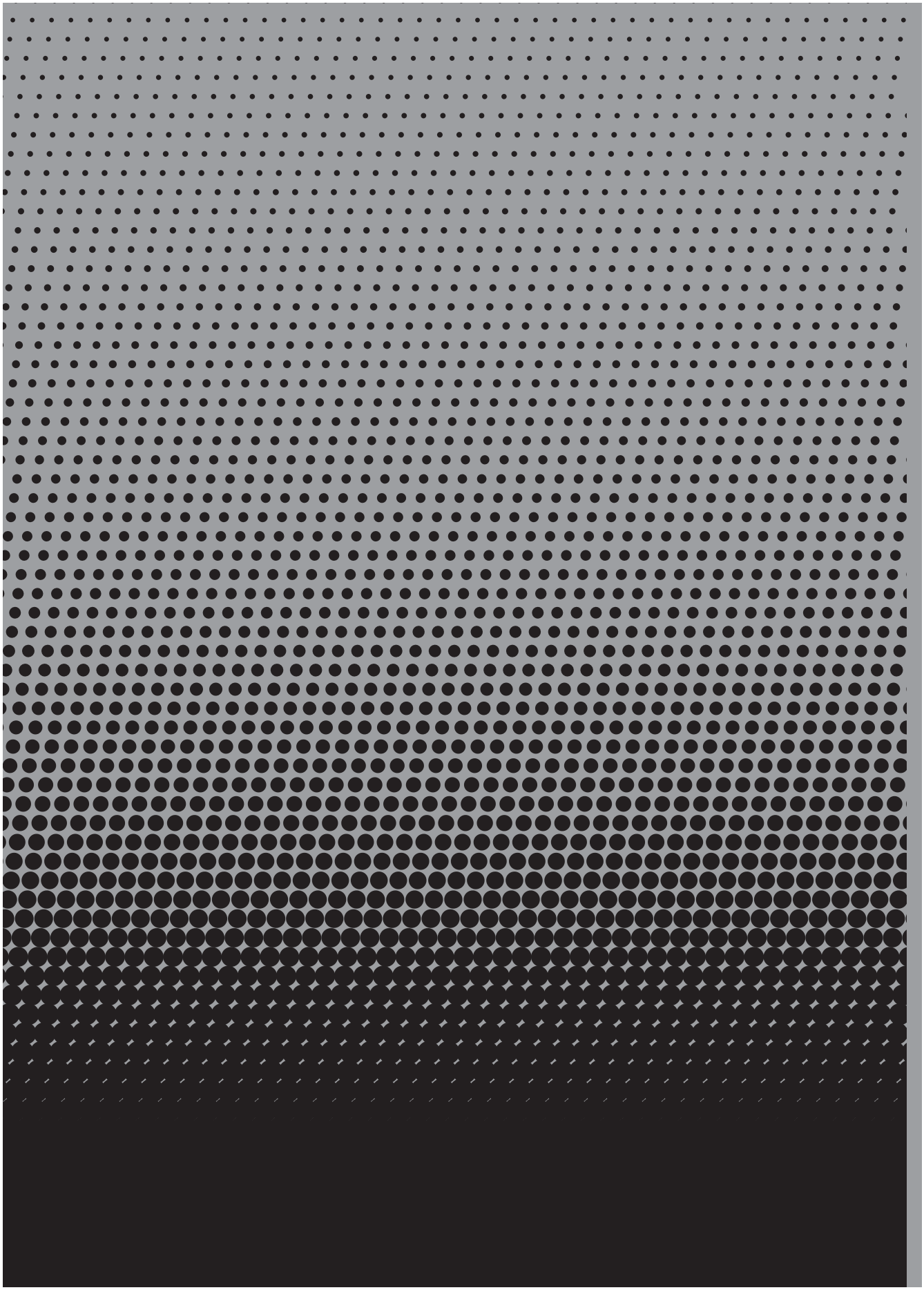

CURRICULUM VITAE



Paula van den Brink was born May 1, 1980 in Nijmegen, the Netherlands. In 1998, she obtained her gymnasium diploma from the Canisius College in Nijmegen.

In 1998 she started studying Bioprocess Technology at Wageningen University. Her first thesis was on the effect of oxygen tension on attachment, proliferation and differentiation of articular chondrocytes in a bioreactor and was performed partly at IsoTis, Bilthoven, the Netherlands, and partly at the department of Food and Bioprocess Engineering of Wageningen University. The project was supervised by dr.ir. Jos Malda and dr ir. Dirk Martens. In 2003 she moved to Christchurch, New Zealand, to carry out an internship at the University of Canterbury on the production of microbial cellulose. In 2004 she finished her M.Sc. degree with a cellular/molecular specialisation. Her final thesis topic was “Iron reduction, EDTA degradation and biomass characteristics within the BioDeNOx concept” under the supervision of dr.ir. Peter van der Maas and prof.dr. Piet Lens.

After her study Paula moved to Delft for a postgraduate program in Bioprocess Design to deepen her biotechnology knowledge and broaden her engineering knowledge. From 2005 to 2010, she worked as a Ph.D. student at the section Environmental Biotechnology of Delft University of Technology. Under the supervision of prof.dr.ir. Mark van Loosdrecht, dr.ir. Hardy Temmink and dr. Arie Zwijnenburg, she performed the research that is presented in this thesis. The research was done at Wetsus, centre of excellence for sustainable water technology, in Leeuwarden.

Since 2010, Paula works as theme coordinator biofouling at Wetsus, and as lecturer water technology at van Hall Larenstein, University of Applied Sciences.

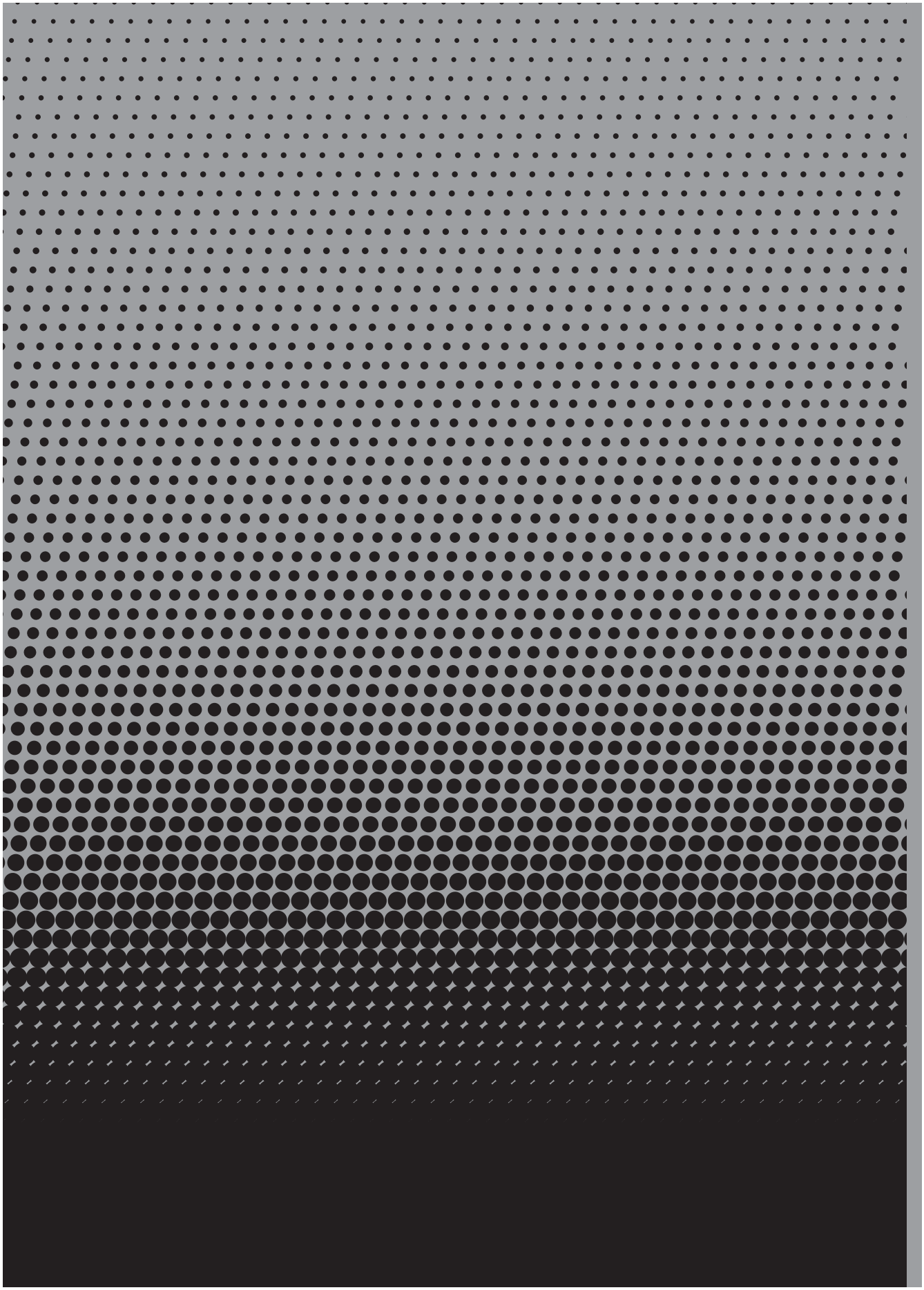

LIST OF PUBLICATIONS

van den Brink P, Faust L, Zwijnenburg A, Temmink H, van Loosdrecht MCM, Bacterial communities in sludge fractions and membrane biofilms in a membrane bioreactor *submitted for publication*

van den Brink P, Zwijnenburg A, Temmink H, van Loosdrecht MCM, Gel layer formation on membranes increases particle retention and fouling *submitted for publication*

Beyer F, Rietman BM, Zwijnenburg A, **van den Brink P**, Vrouwenvelder JS, Jarzembowska M, Laurinonyte J, Stams AJM, Plugge CM (2014) Long-term performance and fouling analysis of full-scale direct nanofiltration (NF) installations treating anoxic groundwater *J. Membrane Sci.* **468**, 339-348

van den Brink P, Vergeldt F, van As H, Zwijnenburg A, Temmink H, van Loosdrecht MCM (2013) Potential of mechanical cleaning of membranes from a membrane bioreactor *J. Membrane Sci.* **429**, 259-267

van den Brink P, Satpradit OA, van Bentem A, Zwijnenburg A, Temmink H, van Loosdrecht MCM (2011) Effect of temperature shocks on membrane fouling in membrane bioreactors, *Water Res.* **45** (15), 4491-4500

Remy M, Temmink H, **van den Brink P**, Rulkens W (2011) Low powdered activated carbon concentrations to improve MBR sludge filterability at high salinity and low temperature *Desalination* **276** (1-3), 403-407

van den Brink P, Zwijnenburg A, Smith G, Temmink H, van Loosdrecht MCM (2009) Effect of free calcium concentration and ionic strength on alginate fouling in cross-flow membrane filtration *J. Membrane Sci.* **345** (1-2), 207-216

van der Maas P, **van den Brink P**, Klapwijk B, Lens P (2009) Acceleration of the Fe(III)EDTA^{-} reduction rate in BioDeNOx reactors by dosing electron mediating compounds *Chemosphere* **75** (2), 243-249

van der Maas P, **van den Brink P**, Utomo S, Klapwijk B, Lens P (2006) NO removal in continuous BioDeNOx reactors: Fe(II)EDTA^{2-} regeneration, biomass growth, and EDTA degradation *Biotechnol. Bioeng.* **94** (3), 575-584

Malda J, **van den Brink P**, Meeuwse P, Grojec M, Martens DE, Tramper J, Riesle J, Van Blitterswijk CA (2004) Effect of oxygen tension on adult articular chondrocytes in microcarrier bioreactor culture *Tissue Eng.* **10** (7-8), 987-994

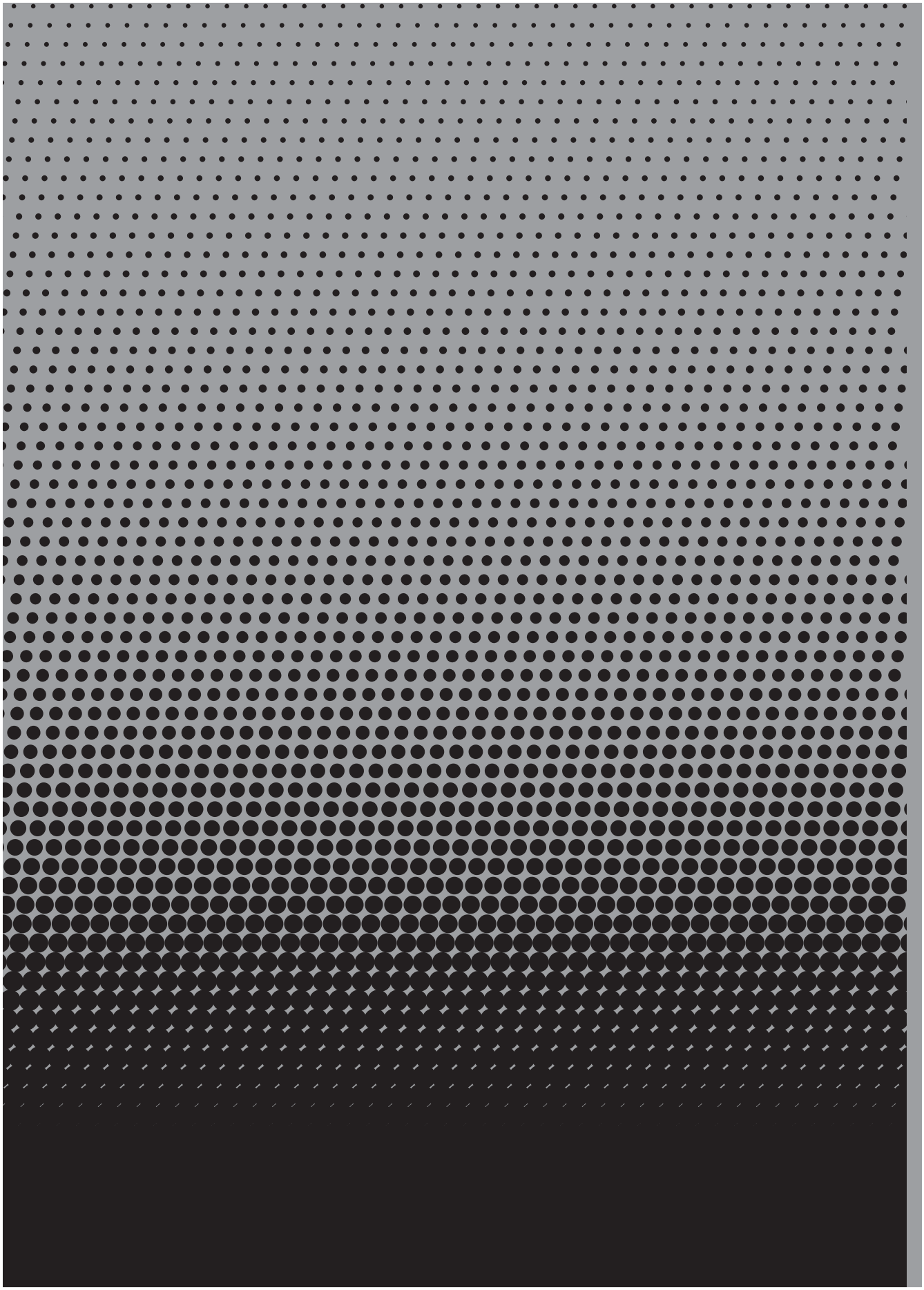

DANKWOORD

Eindelijk, na zoveel jaren…. 9 om precies te zijn. Veel gebeurd, veel geleerd, maar het is mooi geweest. Tijd om weer verder te gaan.

Dat dit proefschrift hier uiteindelijk toch ligt, heb ik te danken aan een heel aantal mensen. Iedereen heeft op zijn of haar eigen manier me geholpen, door het inbrengen van kennis, het kritisch bekijken van mijn onderzoeksresultaten en manuscripten, maar ook door een leuk gesprek of een luisterend oor. Hoe moeilijk en gevaarlijk ook, ik zal proberen op deze plek iedereen te bedanken. Mocht je bij het openslaan van dit boekje direct in het dankwoord zijn gaan zoeken en je naam niet vinden, dan wil ik je op deze plek bedanken.

Allereerst Mark, wat ontzettend fijn dat je me de kans hebt gegeven om promotieonderzoek in jouw groep te mogen doen. Ik herinner me nog goed ons eerste gesprek hierover, waarbij je me het project uitlegde op een A4-tje met allerlei tekeningen over membranen, poriën en bacteriën. Jouw fundamentele kennis beslaat vele vakgebieden en jouw mogelijkheden om hier een technologisch proces mee te bedenken zijn zeer inspirerend. Na een uurtje overleggen in Delft gebruikte ik de terugweg om alles nog eens te overdenken en kon ik weer een hele tijd vooruit. Bij het schrijven van dit dankwoord is net bekend dat je een Spinozapremie zal ontvangen in september. Het is je van harte gegund!

Dear Cristian, in the beginning of our project we had great plans to develop micromodels that would predict fouling in membrane pores. Unfortunately, the data needed as input for these models were lacking, and we decided to take a more experimental route. Luckily, you found an almost perfect PhD student afterwards to do modelling work on fouling in spiral wound membrane modules. Thanks for the nice collaboration during these years and good luck with all your future modelling efforts.

Hardy, als een van mijn dagelijks begeleiders bij Wetsus heb ik veel aan je te danken. Alle discussies over onderzoeksplannen, analyses, interpretatie van resultaten en je hulp bij het schrijven van artikelen zijn erg waardevol gebleken. Je kritische blik bracht soms een schrikreactie teweeg als ik een versie van een manuscript terugkreeg, maar zorgde er ook voor dat het publiceren relatief gemakkelijk ging. Daarnaast zag je ook de kwaliteit in de resultaten, wanneer ik ze al lang had afgeschreven. Jouw tomeloze inzet bij het begeleiden van AIO's is een voorbeeld voor iedere AIO begeleider. Daarnaast was je er ook voor me toen het fysiek wat minder met me ging, bedankt voor alle geduld en vertrouwen. Ik ben erg blij dat je als copromotor deel uitmaakt van mijn commissie. Ik wens je veel succes met het scherp houden van alle volgende AIO's, maar ook genoeg vrije tijd voor je gezin en de andere leuke dingen in het leven.

Moi Arie! Nuchtere Groninger, enthousiaste fietser, communist…. Er valt veel over je te vertellen. Hoewel onze persoonlijkheden behoorlijk verschillend zijn, hebben we elkaar de afgelopen jaren steeds meer leren waarderen. Met jouw nuchterheid en door alles wat je zelf hebt meegemaakt, zet je mijn zorgen en kleine ergernissen in een perspectief. Ik kon (en kan!) altijd bij je binnenlopen voor een vraag over membranen of praktische problemen, maar ook voor adviezen over (race)fietsen, een praatje over van alles en nog wat en een hart onder de riem. Dat heeft me er doorheen geholpen, zeker in de tijd dat het allemaal wat moeizamer liep. Fijn dat je me ook bij wilt staan op die belangrijke dag in september! Ik wens jou, maar ook Lucie en de kinderen, het allerbeste. En ik beloof dat ik, nu echt, op de racefiets naar Oldekerk kom.

Cees, Gert Jan, Johannes en Bert: in deze volgorde leerde ik jullie kennen. Cees, jij haalde me over om naar Wetsus in Leeuwarden te komen, en ik ben zo blij dat je me hebt overtuigd! Jouw directe vragen naar de staat van mijn proefschrift waren niet altijd gemakkelijk, maar hielden me wel scherp en gemotiveerd om af te ronden. Gert Jan, bedankt voor je interesse in mijn onderzoek en mijn persoon in de tijd dat je bij Wetsus werkte, maar ook daarna. Johannes, samen met Cees heb je Wetsus opgebouwd. Ik heb de meeste van deze jaren mogen meemaken en ben nog steeds erg blij een onderdeel hiervan te mogen zijn. Bert, jij kwam bij Wetsus nadat de 'officiële speeltijd' van mijn project al om was. Daarna kwamen de echt drukke jaren pas. Je hebt er altijd vertrouwen in gehad dat ik het ging afronden, en me de ruimte gegeven om me verder te ontwikkelen binnen Wetsus. Jouw rustige manier van werken, echt de tijd nemen voor dingen terwijl er ontzettend veel mensen iets van je willen, is iets waar ik een voorbeeld aan wil nemen.

Tim, Maxime en Perry, ofwel de mede AIO´s in het MBR thema. Tim, je was een vreemde eend in de bijt met je onderzoek over wormen maar altijd bereid om mee te denken over onze vervuilende membranen. Maxime, jouw ongebreidelde 'geloof' in PAC als oplossing voor het vervuilingsprobleem, je artistieke foto´s en hulp bij van alles en nog wat waardeer ik enorm. Ik heb je 'baby', de MBR pilot reactor, met veel plezier van je overgenomen. Perry, jou leerde ik kennen als ontzettend harde werker die me alles kon vertellen over membranen, en daarnaast als een heel creatieve technoloog met altijd nieuwe ideeën tegen membraanvervuiling. Ik ben erg blij dat ik je paranimf mocht zijn en vind het fijn dat je nu eindelijk mijn boekje kan bewonderen. Ook wil ik graag de participanten van het MBR-thema bedanken voor alle input en goede discussies tijdens themavergaderingen en daarbuiten.

Nienke, jij bent zo heerlijk nuchter, dat ik me vaak moest afvragen waarom ik me eigenlijk zo druk had gemaakt over iets. Ook de combinatie van een drukke baan, gezin en vrienden maakt jou niet gek. Onze trip naar Afrika zal ik nooit vergeten. Ik vond het fantastisch om

jouw paranimf en jullie ceremoniemeester te zijn, nu draaien we het even om en ben je paranimf bij mijn verdediging. Ik hoop dat we elkaar nog lang zo trouw blijven opzoeken als nu.

One of the few advantages of a long PhD track is the big diversity of colleagues that shared the office with me. From each of you I have learned things and off course we had great fun too: Ellen, Guillo, Tim, Maxime and Perry in the "early days", in the second round Camiel, Nadine, Claudia, Luewton, Philipp K., Christina, and nowadays Zlatica, Gerwin, Terica, Philipp W. and Lina. Up to the new building!

Dan de oude garde, de Wetsus alumni. Jullie kan ik in het Nederlands aanspreken, omdat jullie allemaal in Nederland zijn gebleven. René, Natasja, Tim, Piotr, Perry, Marthe, Lucia, Bart, Tom, Ingo, Petra, Nienke, Loes, Adriaan, Maxime, Sandra, Elsemiek, Marco, Luewton, Martijn W., Claudia, Philipp K.: die eerste tijd bij Wetsus was toch wel erg speciaal, en dat komt mede dankzij jullie. Bedankt voor alle gezelligheid bij alles wat we ondernomen hebben. Zo fijn om nu ook een nummer te hebben in die mooie rij.

Claudia, Antoine, Thibault, Romain, Xavier, Tomassi, Lucie, Lena, On-Anong, Jean Christophe, Diwan: it is unbelievable that with the help of all of you I could not finish my project earlier… But I am sure that without all your contributions, this thesis would not be here. So, thank you all so much!

Dit dankwoord zou zeker niet compleet zijn zonder een woord van dank aan het labteam en het technisch team van Wetsus. Nu ik meer tijd doorbreng in een ander lab besef ik me pas echt goed wat een luxe het is om jullie ondersteuning te hebben. Ook de dames van het secretariaat wil ik graag bedankten voor hun hulp met de meest uiteenlopende dingen. Ook de wat meer persoonlijke gesprekken met sommige van jullie hebben me veel goed gedaan.

Petra, you know I would write this in English, didn't you? Thank you for the great time we had during all these years. You were there when I came and are luckily still there… We both started in the same way but went into different directions. I am confident that our bond will stay strong. Marthe, Natasja en Nienke, voor elkaar reizen we het hele land door. Heel fijn dat ik jullie als ervaringsdeskundigen van alles kon vragen over het promoveren. Ook erg leuk om bij jullie een uitzicht te hebben naar het leven na de promotie. Bedankt voor al jullie steun! Aleid, in de jaren dat we collega's waren heb ik veel van je geleerd. Je wist vaak de vinger op de zere plek te leggen. Gelukkig woon je nu nog bij me om de hoek dus kunnen we af en toe weer even bijpraten. Ik ben erg blij dat je tijd wilt vrijmaken in je drukke agenda om erbij te zijn op de 16^{e}!

Despite the fact that I was not there very often, I would like to thank my colleagues from the Environmental Biotechnology group in Delft. I have always felt very welcome at the Kluyver Laboratory. Andrea, you just defended your own thesis. Thanks for your great help during the end of both our projects especially with all those administrative issues concerning the printing of the thesis. Good luck in Switzerland! Miranda, bedankt voor al je ondersteuning gedurende het hele proces.

Mijn collega's van van Hall Larenstein: jullie hebben we laten beseffen dat 4 jaar lang werken aan één project een ongekende luxe is die ik niet snel meer zal meemaken. Ik heb veel respect voor jullie inzet voor het onderwijs en hoop jullie in Delft te laten zien waar ik al die jaren druk mee was.

Anke, mede-Wageningse in Leeuwarden, we hebben elkaar pas in Leeuwarden goed leren kennen. In al die jaren hebben we veel etentjes, concerten, avondjes uit en andere leuke dingen beleefd. Laten we dat nog lang zo volhouden! Esther en Nico, oud Dijkgraaf-huisgenootjes: we wonen verspreid over het hele land en ondanks dat we elkaar niet zo vaak zien, is het altijd meteen weer goed. Dat is echte vriendschap! Ik beloof dat ik jullie weer vaker ga opzoeken in het Brabantse land.

Marieke en Jasper, jullie huis was voor mij altijd als een tweede thuis in Groesbeek. Bedankt voor jullie humor en relativeringsvermogen. Een weekendje festivallen is vaak de beste afleiding gebleken wanneer ik weer eens ergens gestressed over was.

Filmhuis Leeuwarden, tegenwoordig Slieker film: de charme van het operateur-zijn is er nu met de digitale film wel wat van af, maar ik ben blij dat ik de laatste jaren van de 35 mm heb mogen meemaken met jullie. Stan, je hebt me de liefde voor de projectietechniek geleerd, en de schoonheid van het "geratel" van de projector. Henk, naast mijn favoriete filmhuis collega ben je ook een fijne buurman!

Volleybaldames van VCL, nu VC058: Volgens mij zijn we al dames 4, 5, 6 en 7 geweest... Gelukkig meestal met de vaste harde kern! Fijn om elke week de frustratie eruit te kunnen slaan, en de zinnen even te kunnen verzetten. Harry, fantastisch dat je ons nog steeds in bedwang kunt houden. Corienne en Inge, we volleyballen niet meer samen, maar daardoor is het niet minder leuk. Fijn dat jullie altijd in zijn voor een lunch, borrel of dagje sauna. Deze afleiding en gezelligheid waren een mooie afwisseling van het werk de afgelopen jaren.

T34-studiegenootjes, "vrienden" is misschien een beter woord: Shakti, Jeroen, Diana, Eva, Suzanne, Jurgen, Jessica, Jeroen, Iris, Sylvia, Packo en alle anderen, ik ben een van de

laatsten van onze groep die promoveert. Bedankt dat jullie al die jaren zijn blijven vragen hoe het ermee stond. Ons jaarlijkse weekend is een leuke traditie geworden om lekker bij te praten en buiten te zijn. Eva en Diana, Jessica, met jullie heb ik geprobeerd wat vaker af te spreken, overal in het land. Nu krijg ik meer tijd en wil ik jullie allemaal vaker opzoeken. Shakti, vanaf de eerste dag in Wageningen zijn we goede vriendinnen. Je gaat nu tijdelijk ver weg wonen en kan daarom niet bij mijn verdediging zijn. Dit vind ik erg jammer, maar het is mooi dat je samen met Jeroen zo'n avontuur gaat meemaken. Bedankt voor al je steun, de goede gesprekken en het er gewoon voor me zijn. Ik ga je missen, het ga jullie goed!

Ook de wat oudere bioprocesgroep van 1996 wil ik hier even noemen. Jullie zijn trouwe bezoekers van promoties, en de Oud & Nieuw feestjes zijn ook altijd erg geslaagd. Fijn dat ik jullie af en toe in wisselende samenstellingen tegen kom. Erik, vooral in de tijd dat je in Groningen woonde zagen we elkaar regelmatig, waarbij we elkaar konden motiveren voor onze beide AIO projecten. Maaike, je bent het beste snowboardmaatje ooit! Daarnaast zie je altijd de zonnige kant van dingen, wat ik een hele mooie eigenschap vind. Kim, je hebt op verschillende manieren een rol gespeeld de afgelopen jaren: toen we beiden in Delft woonden zochten we elkaar regelmatig op, en daarna probeerde ik een afspraak met Mark meestal te combineren met een bezoekje aan Arnoud en jou. Daarnaast zijn we al jaren een goed team bij het organiseren van de wintersport. De twee verschillende weken in Crans Montana gaven mijn gezondheid een duw in de goede richting en de rust om hoofdstuk 5 te schrijven. Bedankt voor alles wat je voor me gedaan hebt.

Gryt, Yldau, Tjallien, Richt en Annemiek, ofwel de kookclub: vele mooie avonden hebben we al gehad samen, met de meest uiteenlopende gerechten. Ik hoop dat er nog vele mogen volgen!

Huisgenoten van de Willemskade, bedankt voor al jullie geduld de afgelopen jaren. Ik was zeker niet altijd gemakkelijk na een lange dag werken, zeker als mijn experimenten niet waren gelukt. Fijn dat jullie toch al die tijd naar mijn verhalen wilden luisteren.

Annemiek en Ton, een speciaal plekje ook voor jullie in het dankwoord. Sinds jij op de Willemskade bent komen wonen, Annemiek, heb ik me bij jullie altijd erg welkom gevoeld. Ik kon me altijd aansluiten bij alles wat jullie ondernamen. Ook waren jullie altijd fijne gasten bij mijn kookacties. Nu komt de tijd dat ik wat kan terugdoen voor jullie. Silvia, jouw tijd in Leeuwarden was kort maar krachtig! Bedankt voor de leuke tijd, maar ook voor je hulp en nuchtere kijk op dingen. Fijn dat je de omslag van mijn proefschrift hebt ontworpen.

Marloes, Willem, Siem en Frank, helaas wonen jullie ver weg en heb ik jullie minder kunnen zien dan ik graag had gewild de afgelopen jaren. Voor jullie was het letterlijk en figuurlijk een ver-van-mijn-bed-show, dat hele promoveren van mij. Ondanks dat bleven jullie me al die jaren wel vragen hoe het ging, waarvoor mijn dank. Oma, u kon het vast niet altijd allemaal helemaal volgen waar ik mee bezig was maar ik weet dat u erg trots bent en het aan iedereen vertelt. Dank u voor uw oprechte interesse en medeleven. Papa en mama, de afgelopen 9 jaren waren niet altijd even gemakkelijk maar jullie waren er altijd voor mij. Dit heeft me er doorheen geholpen en ervoor gezorgd dat het nu toch echt af is. Dank jullie voor alles.

Paula van den Brink
14 juli 2014

This work was performed in the cooperation framework of Wetsus, centre of excellence for sustainable water technology (www.wetsus.nl). Wetsus is co-funded by the Dutch Ministry of Economic Affairs and Ministry of Infrastructure and Environment, the European Union Regional Development Fund, the Province of Fryslân and the Northern Netherlands Provinces. The authors like to thank the participants of the research theme “Membrane processes and operation for wastewater treatment and reuse” for the fruitful discussions and their financial support.